

ENG 287-(EQC 1991/97)

**Earthquake Vulnerability of Existing Unreinforced Masonry
Buildings**

E L Blaikie, D D Spurr (Works Consultancy Services)

Ref: 6/2/2/2 (91/97)
ENS 287



EARTHQUAKE VULNERABILITY
OF EXISTING UNREINFORCED
MASONRY BUILDINGS

E L Blaikie

D D Spurr

This project was sponsored by the
New Zealand Earthquake and
War Damage Commission

Works Consultancy Services
Vogel Building
P O Box 12-003
Wellington
Telephone 04-471 7000
Fax 04-471 1397

December 1992

TABLE OF CONTENTS

1	INTRODUCTION	1
2	PERFORMANCE OF UNREINFORCED MASONRY BUILDINGS IN EARTHQUAKES	2
2.1	Hawke's Bay Earthquake, East Coast New Zealand, 3 February 1931 . . .	3
2.2	Wairarapa Earthquakes, Central New Zealand, 24 June & 1 August 1942	5
2.3	Imperial Valley Earthquake, California & Mexico, 15 October 1979	7
2.4	Coalinga Earthquake, California, 2 May 1983	8
2.5	Whittier Narrows Earthquake, California, 1 October 1987	9
2.6	Loma Prieta Earthquake, California, 17 October 1989	12
2.7	Weber Earthquake, East Coast New Zealand, 13 May 1990	16
2.8	Damage Levels	19
2.9	Correlation with Recorded Accelerations & Dynamic Analysis Modelling	26
2.10	Summary of Failure Modes & Implications for Assessing Vulnerability .	29
2.10.1	Out-of-plane wall failures	29
2.10.2	In-plane wall failures	31
2.10.3	Anchorage failures	32
2.10.4	Diaphragm flexibility and strength	33
2.10.5	Corner damage	33
2.10.6	Interior partition walls	34
2.10.7	Parapet and non-parapet falling hazards	34
2.10.8	Pounding damage	35
2.10.9	Foundation failures / permanent ground deformations	35
2.10.10	Configuration induced failures	35
2.10.11	Soft soil amplification	36
2.10.12	Brickwork and mortar quality	36
2.10.13	Age of construction	36
2.10.14	Windows	37
3	NATURE OF NEW ZEALAND'S UNREINFORCED MASONRY BUILDING STOCK	38
3.1	Introduction	38
3.2	Earthquake Risk Buildings In Wellington City	38
3.3	Earthquake Risk Buildings In Petone and Nelson City	38
4	PREVIOUS RESEARCH	41
4.1	Introduction	41
4.2	Research Carried out by the ABK Joint Venture	41
4.3	The ABK Methodology	42
4.4	Research Carried out at the University of Canterbury	45
4.5	Gilroy Firehouse Response to Loma Prieta Earthquake	46

5	BEHAVIOUR OF CRACKED URM WALLS UNDER STATIC FACE LOADING	48
5.1	Derivation of Static Load Deflection Relationship	48
5.2	Energy Balance	50
5.3	Static Load Deflection Relationship for Uniformity Distributed Loads ...	50
6	DYNAMIC BEHAVIOUR OF FACE LOADED WALLS WITHOUT INTERACTION WITH DIAPHRAGMS	52
6.1	Boundary Conditions for Wall Elements	52
6.2	Computer Model	53
6.3	DRAIN-2DX Computer Program	57
6.4	Face Loaded Wall Behaviour Under Pulse Loading	57
6.4.1	Period of Free Vibration Response	60
6.4.2	Damping of Free Vibration	63
6.4.3	Difference Between Elastic and Inelastic Damping	66
6.5	Comparison Between Computer Modelling and ABK Test Results	68
6.5.1	Introduction	68
6.5.2	Earthquake motion	68
6.5.3	Comparison Between Tests and Modelled Input Motions	69
6.5.4	Comparison Between Test and Modelled Wall Displacement ..	71
6.5.5	Comparison Between Test and Modeled Wall Accelerations ..	74
6.5.6	Anchorage Forces and Vertical Accelerations	77
6.5.7	Comparison Between Predicted and Measured Collapse Earthquake Intensity	78
6.5.8	Damping	78
6.6	Effect of Wall Thickness and Earthquake Intensity on Face Loaded Wall	79
6.6.1	Introduction	79
6.6.2	Wall Displacement Response to the DZ4203 Earthquake Motion	79
6.6.3	Wall Displacement Response to Tabas and Weber Earthquake Motions	83
6.6.4	Anchorage Forces for Rigid Diaphragms	83
6.7	Prediction of Face Loaded Wall Stability Using Displacement Response Spectra	89
6.7.1	Introduction	89
6.7.2	Elastic Response Spectra for DZ4203, Weber and Tabas EQ Records	89
6.7.3	Use of Displacement Response Spectra to Predict Wall Displacements	93
6.7.4	Comparison Between Proposed Formulae, Computer Model and ABK Methodology	95

6.7.5	Example of Calculations Required to Compute the Seismic Stability of Face Loaded Walls	98
7.	BEHAVIOUR OF FACE LOADED WALLS WITH DIAPHRAGM INTERACTION	101
7.1	Behaviour of Walls Subjected to an Acceleration Pulse	101
7.1.1	Wall Modelling	101
7.1.2	Wall Modelled with 0.5 Second Period Diaphragms	101
7.1.3	Energy Loss In Diaphragms	104
7.1.4	Walls Modelled with 1.0 and 2.0 Second Period Diaphragms	105
7.2	Influence of Diaphragms on Seismic Response of Face Loaded Walls ..	108
7.2.1	Diaphragm Modelled Using ABK's Methodology	108
7.2.2	Diaphragms Modelled with Flexibility	111
7.2.3	Interaction Between Wall and Diaphragm Responses	116
7.2.4	Effect of Impact on Damping	119
7.2.5	Diaphragm Anchorage Forces Developed by Flexible Diaphragms	119
7.2.6	Analyses Using Other Earthquake Records	122
8	ANALYSIS OF REGENT THEATRE BUILDING - DANNEVIRKE ..	123
8.1	Details of Building	123
8.2	Computer Modelling	125
8.3	Predicted Response of Regent Theatre Face Loaded Walls	126
9	METHODOLOGY FOR EVALUATING THE SEISMIC RESISTANCE OF FACE LOADED URM WALLS	130
9.1	Introduction	130
9.2	Summary of Proposed Methodology	130
9.3	Details of Proposed Methodology	130
9.3.1	Step 1 : Seismic Resistance of Face Loaded Walls with Rigid Diaphragms	130
9.3.2	Step 2 : Effect of Flexible Diaphragms	131
9.3.3	Step 3 : Effect of Shear Wall Amplification	131
9.3.4	Step 4 : Anchorage Forces and Diaphragm Strengths	132
9.4	Further Research Required	133
10	SUMMARY AND CONCLUSIONS	135
	REFERENCES	139

1 INTRODUCTION

New Zealand still has a large stock of low rise unreinforced masonry (URM) buildings. The performance of this type of building in past earthquakes has sometimes been poor. This has resulted in increasing pressure to strengthen or demolish these buildings. However, despite their poor reputation, many URM buildings have survived strong shaking with relatively little damage. This includes most of the URM buildings in Dannevirke during the May 1990 Weber earthquake and large numbers of domestic buildings in the 1985 Chilean earthquake.

This would indicate that only modest amounts of strengthening may be required for many URM buildings in low and moderate seismicity zones to produce an acceptable level of risk.

Unfortunately the response of URM buildings to earthquake motions is not well understood. This makes it difficult to predict the likely seismic performance of a particular URM building and identify those features of the building that require strengthening.

The most widely applied guidelines for the assessment and the design of strengthening schemes for URM buildings in New Zealand are those published by NZNSEE⁽¹⁾. These guidelines are principally based on an equivalent static load and an elastic stress analysis approach. These traditional methods of analysis often produce an unrealistically conservative assessment of the seismic vulnerability of a URM building. Also, traditional methods of strengthening URM buildings, such as the use of sprayed concrete on walls, are expensive and are very disruptive to a building's fabric. This often makes the strengthening of many commercial buildings uneconomic. It also reduces the value obtained from the strengthening of an Historic building as the value placed on the building's fabric is often a prime reason for its preservation.

With an increased understanding of the performance of URM buildings, cheaper and less disruptive strengthening techniques should be possible particularly in low and moderate seismicity zones. This can be expected to increase the number of at risk buildings being strengthened and hence reduce the amount of building damage and loss of life in future earthquakes.

In this project, damage reports for URM buildings in seven earthquakes are reviewed. Statistical damage data is summarised and building features that have resulted in damage or collapse are identified.

A computer model of a face loaded URM wall is then analysed using inelastic dynamic analysis. Predicted behaviour is compared with test results and the computer model is used to develop a methodology that can be used to assess the seismic resistance of a face loaded URM wall. In this methodology the effective period of the face loaded wall motion is computed using semi-empirical formulae and an elastic displacement response spectrum is used to predict the earthquake magnitude required to cause wall collapse. The proposed methodology is expected to provide more realistic assessments of face loaded wall stability than currently used procedures.

2 PERFORMANCE OF UNREINFORCED MASONRY BUILDINGS IN EARTHQUAKES

Damage to unreinforced masonry (URM) buildings and elements is a pervasive feature of many earthquakes. In many instances the damage has been spectacular, with large quantities of masonry falling and littering streets and in larger earthquakes many buildings have collapsed completely. This extent of damage is both unnecessary and unacceptable, being responsible for much of the loss of life and injury that has occurred in earthquakes. Despite the ensuing conflagration, the deaths of at least three quarters of the 256 people killed in the 1931 Hawke's Bay earthquake were attributed directly to falling brickwork or collapsed masonry buildings (3). However, the spectacular nature of the damage has also tended to obscure the satisfactory performance of many other URM buildings in earthquakes. Even in the Hawke's Bay earthquake where the majority of URM commercial and institutional buildings in Hastings and Napier were severely damaged or collapsed, many one and two storey brick bearing wall dwellings apparently sustained only minor damage.

To help quantify the performance of URM buildings in earthquakes, brief reviews of damage reports from seven New Zealand and Californian earthquakes are presented, followed by a general review of the extent and types of damage in these and several other earthquakes for which statistical damage data are available. Many other similar examples exist.

Californian earthquakes have been included in this review for several reasons. These include the availability of damage data and accelerograph records, and the similarities to the New Zealand situation in terms of URM construction types and histories. In both areas, all URM buildings are pre 1933/35. Outside the central business districts of the main cities, most are 1 or 2 storeys high and typically have timber floors and roof framing and 2 or 3 wythe wall construction. Larger institutional and government buildings often have thicker walls as do "high storey" structures such as theatres and halls. In a number of localities in both New Zealand and California, many of the URM buildings have wall-diaphragm ties or other "reinforcing" elements introduced as part of the original construction, after earlier earthquakes, or as part of recent seismic upgrading to comply with Local Authority requirements. "Government anchors" were used widely in parts of California to tie brick walls to floor and roof diaphragms during the original construction. The wall ends of these anchors had a vertical rod placed through a hook and were set into the brickwork with the rod located between two wythes of bricks.

Although there are many examples of poor quality deteriorated lime mortars in New Zealand, there are indications that at least in some parts of the country, a higher proportion of buildings have better quality cement or lime-cement mortars than is the case in California. Certainly the standard "in-place" brick shear test developed in the US (2) can be very difficult to perform on local buildings. Often a diamond saw is required to clean out the head joints and remove a brick for placing the jack and in some cases the jack capacity can be exceeded or the loaded brick can crush in bearing before the bed joints slip (bed joint shear capacities in excess of 6 MPa).

2.1 Hawke's Bay Earthquake, East Coast New Zealand, 3 February 1931

This was an M_s 7.8 reverse thrust earthquake which occurred at 10.47 am Tuesday 3 February local time. The hypocentre was estimated to be 30 km north west of Napier and 20 - 30 km deep, with the rupture propagating to within about 5km of the surface. The surface projection of the fault plane runs just to the east of Napier and just to the west of Hastings. Surface uplift of 1.5 m - 2 m occurred at Napier, with a maximum uplift of 2.7 m occurring 25 km further north (5). A maximum intensity of MM X shaking occurred over a large area including the towns of Hastings (1931 population 10,850) and Napier (16,025) which are 20 km apart. Two satellite towns were also within this zone.

Both Hastings and much of Napier are located on flexible soils. The near surface soils under Hastings consist of about 15 m of recent sands and silts with interbedded gravel and pumice lenses overlying up to 15 m of recent intertidal and shallow marine sediments. The geology of Napier is more complex and includes some hill and firm ground areas.

Construction:

The business centres of both towns consisted mainly of unreinforced brick buildings of up to three storeys high. No detailed descriptions of the construction standards were found in the literature, but lime mortars appear to have been common, particularly in older brick buildings. Lime mortars in many chimneys had deteriorated badly. The extent of wall-diaphragm ties is not known. A number of buildings did have reinforced concrete bands at the floor and roof levels of the exterior walls, but very few bands were provided at the tops of partition walls that were tied into the main bands.

Damage to URM Buildings:

Eye witness accounts of the earthquake describe two main shocks about half a minute apart. The first shock caused severe damage including partial collapse of buildings but the greatest damage occurred during the second shock, in part due to the damage already inflicted. The total duration of strong shaking was 1½ to 2½ minutes. Many people saved their lives by escaping to the street after the first shock but others were killed by the debris brought down by the second shock while they were escaping.

Damage in the business centres of both towns was severe. Numerous commercial and institutional buildings collapsed and many others were severely damaged. Few brick buildings escaped with only minor damage. Ground disturbance was widespread throughout Napier and in a number of cases exacerbated the extent of damage to brick buildings. Fires broke out within a few minutes of the earthquake and by the next morning had gutted over 4 hectares (about 80%) of the earthquake damaged business area in Napier as well as four blocks in the industrial area at the port. Outside the business area of Napier, some of the larger public buildings were also seriously damaged or collapsed. All wards of Napier Hospital were badly damaged and had to be evacuated, and the Nurses' Home collapsed. Fewer collapses occurred in Hastings and outside the business district damage was less severe than in Napier. One city block and parts of three others were gutted by fires. The fatality

rate in both Hastings and Napier was 1% and it was estimated that 60% lost their lives on the footpaths due to falling masonry or were trapped while trying to escape from collapsing buildings. Four collapsed buildings outside the business districts accounted for a further 15% of the fatalities.

The severity of damage and ensuing conflagrations prevented detailed assessment of the types of damage sustained by URM buildings and components. However some details were reported by Callaghan (3) and Brodie & Harris (4) and are summarised below.

- All domestic brick chimneys in an area extending 75 km north and south of Napier were reported to have collapsed or have been broken.
- There were many examples of one and two storey brick dwellings which suffered little damage other than to chimneys, particularly in areas where there were no permanent ground deformations.
- Inadequate footings and footings not being tied together adequately were significant factors contributing to the damage sustained by buildings founded on silt subsoils.
- Timber partitions were inadequately tied to the exterior brick walls. There were many instances where the exterior brick walls had collapsed and the roof and floor were supported by the interior timber partitions. In the photographs sighted, the plaster linings on the partition walls did not appear to be significantly distressed.
- Poor quality lime mortars and poor filling of vertical joints were considered significant factors affecting the performance of brickwork.
- Inadequate use of bonding-metal (typically wire-mesh or expanded metal every 9 or 10 courses) was regarded as a noticeable feature in the damaged buildings, particularly at corners and in narrow panels between openings. The last part of this observation suggests that corner cracking and diagonal ("X") cracking in piers may have been common.
- Reinforced concrete band courses (generally with 20 mm reinforcement) were considered effective in holding buildings together, but poor detailing of the junction of bands at corners was noted as a frequent cause of failure. The bands were generally provided only at floor and ceiling (roof?) level and it was considered that additional bands should have been used for higher walls. The importance of adequately tying buildings together was well understood by at least some engineers at this time, and even much earlier (see later comments in relation to the 1942 earthquake).
- Brick parapets and gables were responsible for much loss of life. Gables "invariably" proved to be a weakness.
- Massive architectural facades that were inadequately tied to flimsy interior frames of light timber or light brickwork were an additional hazard. The front

portions of these buildings collapsed or were dislodged and had to be demolished.

- Damage due to pounding appears to have been significant, to the extent that "the evidence .. demonstrated the danger of erecting tall buildings" of different heights abutting one another.
- Heavy concrete ceilings and heavy tile roofs were also considered to have had a "dangerous wrecking effect" that was "well demonstrated".

The average damage ratio on insured property in the "earthquake affected area" was estimated to be 50%, but as most of these properties were not insured for earthquake, only about 10% of the losses were paid out by insurance companies (3). It is important to note that the "earthquake affected area" referred to in this case extended well beyond Napier and Hastings, into areas of lesser damage. The population within this larger area was about 100,000 in 1931, which is about three times the population living within the MM X isoseismal at the time.

2.2 Wairarapa Earthquakes, Central New Zealand, 24 June & 1 August 1942

These were M_s 7.2 & M_s 7.0 earthquakes respectively, located 100 km north east of Wellington City and about 40 km deep (6). The peak epicentral intensity in the Masterton area was MM VIII. The intensity in Wellington (1936 population 150,000) varied from c.MM V - MM VI in most of the hill suburbs (weathered rock), to MM VII in the filled areas in the central city. The majority of brick buildings were located on the reclaimed land in the downtown area (MM VII). Recent investigations suggest a "site period" of about 0.9 seconds for the soft soil areas (7). No strong motion instruments were deployed in the area at the time of this earthquake.

Construction - Special Characteristics:

A history of high seismicity in central New Zealand over the hundred year period preceding the 1942 earthquakes had resulted in an average standard of URM construction that was probably somewhat higher than typical in many parts of California. Major earthquakes in 1848 (MM VIII in Wellington) and 1855 (MM X) during the early years of European settlement had a significant impact. Most brick buildings at the time were destroyed or badly damaged and few new brick buildings were built for several years. Subsequently, at least some brick buildings were built with some appreciation of seismic problems. A number of buildings had wall-diaphragm ties included in the original construction and in some cases, light reinforcing was included in occasional horizontal mortar courses. Many other buildings were built with little consideration of earthquake loading. However over the years, the larger ornamental parapets were reduced in height and varying forms of buttressing, strapping and tying have been applied. Cement mortars began to replace lime towards the turn of the century (8).

Few pre 1890 brick buildings remained in existence by 1942 and only two buildings of this age are included in the list of brick buildings surveyed by the City Council in the early to mid 1970's.

Damage to Brick Buildings:

A detailed survey of about 900 buildings in the business area of the city was undertaken after the earthquake. About 550 of the 900 buildings were of brick construction and most were between 2 and 4 storeys high. The survey included data on the type of foundation and subsoil, nature of occupancy, extent of damage and existence of hazards such as parapets, towers, abnormal slenderness, extent of glazing, asymmetric bracing and the like. It is believed that the original data are still in existence but they have not been located. A limited summary of the results was reported by Johnston (8) and the details for brick buildings from this report are reproduced below. No buildings collapsed in Wellington.

	Total No. Examined	No. Damaged	% Damaged
Brick bearing walls, concrete floors	29	11	38%
Brick bearing walls, wood or steel & wood floors	522	269	51%

The lower percentage damage figure for buildings with concrete floors was "believed to be due to better integration and sufficient precompression in the walls to avoid failure However, there were sufficient signs of strain at lower levels in some of the buildings to raise serious doubts of their behaviour in a heavy earthquake" (8).

It was also noted that:

"A few parapets were thrown down and many others damaged but earlier attentions to the more hazardous minimised damage.", and that "Brick buildings were damaged for a variety of reasons but floating floors and roofs requiring the higher levels of walls to cantilever at least a storey were a common cause of damage. The walls of theatres and similar structures which were overlong or over-tall with indifferent lateral support bulged normally to their surfaces. Weaknesses induced by extensive glass facades in one, two or three walls without compensating bracing features resulted in obvious torsional strain while in some cases simple constructional errors such as cold mortar joints, unbonded corners or wall intersections, unbonded additions and the weakening effects of alterations or 'modernising' treatments were the principal cause of damage. At least two substantial brick buildings were severely damaged by the impact of taller and heavier neighbours. A number of well designed buildings suffered no discernible damage, but recent (at c.1960) demolitions have shown that some buildings exhibiting little damage owed that freedom to built-in reinforcement; in one case a complete substantial steel frame"(8).

Buildings founded on reclaimed land sustained more damage than those on firm natural ground. In particular, there was no serious damage to buildings on the landward side of the old shoreline along Lambton Quay and lower Willis Street (two of the main streets in the CBD).

Aked (9) reported details of damage to a number of specific brick buildings in the following categories:

- Theatres and other similar large barn-like structures

- Buildings of more than one storey having large open floor areas
- Hammering of cross walls
- Light well walls and cross walls
- Adjoining buildings.

Damage patterns illustrated by Aked for the first category of buildings show distinctive face load cracking, often resulting from large deflections of the long flexible roof diaphragms. The cracking patterns also reflected points or lines of restraint such as floors, end walls, cross walls and buttresses. This type of cracking appears to have occurred in most buildings of this type, although none of the walls collapsed. "Mid-height" cracks were not evident in the examples illustrated, probably because most of the walls of these buildings were relatively thick and the roof diaphragms relatively flexible.

Damage to the second category of buildings was "often confined to the upper storeys and (had) characteristics similar to the damage in single storey buildings". Also, "In buildings of this type where there are no reinforced concrete bands the tendency is for the long lengths of walls on either side of a cross wall to become a single unit of wall by pulling away from the cross wall by tearing action, ... ". Subsequent pounding between the two walls appears to have primarily damaged the cross walls. Light well walls appear to have suffered "considerable damage" chiefly due to the "swinging movement of the larger walls to which they are attached". The light well walls were weakened by window openings and tended to "fracture vertically, the separated portions of the walls adhering to the main walls".

Aked reported relatively little damage that could definitely be attributed to pounding between buildings during the earthquake.

2.3 Imperial Valley Earthquake, California & Mexico, 15 October 1979 (10)

This was an M_s 6.8 strike slip earthquake on the Imperial Fault. The earthquake epicentre was just south of the US - Mexican border, with the rupture propagating northwards into southern California. Five towns and small cities are located within 5 km - 10 km of the fault rupture; Imperial (5 km from the fault), El Centro (6 km - 9 km, 1991 population 31,000), Brawley (7 km, 19,000), Holtville (7 km) and Calexico (10 km, 19,000). The commercial districts in these towns and cities contain many old, 1-2 storey unreinforced brick buildings. The earthquake intensity in the commercial districts was typically about MM VII (est.).

Accelerograph records were obtained in Brawley, Holtville, El Centro (several locations), Calexico and numerous other locations, including several within 1km to 5km from the surface rupture. Acceleration spectra for several of these records are shown in Figure 2.2.

Construction - Special Features:

The affected area had previously been strongly shaken during the 1940 Imperial Valley earthquake (M_s 7.1) which ruptured the same fault segment, as well as the extension of the fault further south into Mexico. A number of the URM buildings damaged in the earlier earthquake were seismically upgraded when they were

repaired. These retrofits included lightly reinforced wall bands and capping bands on parapets, wall anchors, and/or replacement of damaged brickwork by lightly reinforced concrete walls. Most of the brick buildings in the area had had wall anchors installed at some stage. It was also considered that the quality of brickwork was generally better than is typical in the Los Angeles basin (10).

Observed Damage to URM Buildings:

Damage to URM buildings in the five towns/cities closest to the fault was generally light. The most obvious damage in all cities was broken windows. Other damage due to in-plane loads was largely limited to minor flexural cracking at the tops and bottoms of window mullions and shop front piers. Only one case of diagonal ("X") cracking of a window mullion was observed.

Parapet failure occurred in 10% or less instances, except in Imperial which was the town closest to the fault. No mid-height cracks due to flexure between diaphragm levels were observed, although cracks of this type could have closed after the earthquake.

Separations between the tops of walls and roof structures were not observed, although some anchors did fail, eg. an external anchor plate, together with the four surrounding bricks pulled part way through a wall (10).

Torsional response due to irregularity did not appear to be a significant factor in this earthquake. Also, roof and floor diaphragms of "undesigned" wood framing performed satisfactorily, limiting the displacement of side walls even in cases where static calculations indicated high in-plane shear stresses in the diaphragms.

Recent alluvial soils appear to be common throughout much of this area, though this was not reported (10) as being a factor in the performance of the URM buildings.

2.4 Coalinga Earthquake, California, 2 May 1983 (11,12)

This was an M_L 6.6 thrust fault earthquake, 8 km deep and centred about 15 km north east of Coalinga (1983 population 7000). The peak intensity assigned was MM VIII in and near the town of Coalinga (13). Free-field and basement accelerograph records were obtained from the Pleasant Valley pumping plant switchyard 15 km north east of the fault. The ground conditions at the recording site (fan deposits over marine sediments) are similar to those in Coalinga (14) and it is believed that, except for possible radiation focusing effects, the recorded free-field accelerograph (Figure 2.2) provides a reasonable representation of the shaking experienced in Coalinga (14,15).

Construction:

URM buildings were largely confined to the business district in Coalinga and were either 1 or 2 stories tall. Almost all were built during the period 1900-1930. The standard of construction was considered to be "at the lower range" of average commercial URM construction in California (11), with few if any "substantial" institutional or government buildings. The buildings were generally rectangular in

plan without re-entrant corners. Most buildings had had wall-diaphragm anchors installed at some stage. Most of the anchors were external "through wall" types with exterior bearing plates, although there were some internal "government" type anchors installed as part of the original construction. Chemical analyses made after the earthquake showed that only one of sixteen mortar samples taken from damaged buildings had a significant cement content. In that case the cement:lime ratio was only 17%.

Damage to URM Buildings:

Damage to URM buildings in the business district of Coalinga was widespread. Data presented by Reitherman *et al* (11) indicates that 14% of the URM buildings collapsed with a further 16% assessed as total losses. A further 30% were considered to require replacement of more than 50% of their wall area. As observed in other earthquakes, most wall collapses occurred in single storey buildings or in the top storey of multistorey buildings.

Out-of-plane deformations were the most prevalent cause of major structural damage. This type of damage included wall-diaphragm anchorage failure as well as failure of walls and parapets in flexure. It is believed that anchorage failure (or lack of anchors) was the most common reason for wall collapse. Government type anchors embedded within the brickwork generally proved ineffective in the predominantly lime mortars used in the area and even some ties anchored with bearing plates on the exterior faces of walls failed. In some cases anchorage failure may have been precipitated by prior cracking or collapse of a parapet above the top line of anchors. Wall instability due to out-of-plane flexure between anchor lines was indicated in some of the collapses. However once walls have collapsed, it is very difficult to be certain of the initial cause of failure.

Other common damage included broken shop front windows and "corner damage". This latter category included vertical cracking at the wall junctions and collapse of corner sections of the walls. The second type of corner damage was believed to have been caused by distortions of the timber diaphragms, particularly shear sliding at the diaphragm-end wall junctions. The anchorages provided were not detailed to resist shear sliding.

Examples of diagonal ("X") cracking due to in-plane loads were observed but these were considered to be much less significant as a cause of major damage (11,12). Examples of veneer separation and spalling were also noted (12).

2.5 Whittier Narrows Earthquake, California, 1 October 1987 (17,18,19,20)

This was an M_L 5.9 earthquake, 14 km deep with its epicentre within the Los Angeles metropolitan area. A peak intensity of MM VIII was assigned to a small area (10 sq. km) near Whittier. The surrounding MM VII intensity zone covered several city centres within an area of some 480 sq. km. The estimated population within this area was 1.25 million in 1987 (16). Accelerograph records were obtained from several sites close to damaged URM buildings.

Construction:

The large number of URM buildings affected (7300 in Los Angeles City alone) undoubtedly included a variety of building types, but the majority had timber floors and roof framing.

Prior to the earthquake, about 1100 of the 7300 URM buildings within the LA City area had been fully strengthened in accordance with the City's strengthening ordinance.

Damage to URM Buildings:

Damage surveys were conducted in several cities in the affected area (17,18,19). However other than survey results published by the LA City Building and Safety Section, little of the statistical data obtained appears to be readily available. The LA City study included a preliminary survey of some 2400 URM buildings in the worst affected areas of LA City (downtown - MM VI, Hollywood - MM VI?, and East Los Angeles - MM VII). This was followed by a detailed survey of 25 structurally damaged buildings identified from the preliminary survey results (20). This latter sample was selected with an emphasis on evaluating buildings that had been strengthened. A total of 15 of the 25 buildings surveyed in detail had been strengthened.

Summary results from the preliminary survey are as follows:

Status	Occupancy	Number	Damaged	Vacated
U/PS	Residential	7464 units	53%	5.1%
U/PS	Commercial	1541 buildings	25%	4.3%
S	Residential	432 units	19%	0.4%
S	Commercial	364 Buildings	19%	1.6%
				(see note)

S = Strengthened, U = Unstrengthened, PS = Partially Strengthened

Note: A figure of 1.6% is given for the number of vacated buildings, but 15 "severely damaged" strengthened buildings were selected for the follow-up survey. This is approximately 3% - 4% of total number of strengthened buildings in the preliminary sample.

No buildings appear to have collapsed in any of the affected cities, although there were several collapses or partial collapses of walls.

Qualitative details of the types of damage exhibited in the more severely damaged buildings that were surveyed, are as follows (17,18,19):

- Out-of-plane wall movement damage. This type of damage included partial collapses of exterior walls, wythe separation and cracking along roof line anchors and at lintels. The partial collapses occurred in upper storeys and in one storey

walls. The damage typically was worst in the upper portion of the walls and near the centre of the diaphragms. Separation of wythes was commonly associated with out-of-plane failure of the walls and followed a similar pattern in respect of location of the damage. There appeared to be little mortar in the vertical collar joints between wythes that were exposed by the wythe separations and in one case illustrated, there were no header bricks.

Poor mortar was evident in most failures. The damage patterns also showed the beneficial effect of overburden weight on wall performance under out-of-plane loading.

In a few cases ceilings hammered on the walls, causing damage.

Where wall collapses did occur, roof collapse was prevented by secondary vertical supports (existing walls, or columns added for strengthening).

- Wall separation from floors and roofs. In unstrengthened buildings, out-of-plane failures of walls were characterised by walls separating from roof and floor diaphragms and in-plane cracking of return walls. These failures were caused by a lack of wall-diaphragm anchors or failure of "government" type anchors built into the brickwork during construction. The "government" anchors usually failed at the embedded end, especially where there was poor quality lime mortar. The separation gaps observed were progressively wider up the height of the buildings and were widest near the centre of the diaphragms.
- In-plane cracking. Diagonal tension ("X") cracks occurred in wider "stubby" piers while slender piers rocked on horizontal flexural cracks at the top and bottom of the piers. Cracks were worst in the lower storeys of two of the 25 buildings surveyed in detail, but occurred only in the upper storeys of a third building. There was also extensive cracking of plaster cross walls in one of these buildings. All three buildings had been strengthened.

Three of the unstrengthened buildings surveyed had diagonal cracks at the tops of the end piers, while the internal piers were uncracked or less severely cracked. These diagonal cracks were worst in the upper walls and in non-load bearing walls. Return walls on the end piers were cracked and displaced out-of-plane. This behaviour was thought to be caused by sliding between the ends of the diaphragms and the end walls, resulting in the diaphragm shear loads being reacted primarily by the end piers.

In two of the buildings in the follow-up survey, in-plane cracking occurred in the spandrel beams rather than in the window mullions (piers). In both cases the window openings had arched lintels.

- Corner cracking. Cracks occurred in the top corners of buildings. These extended from the upper corners of openings to the corners of the buildings at roof level. Both strengthened and unstrengthened buildings were affected, but the cracking was more pronounced in the unstrengthened buildings. These cracks were thought to be caused by the ends of the floor and roof diaphragms pushing on the walls, resulting in out-of-plane, in-plane and rotational deformations at the

wall corners.

- Special cases. In one single storey building there was an unusual out-of-plane failure immediately under the line of roof anchors in one wall. This crack extended along almost the entire length of the wall and there was a residual 50mm outward displacement at the top centre of the wall under the crack. Two second storey walls in another building exhibited a similar type of failure.

In another case, there was an out-of-plane horizontal crack extending along a major portion of a common wall between two adjacent roofs that were at different levels. The crack was midway between the two roof levels.

- Cracks in interior plaster walls. Existing lath and plaster partitions and ceilings cracked extensively and it was considered that they would be a hazard in a larger earthquake. Plywood and gypsum board walls in the surveyed buildings sustained the same displacements without cracking.

2.6 Loma Prieta Earthquake, California, 17 October 1989 (21,22)

This was an M_s 7.1 earthquake centred approximately 100 km south east of San Francisco and 15 km east-north east of Santa Cruz. The fault rupture was on or near a segment of the San Andreas Fault and extended about 20 km both north west and south east of the epicentre. Other nearby towns and cities include Watsonville (7 km from the fault rupture), Gilroy (15 km) and San Jose (18 km). A peak intensity of MM VIII was assigned to the epicentral region. The general intensity in the San Francisco - Oakland area was MM VI - MM VII, but there were local pockets of up to MM IX on Bay Mud soil sites around the harbour perimeter.

Strong ground motion records were obtained from more than 130 sites, including locations in Gilroy (0.37g) and Watsonville (0.39g), as well as many locations in San Francisco and Oakland.

URM Construction:

As typical for California, the majority of old URM buildings in the affected area have wood frame floor and roof diaphragms. Only about 3% of surveyed buildings in the area had been strengthened at the time of the earthquake.

Damage to URM buildings:

Surveys of damage to URM buildings were undertaken by several organisations, with much of the data being collated and evaluated by Holmes *et al* (22). The greatest damage to URM buildings occurred in the Santa Cruz - Watsonville area, but there was significant damage as far north as San Francisco and Oakland. Summary damage data extracted from Holmes *et al* are presented in Table 2.1. This table includes data for about half of the total survey sample of 5564 buildings. Data for those areas where separate details were not available for strengthened buildings, have not been included as they could distort the comparisons between strengthened and unstrengthened buildings. The principal omissions are Oakland (2072 buildings, MM VII), San Jose (230, MM VII) and Berkeley (400, MM VI).

The estimated average damage ratio for unstrengthened buildings in San Francisco was of the order of 1.5 times that of the strengthened buildings. However, the difference between the two sets of buildings is less clear in the MM VIII areas. The only difference evident from Table 2.1 is the proportion of demolished buildings and given the very small number of strengthened buildings identified, little significance can be attached to this result. Evaluation of the effectiveness of strengthening in areas outside San Francisco is also complicated by the wide variety of strengthening procedures and design levels used.

An evaluation of the types of damage recorded on survey forms for 1889 unstrengthened buildings in San Francisco yielded the following results (22):

Falling Hazards

- Parapet failure (99 buildings with parapet damage on at least one face). Parapet failure resulted in extensive debris, property damage and one death. This category presumably includes gable failures.
- Non-parapet falling hazards
 - falling units of trim/ornamentation (101)
 - veneer or delamination failure - falling brick (98)
- Failure of a portion of a wall (61)
- Failure of an entire wall (36)

In-plane Cracking Damage

- Cracks at the corner of openings (252)
- "X" cracking in spandrel beams (124)
- Vertical cracking in spandrel beams (179)
- "X" cracking in piers or walls (204)
- Horizontal cracking at the tops and bottoms of piers (199)

Corner Damage

- Distress at first level (167)
- Distress above first level (167)

Separation of walls and diaphragms due to non-existent tension ties or tie failures was also observed in many cases, and appeared to be responsible for most of the wall or partial wall collapses. In other instances, excessive deflections due to diaphragm flexibility were thought to have caused failure of attached walls. Out-of-plane collapses (parapets, walls and portions of walls) were common in the more intensely shaken areas such as Santa Cruz and Watsonville. Poor mortar quality was identified as a factor in many of the failures.

In-plane cracking was common as noted above, but did not appear to result in wall collapses at the intensity of loading experienced in the main commercial districts.

Pounding between buildings caused damage in a number of locations. The worst damage, including partial wall collapse, occurred where the roof or floor levels in the

adjacent buildings did not align, eg. the roof of one building was halfway between the floor and roof levels of the adjacent building.

Failure mechanisms that have been observed in other earthquakes, but which were **observed infrequently or not observed** in the Loma Prieta earthquake were:

- Wall fracture due to bending between diaphragms
- Excessive diaphragm deflections
- Roof and/or floor collapse
- Soft storey or other configuration-induced failures

Statistical evaluations undertaken on the data collected for unstrengthened buildings in San Francisco confirmed that soil conditions had the greatest impact on building damage. Other factors found to affect the level of damage included storey height (in combination with soil condition), occupancy and building age. The influence of soil type and storey height on the estimated average damage ratios of URM buildings in San Francisco is shown in Figure 2.1. Pre-1924 buildings had an average damage ratio about double that of later buildings and assembly/industrial buildings, about three times that of residential buildings. Detailed results are presented by Holmes *et al* (22). However, it is important to recognise that these results are based largely on exterior inspection of the buildings by personnel with widely varying experience. Inclusion of interior wall and partition damage and the relative cost of repairs (including acceptable repair standard) could significantly alter the cost of damage to residential and office buildings relative to industrial buildings.

TABLE 2.1: DAMAGE TO URM BUILDINGS IN THE LOMA PRIETA EARTHQUAKE, 17 OCTOBER 1989

MM Intensity	Total Bldgs	Unstrengthened Buildings				Strengthened Buildings			
		Total	Damaged	Vacated	Demolished	Total	Damaged	Vacated	Demolished
VIII ¹	95	84	74 (88%)	64 (76%)	29 (35%)	11	10 (91%)	7 (64%)	1 (10%)
VII (SF)	2030	1962	721 (37%)	202 (10%)	5 (0.3%)	68	7* (10%)	0	0
VII (Other) ²	246	229	67 (29%)	39 (17%)	11 (5%)	17	4 (24%)	2 (12%)	0
VI ³	137	137	2 (2%)	2 (2%)	0	NA	-	-	-

Data extracted from Table 2 of Holmes *et al*(22). Only includes areas for which "full" data was available for both strengthened and unstrengthened buildings. The "Strengthened Buildings" category includes buildings strengthened to a variety of standards, including many which had been only partially strengthened.

* Table 5 of the same reference indicates that there were 15 buildings with "light" or "moderate" damage (est. 5% & 20% of replacement value respectively), plus a further 18 buildings with "slight" damage (est. 0.5% damage).

1. Los Gatos, Santa Cruz, Watsonville.
2. Campbell, Hollister, Mountain View, Palo Alto, Salinas, Santa Clare County.
3. Fremont, Monterey (City), south San Francisco.

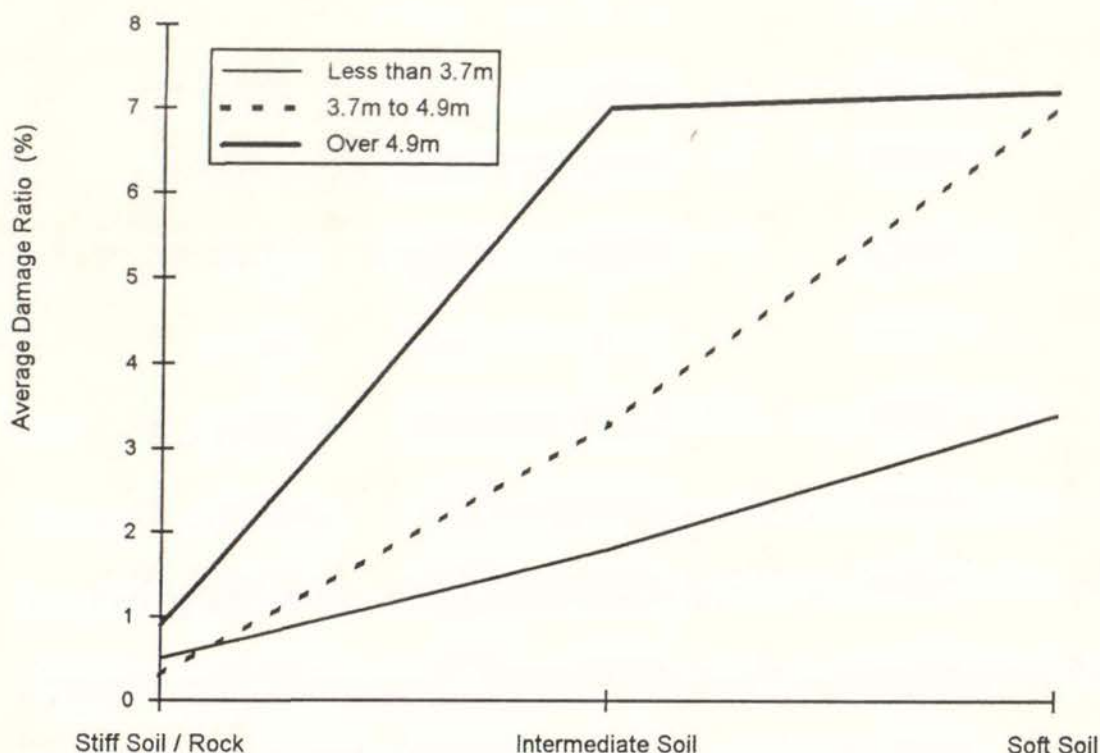


Figure 2.1: Influence of Soil Type and Storey Height on Average Damage Ratio for URM Buildings in San Francisco - 1989 Loma Prieta Earthquake (data from Holmes *et al*)

2.7 Weber Earthquake, East Coast New Zealand, 13 May 1990 (23)

The focus of this M_s 6.5 earthquake was approximately 35 km east of Dannevirke and 17 km deep. The intensity in Dannevirke (population c. 7000) was MM VII. Accelerograph records were obtained from the current Dannevirke Post Office (DPO) at the southern end of the business district, as well as from several more distant locations. The acceleration response spectrum for the N67E component of the DPO record is compared in Figure 2.2 with corresponding spectra for the other records considered. The May earthquake was preceded by a slightly smaller M_s 6.3 earthquake in a similar location three months earlier. The spectral intensities for this earlier event were about 70% of those in the May event. The earlier event caused some minor damage in Dannevirke. Although this contributed to the total insurance cost (some repairs had been undertaken prior to May), it is thought unlikely that the February event significantly affected the amount of damage that occurred in the May earthquake (especially given the past seismic history of the area, as noted below). Fortunately there were no deaths or even serious injuries in the earthquake as it occurred on a Sunday afternoon when almost all businesses were closed.

Construction - Special Features:

Dannevirke has experienced moderate intensity shaking (c.MM VII) several times previously. The most important of these were in 1931 during the M_s 7.8 Hawke's Bay earthquake and in 1934 during the M_s 7.4 Pahiatua earthquake. Both these earthquakes caused as much, if not more damage in Dannevirke than the 1990 earthquake. Following the two earlier events, most of the brick buildings were seismically upgraded to some extent. This commonly included tying walls to floor and roof diaphragms where necessary and/or the removal, replacement or tying of hazards such as parapets and gables. Most wall-diaphragm ties were externally anchored. However in 1990, there were still a few brick buildings without wall-diaphragm ties.

In at least four or five buildings, the ties installed were not anchored to the roof and floor diaphragms themselves, but instead, were carried across the full width of the buildings and anchored at the exterior faces of opposing walls. The tie details used in other buildings are not known. The original floor diaphragms generally had straight T&G floor boards, with plaster ceilings on the underside. Few if any, of these diaphragms were strengthened.

In total there are 40 - 50 URM buildings in Dannevirke, almost all of which are in or near the main business district. All are either 1 or 2 stories high and most have timber floors and roof frames. Mortar quality varies from quite reasonable cement-lime mixes to straight lime mortars that have badly deteriorated and eroded. One damaged building apparently had mortar courses partly filled with old newspaper to stop draughts.

Damage to Brick Buildings:

No formal survey of damage was undertaken for this earthquake but from informal inspection and discussions after the earthquake it was apparent that there was widespread minor cracking and damage, with a comparatively small number of buildings that were more seriously damaged. A lot of the minor damage observed was simply re-opening of existing cracks caused by past earthquakes.

No buildings collapsed and apart from parapets and the free standing rear wall of a makeshift bicycle shelter, no walls or portions of walls collapsed. (The bike shelter wall was the remains of an old brick building that had previously been demolished.)

One building was partly demolished shortly after the earthquake as a safety precaution. Subsequently, a further five URM buildings have been demolished as a result of damage during the earthquake, but it is doubtful that more than one or two of these would have been rated as having more than "moderate" damage based on a "street" level survey of the type conducted in San Francisco after the Loma Prieta earthquake. One of the buildings demolished (a single storey engineering workshop) was one of the few that did not have wall-diaphragm ties. The gable front of this building separated from the roof and bowed outwards, although this was only obvious from inside the building. The two long side walls had significant bows outward at roof level, but it is understood that these probably existed prior to the most recent earthquakes. There were also open cracks in the corner returns at the junctions with the side wall parapets.

The other four buildings that were demolished had cracks in one or more exterior walls and in at least one case, the bricks in one end wall were in a visibly "loosened" state. Undoubtedly there was further damage to the building interiors. The brickwork quality in all four buildings was poor. In addition, the second storey facade of one of the buildings had separated from the side walls during an earlier earthquake and had a slight lean towards the street. This building had steel straps of some age tying the facade back to the sidewalls. However, at least three of the four buildings had externally anchored wall-diaphragm ties and there was no obvious evidence of permanent out-of-plane deformations in any of them due to the recent earthquakes. In all cases, the decision to demolish would have been made after a careful evaluation of the repair costs which would have been affected by the condition and quality of the original structures. All the demolished buildings would have been covered by insurance for at least their indemnity value, with only a minimal deductible.

Cracks spreading from the corners of window and door openings were the most widespread form of damage, but generally these did not open more than a millimetre. In a few instances the cracks were wider and more obvious, particularly where there were other factors such as structural irregularities accentuating local deformations.

As far as is known, only one brick building sustained serious diagonal ("X") cracking. This occurred only in the second storey mullions of the front face of the building, although there was also other damage to the building. The top storey of this building was removed as a safety precaution shortly after the earthquake. The remainder of the building was subsequently demolished, along with the other five buildings noted above. A second building had fine diagonal cracks in the first storey mullions along one wall. However, this was a concrete frame - brick infill building and the mullions that cracked were principally composed of the reinforced concrete columns, with only short "wing" sections on each side that were possibly brick. Part of this building is still in use. Several other buildings had minor diagonal cracks visible in a few locations, but in at least one case these were old cracks that had re-opened.

Broken shop front windows were relatively common and a number of windows set into even reasonably solid walls were broken. In some cases this was despite there being no visible cracks in the walls. These breakages highlight the vulnerability of windows rigidly set in to the walls. In another incident, a large ornamental skylight window fell from the roof of one of the main banks onto the floor of the public area. Other than the broken windows, large open shop fronts at street level do not appear to have caused additional damage in this earthquake.

There is little doubt that the past seismic upgrading significantly reduced the damage that occurred and particularly, the hazards posed by falling masonry. Several parapets did collapse and others were fractured above the top line of anchors. Other than these failures and the damage to the engineering workshop discussed previously, there was very little damage due to out-of-plane wall displacements. As far as is known no gables collapsed, most having been anchored to the roof framing. Also, although there were instances of vertical corner cracks, there was no corner damage of the type that occurred in the Californian earthquakes discussed previously.

There was little evidence of wythe delamination and spalling of the type observed in recent California earthquakes. This discrepancy is unlikely to be related to the

intensity of shaking. The spectrum for the Dannevirke PO record indicates more severe shaking than was recorded at Obregon Park in the Whittier Narrows earthquake, especially for response periods in excess of about 0.4 seconds (Figure 2.2). The duration of strong shaking in the Weber earthquake was also longer, as expected for a larger magnitude earthquake.

Overall, the various seismic strengthening and securing methods used for URM buildings in Dannevirke appear to have been more effective in reducing damage (though possibly not, repair costs) than the c.40% reduction indicated for the MM VII areas in the Loma Prieta earthquake.

2.8 Damage Levels

Damage statistics from the earthquakes reviewed in the preceding sections as well as for several other earthquakes, are collated in Table 2.2. The damage rating scales used in the source references have been retained and no attempt made to rationalise the scales for different earthquakes. Caution is therefore required in interpreting the data. In particular, the lowest damage categories of the Wailes-Horner scale (see notes to Table 2.2) would appear to include buildings with more damage than the first and second categories in most of the other scales. Also, it is important to note that the damage estimates presented have been obtained from a variety of sources and that the experience of the assessors and procedures used vary widely.

Table 2.2 has been subdivided on the basis of MM intensity to provide an indication of damage level versus intensity. To some extent this is incestuous as the MM intensity assignments themselves are to a large extent based on building damage. However, consideration of the earthquake magnitudes and distances, and where available response spectra, suggests that the intensity assignments are approximately consistent. Grouping the data by assigned intensity also provides an indication of inter-event variability in the damage levels arising from differences in construction standards, shaking characteristics, intensity assignments, and the damage estimates themselves.

The majority of the data presented relate to MM VII and MM VIII intensities. The two examples of MM X intensity have been provided largely as a counterpoint to the data for the more moderate shaking intensities.

Ironically the only New Zealand earthquake for which detailed statistics of damage to URM buildings are currently available, is the 1848 Marlborough earthquake which caused considerable damage in Wellington just 8 years after the start of European settlement in the area. Details of the construction of and damage to each building were recorded by Serjeant Miles of the police and later by an examining Board of Damage (24). The data in Table 2.2b is from Miles' summary and covers buildings ranging from private residences to stores, churches, hospital, goal and an army powder magazine. (This last building had 900 mm thick walls plus heavy buttressing, and was one of the few brick buildings only slightly damaged.) At this early stage, construction standards for many of the buildings would have been low. However, it should be noted that the damage in this "event" was the result of three large earthquakes over three days, two of which had magnitudes of M 7 + (one possibly in excess of M7.5) and that the cumulative duration of strong shaking may have been in excess of two

minutes. Considerable additional damage occurred in both succeeding events.

Damage data for the other three New Zealand earthquakes included in the table are mostly qualitative, but nevertheless do contain useable information. The six buildings demolished in Dannevirke (1990 Weber earthquake) needs to be interpreted in the light of comments in Section 2.7. It is doubtful whether any of these would have been rated higher than C on the Wailes-Horner scale.

Whereas in the past a lot of damage was simply plastered over, current legislation and social pressures, usually require a higher standard of repair. Where significant damage has occurred, repaired components will often have to comply with minimum design requirements well in excess of those applying for the original design. Current day standards of finish are also often higher than in the past. Both factors impact on the cost of repair and hence affect the decision on whether to demolish a building. The extent and type of earthquake insurance can also affect this decision, as may the fact that the repaired (URM) building will usually still be deficient relative to current day requirements for new structures.

The San Fernando data in Table 2.2b are for pre 1940 brick buildings in the downtown area of San Fernando (25). The intensity for this area has been interpolated from intensities of MM X and MM VII assigned to adjacent areas (26).

The construction standards for the Tangshan buildings are probably lower than typical in New Zealand, but it is noticeable that the MM VIII losses for this earthquake appear to be lower than those in most of the other earthquakes in Table 2.2b.

The principal comments and conclusions drawn from the data in Table 2.2 are:

- The tabulated data for MM VII and MM VIII indicate a reasonable degree of consistency. The relative damage levels are most apparent from the "No Damage" / "Slight Damage" and the "Collapse" categories.
- The damage levels for MM VII areas are clearly lower than those for MM VIII. Typically no collapses occurred at MM VII as compared with 8% to 45% of brick buildings collapsing at MM VIII. Again at MM VII, c. 50% to 70+% of buildings had slight or no damage as compared with generally less than 20% at MM VIII. Only the Tangshan data deviate from these trends.
- The data indicate that effectively implemented securing, including some wall tying should provide adequate life safety for a design maximum intensity of MM VII. This level of protection may well be sufficient for low seismicity areas such as Auckland.
- A design maximum intensity of MM VIII would probably be more appropriate for moderate seismicity zones in New Zealand and for important buildings in low seismicity zones. The data obtained are not sufficient to assess the effectiveness of current strengthening procedures under this level of loading. Nevertheless it is clear that reasonably comprehensive seismic strengthening would be necessary to minimise the risk of severe damage and collapse at this level of loading. Analytic assessment of the performance of URM walls under this intensity of

loading is discussed in Sections 2.9, 6 & 7, but further evaluation is required.

- Several seismically strengthened multi-storey brick buildings in Tianjin survived MM VIII shaking during the Tangshan earthquake with minimal or no damage (27), but the level and type of strengthening were in excess of the RGA minimum requirements. Similarly, one building in Los Gatos had been retrofitted by guniting the interior faces of the URM walls. This building survived MM VIII shaking in the Loma Prieta earthquake without damage (22). In both this case, and the Tianjin buildings, the strengthening provided intrudes on the building fabric.
- The data for the 1848 Marlborough earthquakes, highlight the progressive nature of damage to URM construction, and the significance of shaking duration. The original eye witness records indicate that the first event (MM VIII) probably caused significantly less than half the eventual damage. Most of the recent earthquakes which have damaged brick buildings in New Zealand and California have had much shorter durations.
- The MM X data clearly indicate that the severity of damage to commercial URM buildings continues to increase significantly at intensities in excess of MM VIII, and that severe damage to this type of construction can be expected in the peak intensity zone of a major earthquake. These data are particularly relevant to high seismicity areas such as Wellington, where there are major active faults in close proximity to the city, compounded by the fact that most of the remaining stock of URM buildings are located on reclaimed land or in other soft soil areas. The Wellington Fault is only 1 - 2 km from most of the brick buildings, and has an estimated effective return period for rupturing of about 300 years.
- The extent of damage in these events, together with analyses undertaken as part of this project (Sections 6 & 7), indicates that the currently favoured retrofit procedures based on the ABK methodology are probably not adequate to ensure reliable performance at this level of loading. Further research into the performance of unreinforced masonry subjected to high intensity loading is required.
- One positive feature of the Hawke's Bay earthquake data is the surprisingly good performance of unreinforced brick dwellings. This result supports the finding by Holmes *et al* (22) that storey height (and presumably horizontal span) was a significant factor in determining damage to URM buildings in the Loma Prieta earthquake.

The preceding discussions have related solely to the performance of URM buildings in earthquakes. However, to provide a benchmark, it is useful to compare the performance of other types of buildings. Two examples are given:

- Timber houses in general, survived both the 1848 Marlborough and the 1931 Hawke's Bay earthquakes with only minor damage other than destruction of brick chimney's and consequential damage due to chimney collapse. At least in the latter event, timber was the most common dwelling material and consequently there were large numbers of this type of building. The main exceptions

(principally in the latter case) were large houses on steep hill sides with different numbers of storeys back and front, houses with inadequate foundation bracing or connections, and houses in areas where there were large permanent ground deformations.

- In Napier and Hastings, there were a small number of substantial, low rise reinforced concrete buildings. These survived the earthquake with only minor cracking, despite having been subjected to loads that were obviously well in excess of current (1992) code requirements.

TABLE 2.2a Damage in Areas of MM VII Intensity Shaking

1942 Wairarapa EQ, NZ (8,9)	No. Bldgs	No Damage	Damaged			Collapse
- Wellington, RC floors	29	62%	38%			-
- Wellington, Ti floors	522	49%	51%			-
1965 Puget Sound EQ, Washington State (29,30)	No. Bldgs	No apparent damage or not readily recognised.	Superficial or light (plaster cracks, etc)	Apparent moderate	Apparent serious or extensive	Collapse
- Seattle (may include all bldgs, not just URM)	1405	67.7%	17.8%	8%	6.5%	-
1976 Tangshan EQ, China (28)	No. Bldgs	Intact	Slight	Medium	Heavy	Collapse
Non-Indust. multi-story	smpl	11%	11%	45%	33%	-
1987 Whittier Narrows EQ, Calif. (17)	No. Bldgs	No Damage	Damaged (incl. Vacated)	Vacated	Collapse	
East LA, LA, Hollywood						
- U/PS Residential	see	47%	53%	5.1%	-	
- U/PS Commercial	Sect.	75%	25%	4.3%	-	
- S Residential	2.5	81%	19%	0.4%	-	
- S Commercial		81%	19%	1.6% ?	-	
1989, Loma Prieta EQ, Calif. (22)	No. Bldgs	No Damage	Damaged, incl. Vacated	Vacated	Demolished	Collapse
- SF, unstrengthened	1962	63%	37%	10%	0.3%	?
- Other MM VII	229	71%	29%	17%	5%	?
- SF, strengthened	68	90% ?	10% ?	-	-	-
- Other MM VII	17	76%	24%	12%	-	-
1990 Weber EQ, NZ (this report)	No. Bldgs	None or Slight Damage		Demolished (see text)	Partial Wall Collapse Below Roof	Collapse
- Dannevirke BD	c. 45	> 50% (probably > 70%)		13%	-	-

LA = Los Angeles

SF = San Francisco

PS = partially strengthened

RC = reinforced concrete

Ti = Timber

S = Strengthened

URM = unreinforced masonry

U = unstrengthened

BD = business district

Refer notes at end of Table 2.2c.

TABLE 2.2b Damage in Areas of MM VIII Intensity Shaking

1848 Marlborough EQ, NZ (24) (refer text)	No. Bldgs	Uninjured	Slightly Damaged	Much Damaged	In Ruins	
- Wellington, Brick	46	9%	9%	41%	41%	
- Wellington, Clay	43	-	4%	26%	70%	
1933 Long Beach EQ, Calif. (11), from (31,32)	No. Bldgs	A (Note 1)	B	C	D	E (Note 6)
- Long Beach	3500	16%	30%	34%	15%	5%
- Compton	?	10%	6%	21%	18%	45%
1971 San Fernando EQ, Calif. (25)	No. Bldgs	No Damage	Slight Damage	Moderate Damage	Severe Damage	
- San Fernando BD	74	14%	34%	34%	19%	
1976 Tangshan EQ, China (28)	No. Bldgs	Intact	Slight	Medium	Heavy	Collapse
Non-Indust. multi-story	smpl	39%	15%	15%	23%	8%
1983 Coaling EQ, Calif. (11)	No. Bldgs	A (Note 1)	B	C	D	E (Collapse)
- Coalinga BD	37	3%	10%	27%	30%	30% (14%)
1989 Loma Prieta EQ, Calif. (22)	No. Bldgs	No Damage	Damaged, incl. Vacated	Vacated	Demolished	Collapse
- Unstrengthened	84	12%	88%	76%	35%	? (several)
- Strengthened	11	9%	91%	64%	10%	- (?)

Refer notes at end of Table 2.2c.

TABLE 2.2c Damage in Areas of MM X Intensity Shaking

1931 Hawke's Bay EQ, NZ (4)	No. Bldgs	No damage or Slight		Moderate	Heavy	Collapse
- 1 & 2 stry dwellings (excl. ground failure)	?	Many		?	?	?
- Commercial 1 -3 stry	>100	Very few		?	Numerous	Numerous
1976 Tangshan EQ, China (28)	No. Bldgs	Intact	Slight	Medium	Heavy	Collapse
Non-Indust. multi-story	smpl	-	-	2%	22%	76%

Notes to Table 2.2:

- The Wailes-Horner damage scale (31) used for two of the Californian earthquakes is as follows: (abbreviated from ref. 11)
 - No damage, plaster cracks or other minor damage not affecting structural safety, including minor parapet and wall corner cracks.
 - Parapets down; extensive interior partition damage; rupture of brick or tile filler or partition walls, requiring minor replacement and extensive plaster repairs; separation of veneers; minor structural damage.
 - Masonry walls ruptured below roof line; failure of structural parts requiring major repairs to or replacement of somewhat less than 50% of exterior walls or framework.
 - More than 50% of wall area requires replacement; extensive damage to interior partitions, floors, foundations, or roof structures; failure of structural frame requiring considerable replacement.
 - Building demolished to an extent making repairs impracticable.
- As far as possible the rating scale terminology used in the source references has been retained. No attempt has been made to rationalise the various rating scales for different earthquakes. Refer source references for details of the rating scales.
- smpl = damage estimates based on a sample of buildings. Size of sample not stated.
- Refer relevant Section 2.1 - 2.7 for details relating to specific earthquakes.
- Except as noted for the Puget Sound earthquake (Table 2.2a), all data are for URM buildings.
- A number of buildings in both Long Beach and Compton collapsed completely.

2.9 Correlation with Recorded Accelerations & Dynamic Analysis Modelling

Acceleration response spectra from four of the earthquakes reviewed in Sections 2.1 - 2.7 are compared in Figure 2.2. Four records are shown from MM VII zones (Obregon Park from the Whittier Narrows earthquake; Holtville PO and Imperial County Services Building FF from the Imperial Valley earthquake; and Dannevirke PO from the Weber earthquake). The fifth record is from an MM VIII zone (Pleasant Valley pumping plant free field record from the Coalinga earthquake). In all cases the spectra shown are the stronger of the two horizontal components of the motion recorded. The 450 year design seismic hazard spectrum specified in the new SANZ Loadings Standard NZS 4203:1992 (33) for the high seismicity zone in central New Zealand, is also shown for comparison.

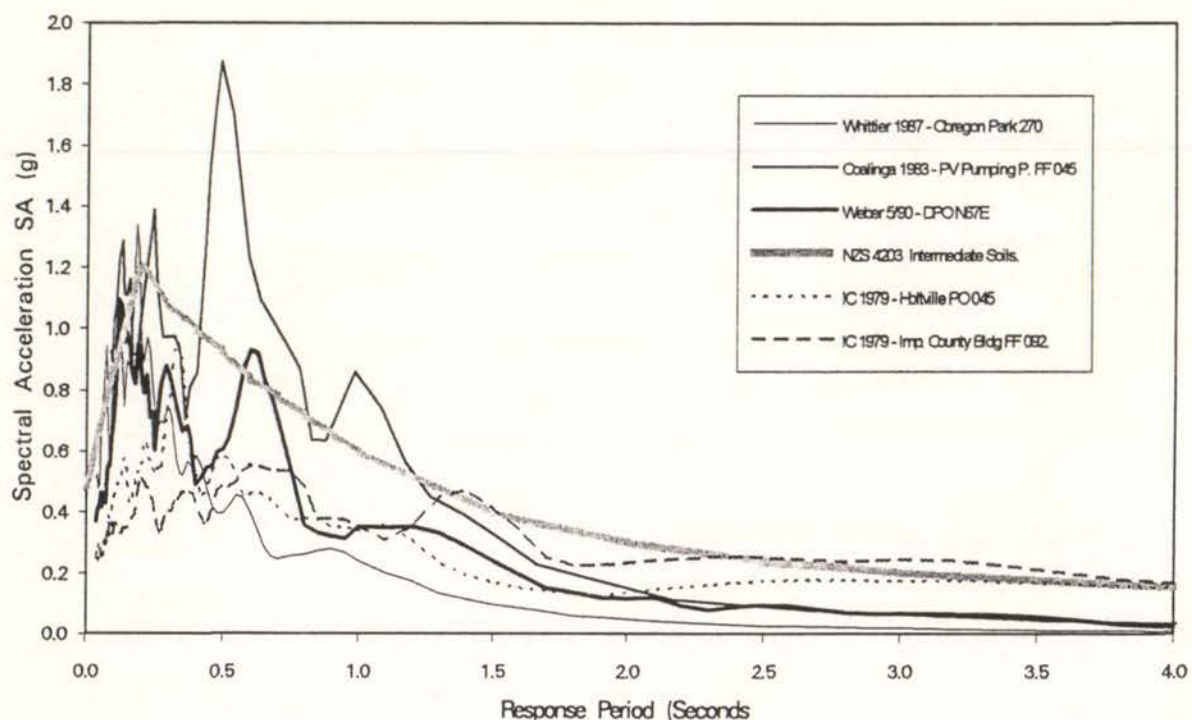


Figure 2.2: Acceleration Response Spectra From MM VII and MM VIII Zones

Although there is inevitable scatter between the MM VII spectra, they nevertheless fall into a reasonably distinct band over the period range 0.4 seconds to 1.3 seconds. The Dannevirke PO record is similar to the Obregon Park record up to 0.4 seconds and is stronger than the other MM VII records over a short period range around 0.6 seconds. The two Imperial Valley earthquake records are weaker for short periods (up to 0.25 seconds - 0.4 seconds) but are significantly stronger than any of the other records for periods in excess of 2 seconds. In the intermediate period range, the spectral intensities for these records are similar to the other two MM VII records. The corresponding spectra (not shown) for the Brawley and Calexico records from the 1979 Imperial Valley earthquake show similar trends.

The spectrum from the Coalinga earthquake (MM VIII zone) is stronger than the other records for almost all periods up to 1.4 seconds and over the period range 0.5 seconds to 1.3 seconds it is about double the average of the MM VII spectra. Beyond a period of 1.4 - 2 seconds, the Coalinga record is significantly weaker than the two Imperial Valley earthquake records shown.

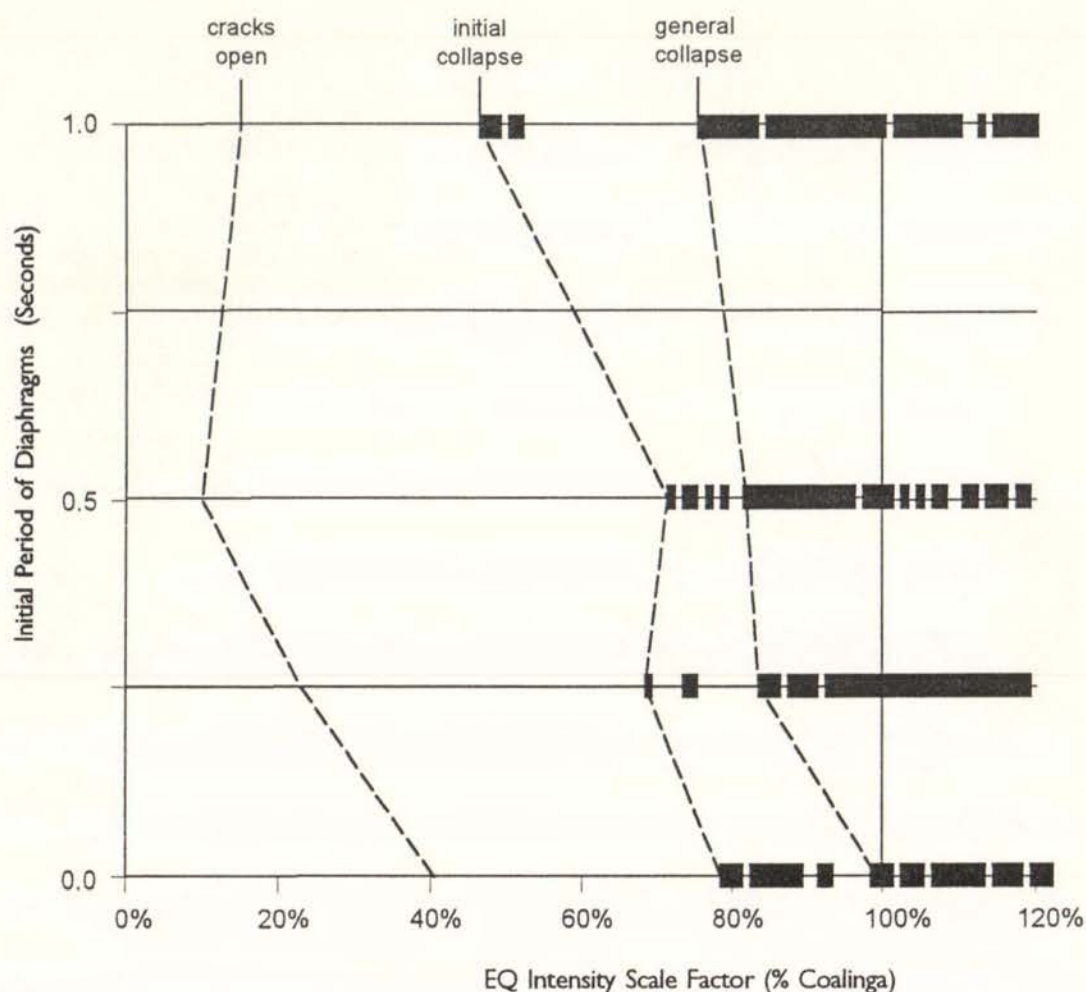
The NZS 4203 hazard spectrum forms an approximate upper bound to the MM VII and MM VIII spectra in Figure 2.2, except over the 0.4 second - 1.2 second range where it is generally lower than the MM VIII Coalinga spectrum. The MM VII spectra are typically 50% - 80% of the code values over this range. The code spectrum for flexible/deep soils would normally be more appropriate for comparison with the Coalinga record (refer Section 2.4). However, the intention in this case is mainly to assess the design spectrum in terms of the intensity of shaking likely to cause URM buildings to collapse, as indicated by historical performance rather than analytic assessment.

Too few spectra have been obtained from sites that can be correlated with URM damage to draw definite conclusions. Nevertheless, the relative intensities of the historic spectra in Figure 2.2 are consistent with the assigned MM intensities and particularly with the significantly greater damage that occurred in Coalinga relative to the other areas. Coalinga was the only one of these events where URM buildings collapsed. The relatively light damage to URM buildings in the Imperial Valley earthquake can in part be explained by the quality of construction. However, the moderate intensity of the short period shaking experienced in areas where the URM buildings were located was also a factor, and is presumably the reason that in-plane cracking damage was infrequently observed.

Including a larger number of earthquake spectra would undoubtedly result in a more uniform spread of spectral intensities, but the general trends are expected to be similar to those in the above comparisons.

To further investigate expected damage levels due to face loading, a limited series of inelastic dynamic analyses were performed for three of the records in Figure 2.2. The wall element modelled in these analyses is described in Section 6.2 (full scale element, 3 wythes thick by 4.8 m high, ie. $h/t \approx 14$). Analyses were carried out for a range of diaphragm response periods. In each case the load intensity (fraction of the acceleration record) was increased in small steps until general collapse occurred due to face load instability. All analyses were carried out using the DRAIN 2DX program (34) with comparatively low damping in the diaphragms. Modelled collapse of the wall element occurred when the maximum out-of-plane deflection of the wall relative to the top and bottom diaphragms exceeded a critical value (approximately the wall thickness) at which the wall became unstable under gravity loading. Further details of the analysis procedure and model are described in Sections 6 & 7.

Results of the analyses for the Coalinga earthquake record (free field record from the Pleasant Valley pumping plant) are illustrated in Figure 2.3. Initial collapse of the modelled wall element occurred at a load intensity of between 0.47 and 0.79 times the Coalinga record, and general collapse at between 0.75 and 0.99 times the Coalinga record. Lower failure loads would be obtained for a two wythe wall with the same height/thickness (h/t) ratio. In practice, the capacity of many walls would be higher



- Note:
- "Initial collapse" is the lowest load at which collapse occurred in the analyses.
 - "General collapse" is the load above which collapse generally occurred. Above this limit, the wall is only "stable" over load ranges of 2% or less of the full earthquake record. Some of the stable responses at high load intensities may be due to the top and bottom diaphragms responding out of phase with each other in the analyses.
 - Heavy black line shows ranges of EQ intensities over which the wall element collapses.

Over critical ranges of load intensity, analyses were carried out for 1% increments in the acceleration record, generally up to a maximum intensity of 1.2 times the Coalinga record.

Between the "initial" and "general" collapse loads, the wall is in a state of what might be termed "marginal stability". Over this range, the wall collapses at some load intensities but may be stable at other higher intensities. Whether the wall collapses or not depends on the relative phase between the earthquake loading and the wall response, i.e. on the displacement of the wall at the time that each large pulse in the earthquake motion is imposed. Below the initial collapse load, an increase in the intensity of loading is required to induce collapse.

Figure 2.3: Dynamic Stability of Face Load Wall Element Subjected to the N45E Component Pleasant Valley Pumping Plant FF Record from the 1983 Coalinga Earthquake

than modelled because of nonlinear diaphragm response, the support provided by end walls and cross walls, higher damping and other factors. However, the modelled element does approximately represent the situation at the centre of some diaphragms, especially for sections of wall with large window openings on either side. Even if these walls had 20% - 30% greater capacity than modelled, the results indicate that the earthquake loading was probably sufficiently strong to have caused some of the walls to collapse under face loading, without the diaphragm anchorages having to fail first.

By contrast, analyses of the same wall element model for the MM VII intensity zone acceleration records from Dannevirke PO (1990 Weber EQ) and Obregon Park (1987 Whittier Narrows EQ) yield initial collapse loads of c.1.5 and 2.3 times the respective earthquake records. That is, earthquake loads significantly in excess of those recorded are required to cause face load collapse if the walls are adequately anchored to the top and bottom diaphragms and the brickwork integrity is maintained (eg. no wythe delamination).

Results from these analyses and the comparisons of the spectra in Figure 2.2, suggest that the level of damage due to walls bowing out-of-plane between diaphragm levels is principally dependant on the strength of shaking in the intermediate period range (c. 0.4 - 1.3 seconds ?). Strong long period shaking such as that recorded in the 1979 Imperial Valley earthquake, appears to be less important as a cause of significant damage to typical URM commercial buildings. Both the analysis results, and the recorded spectra, are consistent with the observed extent of damage in the respective events.

One further point noted in relation to Figure 2.3 is that even for the Coalinga record, the flexible diaphragms had only a relatively moderate effect on the intensity of shaking required to cause face load collapse. This record is very strong in the 0.5 - 1.2 second period range (Figure 2.2). The magnitude of this effect is less than indicated in the ABK methodology (38), but further investigation is required to verify this result as the element model used did not constrain the top and bottom of the walls to have identical displacements. The diaphragms did significantly amplify the elastic response, as indicated by the fact that the first cracks in the walls opened at a much lower intensity of loading in the analyses with flexible diaphragms (as would be expected). For the Obregon Park record, which is relatively weak for periods above 0.4 seconds, both the 0.5 and 1.0 second diaphragms increased the predicted collapse load of the face loaded wall element (results not shown).

2.10 Summary of Failure Modes & Implications for Assessing Vulnerability

The following is a summary of the principal modes of failure and factors affecting the performance of unreinforced masonry buildings in earthquakes. Where appropriate, modifications to existing design procedures or requirements are suggested.

2.10.1 Out-of-plane wall failures

Wall failures are usually classified according to whether they result from either in-plane or out-of-plane loading. Cracking and more substantial damage due to out-of-plane loading has been observed frequently, even in moderate magnitude earthquakes.

No total collapses of buildings were reported in the MM VII intensity zones of the earthquakes reviewed, but there were a number of out-of-plane collapses or partial collapses of walls. Other walls cracked or bowed outwards under face loading. These failures were largely confined to single storey walls or the top storeys of higher buildings. In most cases, the tops of the walls displaced outwards at roof level due to anchorage failure, lack of anchors or flexibility of the roof diaphragm. These failure modes are discussed separately in following subsections.

Where walls have been adequately supported top and bottom, there appear to have been very few instances of out-of-plane damage due to walls bowing outwards between diaphragm levels in zones of MM VII intensity shaking. The main exceptions to this have been where wythe delamination and spalling has occurred (eg. 1987 Whittier Narrows EQ) or where walls have been only one wythe thick (eg. 1989 Newcastle, Australia EQ). The behaviour of buildings in Dannevirke (1990 Weber earthquake) and in the 1979 Imperial Valley earthquake indicates that damage due to out-of-plane loading in MM VII zones can be greatly reduced if walls are adequately tied to floor and roof diaphragms. This behaviour is consistent with results obtained from dynamic analyses of walls subjected to earthquake accelerations recorded in the MM VII intensity zones (Section 2.9).

Between 8% and 40% of URM buildings in the MM VIII zones collapsed or were "in ruins". Out-of-plane deformations were the most prevalent cause of major structural damage in the MM VIII zones of the Coalinga and Loma Prieta earthquakes and in a number of cases resulted in building collapse. Anchorage failure or lack of anchors were believed to be the most common cause of wall failure at this intensity of shaking. However, it is possible that a number of the collapses were a result of excessive out-of-plane displacements of walls spanning between the floor and roof diaphragms. In a number of cases, through-wall diaphragm anchorages remained in place after the walls had collapsed and it was noted that it was very difficult to determine the initial failure mechanism from the wall remnants.

Analyses of the face load response of a wall element subjected to MM VIII intensity shaking were undertaken in this project using the Coalinga earthquake record from the Pleasant Valley pumping station (Section 2.9). The results of these analyses indicate that in some instances face load collapses due to out-of-plane wall displacements between diaphragm levels could be expected at only 80%, and possibly as low as 50% of the Coalinga record. These results suggest that the extent of damage to URM buildings in Coalinga (MM VIII) can be explained by the intensity of the shaking, regardless of the brickwork quality. Although further investigation is required, the results obtained indicate that many commercial and industrial URM buildings may be particularly vulnerable to earthquake motions rich in 0.5 sec - 1.2 sec period shaking. Strong amplification of shaking over at least part of this period range can be expected on reclaimed land in Wellington City (7) and in some other soft soil areas.

Damage to commercial and industrial URM buildings in the MM X zones of the 1931 Hawke's Bay and 1976 Tangshan earthquakes was severe, with three quarters of non-industrial multistorey brick buildings collapsing in the latter case. However the reported survival of many URM dwellings in Napier with only slight damage (other than to chimneys), indicates that adequately supported walls can survive even this intensity of earthquake loading.

One feature of damage to URM walls in earthquakes that appears to be almost universal, but is rarely if ever commented on, is that the debris from collapsed exterior walls invariably ends up on the outside of buildings. It is probably "obvious" that this should occur, but it does imply that the face load response is not symmetrical as is normally assumed in dynamic analyses of walls. Inwards displacement of walls is impeded by the physical depth of floor and roof diaphragms and when present, by cross walls. These factors tend to mitigate against wall flexural failure modes involving an increase in the amplitude of displacements over several cycles.

2.10.2 In-plane wall failures

The main types of in-plane cracking reported at moderate-strong shaking intensities (MM VII & VIII) were:

- Cracks at the corner of openings
- Vertical and "X" cracking in spandrel beams
- "X" cracking in piers and walls, and
- Horizontal cracking at the tops and bottoms of piers.

These types of cracking were common in most areas of moderate-strong shaking intensity, with a notable exception being the 1979 Imperial Valley earthquake (discussed in Section 2.9). Arched lintels have also proved to be a weakness in many earthquakes, especially for window openings near the ends of a wall where there is insufficient restraint to prevent the arch footings from spreading under lateral loading.

Diagonal "X" cracking in piers and walls can occur in both the upper and lower storeys of buildings. These cracks do have a certain amount of post-crack displacement capacity and do not appear to have been responsible for collapse in any of the moderate-strong shaking intensity areas reviewed. Even in Coalinga, it was noted that the vertical load capacity of all piers with in-plane shear displacements was retained, and that "the risk posed to life safety by the in-plane cracking was minimal or nil" (12).

Diagonal cracking of walls and piers have, however, been a serious cause of failure and collapse in the more intensely shaken areas of large earthquakes. In Tangshan, hundreds of multistorey brick buildings were reported to have collapsed mainly as a result of shear failures in load bearing walls (28). Extensive brittle in-plane shear failures also occurred in the 1990 Manjil, Iran earthquake (35) and in the Hawke's Bay earthquake, "racking effects" on piers and walls were noted as one of the factors "responsible for much of the damage" (4).

In-plane rocking or sliding on horizontal flexural cracks at the top and bottom of mullions can be an effective means of absorbing earthquake deformations and at the same time, limit the forces generated within a building.

Some concerns have been expressed about potential collapse resulting from progressive splitting and crushing of the corner compression blocks of rocking piers. This type of failure was common in slender walls, piers and columns in the 1990 Manjil earthquake in Iran (35). A further problem can occur at the ends of walls. When the outside toe of the end pier is in compression, the shear and axial forces from the pier have to be resisted by a short length of brickwork at the end of the wall. This can result in an

inclined fracture in the brickwork under the pier, leaving a small triangular section of wall supporting the pier compression block. This type of cracking was not specifically noted in the damage reports reviewed, but it has been evident in a number of other moderate earthquakes, eg. Newcastle (36). Failure of the compression zone support at the ends of the walls can be prevented by installing drag bars to distribute the shear forces from the end piers further into the wall.

Where rocking is relied on in a retrofit, the piers in any line should preferably have similar dimensions and strengths. If the strengths or dimensions vary significantly, the stiffest piers can attract a disproportionate share of the loads and fail in unexpected or less desirable modes.

2.10.3 Anchorage failures

Anchorage failure, or lack of anchors, has been the most frequent cause of wall and gable collapse in moderate earthquakes in California and New Zealand. In the majority of cases, the failures occurred at or near the tops of the walls where there is little overburden. Most of the failures were within the brickwork, rather than at the diaphragm end. At higher load intensities, progressive anchorage failure can occur at lower floor levels due to the removal of overburden following collapse of the upper storey walls.

The "Government" anchors used in California have generally proved ineffective in lime mortars, even though the ends are well set into the brickwork with a vertical rod engaging the brick courses above and below the anchor line. There have also been many instances where externally anchored diaphragm ties have pulled through brickwork. In almost all instances, these failures occurred in brickwork with deteriorated or poor quality lime mortar. Some of the anchorage failures may have been precipitated by parapet collapse, but in other cases the walls appeared to have disintegrated around the anchors. In some cases, this may have been due to the wall collapsing from under the anchors.

In several buildings in Santa Cruz (1989 Loma Prieta earthquake), anchorages failed by tearing out part of the diaphragms. Similar types of failure have occurred in new tilt-up concrete buildings in the past (eg. 1971 San Fernando earthquake). These failures indicate that if brickwork anchorage details are strengthened, more failures may occur within the diaphragms. The adequacy of design procedures for diaphragm connections needs to be reviewed.

As noted in Section 2.7, at least some of the ties used in Dannevirke were not anchored in the diaphragms but instead, were carried across the full width of the building and anchored at the exterior faces of opposing walls. These ties were installed in the early 1930's, generally without any strengthening of the diaphragms. Both anchorages and diaphragms performed well in the 1990 Weber earthquake.

In the Whittier Narrows earthquake, full length out-of-plane "shear" failures were discovered just below the top line of anchors in three walls. The lower section of these walls had displaced outwards by up to c.50 mm. While these were the only such reports found in the literature, it is possible that this type of failure has occurred more frequently as it is often impossible to identify the initial cause of failure once a wall or

part of a wall has collapsed.

Mortar quality and "overburden" are clearly important to achieving anchorage in brickwork. Where there is a strong cement or lime-cement mortar with good bond to the bricks, a simple through-wall anchoring detail is probably adequate. However, where the integrity of the brickwork under earthquake loading is uncertain, further measures are necessary. Possible options include repointing walls and retaining parapets (braced) to provide overburden, or for more reliability, centre core reinforcing the top of the wall to 1 m - 1.5 m below the roof diaphragm anchors (in conjunction with repointing, if necessary).

This issue is fundamental to the success of a "minimum interference" seismic retrofit and there is a need for more tightly specified design requirements in this area. Some details currently being used are not providing adequate protection against wall collapse.

2.10.4 Diaphragm flexibility and strength

The effect of diaphragm flexibility on the performance of URM buildings is complex and not well understood. The main concern is the effect on wall damage. No incidence of gross diaphragm failure was found in the damage reports for any moderate intensity earthquake.

Diaphragm flexibility appeared to cause little damage in Dannevirke but much of the wall distress in theatre and similar large barn-like buildings in Wellington in the 1942 earthquakes was a result of excessive deflection of the roof diaphragms. Diaphragm flexibility was also suggested as a possible cause of wall damage in several of the Californian earthquakes. In other cases, it has been suggested that over strengthening diaphragms increased the amount of damage because the reduced diaphragm period resulted in higher amplification of the earthquake accelerations.

Limited analyses of the influence of diaphragm flexibility have been undertaken in this project (Section 7), but further investigation is required. This should include consideration of the characteristics and intensity of earthquake shaking expected in different areas. However, for the majority of typical commercial URM buildings similar to those in Dannevirke, specific strengthening of floor diaphragms should not be necessary for design intensities of MM VIII or less, providing that there are adequate cross walls and no large openings or other weaknesses in the floors.

2.10.5 Corner damage

Corner damage was reported in several of the earthquakes and included vertical cracks at the junctions between walls and collapse of a section of wall adjacent to an upper corner. In some cases the vertical corner cracks were diverted to nearby window openings. Similar cracks occurred at junctions with internal cross walls and partitions (4,9,28).

Vertical cracks at the wall corners and junctions result in separation of the exterior walls and hence significantly increase their vulnerability to face loading. Wall collapses were attributed to this cause in both the Hawke's Bay (4) and Tangshan (28)

earthquakes. This type of cracking has been attributed to poor bonding at the wall junctions and/or, in the case of corner cracks, to opening and closing bending moments induced in the brickwork by excessive distortion of floor and roof diaphragms. However, fine vertical cracks can be found at the corners of many multistorey URM buildings in Australia which have never been subjected to significant earthquake loading. The causes and significance of corner cracks need further investigation. To survive shaking of the intensity experienced in the Hawke's Bay and Tangshan earthquakes may require wall junctions to be mechanically anchored, especially if the brickwork quality is deficient.

Collapse of sections of wall adjacent to the upper corners of URM buildings has been reported in several Californian earthquakes. This type of damage highlights the need to provide effective transfer of in-plane diaphragm forces into the end walls and to minimise shear sliding between the elements. A number of suitable details have been developed. Performance requirements and/or design guidance should be provided.

2.10.6 Interior partition walls

Interior masonry partitions are particularly vulnerable in earthquakes as they are often only one wythe thick and normally have no overburden other than their own self weight. Both in-plane and out-of-plane damage are common. Inadequate tying of partitions to exterior walls was also suggested as a problem in some of the damage reports.

There have been many instances where buildings have lost all external bricks walls during an earthquake, but the floors and particularly roofs have been prevented from collapsing by the internal timber frame partitions. This occurred even at the severe shaking intensities experienced in the 1931 Hawke's Bay earthquake. It is not possible to rule out the possibility that the partitions actually contributed to the wall collapses, eg. by removing much of the overburden from the tops of the brick walls. However, tying exterior walls to the timber partitions would almost certainly have reduced the risk of collapse by improving the overall wall-structure anchorage and by helping to restrain the walls from bowing outwards between diaphragm levels.

2.10.7 Parapet and non-parapet falling hazards

Parapets and gables have long been recognised as a serious threat to life in earthquakes and some of the earliest seismic retrofit regulations were directed at securing these hazards. Other potentially lethal falling hazards include veneers with inadequate or corroded ties and insecure ornamentation. Parapet collapses occurred in all the earthquakes reviewed and were responsible for loss of life in at least two of them. In addition considerable material damage, including building collapse, has been caused by heavy units of masonry falling on adjacent buildings or on lower parts of the same structure.

Observations from several earthquakes suggest that unsecured gables are even more vulnerable than parapets, probably because of impact from the roof structure. This was particularly noticeable in the 1989 Newcastle, Australia earthquake (36). In a number of instances gables collapsed while parapets and even chimneys with badly eroded mortar on the same buildings were undamaged.

2.10.8 Pounding damage

Pounding between buildings caused partial wall collapses in both San Francisco and Santa Cruz during the Loma Prieta earthquake and considerable damage during the Hawke's Bay earthquake. Similar pounding damage has occurred in other earthquakes. Pounding has the potential to cause collapse in situations where the floors and roofs of the adjacent buildings are misaligned, particularly if there is a strong lower building abutting a taller building with masonry bearing walls or columns.

There are limited remedial options for reducing potential damage from pounding between two existing buildings, but in particularly adverse situations some form of mitigation would need to be undertaken as a part of any retrofit scheme.

2.10.9 Foundation failures / permanent ground deformations

Foundation failures and permanent ground deformations do not appear to have contributed significantly to URM damage in any of the MM VII - MM VIII intensity zones reviewed, but foundation failure may need to be considered where soils are particularly prone to liquefaction .

Foundation soils failure can however be a significant factor in weak soil areas at higher shaking intensities, as evident in the Hawke's Bay earthquake. Damage levels were noted to be significantly higher in areas where ground failure occurred (although at this intensity of loading, catastrophic collapses also occurred in firm ground areas). Rotation and displacement of a foundation markedly increase the vulnerability of unreinforced masonry walls in an earthquake.

The importance of strong foundations and adequately tying building footings together in areas susceptible to ground failure were emphasised by Brodie & Harris (4) in their report on damage in the Hawke's Bay earthquake. Specific provisions to address these problems should be considered when retrofitting buildings located on vulnerable soils. This would include a number of areas in Wellington and Lower Hutt.

2.10.10 Configuration induced failures

The San Francisco damage data evaluated by Holmes *et al* (22) after the Loma Prieta earthquake indicate that square shaped buildings, with or without re-entrant notches, have a lower susceptibility to earthquake damage than either irregular or rectangular buildings. The differences in the sample average damage ratios were in the order of 40%. Insufficient data are available to assess the effect of configuration for moderate and strong (VII & VIII) intensity areas in the other earthquakes reviewed. Usually, it was not raised as an issue.

Severe damage and collapse were too general, and insufficient detail recorded to evaluate the importance of configuration in the MM X zones for the earthquakes reviewed. The three storey Nurses Home in Napier was located on firm ground and collapsed catastrophically. This building had an irregular plan layout, but the evidence is insufficient to attribute configuration as a factor in this collapse or in the collapse of

other buildings.

In moderate and strong intensity zones, open shop fronts do not appear to have exacerbated damage other than window breakage. In some areas, buildings with soft bottom storeys sustained less damage than nearby stiffer buildings. However, in comments on buildings with reinforced concrete frames, Brodie and Harris (4) noted that "the disastrous result" of sacrificing lateral rigidity in the front of shops "was well illustrated in many shops" in the 1931 Hawke's Bay earthquake.

2.10.11 Soft soil amplification

The effects of soft soils on earthquake shaking characteristics and intensities have been intensively investigated in recent years and understanding of the phenomenon has advanced considerably.

In practice, the fact that building damage can be much higher in soft soil areas has long been recognised. These effects were specifically noted in contemporary reports on damage in Wellington in 1848, 1855, and 1942, and have been similarly reported for many other historic earthquakes (including the Hawke's Bay earthquake, and in Wanganui). Unreinforced masonry is particularly vulnerable to soil amplification effects. In the Loma Prieta earthquake the increase in damage to URM buildings in San Francisco due to soft soils, was up to a factor of ten (Figure 2.1).

It has been argued that effects of soft soils are most pronounced for moderate shaking intensities resulting from larger distant earthquakes, and that the effect on the severity of shaking would be much less at high shaking intensities. The historical evidence suggests otherwise, at least in terms of damage potential. Buildings located on soft soils in areas of general MM X shaking were reported to have sustained much greater damage in both the 1855 Wairarapa and 1931 Hawke's Bay earthquakes.

2.10.12 Brickwork and mortar quality

Poor mortar quality, particularly deteriorated and/or eroded lime mortars, have almost universally been noted as significant contributory factors in earthquake damage to URM buildings. Mortar quality is particularly important in the upper part of walls and for roof anchors where there is little overburden to resist the high out-of-plane loads that are imposed. City of Los Angeles requirements for mortar testing in the upper parts of walls have been significantly tightened following surveys of buildings damaged in the Whittier Narrows earthquake (37).

Similar tightening of provisions for mortar testing needs to be considered in New Zealand.

2.10.13 Age of construction

A common observation after recent earthquakes has been that newer buildings designed to modern day standards performed much better than older types of construction. This type of statement is often directed at "old" buildings constructed in the 1930's and earlier. However almost identical statements were made shortly after the 1931 Hawke's Bay earthquake. Some of the new buildings referred to are now

considered old and beyond redemption. The implication of this is that age *per se*, not just date of construction, is an important factor even for purportedly permanent building materials. As noted previously lime mortars can deteriorate badly and both the brick and mortar can be eroded by the weather. The effects of deterioration with age were particularly evident after the 1989 Newcastle earthquake in Australia . In many walls, metal veneer ties had completely corroded through, leaving veneers two and three storeys high without lateral support. Many of these veneers collapsed. In most cases the ties had corroded just within the mortar at the cavity face of the veneer. Well planned exploratory investigations are needed to determine the extent of this type of deterioration.

2.10.14 Windows

Both large shop front windows and smaller windows set into masonry walls have commonly been broken in earthquakes. Failure of the smaller windows is principally due to the rigid window settings used in the original construction. Provided that there is not a significant life risk, it would not normally be cost effective to replace window frames, except as part of a planned refurbishment.

3 NATURE OF NEW ZEALAND'S UNREINFORCED MASONRY BUILDING STOCK

3.1 Introduction

A number of Local Authorities in New Zealand have surveyed the unreinforced masonry buildings in their jurisdictions and listed the buildings that are considered to be earthquake risks in terms of Section 624 of the Local Government Act, 1979.

Details of surveyed buildings were obtained for Wellington City, the Petone suburb of Lower Hutt City and the Nelson Central Business District.

Although not typical, these locations were assumed to be representative of a main city, a suburban shopping district and a provincial city respectively.

3.2 Earthquake Risk Buildings In Wellington City

The list of Wellington City buildings identified as earthquake risks in terms of the Local Government Act, was sorted to identify the number of buildings with 1,2,3 or more storeys. Results are shown in Figure 3.1

All the buildings were principally of brick construction and the list obtained was last updated in May 1988. The number of storeys in the buildings includes basements but excludes mezzanines and penthouses. Some of the buildings on the list have been strengthened and the number of storeys for 23 additional buildings were not identified and have not been included.

3.3 Earthquake Risk Buildings In Petone and Nelson City

Figure 3.2 shows the frequency distributions of the earthquake risk buildings in Petone and Nelson when classified according to number of storeys.

The number of storeys for a significant proportion of the Petone buildings was not available. However, these were mainly small single storey buildings. These buildings have been included in the total number of single storey buildings shown but have been identified separately.

For Nelson City only the 42 buildings still requiring further work are included in Figure 3.2(b).

In the early 1980's 92 buildings in Nelson's Central Business District were identified as potential earthquake risks.

On closer examination it was found that 11 of the buildings did not come within the Act and (as at the 21.01.91) 29 have been demolished. A further 22 have either been strengthened (6), secured (14) or have had local hazards removed (2). Five buildings are yet to be inspected and classified. Of the 42 remaining buildings 13 only require attention to a brickwall to meet the Local Body Act's requirements. These buildings have been separately identified in Figure 3.2.(b).

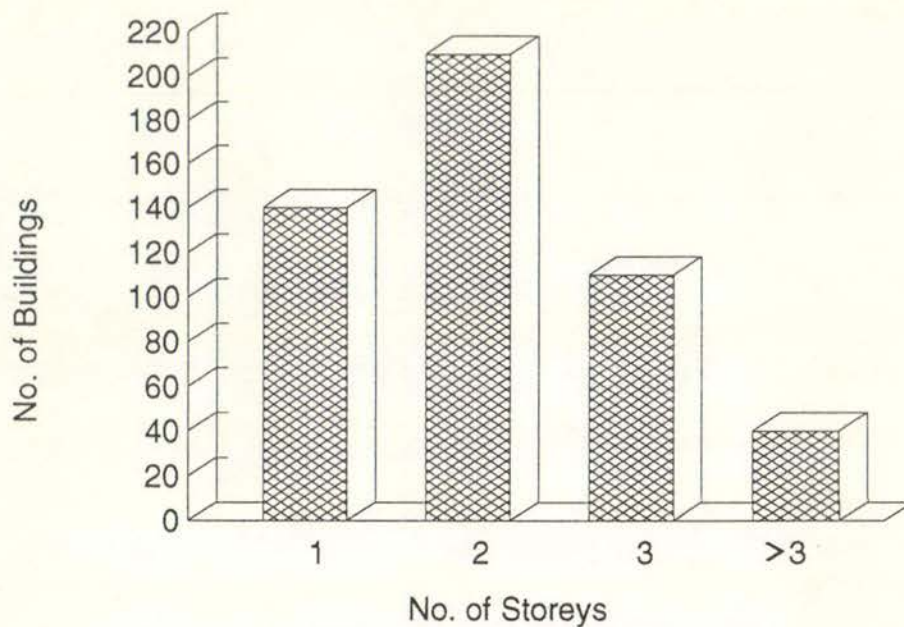


Figure 3.1 Earthquake Risk Buildings in Wellington City Classified According to Number of Storeys

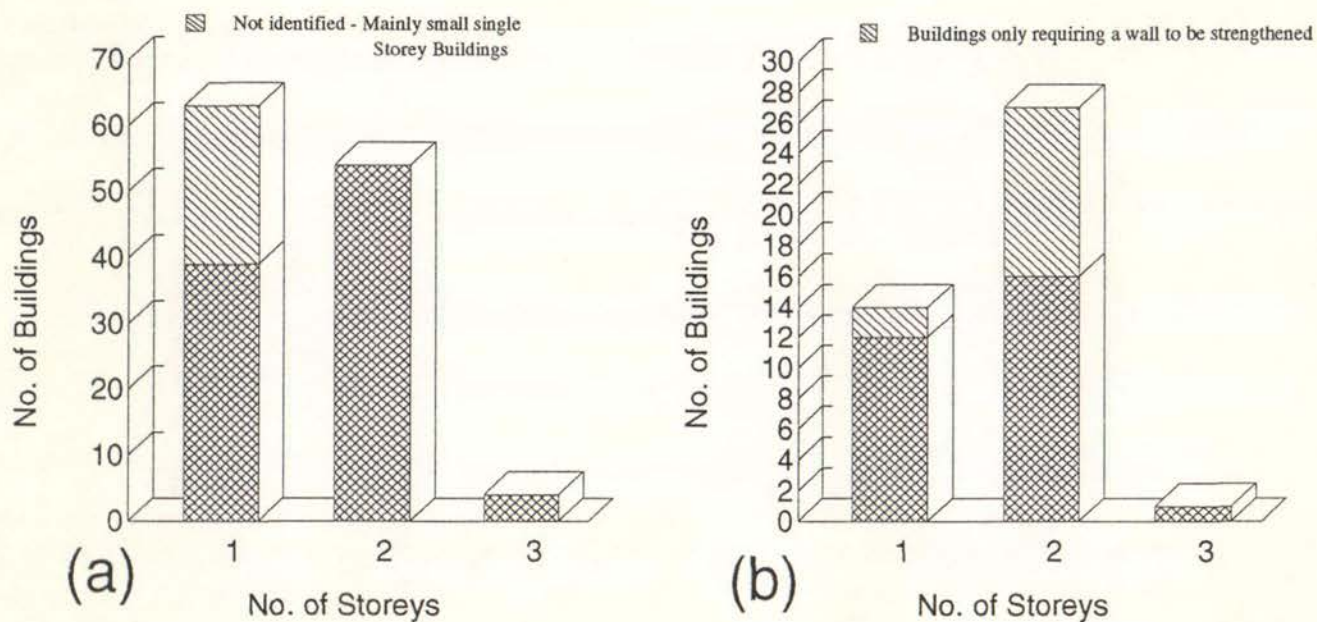


Figure 3.2 Earthquake Risk Buildings, Classified According to Number of Storeys in:

- the Petone suburb of Lower Hutt City
- Nelson City Central Business District (requiring further work as at 21.01.91)

It is evident from Figures 3.1 and 3.2 that the bulk of New Zealand's earthquake risk building stock will have 1 or 2 storeys.

Consequently this project will be directed primarily at 1 and 2 storey buildings although it should be noted that the buildings with 3 or more storeys will generally be larger so that Figures 3.1 and 3.2 will tend to under estimate their relative importance.

It may be concluded that New Zealand's URM building research effort should be directed towards buildings having 3 or less storeys.

4 PREVIOUS RESEARCH

4.1 Introduction

When traditional methods of structural analysis are used to assess URM buildings they often result in an unrealistic assessment of seismic risk. Many engineers assume that the building is uncracked and try to assess seismic risk by evaluating the earthquake intensity required to cause cracking. However, the tensile strength of masonry is highly variable and URM buildings are often already cracked due to stresses induced by settlement, or temperature and moisture changes. They may also have been cracked in previous earthquakes.

It has also been observed that many masonry buildings that are severely cracked are often still standing after earthquakes and that they are still able to resist strong aftershocks.

These observations have led researchers to investigate the post-cracking seismic resistance of URM buildings.

4.2 Research Carried out by the ABK Joint Venture

In the early 1980's a consortium of Californian engineers called the ABK Joint Venture (ABK), carried out pioneering research into the post-cracking behaviour of URM. This research led to the development of a new methodology for assessing the seismic risk associated with a URM building (38 h).

The methodology developed by ABK was based on the results obtained from tests on full scale test specimens representing wall and diaphragm elements found in URM buildings.

Initially tests were carried out on 18 x 6m diaphragms that represented the various types of roof and floor diaphragms found in URM buildings in California. Results of these test were used to calibrate a nonlinear diaphragm computer model (38 (c)).

The diaphragm computer model was then used to produce representative diaphragm displacement time histories that could be used in the testing of full scale face loaded wall test specimens.

The face loaded wall specimens tested by ABK, represented a section of URM wall spanning between two diaphragms. To test the specimens, earthquake motions derived from the diaphragm computer model were imposed on the wall at the levels of the top and bottom diaphragms.

ABK found that a single horizontal crack tended to form near mid-height of the test specimens and another crack formed near its base. During the test these cracks opened up and allowed the centre of the wall to undergo large displacements. This ability to withstand large displacements without collapse resulted in the walls having a significant post cracking seismic resistance. ABK used the term "dynamic stability" to distinguish this type of behaviour from the behaviour that might have been expected from static force calculations.

ABK concluded from their test results that the collapse of unreinforced face loaded walls under seismic loading would be dependant on the kinetic energy imparted to the mid-storey area of the wall mass. They hypothesised that the kinetic energy transmitted to the wall during an earthquake would be dependant on the peak velocities of the motions that the diaphragms imposed on the wall.

4.3 The ABK Methodology

ABK found that 3 parameters had a significant effect on the stability of their face loaded wall test specimens. The relationship between these three parameters is shown in Figure 4.1 (a). The parameter that ABK used as a measure of earthquake intensity is the square root of the sum of the squared velocities at the top and bottom of a wall element. (SRSS velocity). The other two parameters were the slenderness ratio of the wall elements ($=H/t$ where H is the wall element height and t is its thickness), and the overburden to weight ratio ($=O/W$, where O is the overburden load representing the weight of a parapet or any upper storey and W is the weight of the wall element being considered).

Figure 4.1(a) can be used to assess the seismic resistance of a face loaded wall element spanning between diaphragm supports (or the ground and a diaphragm) if the peak velocities of the earthquake motions imposed by the diaphragms are known.

ABK also concluded that diaphragms would amplify the peak ground velocity and that the amount of amplification would be dependent on the strength and stiffness of the diaphragms.

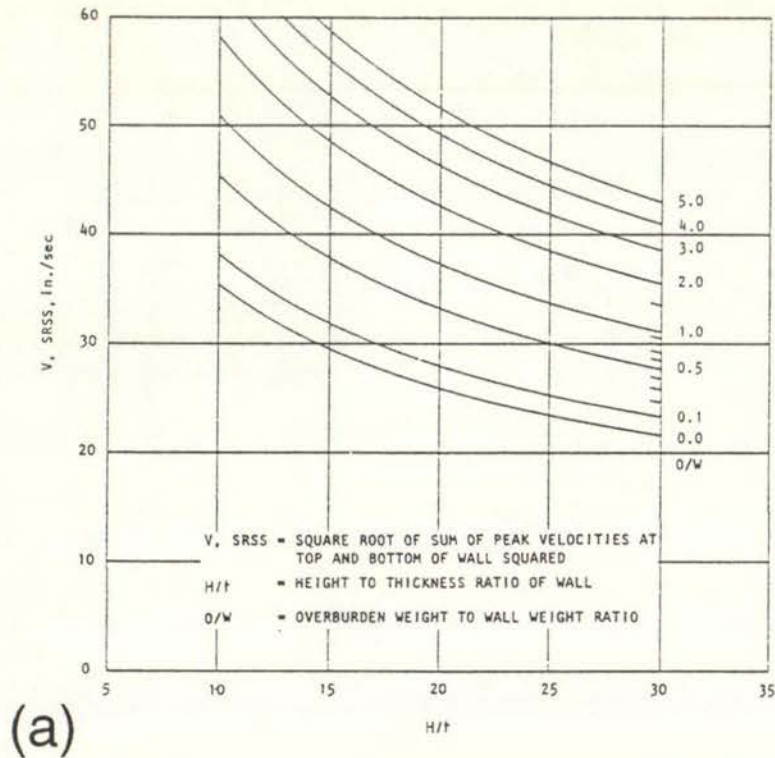
The criteria used to evaluate the diaphragms in the ABK methodology is shown in Figure 4.1.(b). The diaphragm strength is expressed in terms of a Demand - Capacity ratio; $W_D / (2v_u D + \Sigma V_c)$

Where W_D = total seismic weight for the diaphragm span
 v_u = yield capacity of diaphragms in shear
 D = diaphragm depth
 V_c = total yield capacity of timber cross walls within the diaphragm span

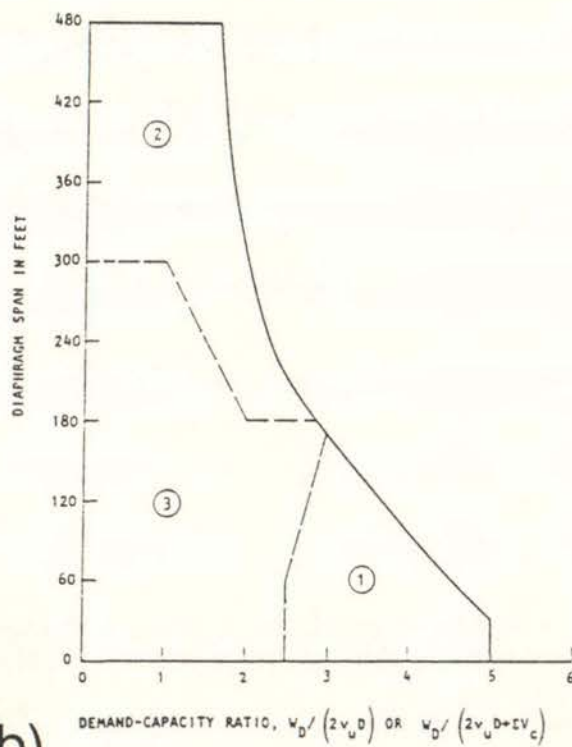
It should be noted that the inverse of the Demand-Capacity ratio is essentially the more familiar lateral load coefficient, C_d .

The criteria used to construct Figure 4.1 (b) is unknown as it would appear that the background report (38(e)) explaining its development has never been published. However, the ABK researchers seem to have concluded that a minimum diaphragm strength is required to limit diaphragm displacements because large diaphragm displacements could affect the stability of any face loaded walls fixed to it.

Figure 4.1.(b) indicates that the minimum diaphragm strength required by the ABK methodology increases with diaphragm span.



(a)



(b)

Figure 4.1 Criteria used in ABK Methodology to assess URM Buildings:

- Criteria for 98% Probability of Survival of Face Loaded URM Walls
- Criteria used to Evaluate the Minimum Strength of Diaphragms Required to Control Displacements and also to Evaluate the Amplification of Ground Motions by Diaphragms. (diagrams reproduced from Ref 39 - note imperial scales)

It can also be seen that a minimum strength corresponding to a lateral load coefficient $C_d = 0.2g$ (Demand-Capacity Ratio = 5.0) is required for short span diaphragms and that a relatively high minimum strength corresponding to $C_d = 0.5g$ would be required for long span diaphragms.

The degree to which diaphragms are expected to amplify the peak velocity of the ground motion varies with the diaphragm characteristics as indicated by the 3 zones shown in Figure 4.1.(b).

In zone 1 diaphragms will be comparatively "weak" and will be forced well beyond their yield limit and also have high levels of effective damping. When diaphragms lie within this zone ABK recommends the use of 1.75 x the peak ground velocity in conjunction with Figure 4.1.(a) to assess the stability of any face loaded walls fixed to the diaphragm. The same amplification factor is recommended for zone 2 as a diaphragm in this zone will have a relatively long period that will be outside the range where peak amplification of the earthquake motion is expected.

Diaphragms in zone 3 will be relatively strong and stiff and are therefore expected to respond elastically with a lower level of damping and a higher amplification of the peak ground velocity. For diaphragms in this zone a higher amplification factor of 2.25 is recommended by ABK. This suggests that the seismic resistance of face loaded walls in a URM building would be reduced if the floor diaphragms were strengthened more than the minimum amount required to control displacements.

It should be noted that Figure 4.1(b) is only applicable when assessing the seismic resistance that a URM building would have when subjected to an earthquake with an Effective Peak Acceleration (EPA) of 0.4g.

An earthquake with an EPA of 0.4g is defined (38 (k)) as an earthquake motion that would have a smoothed peak 5% damped spectral response value of 1.0g. Therefore, it corresponds to an earthquake intensity close to that represented by the "equal risk" spectra for normal soils given in New Zealand's draft loading code, DZ4203/2 (40). Within limits, it is probably reasonable to use Figure 4.1(b) for other earthquake intensities if the Demand-Capacity scale is adjusted to reflect the increase/decrease in earthquake intensity.

This is effectively the approach used in the Los Angeles Municipal Code (41). In this code a modified form of the ABK methodology is permitted as an "alternative design method" for the assessment and strengthening of URM buildings.

An apparent limitation of Figure 4.1(b) is its lack of dependence on the thickness of the face loaded walls that are fixed to the diaphragms.

By considering the static equilibrium of a face loaded wall element it is apparent that its stability is mainly affected by the relative displacement between the diaphragms at the top and bottom of the wall element and that it is the ratio of the relative diaphragm displacement to the wall thickness that is likely to be the important parameter. Therefore, a series of curves corresponding to a range wall thickness would be expected in Figure 4.1(b), not just a single curve.

The ABK methodology also includes a procedure for assessing the seismic resistance of URM loaded in-plane as shear walls. However, this aspect of the methodology has not been considered in this project.

4.4 Research Carried out at the University of Canterbury

Research in New Zealand at the University of Canterbury by Priestley (42) and Zoutenbier (43) has extended ABK's research effort.

Priestley used energy and static stability considerations to predict the peak diaphragm acceleration that would cause collapse of face loaded URM wall elements. This research indicated that the elastic modulus of the brickwork could be an important parameter when considering the stability of face loaded URM walls.

Zoutenbier extended Priestley's research using inelastic dynamic analysis to model face loaded wall elements. This included some preliminary analysis of a five storey URM face loaded wall. Unfortunately Zoutenbier's wall computer model appears to assume that the moment-curvature relationship that is applicable at a wall crack also applies at every section throughout the wall height. However, ABK's testing indicated that only single cracks are likely to form in a face loaded wall element at the diaphragm and mid-storey levels. The reduced elastic stiffness associated with a crack will, therefore, only apply to very short sections of wall in the vicinity of the cracks and not over the full wall height as assumed by Zoutenbier.

The walls modelled by Zoutenbier were also relatively slender with an inter-storey height of 5.0m and a thickness of 200 or 220mm. Use of slender walls and a reduced cracked stiffness throughout the wall height would have resulted in relatively large elastic deformations in the wall. This may explain why Zoutenbier found that the stability of face loaded walls was strongly influenced by the elastic modulus (E) assumed for the brickwork. No significant correlation with the magnitude of the E value assumed for the brickwork was found in the research carried out as part of this project (See Section 6.6).

The face loaded wall specimens tested by ABK were only one storey high. This meant that any interaction between the response of the test specimens and any wall in a storey above or below the test specimen could not be included in the test setup. Zoutenbier's analysis of multi-storey face loaded walls indicated that the first mode response of the wall would involve alternate storeys moving in opposite directions (ie out-of-phase) as indicated in Figure 4.2. In this mode the wall elements in each storey have their lowest effective stiffness and hence the wall has its longest response period. This finding has implications when the boundary conditions are being modelled for a wall element that represents a single storey in a multi-storey wall. These implications will be discussed more fully in Section 6.1.

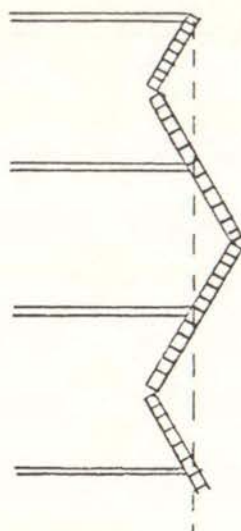


Figure 4.2 First mode Response of Face Loaded wall (reproduced from (43))

When Zoutenbier substituted flexible diaphragms for the rigid diaphragms in his computer model he found that the wall displacements did not necessarily increase and in some cases decreased. Using ABK's methodology an increase in the face loaded wall response would have been expected because the flexible diaphragms should have amplified the peak velocities of the earthquake motions imposed on the wall.

In the ABK methodology masonry shear walls, loaded in-plane, are assumed to be so stiff that they transmit the ground motion to the ends of the diaphragms unmodified. This is a controversial aspect of the ABK methodology (44). The University of Canterbury researchers proposed a relatively simple procedure that would take into account amplification of ground motion with height in multi-storey structures (43).

4.5 Gilroy Firehouse Response to Loma Prieta Earthquake

The need to allow for amplification of earthquake motions by the shear walls of a URM building is supported by the response of the Gilroy fire house in the recent Loma Prieta Earthquake (45). Accelerograms from instruments installed in this building showed that peak ground accelerations at the top of the building's two storey URM walls was 45% greater than the peak ground acceleration (0.29g). The records also showed that the peak EW acceleration at the centre of the roof diaphragm was 2.7 times the peak ground acceleration.

The floor and roof diaphragms of the building were diagonal boarding with a ply overlay and appear to have responded in an essentially elastic manner. Computer modelling of this building (45) indicates that the in-plane shear walls may respond with a higher level of damping than the 5% assumed by the Canterbury researchers. The modelling indicted that 10% damping was appropriate even though the walls were not significantly cracked in-plane. This relatively high level of damping in the modelling appears to be necessary to allow for the effects of soil structure interaction.

The best match between the recorded and modelled response of the building was obtained when an effective first mode damping ratio of 16.4% was used.

This appears high, given that the diaphragms appear to have responded elastically and may indicate that the face loaded walls were not modelled realistically by treating them as lumped masses.

5 BEHAVIOUR OF CRACKED URM WALLS UNDER STATIC FACE LOADING

5.1 Derivation of Static Load Deflection Relationship

Face loaded walls in URM buildings normally span vertically between floor diaphragms. They may also be supported by roof diaphragms or by the ground. In many instances the walls also span horizontally between walls or returns. For the current investigation only vertically spanning walls are considered.

When subjected to sufficient load, the walls can be expected to crack at the level of the supports and near the mid-height of the wall elements that span between the supports. Figure 5.1(a) shows the forces assumed to act on a cracked wall element spanning, H , between supports. The wall has a total weight, W , and effective thickness, t . The overburden load, O , represents the weight of a parapet or the weight of any upper storey walls and is assumed to act at the wall centre line.

At the base of the wall element the vertical reaction, $O + W$, is assumed to act near the face of the wall at a point that is $t/2$ from the wall centreline. As a small compression zone depth would be required to develop the reaction and, as the mortar may not extend to the outside face of the wall, the effective wall thickness, t , will be slightly less than the nominal wall thickness. The reduction factor used to reduce the nominal wall thickness to an effective wall thickness can also be selected to make an allowance for 2nd order geometric effects which may be significant when the wall mid-height displacement, Y , is large.

At the mid-height crack, the reaction between the upper and lower halves of the wall is also assumed to be located $t/2$ from the deflected centre line of the wall or $(t/2 - Y)$ relative to the undeflected wall centre line as indicated. Figure 5 (b) shows the bending moments developed in the wall when the wall is subjected to a point load, V , acting at the mid-height crack. The bending moments given are relative to the undeflected centre line.

Equating the simply supported bending moment to the wall moments at the mid-height crack:

$$\frac{VH}{4} = (O+W) \frac{t}{4} + (O + \frac{W}{2}) (\frac{t}{2} - Y) \dots\dots\dots 1$$

$$\therefore V = \frac{2}{H} [W(t - Y) + O(3t/2 - 2Y)] \dots\dots\dots 2$$

V will have a maximum value, V_{\max} when $Y = 0.0$

$$\therefore V_{\max} = \frac{t}{H} (2W + 3O) \dots\dots\dots 3$$

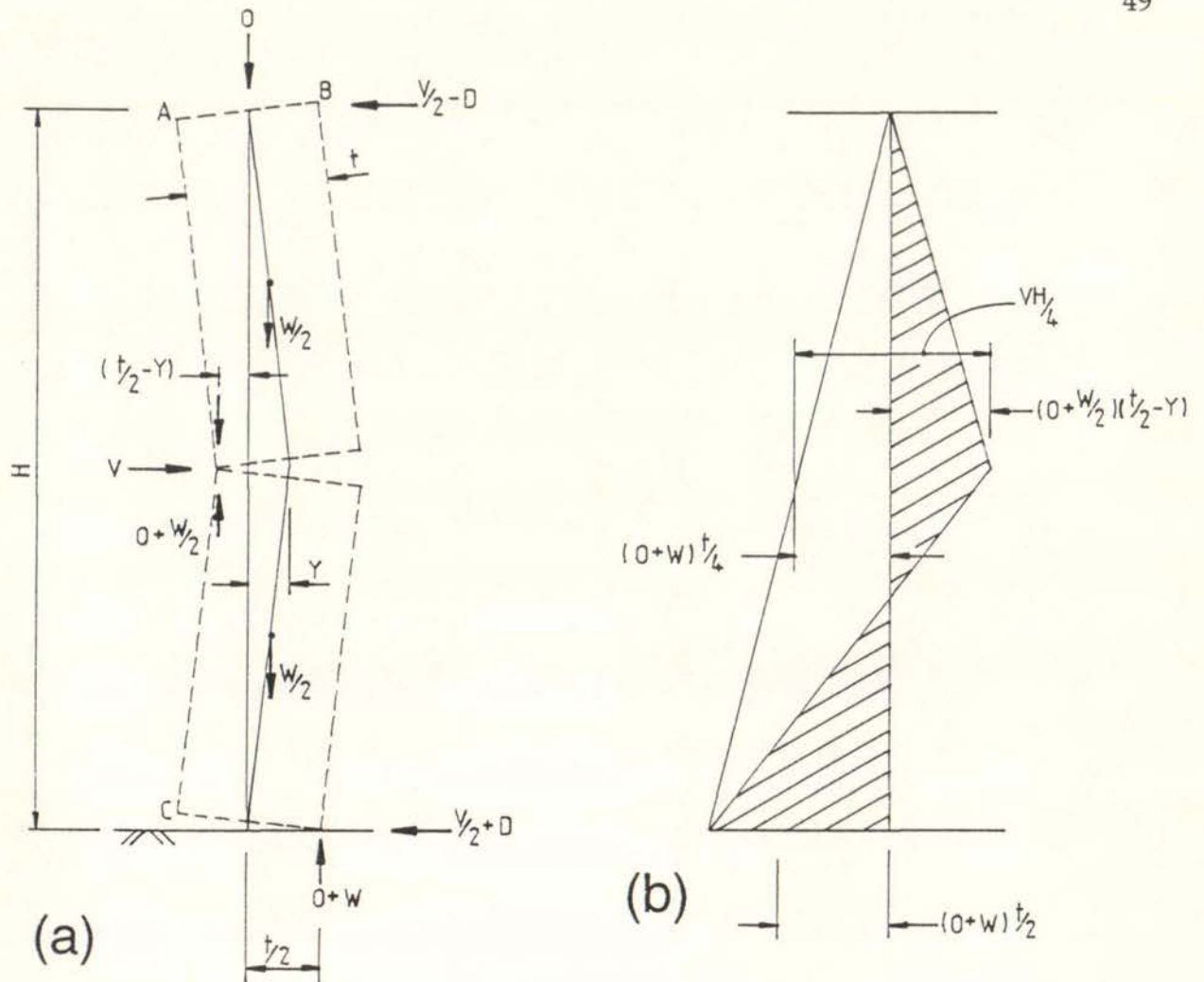


Figure 5.1 : Behaviour of face loaded wall under static loading

- forces assumed to act on the wall
- bending moments in the wall
- load deformation relationship for point load acting at mid-height crack

The wall will become unstable when $V = 0.0$ and the wall displacement, Y , will then have its maximum static value, Y_{\max} . Therefore rearranging equation 2 and substituting $V = 0.0$:

$$Y_{\max} = \left(\frac{W + 1.5O}{W + 2O} \right) t \dots\dots\dots 4$$

Using equation 3 and 4 to replace O and W in equation 2 and rearranging equation 2 it can also be shown that:

$$V = V_{\max} (1 - Y/Y_{\max}) \dots\dots\dots 5$$

This equation is shown graphically in Figure 5.1.(c).

The difference in reactions at the top and bottom support levels, D , that is indicated in Figure 5.1.(a), can be obtained by taking moments about the undeflected wall centre line at the mid-height crack. This results in the expression:

$$D = (O + W) \frac{t}{2H} - \frac{WY}{2H} \dots\dots\dots 6$$

5.2 Energy Balance

Figure 5.1.(a) shows that the wall weight and overburden load will be displaced vertically as the wall is deflected horizontally. The resulting potential energy stored in the wall will be equal to the area under the load deformation curve as indicated in Figure 5.1.(c). When wall displacements are large, calculation of the wall potential energy directly, using the wall's vertical displacements is relatively complex as it is dependant on second order vertical wall displacements. Figure 5.1.(c) and the related equations are, therefore, a convenient method of calculating the potential energy stored in the wall for a given displacement Y . The method is also applicable under dynamic conditions.

When a real URM wall is subjected to face loads there will be some elastic deformation of the wall prior to the cracks opening. This elastic part of the static response is also indicated in Figure 5.1.(c). Except where the wall displacements are small or the wall is very slender these displacements are relatively small and can normally be neglected.

5.3 Static Load Deflection Relationship for Uniformity Distributed Loads

Figure 5.1.(b) indicates how the simply supported bending moment for a point load, V , may be equated to the wall moments. The resulting relationship is given in equation 1. If the point load is replaced by a uniformly distributed load, wH , the simply supported bending moment will be $wH^2/8$. Therefore the load, V , in equations

1 to 5 would need to be replaced by $wH/2$ if the load applied to the wall was uniformly distributed,

$$\text{ie, } wH = 2V \dots \dots \dots 7$$

Therefore, if the load is uniformly distributed, twice the load is required to produce the same wall displacement.

The equations used to calculate Y_{\max} and D (equations 4 and 6) are not affected by the load distribution and remain the same for a uniformly distributed load.

Equations 3 and 7 can also be used to find the seismic lateral load coefficient, C_d , at which the cracks in the wall will start to open:

$$C_d = \frac{wH}{W} = \frac{2V_{\max}}{W} = \frac{2t}{H} \left(2 + \frac{3O}{W} \right) \dots \dots \dots 8$$

The basic equation describing static equilibrium of a cracked face loaded wall (equation 1) can also be derived by considering equilibrium of the upper and lower halves of the wall element separately. As this proof was more complex and was not as intuitive as considering bending moments it is not included here. However, it was used to check the validity of the derivation method used.

6 DYNAMIC BEHAVIOUR OF FACE LOADED WALLS WITHOUT INTERACTION WITH DIAPHRAGMS

6.1 Boundary Conditions for Wall Elements

The boundary conditions assumed at the top and bottom of a wall element were the same as used for the static analysis and shown in Figure 5.1.(a).

The overburden load is shown acting at the wall centreline at the top of the wall. This is the position of the overburden assumed by previous researchers (42, 43) and is also the position at which the overburden load was applied in the walls tested by ABK (38(d)).

During dynamic response to earthquake loads the displacements of a parapet, for example, would be out-of-phase at least part of the time with the response of the wall element supporting it. Therefore, the actual position that the parapet applies the overburden load to the wall would fluctuate between positions A and B shown in Figure 5.1(a). When the parapet and wall element motions are in-phase the overburden load will be applied at B and exert a clockwise moment at the top of the wall element. This would reduce the moment shown in Figure 6.1.(b) acting at the mid-height of the wall element and therefore improve the wall element's stability.

Conversely, if the wall element and parapet motions are out-of-phase the overburden load would act at point A and this would reduce the stability of the wall element.

If the overburden load is the result of an upper storey wall element its effect on the wall would be similar depending on whether it is moving in-phase or out-of-phase with the wall element under consideration.

The reaction at the base of the wall, $O + W$, is shown in Figure 5.1(a) in a position that increases the wall's stability. For a wall supported on a foundation that can develop the reaction this would be the reaction's position. However, if the wall element under consideration was supported on a lower storey wall the reaction could move to the position indicated as C in Figure 5.1(a). This location for the reaction would apply when the lower storey wall element is moving out-of-phase with the wall element under consideration. Under these conditions the upper storey's stability would be reduced while the lower storey wall's stability would be improved.

If the reaction at the base of the wall was assumed to act at the wall centre line the displacement at which the wall becomes unstable, Y_{\max} , would be reduced. For example, if the reaction develops at the outside edge of the wall, and the overburden load is zero, equation 4 indicates that $Y_{\max} = t$. When the reaction is assumed to act at the wall centre line Y_{\max} reduces to $0.5 t$.

Also, if the wall reaction at the base of the wall acts at the wall centreline, the wall will be less stiff under lateral loads. It will then have a lower frequency of vibration. This is the basic reason why the first mode (or lowest frequency) of vibration of a multistorey wall has alternate wall elements between the floors moving out-of-phase as was shown in Figure 4.2.

For an elastic system, the lowest frequency mode usually makes the greatest contribution to the dynamic response. This implies that the boundary conditions shown at the base of the wall in Figure 5.1(a) may be unconservative under dynamic conditions when modelling an upper storey of a multistorey wall, or if the wall foundation is not rigid and rotates.

However, the seismic stability of a multistorey face loaded wall generally increases from the top towards the bottom storey because of increasing overburden, increasing wall thickness and reducing dynamic loads. The response frequency of wall elements in adjacent storeys is also likely to vary, especially after cracking. Therefore, it is unlikely that wall elements in adjacent storeys will become unstable simultaneously. Wall elements can, therefore, expect to have stabilising moments imposed by wall elements in adjacent storeys as they approach collapse. For these reasons it is expected that the combined top and bottom boundary conditions shown in Figure 5.1(a) will be reasonably conservative in most cases for wall elements subject to dynamic loads.

However, the boundary conditions may be unconservative for a top storey wall element if the supporting element in the storey below has a similar level of dynamic stability and frequency of vibration. This is more likely to be the case when the supporting wall in the lower storey is relatively slender or has a non-rigid foundation.

6.2 Computer Model

Figure 6.1 gives details of the computer model used to evaluate the inelastic dynamic behaviour of face loaded walls.

The model allows the wall to deform as indicated in Figure 5.1(a). Opening of cracks at mid-height and at the base of the wall is accommodated by the link members indicated in Figure 6.1. These members buckle when subjected to compression.

The wall properties selected for the computer model were based on one of the brick walls tested by ABK (38(d)). This allowed results from the computer model to be compared with the ABK test results. The wall tested by ABK (ABK test wall No. 1) had an effective height of 4.8m allowing for the position of the crack at the base of the wall and the support location at the top of the wall. The full thickness of 350mm was used to calculate the wall mass, area and flexural rigidity. The wall's effective thickness, t , allowing for the depth of the compression zone and raking of mortar joints was assumed to be 330mm.

Half scale and 2 x scale walls were also evaluated. These walls had the same slenderness ratio, H/t , as the "full scale" ($4.8 \times 0.33\text{m}$) walls but had half or double the effective wall thickness respectively.

Table 6.1 shows the properties assumed for various elements in the computer model and the scaling factors used to calculate the properties of the 1/2 and 2 x scale walls. These properties were used for all analyses except where explicitly stated otherwise. As noted in the table, the end block members were modelled as essentially rigid.

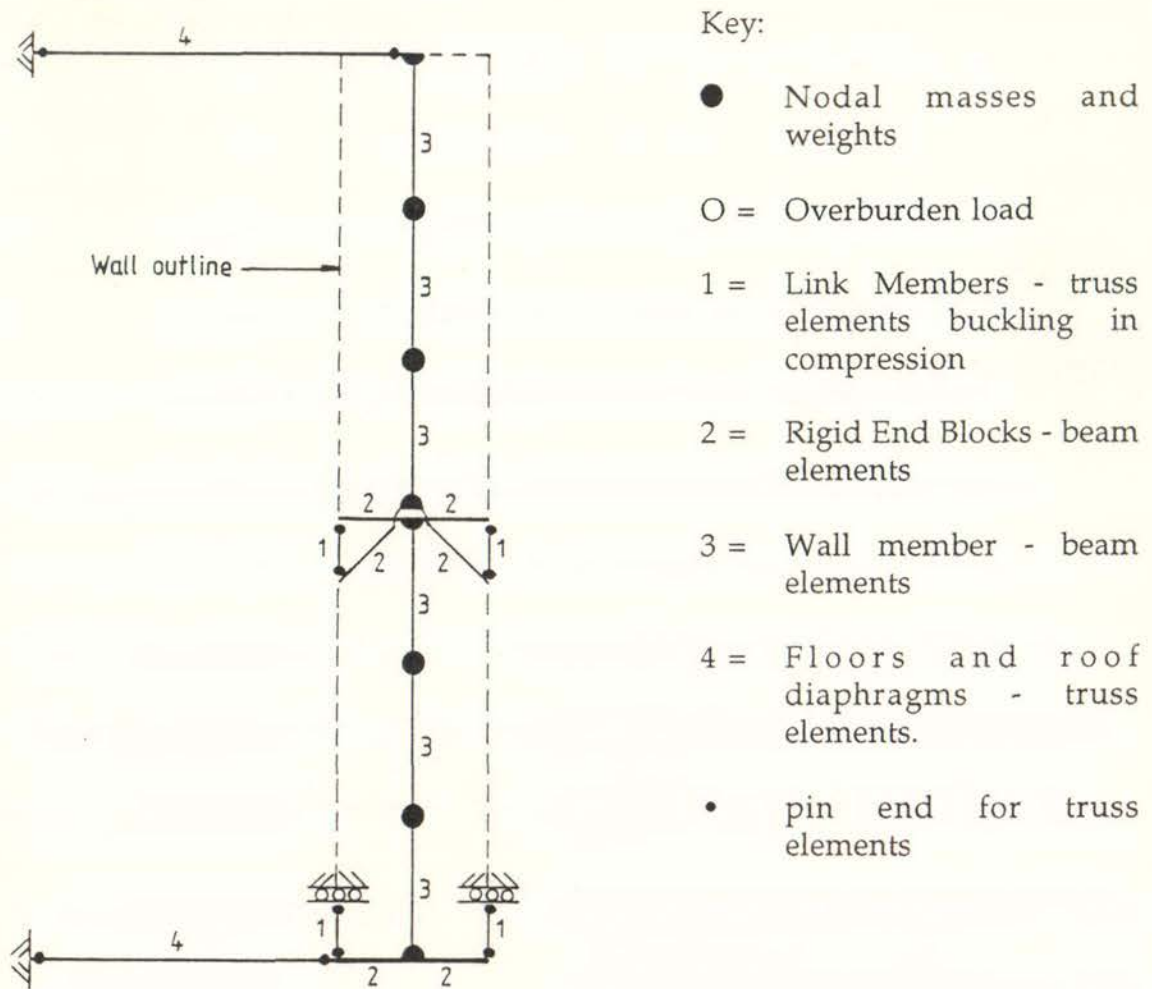


Figure 6.1 Computer Model for Face Loaded Wall. (Exaggerated Horizontal Scale)

The two nodes at the mid-height crack of the model were "slaved" in the horizontal direction so that no relative horizontal displacement would occur. Slaving was also used at the base of the wall so that the supports providing vertical restraint would move with the base of the wall when the lower diaphragm extended. Initially the diaphragms were modelled as essentially rigid or were removed from the model.

ELEMENT AND PROPERTY (Wall assumed 1m long)	VALUE	SCALING FACTOR USED FOR:	
		1/2 Scale Walls	2 x Scale Walls
Wall Members			
Wall height & thickness	4.8 x .33m	1/2	2
Modules of elasticity (E)	1.0 GPa	1	1
Area of wall	.35m ²	1/2	2
Moment of inertia	.0036m ⁴	1/8	8
Total wall weight	36 kN	1/4	4
Mass (tributary wall length = H/6)	.6 tonne	1/4	4
Overburden load	5.0 kN	1/4	4
Link Members			
Length	0.1m	1	1
Area	0.25m ²	0.6	1
Modulus of elasticity	1.0 GPa	1	1
End Block Members (rigid)			
Area	10.0m ⁴	1	1
Moment of inertia	3.0m ⁴	1/2	4
Modulus of elasticity	1.0E3 kN/m ²	1	1
Diaphragm (essentially rigid)			
Elastic Modulus (E)	1 GPa	1	1
Area	2.0m ²	1	1
Instability Displacement (Y_{max})	310mm	1/2	2
Wall Period (prior to link buckling - evaluated by solving eigen vector problem using DRAIN-2DX)	0.166 sec	approx 1/2 (0.087)	approx 2 (0.366)

6.3 DRAIN-2DX Computer Program

The model was analysed using the inelastic dynamic analysis program DRAIN-2DX Version 1.01 (34, 46). The program uses step-by-step numeric integration to perform inelastic dynamic analysis. An option permits the detection of events (ie detects stiffness changes) during a time step and then uses an event-to-event type solution.

Another option allows the time step used for the analysis to vary automatically depending on error tolerances selected by the user. These options were used for the analysis. However, options permitting "velocity correction" and "acceleration correction" were not used.

6.4 Face Loaded Wall Behaviour Under Pulse Loading

The face loaded walls were subjected to a short duration (0.2 sec) acceleration pulse applied to the top and bottom of the walls. This was a convenient method of applying an initial displacement to the centre of the wall. The free damped responses of the walls could then be studied. Figures 6.2(a) to (c) show 3 of the free vibration wall responses. The damping coefficients, α and β given, are explained in detail in section 6.4.2.

The response shown in Figure 6.2(c) is for the 2 x scale wall when it almost reached the displacement at which it becomes unstable, Y_{max} . If the displacement had reached Y_{max} , theoretically the wall would have stopped moving and the vibration period of the wall motion would have been infinite.

Figure 6.3 indicates how the displacement at the mid-height of the walls varies with the magnitude of the acceleration pulse. The wall displacements have been normalised using the displacement at which the walls become unstable, Y_{max} . The instability displacement, Y_{max} , was calculated using equation 4. The pulse magnitude corresponding to C_{dr} , calculated using equation 8, is also shown. This acceleration value corresponds to the uniformly distributed static face load that would need to be applied to the walls to just open the cracks at mid-height and at the base of the wall.

As all the walls had the same slenderness (H/t ratio) the ABK methodology would predict that they would have the same seismic resistance. However, Figure 6.3 suggests that seismic resistance may increase with wall thickness. It can also be seen that wall response increases with reduced damping as would be expected.

Perhaps the most important conclusion to be drawn from Figure 6.3 is that once the wall displacement exceeds approximately 60% Y_{max} the response becomes very sensitive to small changes in the pulse magnitude. This sensitivity could have been anticipated from the load-deformation relationship shown in Figure 5.1(c) where it can be seen that as the displacement approaches Y_{max} the energy that needs to be input into the wall to increase the displacement incrementally becomes progressively smaller.

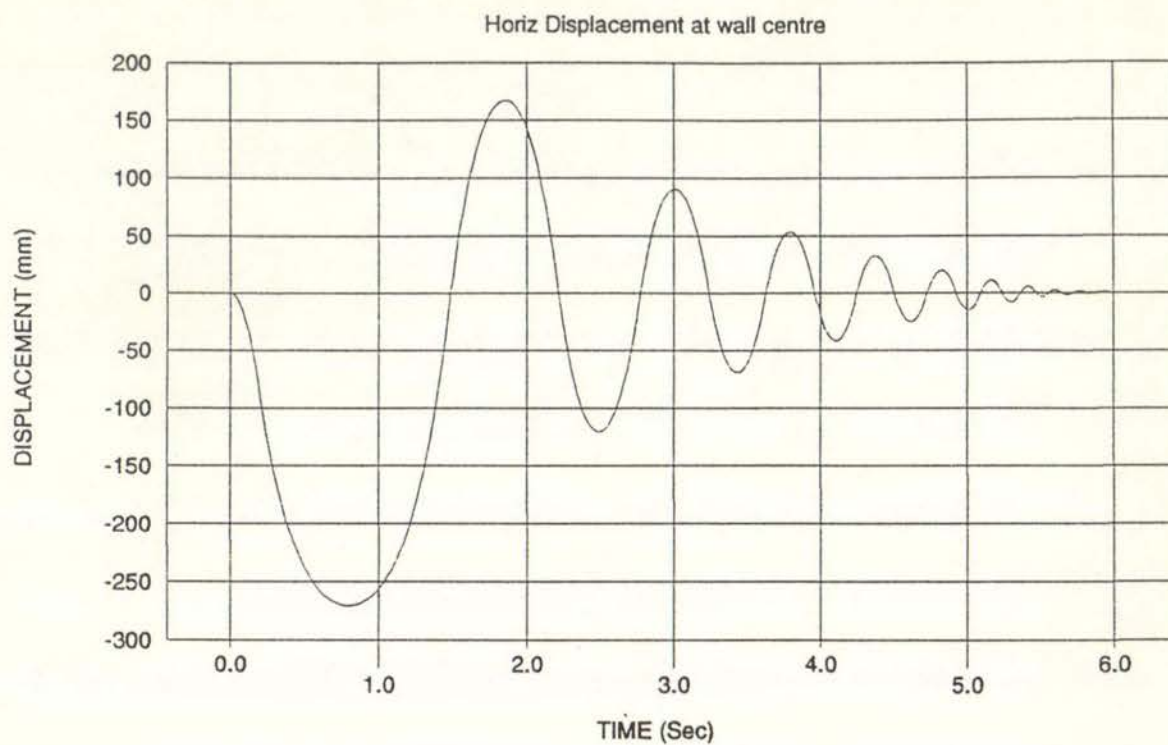


Figure 6.2(a) : Horizontal Displacement at Centre of 4.8 x .33m Wall When Wall Subjected to a 0.64g Pulse for 0.2 Seconds ($\alpha = .006$, $\beta = .004$)

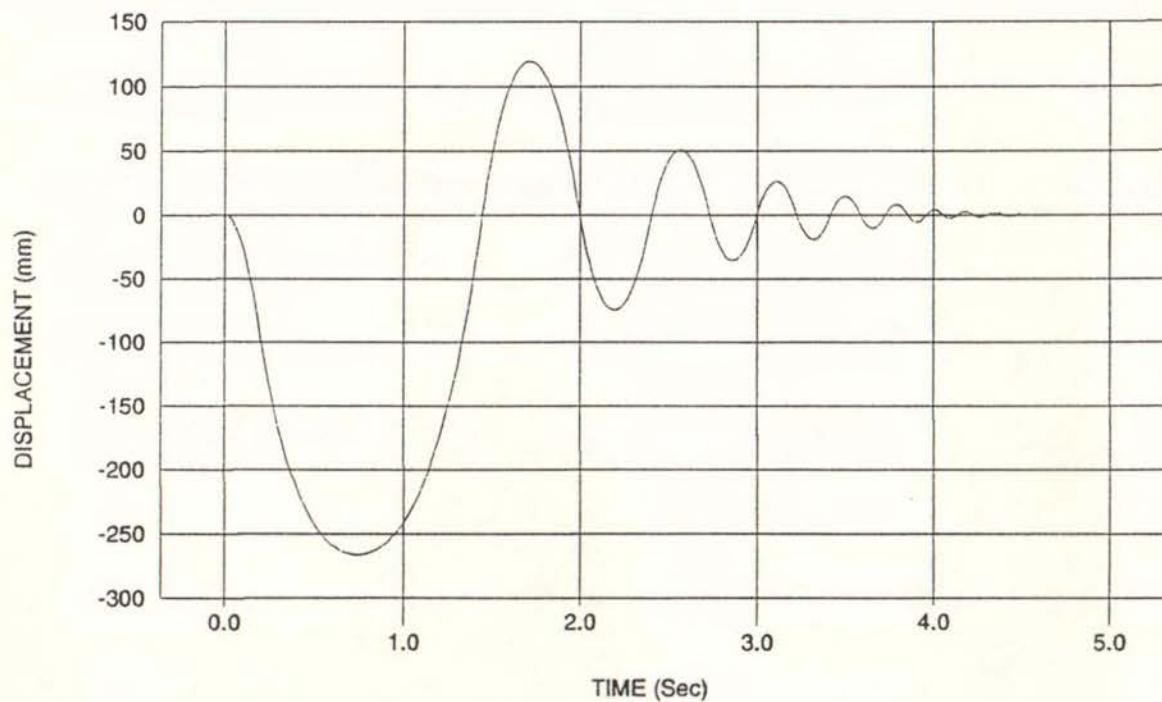


Figure 6.2(b) : As for (a) Except Pulse Magnitude Increased to 0.675g and Mass Damping Factor, α Increased to 0.6

0.875g Pulse (9.6 x 0.66 wall)

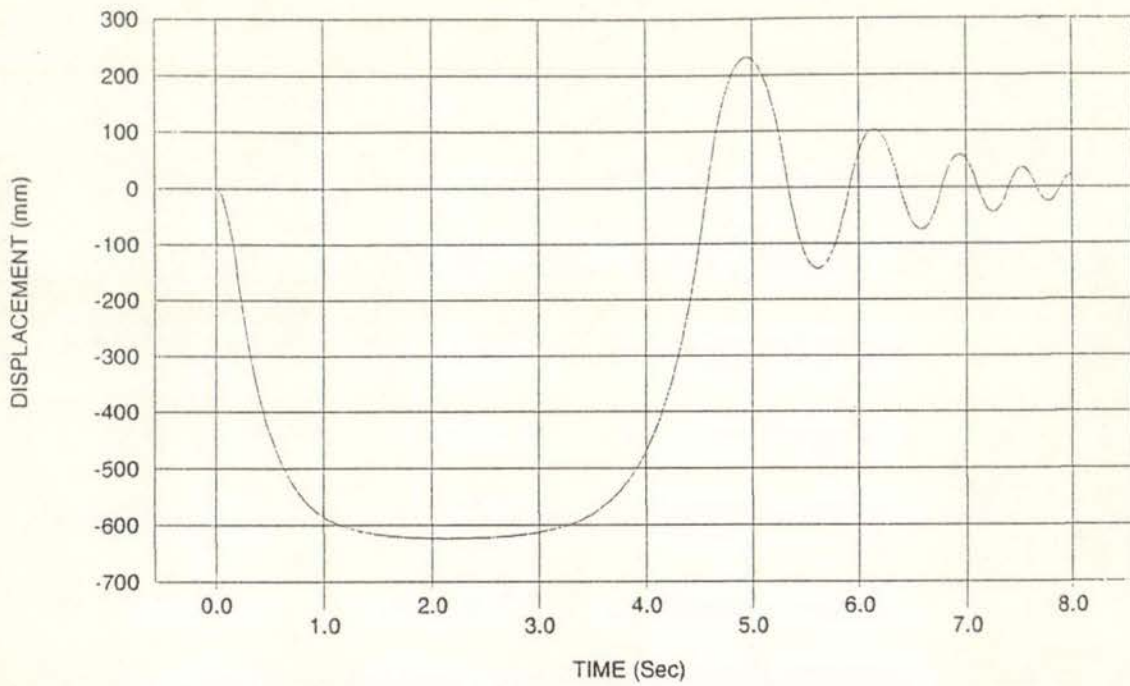


Figure 6.2(c) : Horizontal Displacement at Centre of 9.6 x 0.66 Wall When Wall Subjected to a 0.875g Pulse for 0.2 Seconds ($\alpha = .006$, $\beta = .004$)

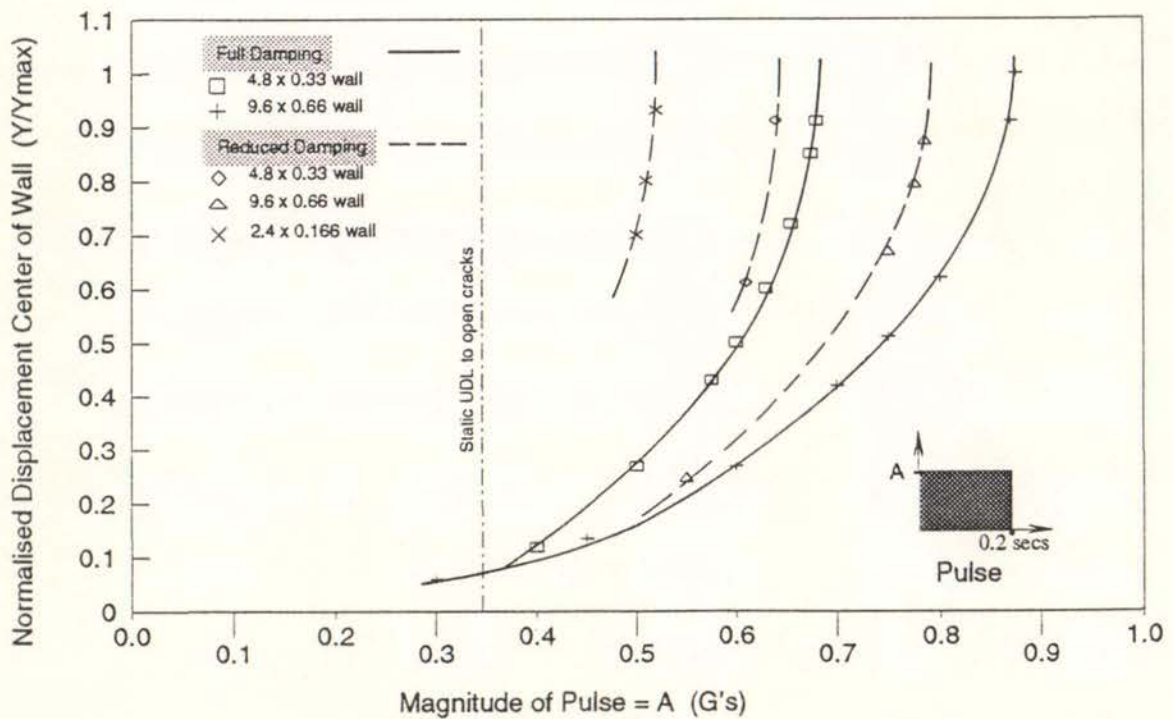


Figure 6.3 : Response of Face Loaded Walls to a 0.2 Second Pulse of Varying Magnitude.

6.4.1 Period of Free Vibration Response

It can be seen from Figures 6.2(a) to (c) that the free vibration period of the wall increases with the wall displacement. This relationship is shown graphically in figure 6.4(a). The periods and displacements for the graph were obtained from plots like those shown in Figures 6.2(a) to (c) by considering the half cycles on each side of the zero displacement line separately. For the first half cycle only the second quarter cycle was used to avoid including the effect that the initial 0.2 second acceleration pulse has on the period. The periods were then normalised using the period that corresponded to a displacement of $0.75 Y_{max}$ as given in Table 6.2.

TABLE 6.2 : VIBRATION PERIOD WHEN WALL DISPLACEMENT = $0.75 Y_{max}$		
WALL SIZE	NORMAL DAMPING ($\alpha = .6, \beta = .004$)	REDUCED DAMPING ($\alpha = .006, \beta = .004$)
Full Scale Wall (4.8 x .33m)	2.3	2.12
2 x Scale Wall (9.6 x .66m)	3.3	3.0
1/2 Scale Wall (2.4 x 0.166m)	-	1.4

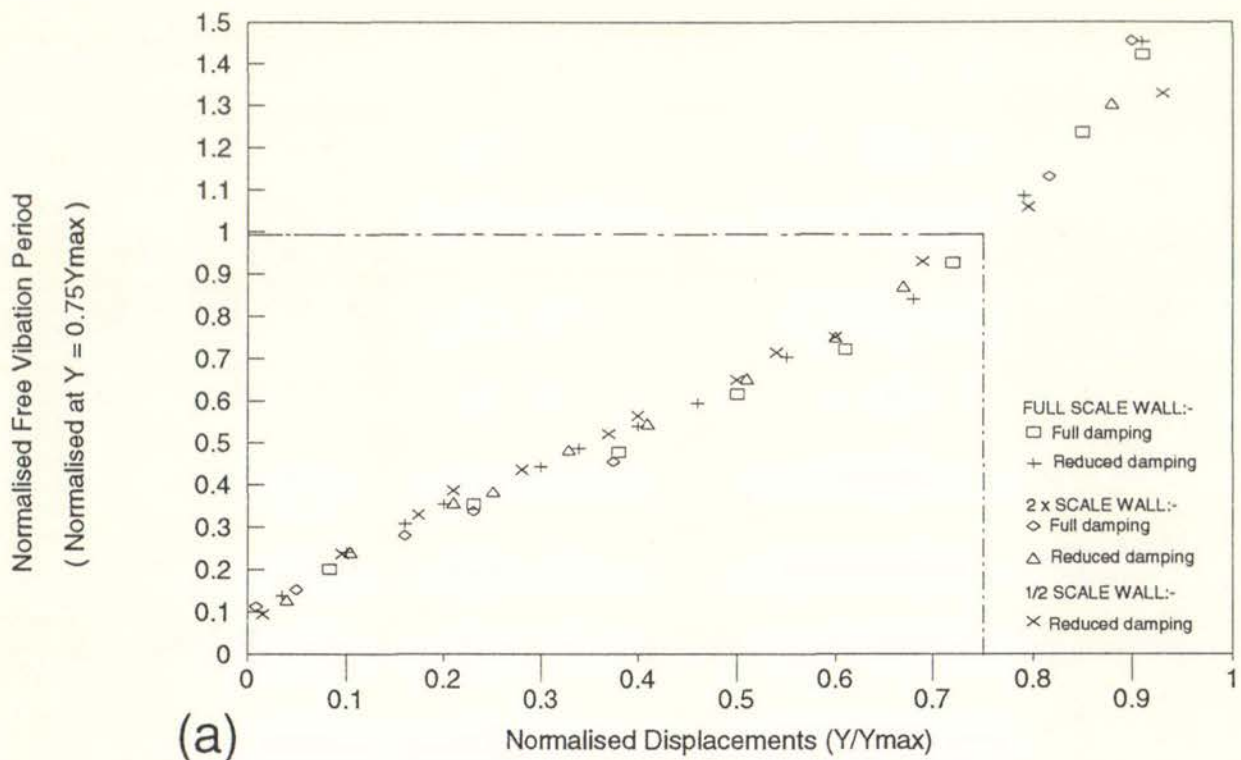
It can be seen from Figure 6.4(a) that the relationship between normalised period and wall displacement is practically independent of the scale factor used for the wall.

The inset diagram shown in Figure 6.4(b) defines a free vibration period shape factor, R , where RT_1 is the quarter cycle period and T_1 is calculated from the peak velocity, V_o , for the half cycle using the relationship $T_1 = Y/V_o$. An examination of the free vibration responses of the walls suggested that the shape of each half cycle of the response was likely to be primarily dependent on the normalised displacement Y/Y_{max} . As R and V_o define the shape of the half cycle response a relationship between R , V_o and the normalised displacement Y/Y_{max} is to be expected.

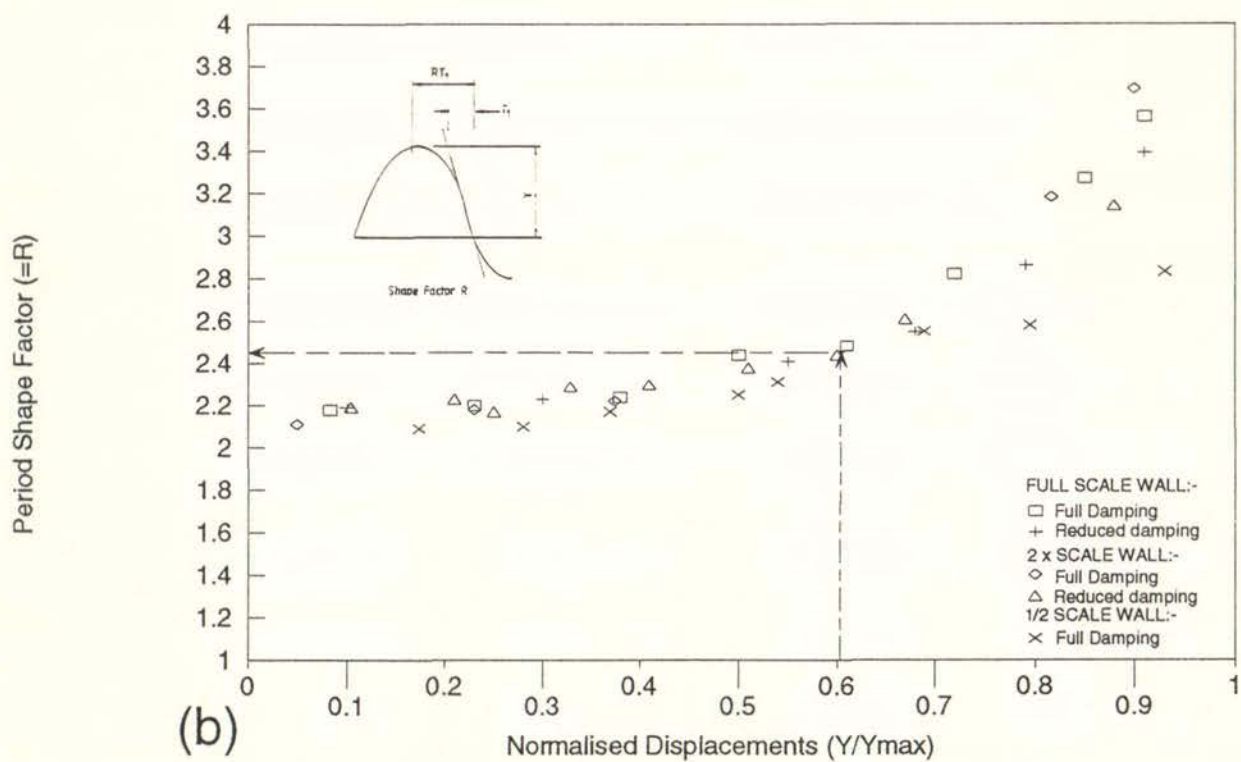
This relationship can be derived using Conservation of Energy principles.

When a face loaded wall, like that shown in Figure 5.1(a) responds to free vibration, all the energy within the wall will be kinetic energy when the displacement, Y , is zero and all the energy will be in the form of potential energy when it reaches its maximum displacement Y . Ignoring energy loss due to damping the peak kinetic energy, E_k , and peak potential energy will be equal.

Assuming uniformly distributed mass over the depth of the wall and ignoring small elastic deformations the total peak kinetic energy stored in the wall at zero displacement is given by the relationship : $E_k = MV_o^2/6$ where M is the total mass of the wall and V_o is the peak velocity at the mid-height crack in the wall.



(a)



(b)

Figure 6.4 (a) Free Vibration Period of Face Loaded Walls vrs Displacement at the Centre of the Wall.
 (b) Variation in Free Vibration Period Shape Factor (R) with Wall Displacement.

The peak potential energy stored in the wall at a displacement Y , can be calculated with reference to Figure 5.1.(a) using the relationship:

$$\begin{aligned} E_o &= (V_{\max} + V)Y/2 \\ &= V_{\max} (2 - Y/Y_{\max})Y/2 \end{aligned}$$

Equating peak kinetic and potential energy:

$$V_o^2 = \frac{3Y V_{\max}}{M} (2 - Y/Y_{\max}) \dots \dots \dots 9$$

where V_{\max} and Y_{\max} are given by equations 3 and 4 respectively.

Equation 9 was used to calculate the peak velocity V_o for the half cycles of the free vibration wall response. This allowed the period shape factor, R , to be calculated from the observed period of the 1/2 cycles. The resulting relationship between the period shape factor, R , and the normalised peak displacements of each half cycle is shown in Figure 6.4.(b). It can be seen that for peak displacements below approximately $2/3 Y_{\max}$, R is not dependent on the scale of the wall or the level of damping within the range of variables considered.

The assumption made above, that the peak kinetic and potential energies will be equal, will not be valid because of energy losses due to damping. Therefore, an energy loss reduction factor should have been included on the right hand side of equation 9. However, the effect that this reduction factor would have has been included within a single overall period shape factor, R , which in effect also allows for energy loss.

For a peak displacement of $0.6 Y_{\max}$ the period shape factor read from Figure 6.4.(a) is 2.45. The period of the free vibration response with this peak displacement is, therefore:

$$\begin{aligned} T &= 4RT_1 = 4 \times 2.45 T_1 \\ &= 9.8 T_1 \\ &= 9.8 \times 0.6 Y_{\max} / V_o \end{aligned}$$

substituting for V_o using equation 9 and rearranging:

$$T = \frac{\sqrt{1.14 Y_{\max} W}}{V_{\max}} \dots\dots\dots 10$$

where V_{\max} and Y_{\max} are given by equations 3 and 4 in kN and metres respectively.

This relatively simple formula for predicting the period of motion for walls displaced to a peak displacement of $0.6 Y_{\max}$ is used in Section 6.7 to help predict the seismic stability of face loaded URM walls.

6.4.2 Damping of Free Vibration

The main source of energy loss in a face loaded wall, such as that shown in Figure 5.1(a), will be due to the impact that occurs when the cracks close.

The analysis procedure employed by DRAIN-2DX attempts to ensure no energy loss during each step of the analysis except for the work done by viscous damping. Therefore, in the computer model, energy loss due to impact has to be modelled as viscous damping with energy loss occurring throughout the response.

DRAIN-2DX makes provision for two types of damping to be provided in the computer model. For an elastic structure the proportion of critical damping, λ , is given by:

$$\lambda = \frac{\alpha T}{4\pi} + \frac{\beta\pi}{T} \dots\dots\dots 11$$

where: α and β are the coefficients for mass and stiffness damping respectively and: T is the elastic period of the motion.

The relationship between the damping components and the period, T , should be noted. When a structure has a range of response modes and both types of damping, the mass damping component $\alpha T/4\pi$, will dominate for long period motions while the stiffness damping component $\beta\pi/T$, will dominate for short period motion.

The stiffness component can be varied for each element in the computer model and may be visualised as a viscous damper placed in parallel with the member. The resulting damping is dependent on the strain and strain rate in the member and is proportional to its initial elastic stiffness. This presents a problem when modelling damping in the link members of the computer model. These members must have a high elastic stiffness to limit their contribution to the elastic displacement of the wall and they are subject to relatively large strains and strain rates after buckling. Adjustment of the stiffness damping co-efficient, β , so that the contribution of stiffness damping would be effectively based on the secant stiffness of the links was considered. However, this would produce damping similar to mass damping which

was easier to use as it was not dependent on peak displacements. The damping coefficient, β , for the links was therefore, set at zero for all wall computer models used in this project.

In the remaining members of the computer model, the elastic deformation and strain rates would be quite small once the wall cracked. Therefore it was not expected that stiffness damping would make a significant contribution to the damping during the wall's post cracking response.

The mass damping provided in the computer model may be visualised as viscous dampers placed between the nodal masses and the supports. Mass damping is, therefore, dependent on the displacement of each mass, its velocity and is also proportional to the nodal mass.

The free vibration responses of the computer modelled walls like those shown in Figure 6.2(a) to (c) were used to evaluate the actual amount of damping present. It was assumed that the logarithmic decrement method, which is applicable to linear elastic systems, was also applicable to the inelastic computer model of the face loaded walls. This was justified on the grounds that any future experimental tests of face loaded walls would probably use free vibration tests to determine damping and the results would probably be evaluated using the logarithmic decrement method. The test results could then be compared with the range of damping assumed in this project.

For a free vibration response such as that shown in Figure 6.2(a) the logarithmic decrement method gives the proportion of critical damping, λ , as:

$$\lambda = 1/n (Y_1/Y_2)/\pi \dots\dots\dots 12$$

where Y_1 and Y_2 are the peak displacements of successive 1/2 cycles on opposite sides of the zero displacement axis. The logarithmic decrement method actually requires the displacements Y_1 and Y_2 to be measured to the tangent point of the curve that forms an envelope for the response. This refinement was only used for the first 1/2 cycle when it made a significant difference.

The resulting damping for the two levels of damping generally assumed in this project are shown in Figures 6.5(a) and (b).

In each case the damping curves for the various scale walls are shown starting at the damping value corresponding to the elastic response. This value is applicable until the wall cracks open and was calculated using equation 11 and the period in Table 6.1. The calculation ignores the use of zero stiffness damping for the link members.

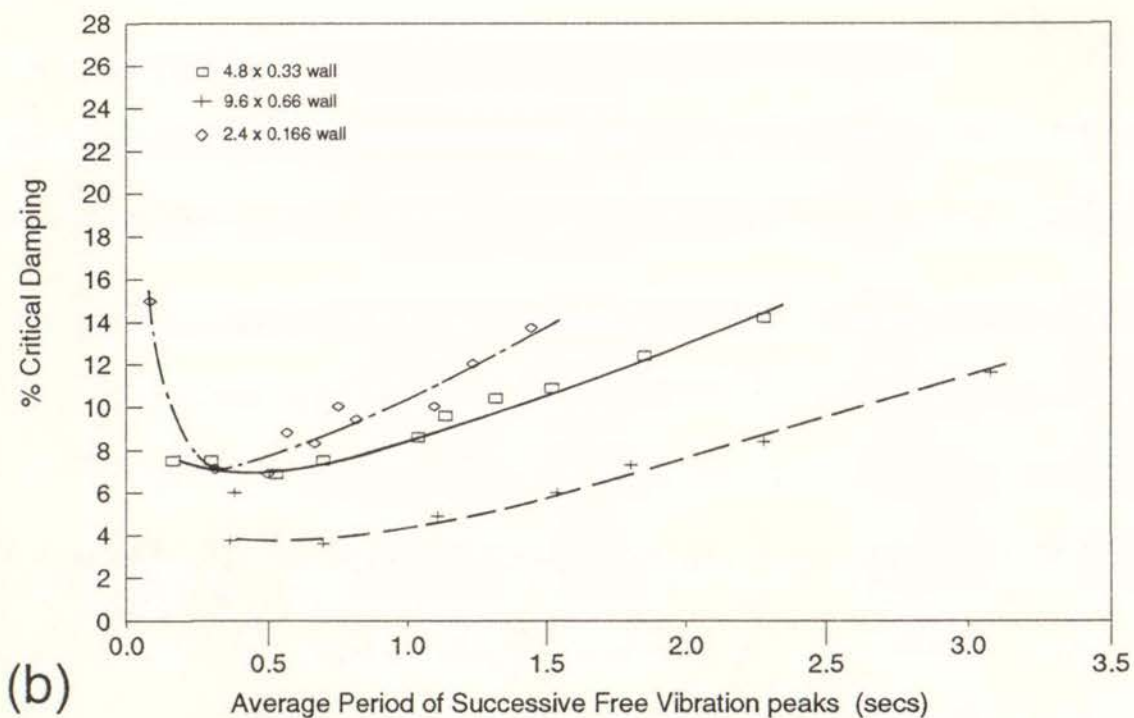
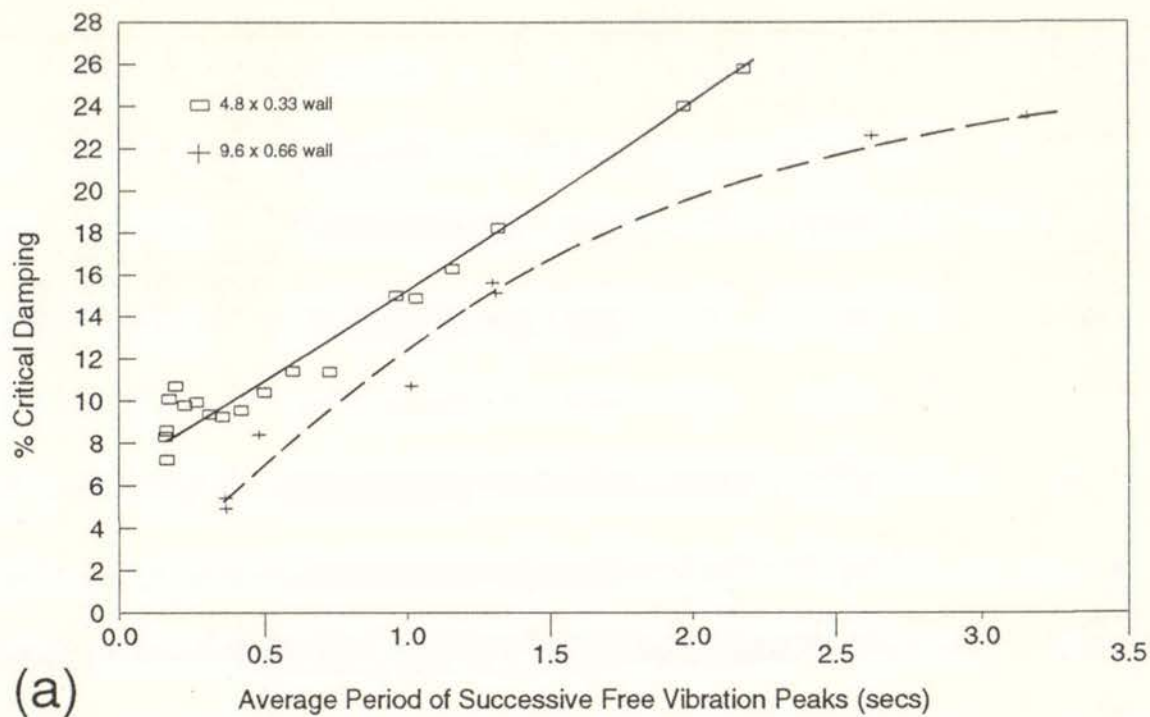


Figure 6.5 Damping calculated from free vibration response of walls using logarithmic decrement method.

(a) Full damping with $\alpha = .6$, $\beta = .004$

(b) Reduced damping with $\alpha \approx 0.0$, $\beta = .004$

It was found that the level of damping in the modelled walls was significantly higher than would be expected from a consideration of the α and β factors used. When the α and β factors were set equal to zero, so that the wall should have had no damping, it was found that the response still damped out slowly. Professor G H Powell, one of the principal authors of the DRAIN-2DX program, was asked to comment on this behaviour. Although uncertain as to the exact cause of this additional damping, Professor Powell was confident that it was related to the effect of impact forces on the geometric stiffness that is used by DRAIN-2DX to model P-Delta effects.

DRAIN-2DX bases the geometric stiffness on the static axial load which will be incorrect when large vertical forces are generated by impact. Apparently the resulting force imbalance is not reported by DRAIN-2DX as a force error and results in additional damping in the system. When the vertical inertia of the masses are set equal to zero in the computer model, there are no impact forces generated because additional forces cannot be generated in the vertical direction without violating vertical equilibrium. Under these conditions the additional damping due to impact disappeared. However, the solution was not very numerically stable and required very short time steps to produce acceptable force balance errors.

It was also observed from studying time histories of the wall responses that the forces generated by impact produced a high frequency, highly damped overlay on the response (See Section 6.5.4). The damping of this high frequency component of the response would produce energy loss in the system and be an additional source of overall damping.

As noted above, high frequency components of the response are affected mainly by the stiffness component of the damping provided. It was observed that the addition of only stiffness damping to walls modelled with impact, had a greater affect on the level of post cracking damping than would have been expected from the physical model described above for stiffness damping. This is probably explained by the effects of stiffness damping on the high frequency overlay in the wall response that was generated by impact.

Part of the damping provided in the model was provided by the above mechanisms involving impact. This had a number of advantages. The energy loss due to impact was closer to the energy loss mechanism expected in a real URM wall. It also produced a more uniform level of damping across the full period range of the wall's dynamic response to earthquake motions than would have been possible using only mass and stiffness viscous damping.

6.4.3 Difference Between Elastic and Inelastic Damping

Figure 6.5(a) indicates that the higher of the two levels of damping considered in the computer modelling of the walls is above 20% for longer period motion. These high damping values occur when the wall motion approaches the instability displacement, Y_{\max} .

However, the use of the logarithmic decrement method to evaluate the proportion of critical damping is strictly only applicable to linearly elastic systems with a single of

degree of freedom. The 20% damping value calculated for the non linear face loaded computer modelled wall represents a much smaller proportion of energy loss than it would for a linearly elastic system.

This can be illustrated by considering the example of 25% energy loss in both types of system as shown in Fig 6.6.

Figure 6.6 (a) is similar to Figure 5.1(c) and represents the load displacement relationship for a face loaded wall. In this example the wall is assumed to reach a peak displacement, $Y = Y_{\max}$ in the first half cycle of its free vibration response.

In the following half cycle the peak displacement is assumed to reduce to Y_2 . For 25% energy loss in the half cycle between the peaks, simple geometry dictates that $Y_2 = \frac{1}{2} Y_1$. Substituting $Y_1/Y_2 = 2$ in equation 12, the damping is evaluated using the logarithmic decrement method and results in a damping value of 22.% for the nonlinear face loaded wall system.

For a linearly elastic system undergoing the same 25% energy loss in a half cycle, the ratio of Y_1/Y_2 is much smaller as illustrated in Fig 6.6 (b). In this case it can be shown, using simple geometry, that $Y_1/Y_2 = 1.155$. The corresponding damping evaluated using equation 12 is then only 4.5%.

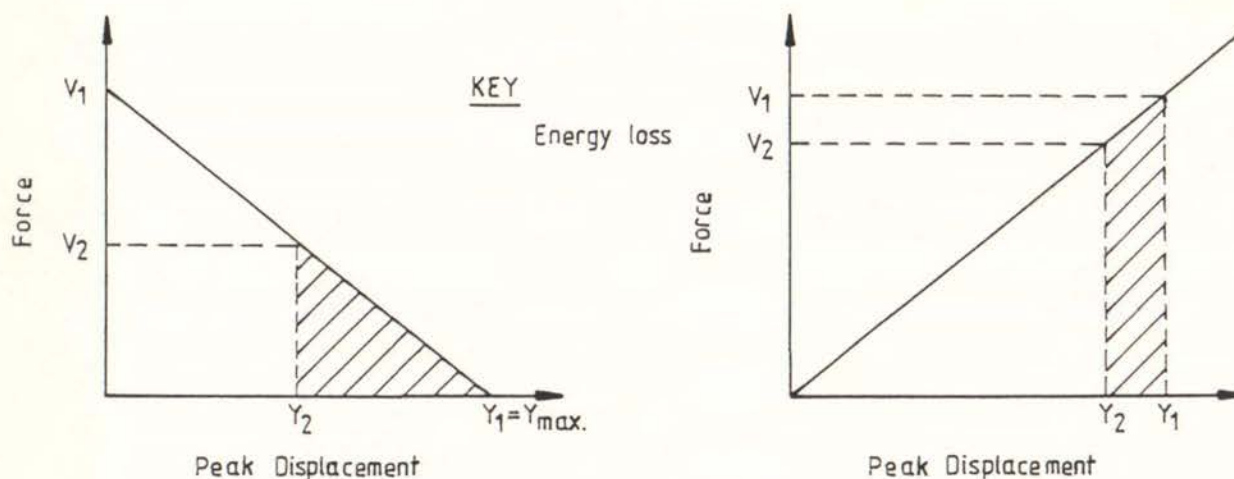


Fig 6.6 Reduction in Peak Displacement (Y_1 to Y_2) corresponding to 25% energy loss (a) for inelastic system representing a face loaded wall and (b) a linearly elastic SDOF system

When the peak displacement of a face loaded wall is significantly less than the instability displacement, Y_{\max} , the difference in damping evaluated for the two systems for a given energy loss is not as dramatic. For example, if the displacement of the face loaded wall in the first half cycle Y_1 is only $\frac{1}{2} Y_{\max}$, 35% energy loss in the next half cycle would correspond to 10% damping. The same 35% energy loss for a linearly elastic system would correspond to 7.1% damping.

No experimental damping test results applicable to the long period motion of face loaded walls were found during the literature search phase of this project.

Some testing of rocking URM piers was carried out by the ABK researchers (38(h)). However, the piers were relatively squat (3.35 high by 1.2 or 1.5m wide) and the maximum displacement applied at the top of the piers was relatively small (18mm). Damping values of 6.0 and 12.4% were obtained using the logarithmic decrement method for two of the piers in the first cycles of their responses. It was also noted that the damping decreased during cycles occurring later in the response when the peak displacement decreased. These damping values indicate that the short period damping levels shown in Fig 6.5 are reasonable.

The "Full" and "Reduced" levels of damping shown in Figures 6.5(a) and (b) respectively were generally the levels of damping considered for the computer modelling of face loaded walls in this project.

Experimental tests to determine damping values applicable to face loaded walls subjected to displacement near their instability displacement, Y_{max} , are required.

6.5 Comparison Between Computer Modelling and ABK Test Results

6.5.1 Introduction

Of the face loaded URM walls tested by ABK only three were constructed using clay bricks. The most comprehensive test results were published for the first of these walls (ABK wall specimen No. 1). Consequently this wall was selected for comparison with the results predicted by the computer model.

The face loaded wall model used in this phase of the project was practically the same as that previously used for the pulse loading study described in section 6.2. However, the location of the intermediate height crack shown in Figure 6.1 was moved up one node so that it was located at the $\frac{2}{3}$ wall height position. This was close to the position where the principal crack occurred during the testing of ABK's wall specimen.

6.5.2 Earthquake motion

As previously noted in Section 4.1, ABK used the output from a floor diaphragm computer model as the input motion at the top and bottom of their wall test specimens.

The earthquake motion used in the testing of the ABK wall specimen corresponded to the response of a stiff floor diaphragm responding to 1.25 times the N-S component of the 1940 E1 Centro Earthquake.

A time history of the actual input motion that the test wall was subjected to was not available for use in this project. This required an approximation of ABK's input motion to be used for the wall computer modelling. The approximate input motion was derived using a single degree of freedom (SDOF) oscillator as a diaphragm model. The SDOF diaphragm model was analyzed using DRAIN-2DX and subjected

to 1.3 times the 1940 N-S El Centro record. The acceleration time history obtained from the SDOF diaphragm model was then used as the input motion for the computer model of the face loaded walls.

This approximation assumes that an elastic SDOF system can capture the important features of the response produced by ABK's nonlinear, multi-degree of freedom floor diaphragm model. It also assumes that ABK were able to apply the intended motion to the test specimen. For the SDOF approximation, the effective period and damping were unknown. However, the peak velocity and acceleration of the ABK diaphragm model were given by ABK as 0.701 m/sec and 0.9g respectively. These values allowed the effective period of ABK's diaphragm motion to be estimated as 0.5 seconds using the relationship for peak pseudo velocity;

$$V_s = \frac{T}{2\pi A} \dots\dots\dots 13$$

where T is the period of an elastic oscillator and A is the peak acceleration, (in m/sec²).

The effective level of damping was then estimated using elastic velocity and acceleration response spectra for 1.3 times the El Centro earthquake motion. Peak velocities and accelerations obtained from the spectra for a 0.5 second period oscillator are shown in table 6.3 for three levels of damping.

Table 6.3 Peak Elastic Response of 0.5 sec SDOF oscillator

Damping	Velocity	Accel
5%	0.9	1.08
10%	.711 or .701	0.912
15%	0.6	0.8

A velocity response spectra at the 10% damping level was not available and the two velocity values shown in the table are the pseudo velocities calculated respectively from the spectral acceleration and displacement. It can be seen that the peak response values in the table corresponding to 10% damping are close to the peak values produced by ABK's diaphragm computer model. A damping value of 10% was, therefore, used in the SDOF computer model to derive the approximate diaphragm motion. This approximation of ABK's diaphragm motion was then used as the input motion for the wall model.

6.5.3 Comparison Between Tests and Modelled Input Motions

Figure 6.7 (a) shows the time history for the accelerations obtained using the SDOF diaphragm model. This is the acceleration time history used as the input motion at the top and bottom of the wall element in the wall computer model. The first 10

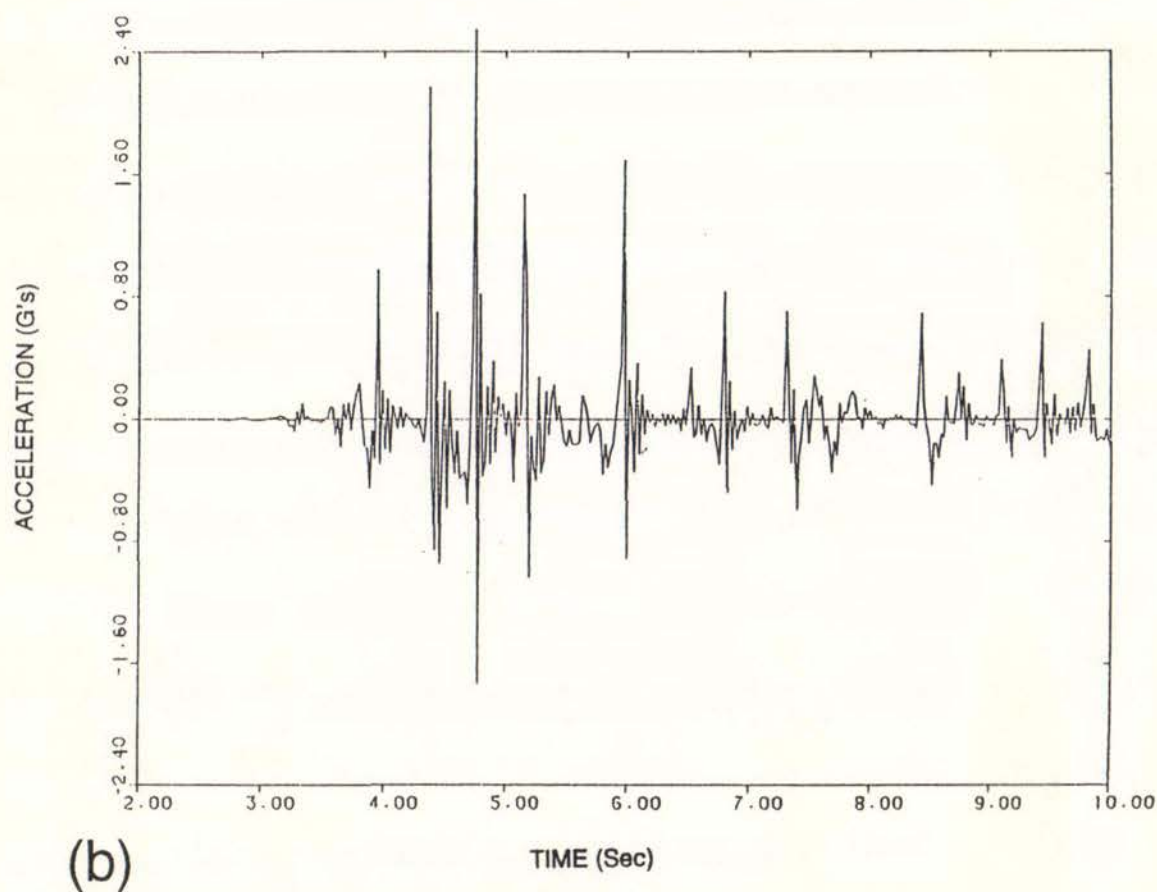
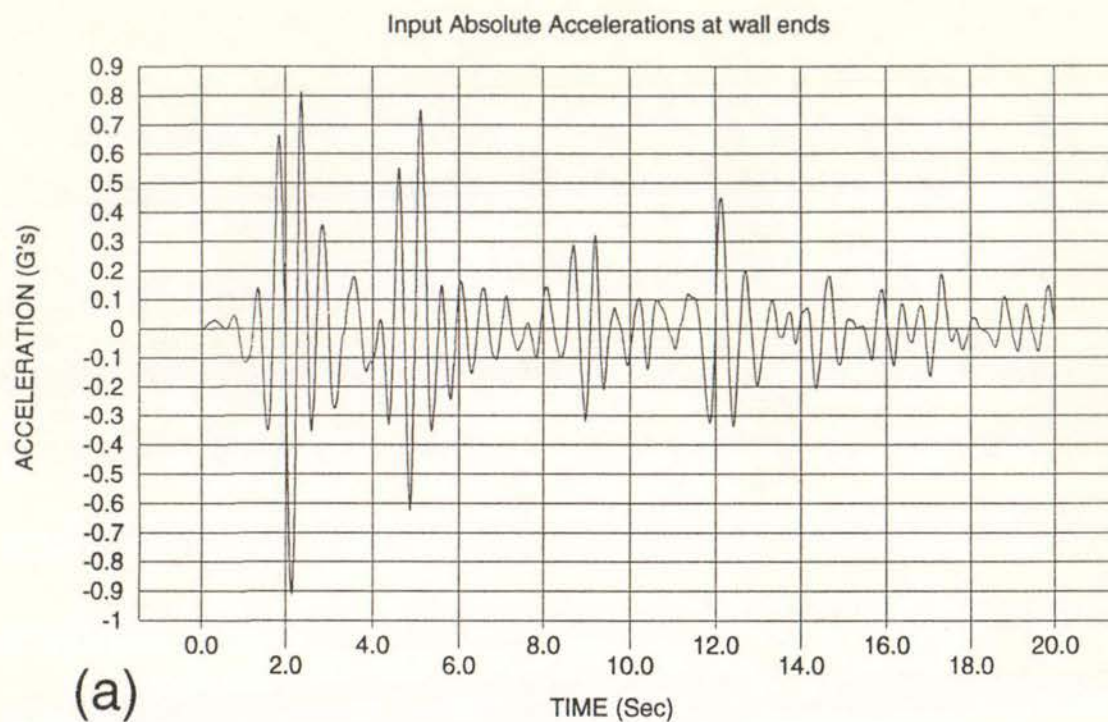


Figure 6.7 Input Accelerations at Top and Bottom of Wall
a) as used in computer model, and
b) as measured during testing of ABK wall 1

seconds of this history may be compared with the accelerations that were measured at the top of ABK's wall test specimen using an accelerometer. It can be seen that there is no agreement and that the 2.5g peak acceleration recorded by ABK is well in excess of their planned peak value of 0.9g. However, the SDOF diaphragm model did produce the peak value of 0.9g expected.

ABK (38 [f]) used displacement control in their tests and seem to have been unconcerned about discrepancies in the measured accelerations compared with those intended. They did conclude that jack forces measured during the tests could not be used to predict anchorage forces because the jack force time history was overlain with high frequency noise "generated by the displacement control system". This high frequency noise may also have effected the acceleration recorded at the top of the wall adjacent to the jacks.

Generally ABK appear to have practically ignored the accelerations they recorded at the top and bottom of the test walls and used velocities as a measure of the intensity of the imposed earthquake motion instead.

Figure 6.8(b) shows the input velocities derived using ABK's diaphragm computer models. ABK (38(f)) noted that "plots of velocity obtained by differentiating the recorded displacements fit the anticipated peaks" and that their "statistical analysis of the test results assumed the planned peak velocities were attained in the test runs". However, the agreement between the input velocities that ABK planned to apply to their test specimens and the input velocities actually applied to the specimens was not published by ABK.

Figure 6.8 (a) shows the input velocities obtained using the approximate SDOF diaphragm computer model used in this study. The velocities were calculated by integrating the acceleration time history shown in Figure 6.7(a).

It can be seen that the velocity time history shown in Figure 6.8 (a) is a reasonable approximation of that shown in Figure 6.8(b). However, the SDOF model produced a significantly higher peak velocity (1.03m/sec) than the 0.71m/sec targeted.

Agreement between the time histories would be improved by a baseline correction in Figure 6.8 (a) of -0.1 m/sec. This would be equivalent to giving the wall ends an initial velocity of 0.1 m/sec. The effect that this would have on the wall response was not evaluated.

It can also be seen that the time history in Figure 6.8(b) has some higher frequency content not evident in Figure 6.8(a). This is probably due to the higher mode responses of the multi-degree of freedom diaphragm computer model used by ABK.

6.5.4 Comparison Between Test and Modelled Wall Displacement

A comparison between the wall displacements predicted by the computer model and those measured during the testing of ABK's wall specimen is shown in Figure 6.9 (a) for the first five seconds of the walls response.

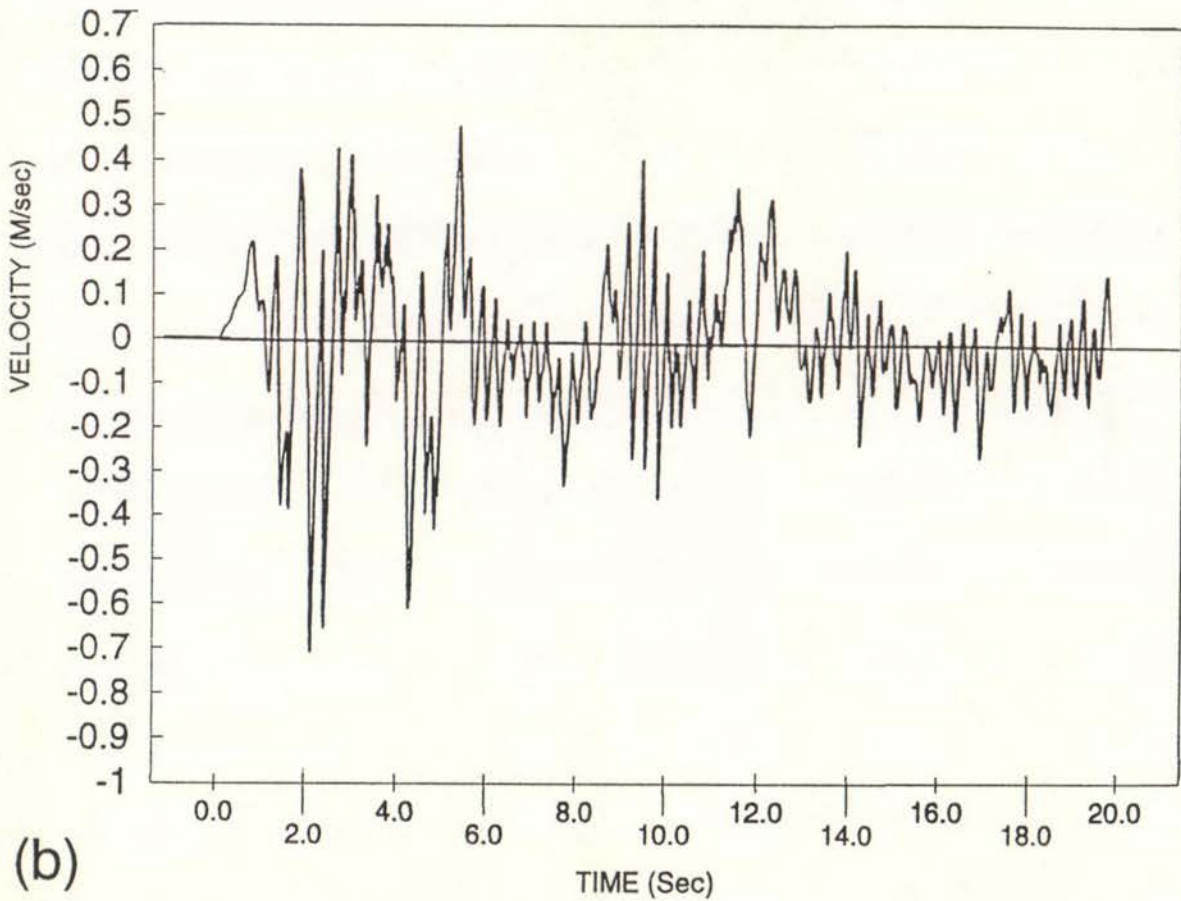
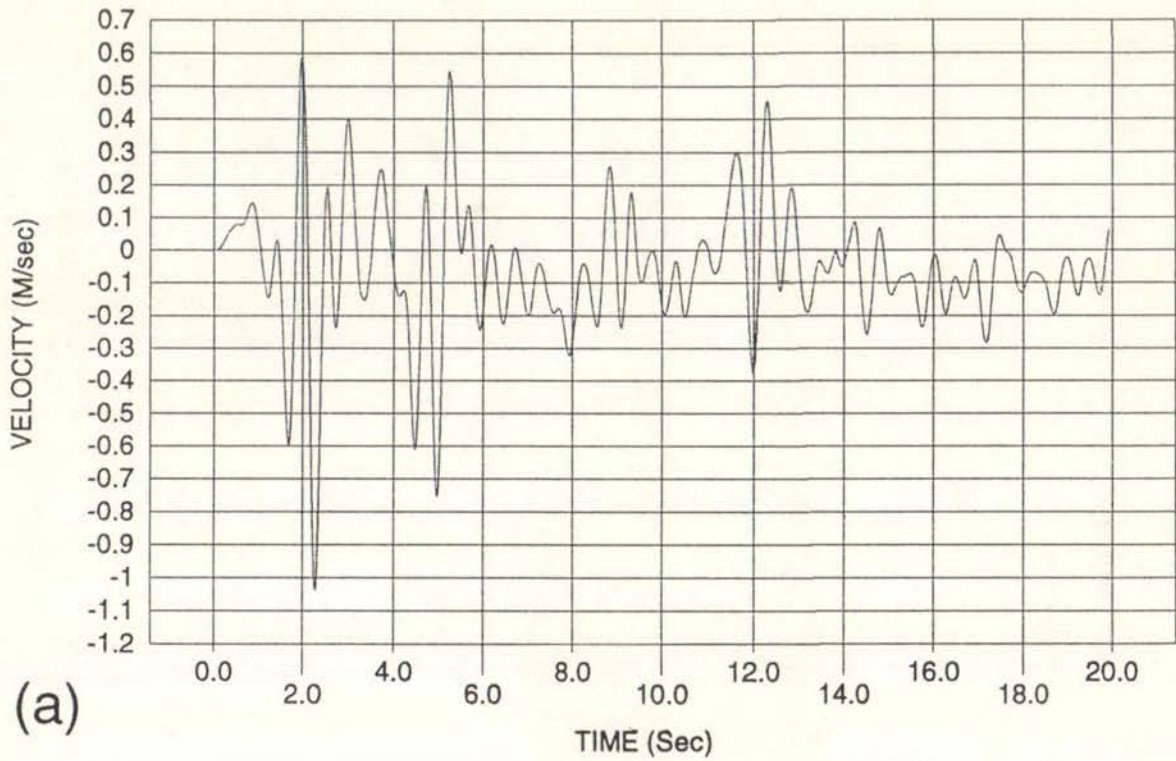


Figure 6.8 Input Velocity at Top and Bottom of Wall
a) as used in computer model, and
b) as measured during testing of ABK wall 1

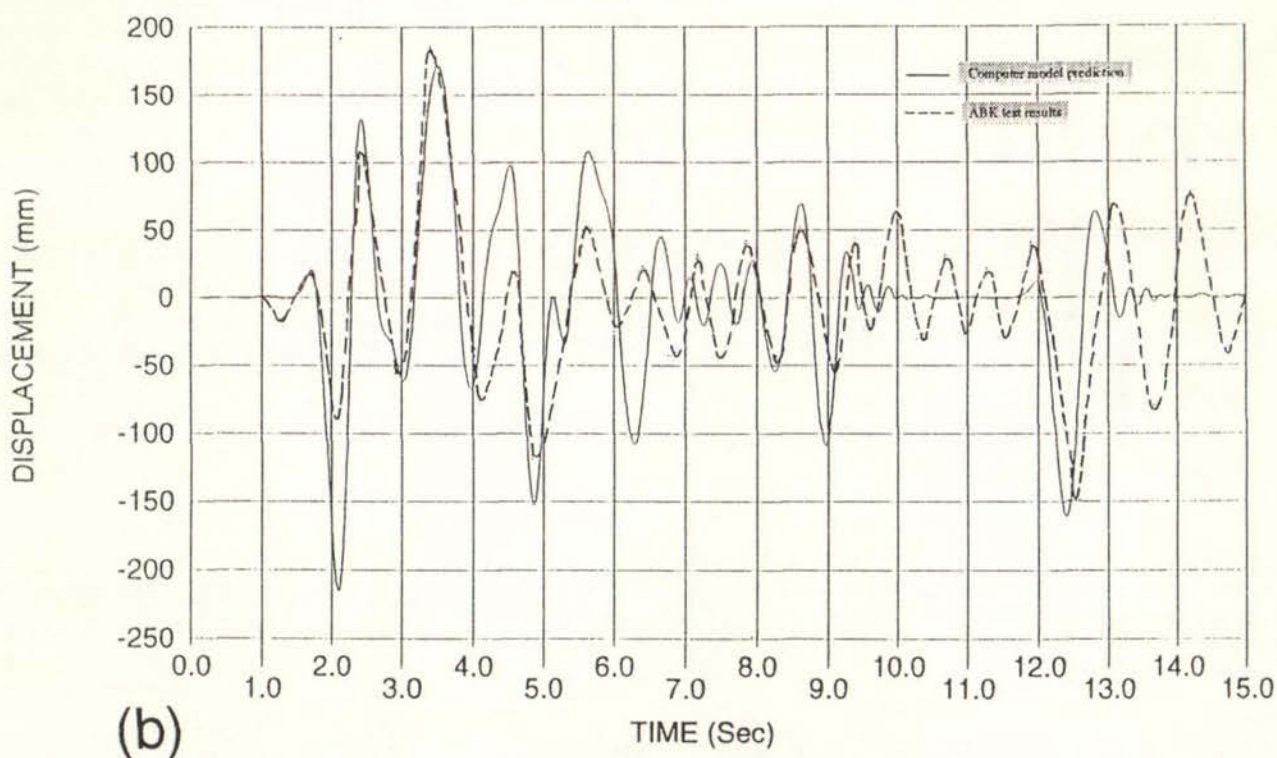
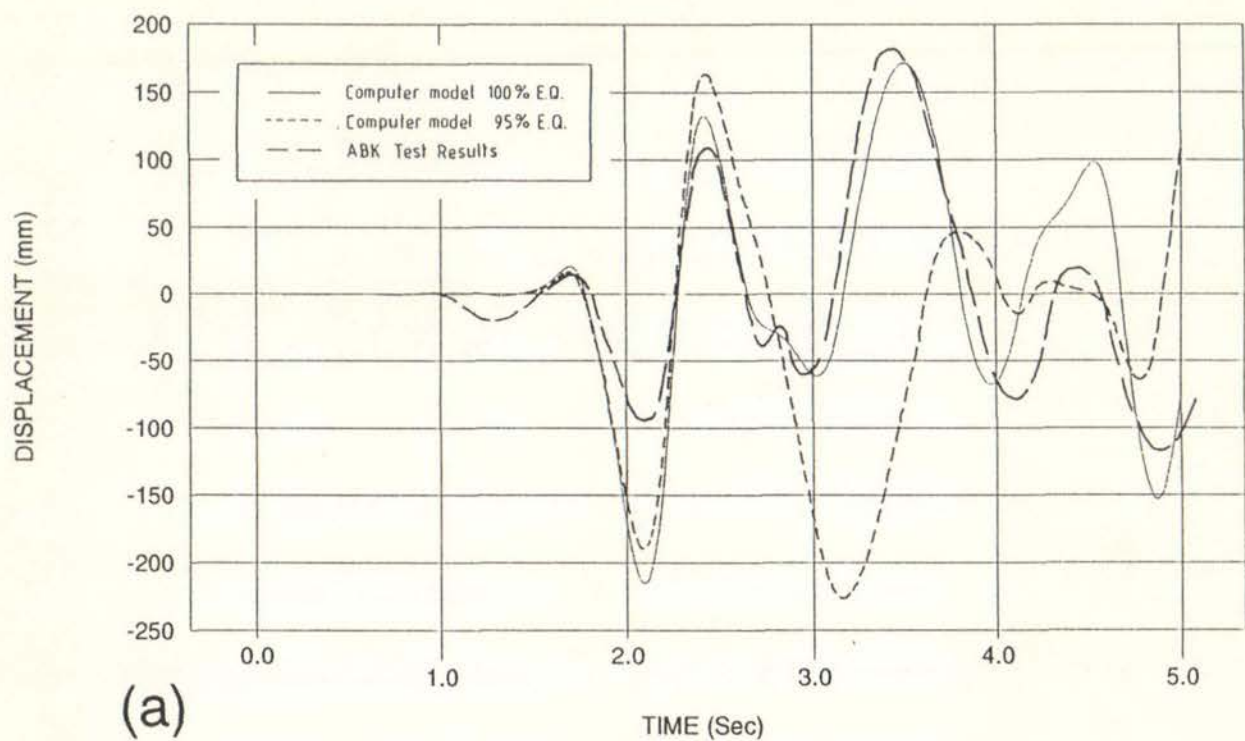


Figure 6.9 Comparison Between Face Loaded Wall Displacements Predicted by Computer Modelling and those Measured During Testing of ABK Wall Specimen No.1 for:

- a) first 5 seconds of response, and
- b) for first 15 seconds of response

The displacements were measured at (or close to) the crack occurring at the 2/3 wall height position in both the computer model and test specimen. For the comparison, the signs of the displacements published by ABK were reversed and a lead in period of 2.2 seconds for their published displacement time history was assumed.

When the acceleration time history shown in Figure 6.7(a) was used in an unmodified form as the input motion for the wall computer model, it was found that the peak wall displacement occurring at about 2.1 seconds into the time history approached the instability displacement, Y_{max} , of 306mm. This large displacement was generated by the acceleration pulse that is shown in Figure 6.7(a) with its peak about 1.9 seconds from the start of the time history.

To obtain the level of agreement between the predicted and test specimen displacements shown in Figure 6.9(a) for the 100% EQ load level, it was necessary to truncate the acceleration pulse occurring at 1.9 secs so that it had a maximum value of only 0.44g.

It was found that the detailed response of the wall predicted by the computer model was very sensitive to small changes in the input motion. This is illustrated in Figure 6.9(a) where the effect of reducing the intensity of the (truncated) input motion by 5% is shown. Similar large changes in the detailed response were also generated by relatively small changes in the truncation level of the input motion acceleration pulse occurring at 1.9 seconds. However, the detailed response was found to be less sensitive to changes in damping and wall stiffness.

The comparison between predicted and measured wall displacement at the 100% earthquake load level shown in Figure 6.9(a) is repeated in Figure 6.9(b) as part of the full 15 seconds of the time history analysed. Given the sensitivity of the detailed response to small changes in the input motion and the uncertainty regarding the actual motion applied by ABK to their test specimen the agreement is generally good.

It can be seen that the predicted response in Figure 6.9(b) is relatively flat between 9.5 and 12 seconds and after 13 seconds. The agreement between predicted and measured response between 9.5 and 12 seconds was improved when the stiffness damping coefficient was reduced from .006 to .002. The agreement after 13 seconds, was also quite good when the input earthquake motion used for the computer model was increased by 10%. However in both these cases agreement elsewhere in the response time history deteriorated.

6.5.5 Comparison Between Test and Modeled Wall Accelerations

Predicted and measured horizontal accelerations at wall mid-height are shown in Figure 6.10. Those predicted by the computer model are shown in Figure 6.10(a) and those measured by ABK during wall testing are shown in Figure 6.10(b).

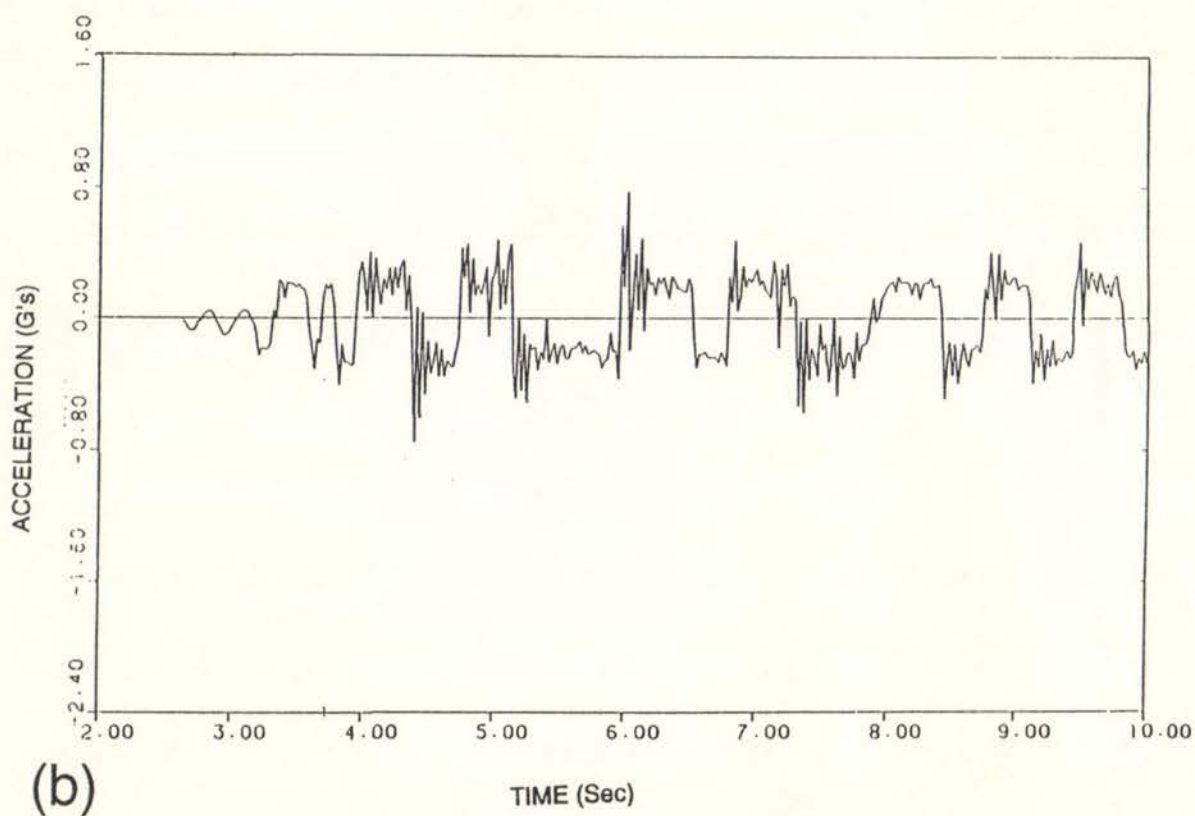
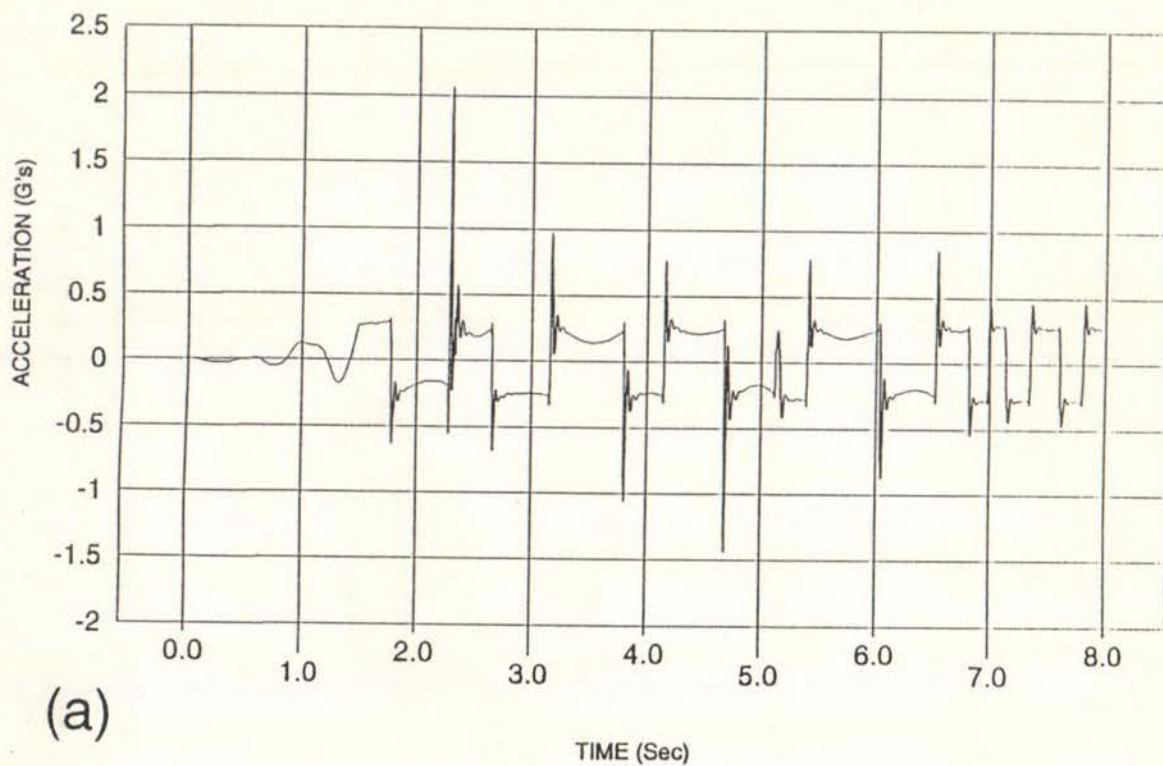


Figure 6.10 Accelerations at mid-height of the face loaded wall element

- (a) as predicted by the computer model and;
- (b) as measured during testing of ABK wall 1

By comparing the time histories in Figures 6.9(a) and Figure 6.10.(b) it can be seen that the high accelerations spikes, predicted by the computer model, correspond to the time intervals when the wall passes through its zero displacement position. At these time intervals the wall cracks close and impact occurs.

The impact forces only act for a short time and are unbalanced by static forces. Consequently they generate a high frequency motion that quickly damps out. This type of impact response has recently been studied theoretically by Psycharis (47) and will not be described here in more detail.

It can be seen that the main difference between the measured and the predicted responses is that the measured response does not have a sharp impact spike and the high frequency impact motion does not damp out as quickly. This reflects the limitations of the computer model. DRAIN-2DX aims to achieve an energy balance at each time step and the damping has to be provided by viscous damping throughout the response. In the wall test specimen most of the energy loss probably occurs on impact so that the damping in the remainder of the response does not have to be as high to achieve the same energy loss.

The "flat" part of the acceleration response shown, corresponds to the period when the wall cracks are open. It can also be seen that the accelerations are lower near the centre of this flat portion of the response.

This reduction in acceleration corresponds to the reduced lateral load capacity of the face loaded wall as its displacement tends towards the instability displacement, Y_{max} (see Fig 5.1.(c).)

A formula similar to equation 8 (adjusted for cracking at $\frac{2}{3}$ wall height) was used to calculate the acceleration corresponding to the uniformly distributed load required to just open the wall cracks. The calculated value of 0.27g appears on average to be less than the "flat" portion of the acceleration responses shown in Figure 6.10.

Nevertheless the slope of the acceleration response at impact shown in Figure 6.10(a) can be used to estimate the time after impact that the cracks open. Using this time interval and the velocity given by the slope of the displacement response, shown in Figure 6.9(b) it is possible to estimate the wall displacement at crack opening.

On average this was computed to be 3.4 mm at the $\frac{2}{3}$ wall height crack. Using an elastic modulus for the brickwork of $E = 1.0\text{GPa}$, the elastic deflection of the wall at crack opening was calculated to be approximately half this displacement for a uniformly distributed load. The area of the link members used in the computer model (0.025 M^2) was selected so that the deformation of the links at opening of the crack at the base of the wall contributed the remaining 50% of the estimated deformation.

As the actual E value of the brickwork used by ABK is not known this allocation of flexibility between the links and wall is arbitrary. However the wall response was found to be relatively insensitive to changes in the stiffness of the wall and link elements.

6.5.6 Anchorage Forces and Vertical Accelerations

Forces developed in the diaphragms at the top and bottom of wall element are important because they represent the forces that need to be resisted by the diaphragms and by the anchorages that tie the diaphragms to the walls.

The anchorage forces developed at the top of the computer modelled wall are shown in Figure 6.10(c). As noted above, ABK were unable to record meaningful anchorage forces so that a comparison between predicted and measured anchorage forces is not possible.

However, it is unlikely that the sharp spikes in the anchorage force response evident in Figure 6.10(c) would have been present in the test specimen response as these spikes correspond to impact. The reader can confirm the influence of impact on the anchorage forces by comparing the time histories in Figures 5.9(b) and 6.11.

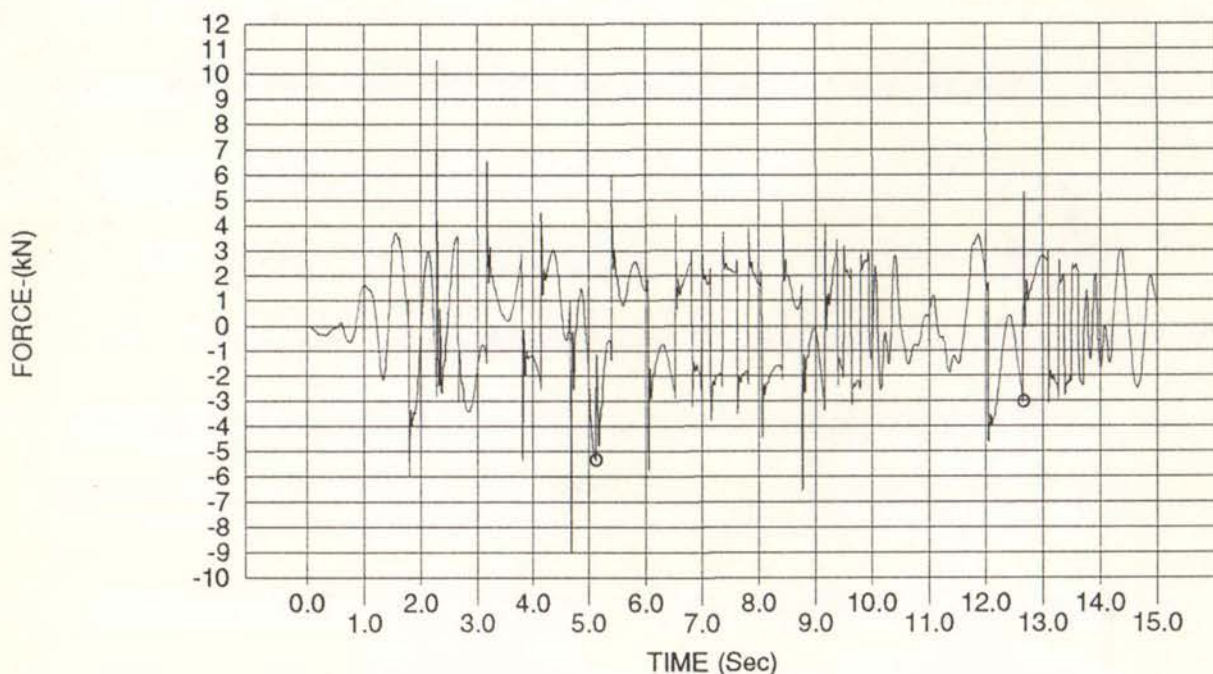


Figure 6.10(c) Force in top Diaphragm as predicted by Computer model (for rigid Diaphragm)

ABK also recorded vertical accelerations at the top of their wall test specimen. The maximum recorded acceleration was 1.6g and this can be compared with the maximum acceleration spike in the response predicted by the computer model of 12.5g. However the maximum axial load at the base of the wall, as predicted by the computer model, indicated that the average vertical acceleration in the wall was only 4.0 g.

It may be concluded that DRAIN-2DX is unable to model accurately the short time interval during which impact occurs.

However, the high impact forces only act for a short time interval and are imposed on the wall when it is at its zero displacement position. At this time the wall is in its most stable condition. Consequently, it would appear that the impact forces do not significantly affect the wall's displacement response. Hence they do not prevent the computer model from being used to predict the stability of face loaded walls. However, the effect of impact forces on damping and predicted anchorage forces can not be ignored, at least when the diaphragms are modelled as essentially rigid.

6.5.7 Comparison Between Predicted and Measured Collapse Earthquake Intensity

When ABK increased the intensity of the input motion for their wall test specimen by 20% the wall collapsed.

When the input motion for the wall computer model was increased in 10% increments and the acceleration pulse at 1.9 seconds was truncated (at 0.44 g) the wall did not collapse until the input motion was increased by 40%. With the acceleration pulse not truncated, collapse occurred when the input motion was increased by 20%.

The effect of moving the crack position from $\frac{2}{3}$ the wall height to mid-height will be seen from the results presented in Section 7.2.1. However, in this case the maximum stiffness damping coefficient used was also reduced to 0.004.

6.5.8 Damping

The damping coefficients used for the comparative computer modelling of ABK's test wall were $\alpha = 0.6$ and $\beta = 0.006$. It was hoped that the comparison between the response predicted by the computer model and the test results would provide an indication of the appropriate level of damping to use in the computer model.

However, the relative sensitivity of the computer model's response to small changes in the input motion and uncertainty regarding the actual input motion applied by ABK to their test wall specimens made this impossible.

Two levels of wall damping were generally used for the computer modelling of the walls in this project. The "full" level of damping used $\alpha = 0.6$ and $\beta = .004$ and the "reduced" level of damping used $\alpha = 0.0$ (or .006) and $\beta = .004$. A reduced level for the component of damping generated by impact (section 6.4.2) was also considered when the walls were modeled with flexible diaphragms. These damping levels are less than the values assumed for the comparative computer modelling of ABK's test wall and can be expected to produce conservative predictions of face loaded wall stability.

6.6 Effect of Wall Thickness and Earthquake Intensity on Face Loaded Wall Stability

6.6.1 Introduction

The computer model used in this part of the project to study the seismic stability of face loaded walls was the same as that described in section 6.2.

The intermediate height crack was assumed to be at the mid-height of the wall and the diaphragms were modelled as essentially rigid. Three earthquake motions; DZ4203, Weber and Tabas were used to assess effect of different earthquake motions and intensities.

For each earthquake motion, walls with 3 thicknesses were studied. However the wall slenderness (H/t) was kept constant so that the 3 wall thicknesses corresponded to the $\frac{1}{2}$, 1 and 2 x scale walls that were previously described in section 6.2. The factors used to scale the properties of the elements in the face loaded wall computer model are given in table 6.1.

Two levels of damping, as described in sections 6.4.2 and 6.5.6, were generally considered for each scale of the wall model and the effects of varying the wall stiffness was also considered in some instances. Where non standard damping or wall properties were used this is noted on the graphs where the analysis results are plotted.

6.6.2 Wall Displacement Response to the DZ4203 Earthquake Motion

A computer program (WAVE) was used to modify the acceleration time history of the 1940 El Centro NS earthquake motion so that its 5% damped spectra more closely matched the "equal risk" spectra given in New Zealand's draft loading code (40). Further details of this earthquake motion are given in a later section (6.7.2) of this report. This modified earthquake will be referred to in this report as the DZ4203 earthquake motion.

To evaluate the effect of earthquake intensity on the stability of face loaded walls the intensity of the input motion used for the computer analysis was gradually increased by scaling until the wall "collapsed". The relationship between the displacements at the mid-height crack in the wall and the DZ4203 earthquake intensity is shown in Fig 6.11(a) for the full scale wall model. The wall displacements shown have been normalised using the displacement at which the wall becomes unstable, Y_{max} , which was calculated using equation 4.

It can be seen that the results for the lower (reduced) level of damping considered fall into two zones. The upper and lower envelopes of these zones are also shown. It can also be seen that the results that lie near the upper envelope correspond to narrow bands or windows of earthquake intensity. This behaviour demonstrates the sensitivity of the wall response to small changes in the earthquake motion.

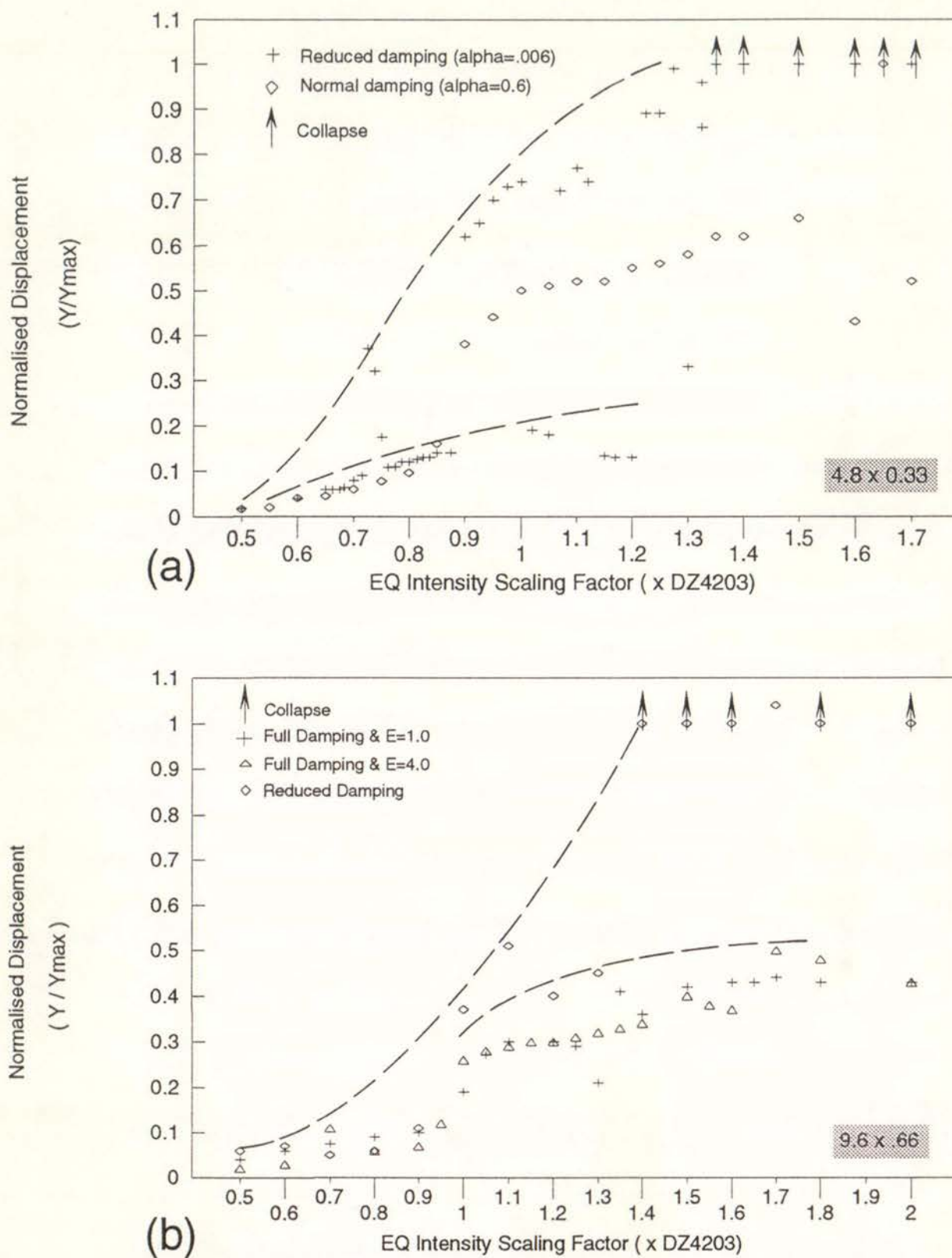


Figure 6.11 Normalised Displacements of wall at the Mid-height crack level vs the Scaling Factor applied to the DZ4203 Earthquake Motion.

a) For full scale (4.8 x .33 m) wall; and
 b) for 2 x Scale Wall

When the wall is displaced beyond about $0.6Y_{\max}$ only a small additional adverse acceleration pulse is required to make the wall unstable. As the wall is responding inelastically, a change in the earthquake intensity generates a phase shift between the earthquake loading and the wall displacements. Hence, a small increase in earthquake intensity can result in a pulse that was causing wall instability to act at a different time in the response and stabilise the wall instead. With increasing earthquake intensity the average wall displacement tends to increase and a smaller adverse pulse is required to cause collapse. Therefore the wall tends to become less stable.

It is unlikely that this aspect of the wall behaviour would have been evident during the testing of face loaded wall specimens by ABK. Although ABK gradually increased the intensity of the earthquake motion during their test sequence they also varied the nature of the motion by using motions that corresponded to a variety of diaphragm or ground motions for each wall tested. It can be seen from Figure 6.11(a) that a large number of analyses with a single earthquake record are required to establish any pattern for the results.

For the "full" damping case considered, the wall displacements were reduced significantly and appeared to be more stable. However at an earthquake intensity scaling factor of 1.65 the wall displacement suddenly increased beyond Y_{\max} and the wall collapsed.

Similar results for the 2 x scale wall are shown in Figure 6.11(b). For the analyses with full damping, collapse did not occur for the range of earthquake intensity considered. To investigate whether changes in the wall properties could cause a sudden increase in the displacement, the stiffness of all wall elements, except the links, was increased by a factor of 4. It can be seen that this made no significant difference to the fully damped wall response.

This contradicts the findings of Zoutenbier (43) who concluded that the stiffness of the wall was a significant factor affecting wall response.

Results from the computer analysis of the $\frac{1}{2}$ x scale wall and the DZ4203 earthquake motion are given in Figure 6.11(c). It is evident that the wall responded practically elastically without significant opening of the wall cracks up to an earthquake intensity scaling factor of approximately 0.8. Only a small increase in the earthquake intensity was then required to cause the wall to collapse. With reduced damping the response of the wall increased but the collapse earthquake intensity was not significantly effected. Once again increased wall stiffness ($E = 4.0$ case) did not affect the results significantly.

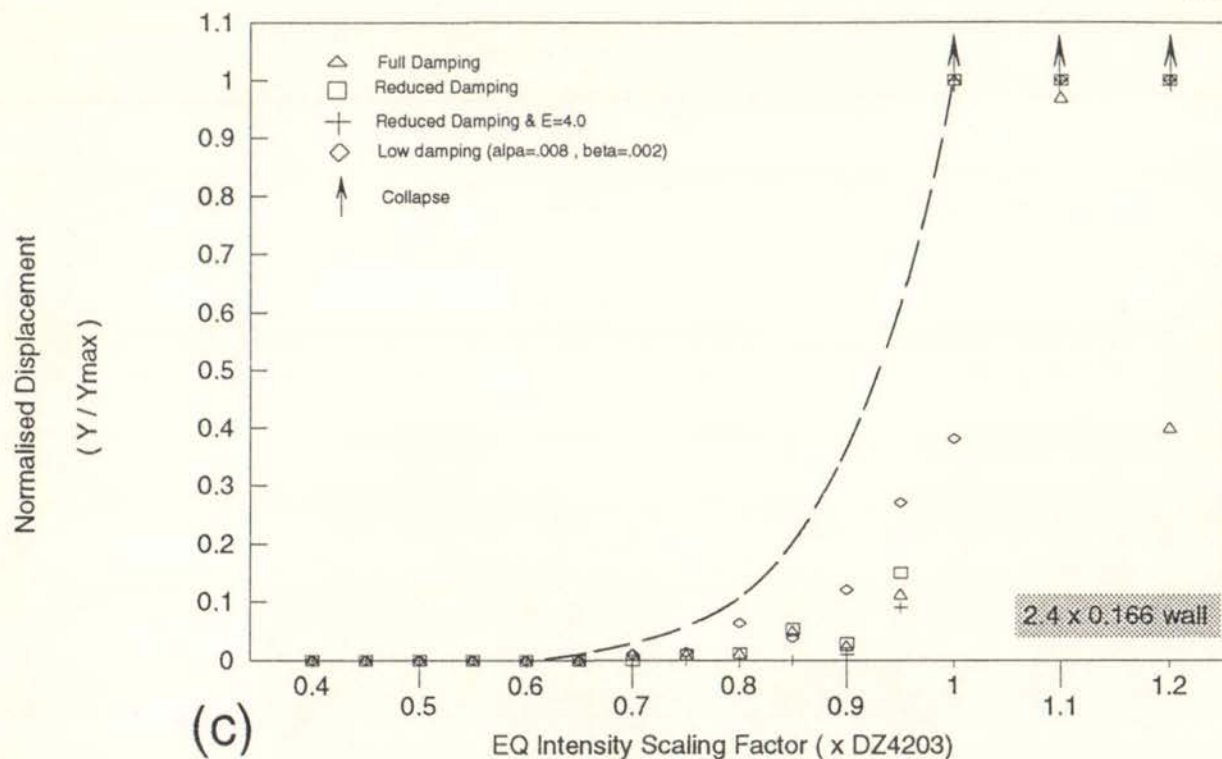


Figure 6.11(c) Normalised Wall Displacement at the Mid-Height Crack Level for 1/2 Scale Wall and DZ4203 EQ Motion

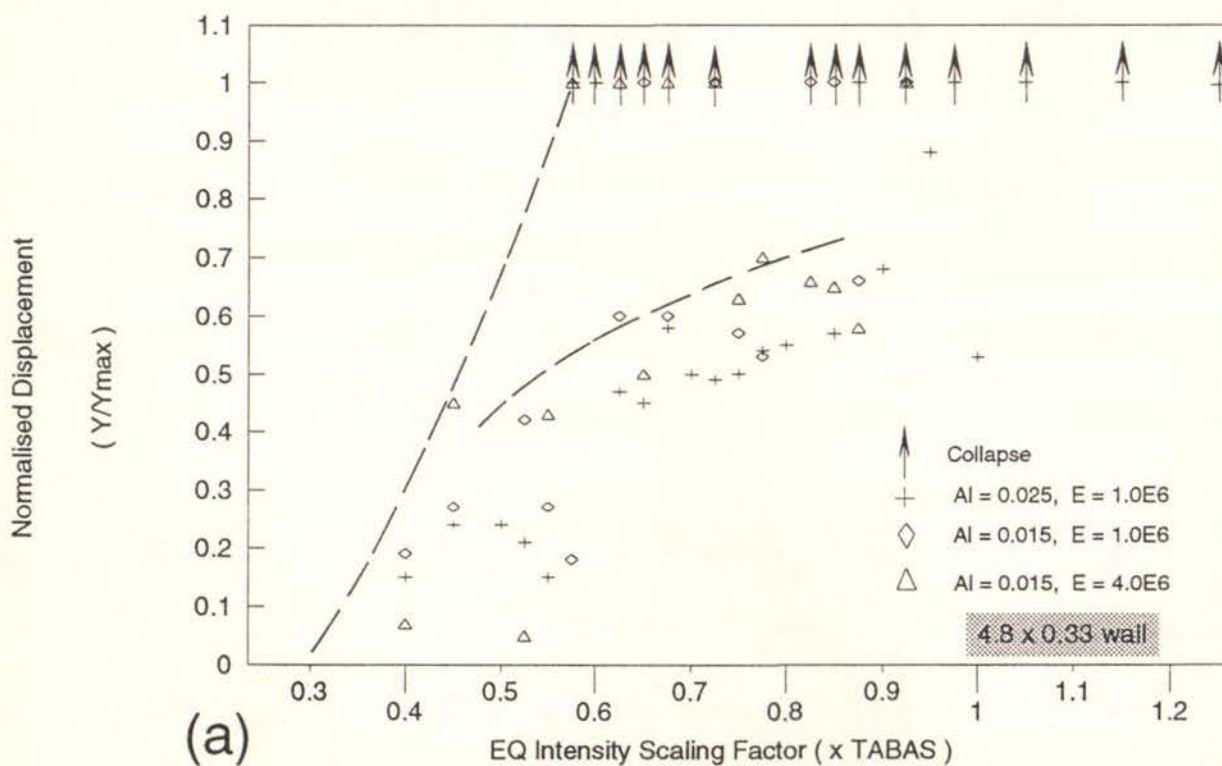


Figure 6.12(a) Normalised Wall Displacement at Mid-Height Crack Level for Full Scale Wall and TABAS EQ Motion. Reduced Damping Case Only ($\alpha = 0.0$, $\beta = 0.006$).

Note : Al = area of buckling links in m^2

6.6.3 Wall Displacement Response to Tabas and Weber Earthquake Motions

The transverse component of the Tabas earthquake (16 September 1978) is one of the strongest ground motions ever recorded. It was selected for this study to represent the ground motion that could be expected close to the epicentre of a catastrophic earthquake. An examination of the response spectra details for this component of the earthquake record indicated that elastic structures with periods between 0 and 4 seconds would have had their peak responses within the first 16.5 seconds. Consequently the first 16 seconds of the record was selected for the analysis.

The Weber earthquake (13 May 1990) was selected for this study because it is the strongest earthquake motion recorded in New Zealand. Also this earthquake caused significant damage to some masonry buildings in Dannevirke so that the observed damage could be correlated with that predicted by this study. The earthquake input motion used in the analysis was the transverse N67E component of the ground motion recorded at Dannevirke Post Office. Further details of this earthquake were given in Section 2.7.

The response spectrum for the Weber earthquake motion selected, indicated the peak response for elastic periods between 0 and 4 seconds would occur in the first 23 seconds of the motion. However, preliminary wall analyses indicated that the response in the first 5 seconds was not significant and that a peak response was unlikely in the last 5 seconds. Consequently the analysis was "switched off" for the first 5 seconds and was terminated at 18 seconds from the start of the record.

Results of the analyses for the Tabas and Weber earthquake records are shown in Figures 6.12 and 6.13 respectively. The general form of the result is similar to that described above for the DZ4203 motion.

In most cases a lower envelope as well as the upper envelope could be discerned in the results. The lower envelopes suggest that it only takes a small adverse fluctuation in the response or earthquake input motion to cause collapse when the wall reaches a displacement of about 60% of the instability displacement, Y_{max} . This type of behaviour and the general shape of the upper envelopes are consistent with the wall response under pulse loading previously described in section 6.4 and indicated in Figure 6.3.

6.6.4 Anchorage Forces for Rigid Diaphragms

As previously discussed in Section 6.5.4 the peak diaphragm forces predicted by the computer model are affected by the forces that develop in the wall during the very short time interval corresponding to impact. The comparison with the ABK test results indicated that these forces will probably not develop in a real URM wall.

Figure 6.10(c) is typical of the time histories obtained for the anchorage forces developed in the diaphragms using the computer model. If the short spikes associated with impact are ignored the peak diaphragm force in this time history occurs at approximately 5.1 seconds (as indicated by a small circle). The peak force in the top diaphragm of the full scale walls were evaluated from similar time history plots ignoring the sharp spikes and are shown in Figure 6.14(a).

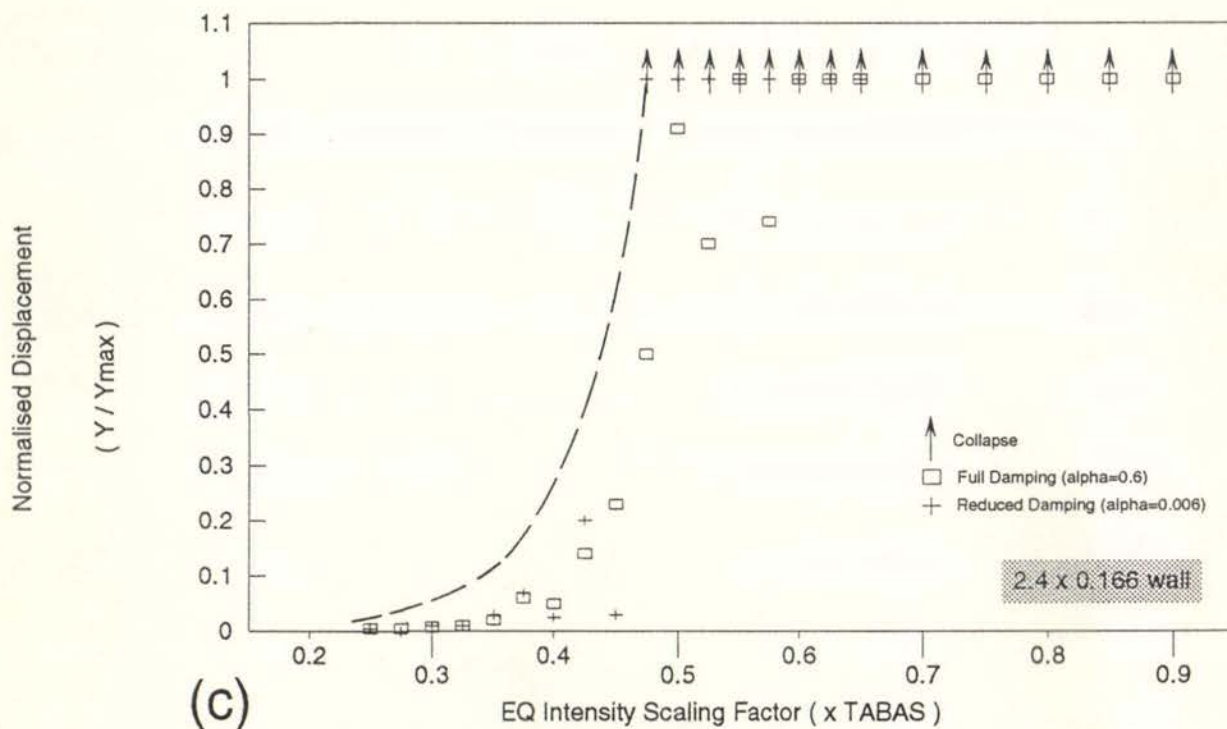
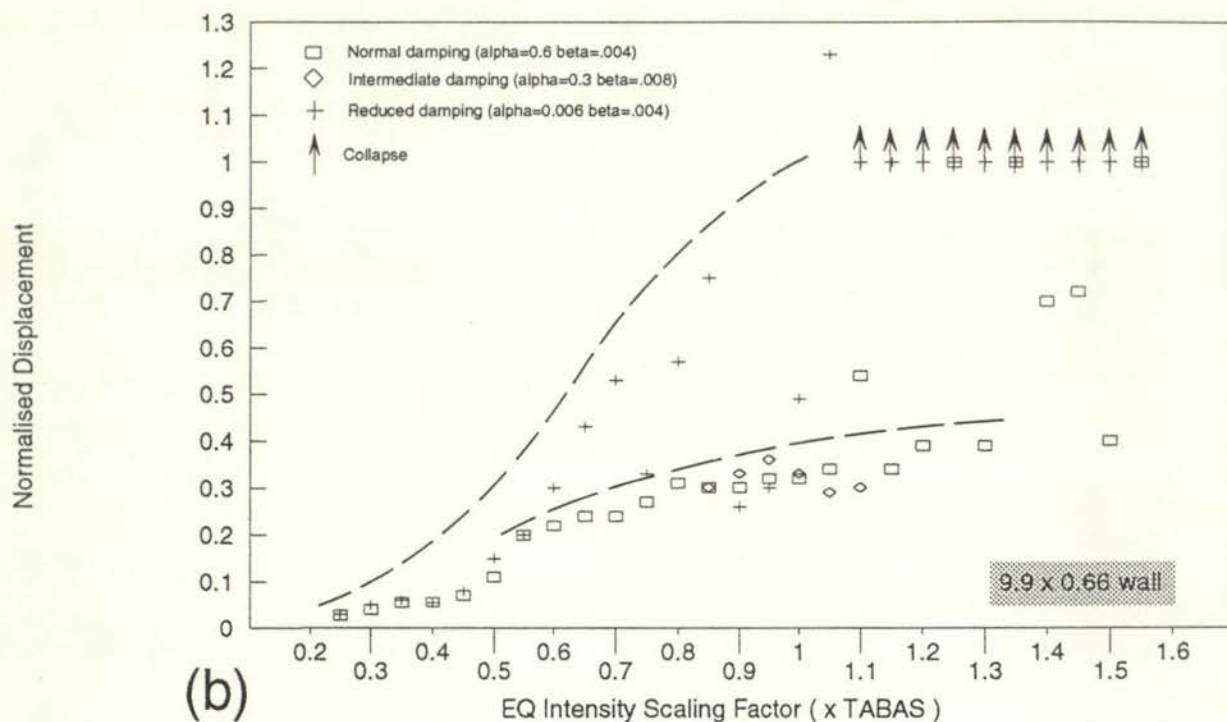


Figure 6.12(b) and (c) Normalised Wall Displacement at Mid-height Crack Level vs the Scaling Factor Applied to the TABAS EQ Motion. (b) for 2 x Scale Wall; and; (c) for 1/2 x Scale Wall

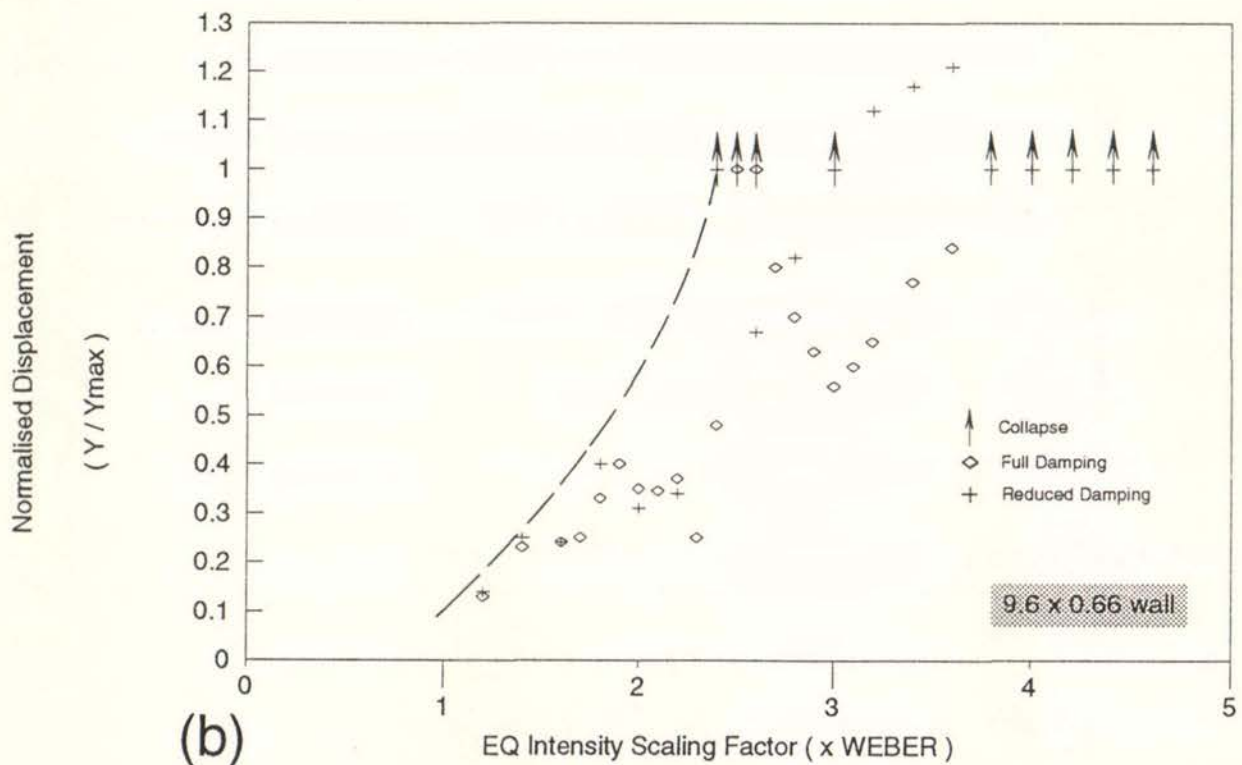
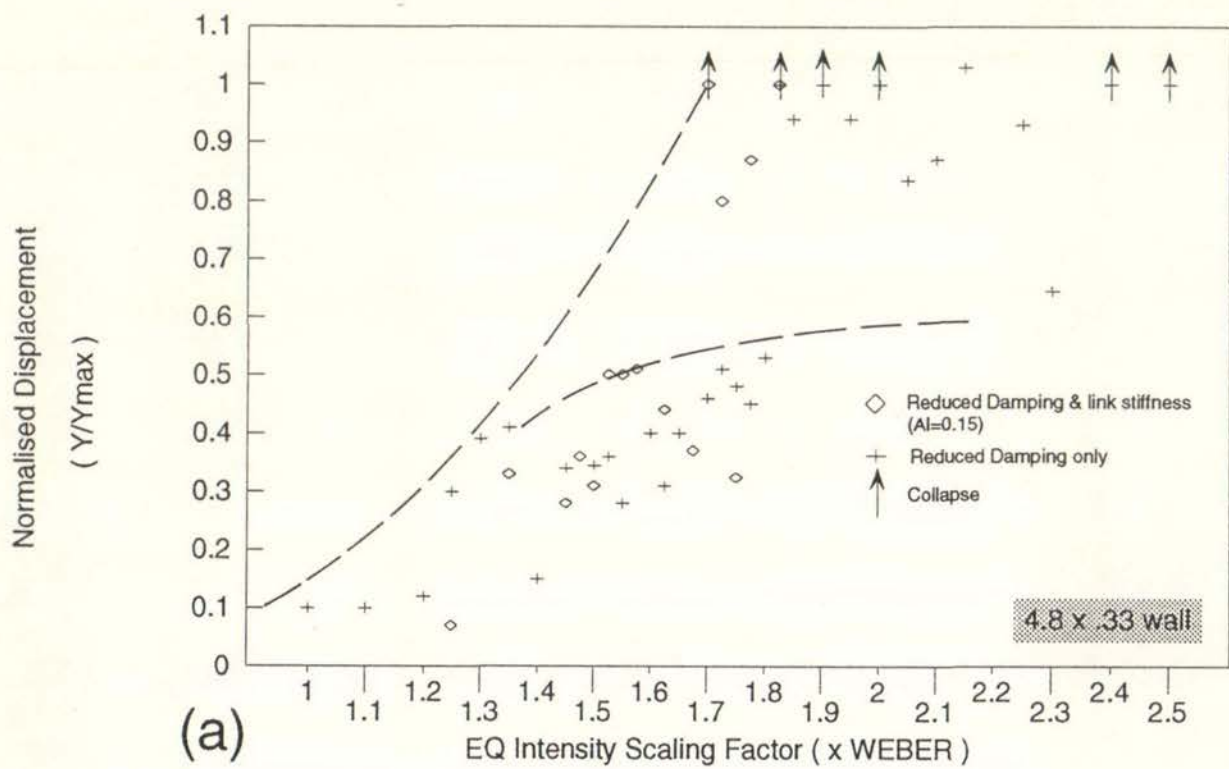


Figure 6.13 Normalised Wall Displacement at Mid-height Crack Level vs the Scaling Factor Applied to the WEBER EQ Motion. (a) for Full Scale (4.8 x .33m Wall) and; (b) for 2 x Scale Wall

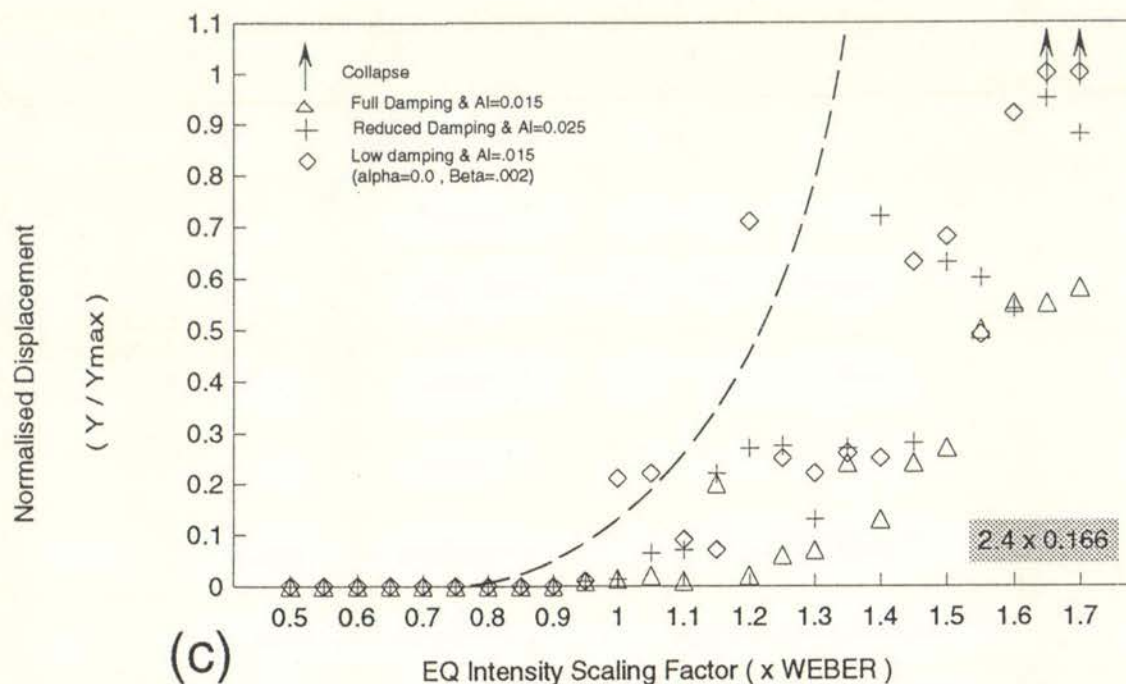


Figure 6.13(c) Normalised Wall Displacement at Mid-height Crack Level 1/2 Scale (2.4 x .166m) Wall and WEBER EQ Motion

Also shown (dotted) is the reaction (of 4.6 kN) that would develop at the top of the wall if the wall was loaded with the static uniformly distributed load that was just sufficient to start opening the cracks in the wall. This reaction was evaluated using equations 3, 7 and 8 given in Section 5.1.

It can be seen that the anchorage force is not dependent on the type of earthquake motion and is practically independent of the wall displacement and hence earthquake intensity. It would appear that the wall cracking acts like a fuse, limiting the anchorage force that can be developed. However, the results indicate that the anchorage force under dynamic conditions can be up to 50% greater than that calculated using a static analysis of the wall.

An examination of Figure 6.10(c) indicates that the Anchorage force tends to have a peak just before impact. This peak force is unlikely to be affected by the sharp spike in the anchorage force that develops at impact and, therefore, should set a lower limit on the Anchorage force that would develop in a real URM wall. The peak force evaluated using this method would occur at 13.7 seconds in the typical anchorage force time history shown in Figure 6.10(c) (and is indicated by a small circle).

The anchorage forces predicted by the computer model and evaluated using this methodology are shown in Figure 6.14(b). It can be seen that the anchorage force in this case is generally less than would be predicted by a static analysis of the face loaded wall.

Similar results are given in Figures 6.14(c) and (d) for the bottom diaphragms of the full scale wall and in Figure 6.15(a) to (d) for 1/2 and 2 x scale walls.

Diaphragm anchorage forces are also discussed in section 7.2.4.

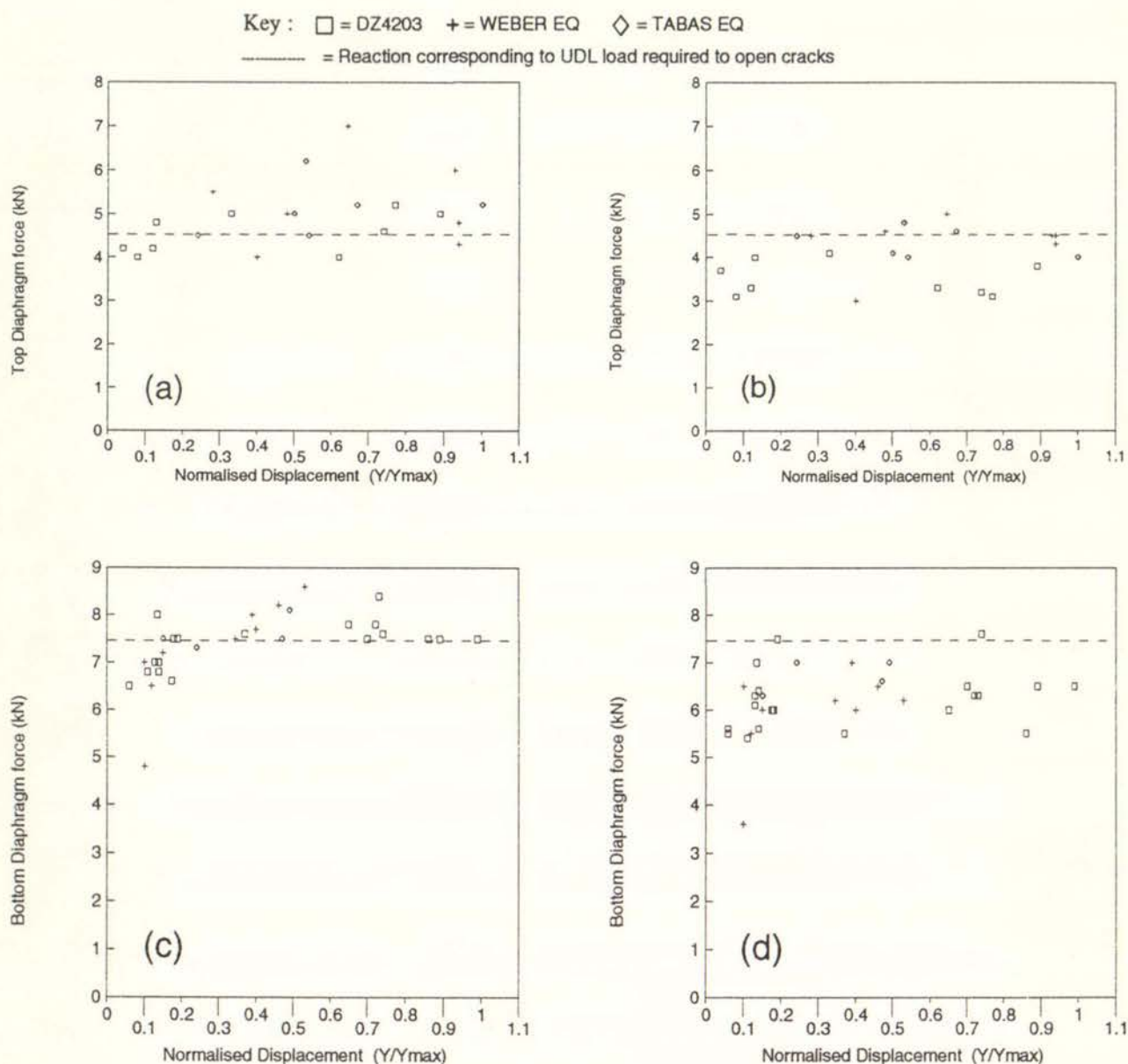


Figure 6.14 Anchorage Forces for Rigid Diaphragm and the Full Scale (4.8 x .33m) wall.

- (a) Peak Force in Top Diaphragm (ignoring 1st peaks due to Impact)
- (b) Force in Top Diaphragm (Maximum of Peaks Occurring just before Impact)
- (c) Peak Force in Bottom Diaphragm (ignoring 1st Peaks due to Impact)
- (d) force in Bottom Diaphragm (Maximum of Peaks Occurring Just Before Impact).

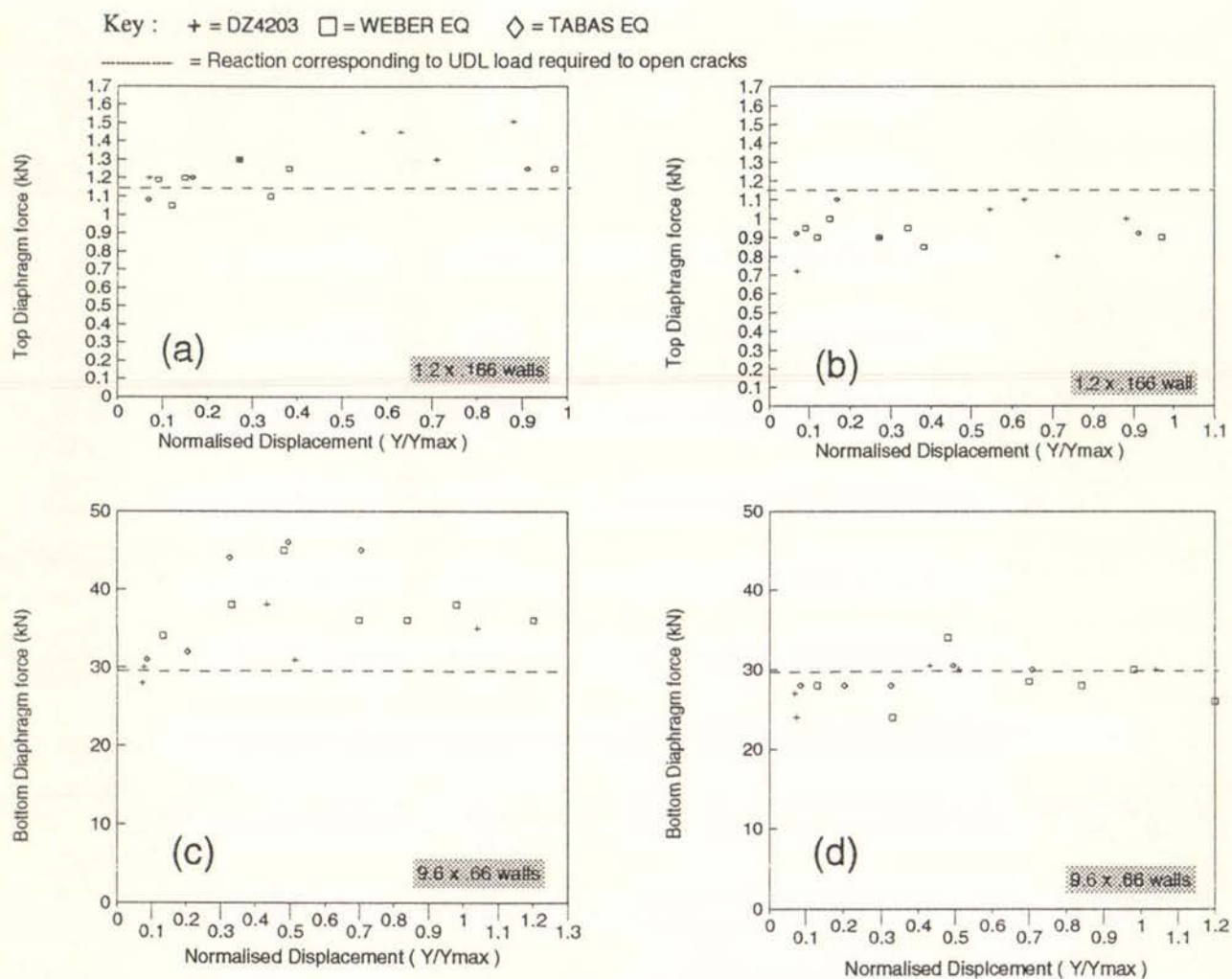


Figure 6.15 Anchorage Forces for Rigid Diaphragm;

- Peak Force in Top Diaphragm for 1/2 x Scale Walls (ignoring 1st peaks due to impact)
- Force in Top Diaphragm for 1/2 x Scale Walls (maximum of peaks occurring just before impact)
- Peak Force in Bottom Diaphragm for 2 x Scale Walls (ignoring 1st peaks due to impact)
- Force in Bottom Diaphragm for 2 x Scale Walls (maximum of peaks occurring just before impact)

6.7 Prediction of Face Loaded Wall Stability Using Displacement Response Spectra

6.7.1 Introduction

The ABK joint venture (38) used peak velocity as the indicator of earthquake intensity in their analysis of the seismic stability of face loaded walls. Zoutenbier and Priestley (42,43) used peak acceleration as their indicator. Peak velocity is likely to be a better indicator of intensity than peak acceleration, as it takes into account the length of time an acceleration pulse acts.

However, the stability of face loaded walls depends mainly on displacements and the displacement that a velocity pulse generates also depends on the time that the velocity pulse acts. It was postulated for this project that the displacements predicted by an elastic response spectrum would be a better indicator of earthquake intensity, as the use of displacement spectra should automatically take into account the duration of a velocity pulse as well as the magnitude of its peak.

6.7.2 Elastic Response Spectra for DZ4203, Weber and Tabas EQ Records

Figure 6.16 shows acceleration and displacement response spectra for the DZ4203 earthquake motion. The derivation of this motion was described previously in section 6.6.2.

The match between the DZ4203 acceleration spectrum and the 5% damped acceleration spectrum for the DZ4203 motion achieved by the WAVE program can be seen to be quite close in the period range 0 - 2 seconds (Fig 6.16(a)).

A pseudo displacement response spectrum can easily be derived from the DZ4203 acceleration design spectrum using the relationship:

$$Y = (T/2\pi)^2 A \dots\dots\dots 14$$

where A is the spectral acceleration (in m/sec²) for a SDOF elastic oscillator with period T and Y is the pseudo spectral displacement.

The resulting pseudo displacement spectrum for the DZ4203 EQ motion is shown in Figure 6.16(b). Agreement with the 5% spectrum for the DZ4203 motion derived using the WAVE program is not good above 2 seconds because the WAVE program was only required to match the spectrum at 2.0 and 3.0 seconds. In retrospect, better agreement would probably have been achieved if the WAVE program had also been required to match the spectrum at 2.5 and 4.0 seconds. Nevertheless the plots do indicate that displacement spectra can be derived with sufficient accuracy from acceleration spectra. This is significant because the methodology that will be proposed in this project for predicting the stability of face loaded walls uses displacement spectra and design spectra are usually only readily available as acceleration spectra.

Response spectra for the Weber and Tabas earthquake records using 15% damping are also given in Figures 6.17 and 6.18 respectively.

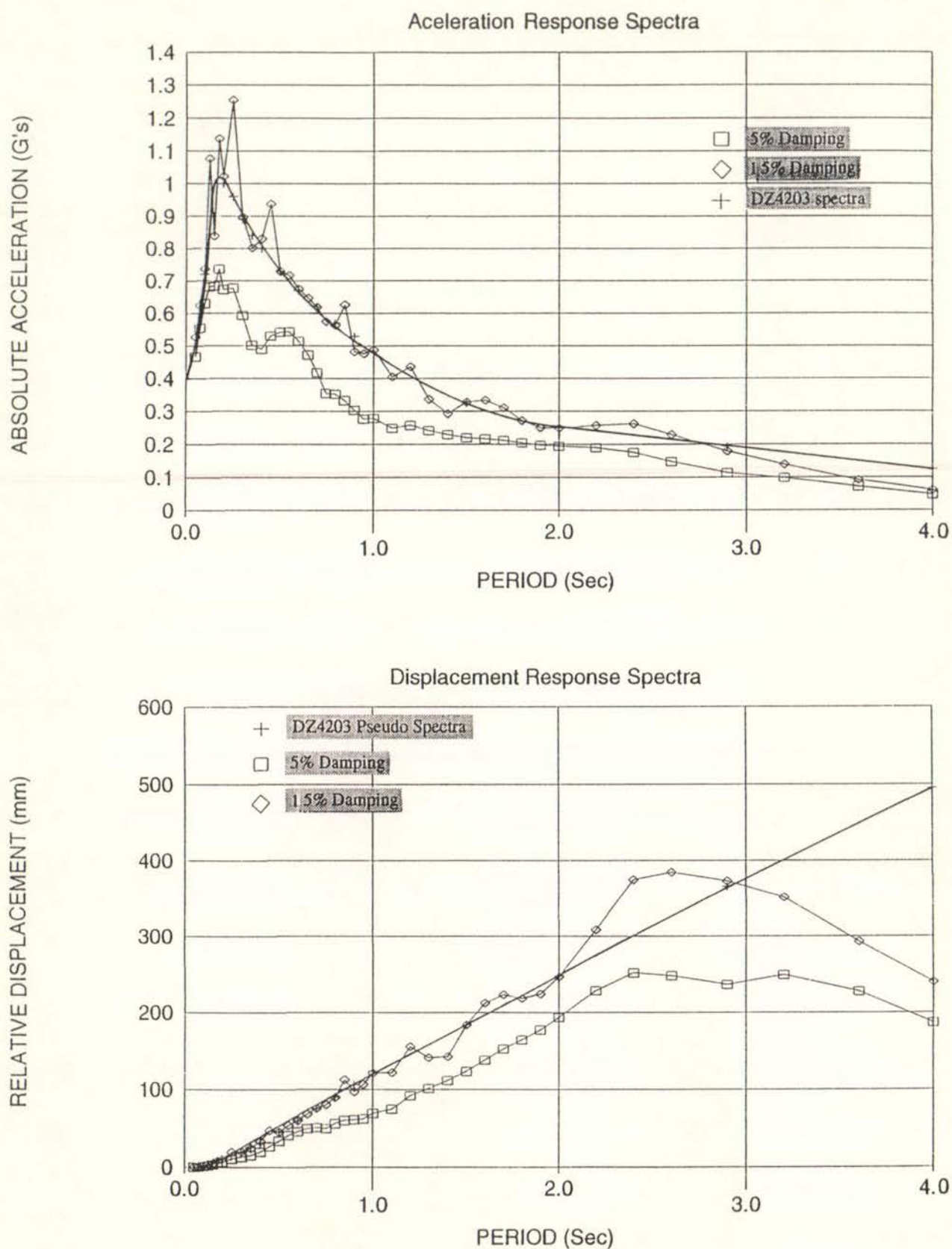


Figure 6.16 Elastic Response Spectra for first 15 seconds of the DZ4203 EQ Motion for:
 a) Acceleration and;
 b) Displacement

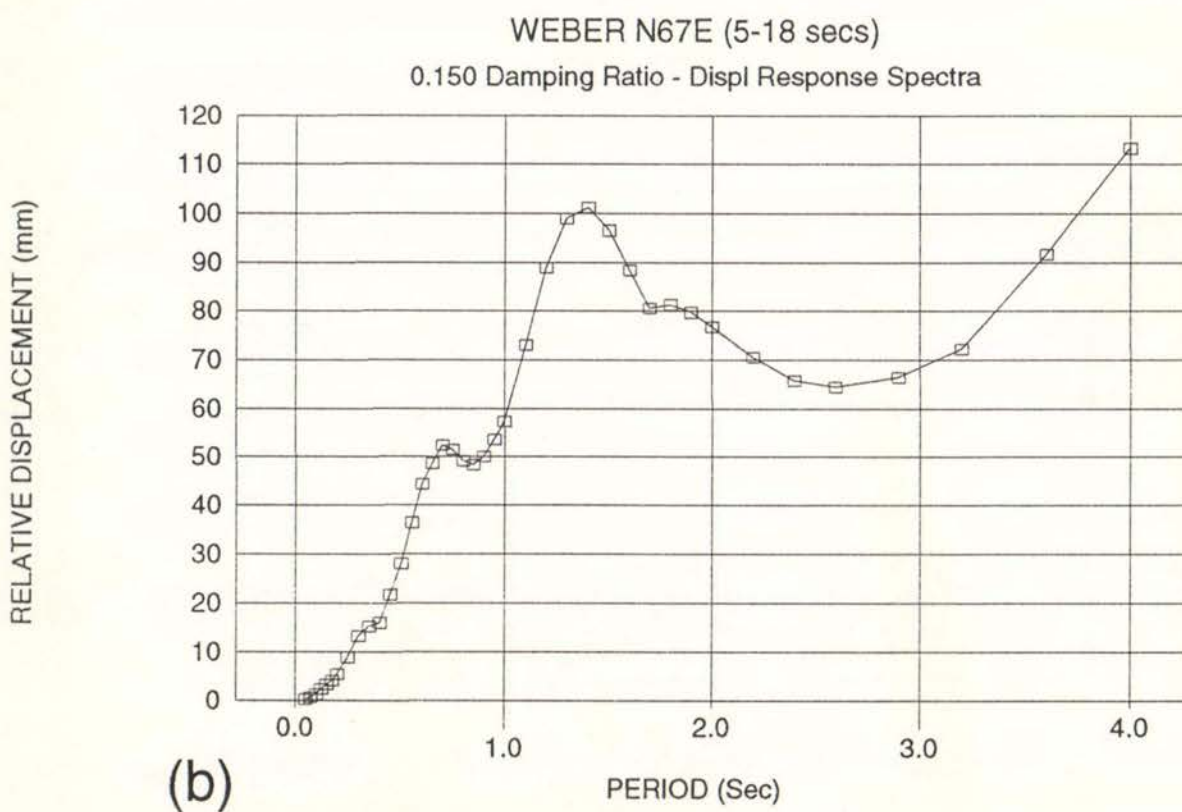
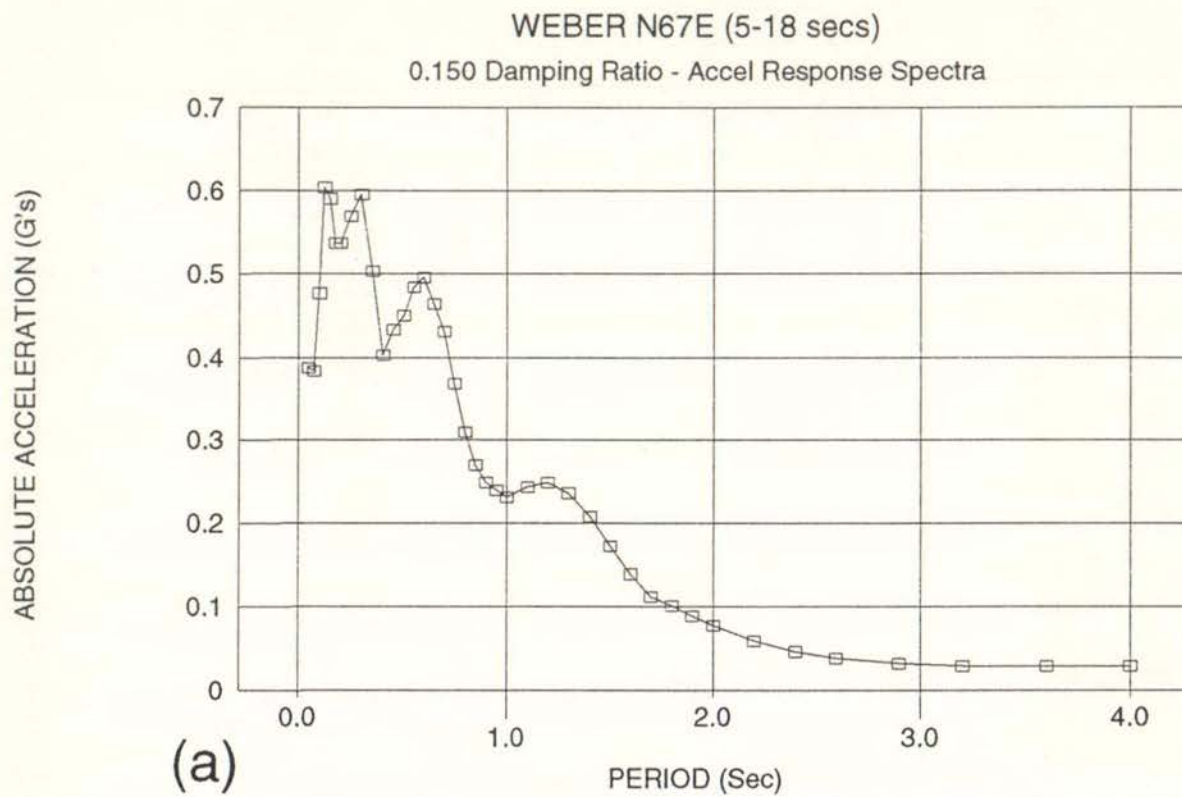


Figure 6.17 Elastic Response Spectrum for the Weber EQ Record.
a) Acceleration spectra and;
b) Displacement Spectrum

TABAS EQ (0-25 Sec, Trvs Comp)
0.150 Damping Ratio - Accel Response Spectra

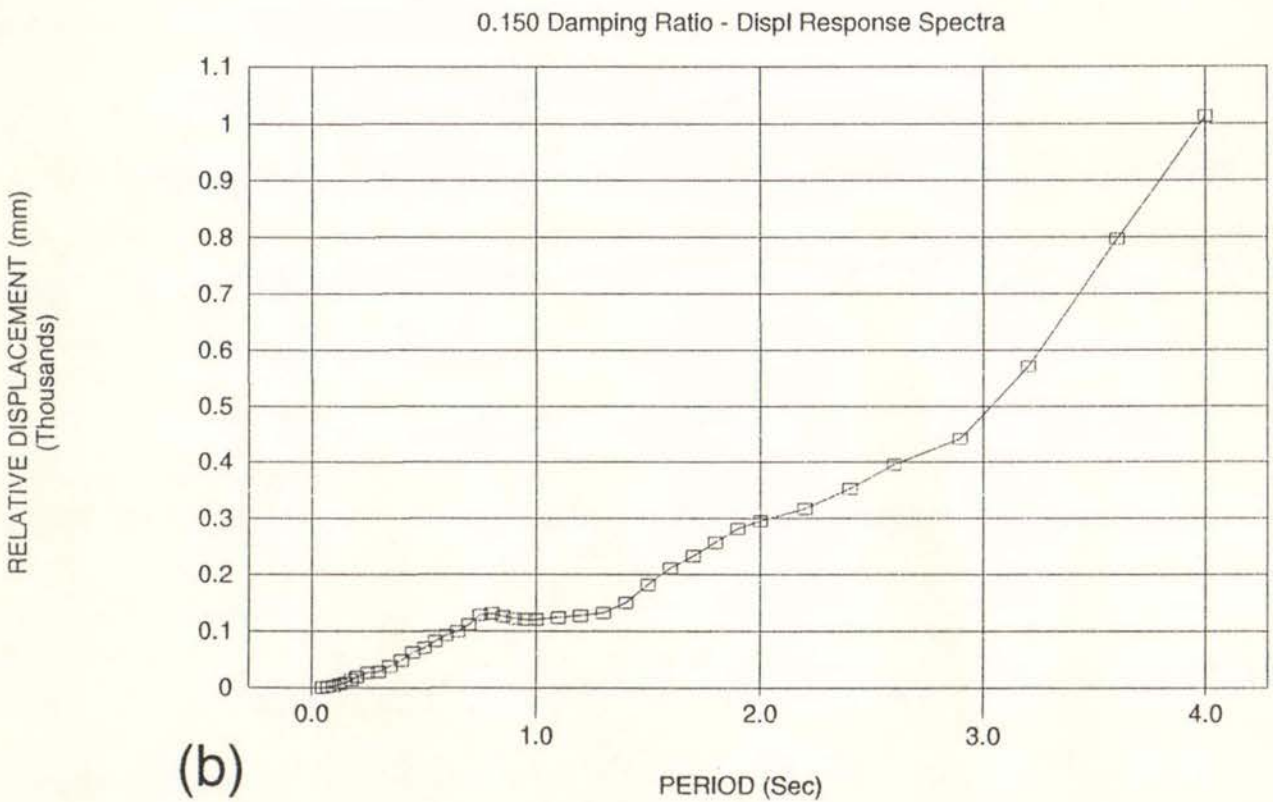
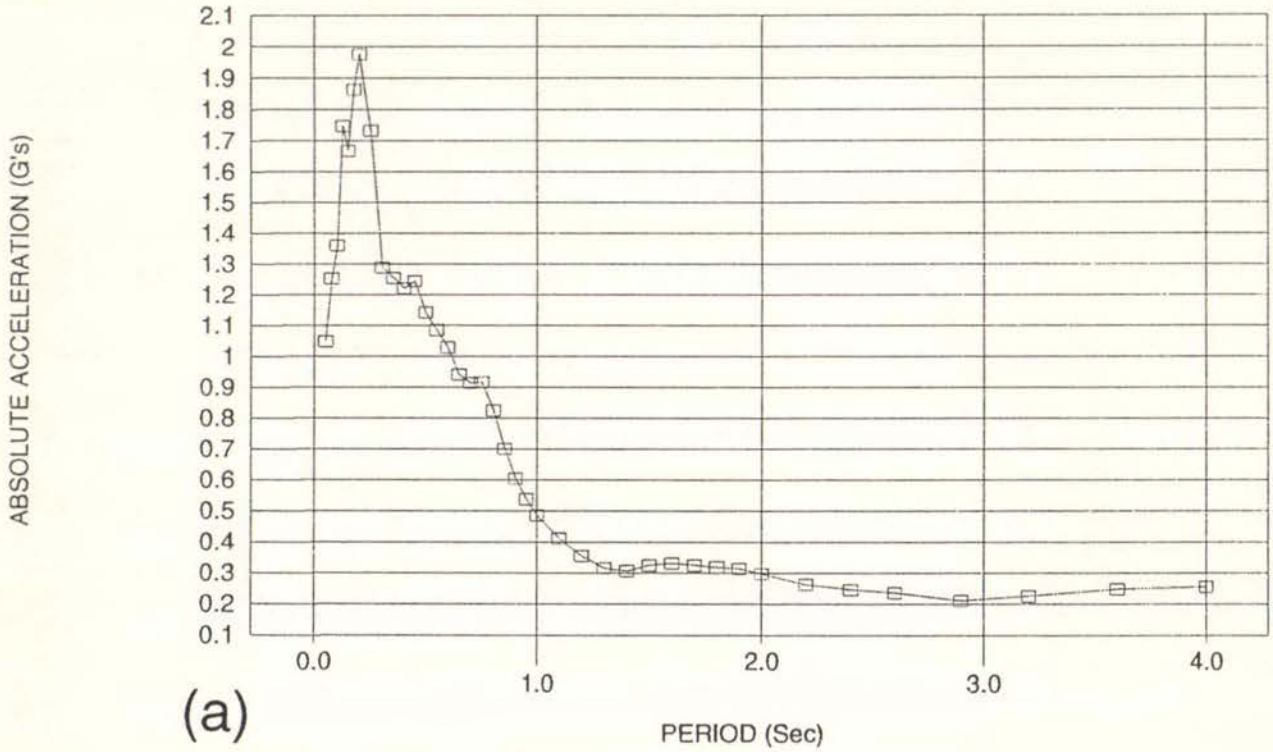


Figure 6.18 Elastic Response Spectra for the TABAS EQ Record. (a) Acceleration Spectrum and; (b) Displacement Spectrum

6.7.3 Use of Displacement Response Spectra to Predict Wall Displacements

In section 6.4.1 a relatively simple formula was derived to predict the free vibration period for a face loaded wall displaced to 60% of Y_{\max} (see equation 10).

It was also demonstrated using computer modelling (section 6.6) that the face loaded wall stability becomes somewhat erratic once the peak wall displacement exceeds approximately $0.6Y_{\max}$. Therefore, it was decided to use the displacement response spectra to predict the earthquake intensity required to generate a peak wall displacement of $0.6Y_{\max}$.

A summary of the calculations is given in Table 6.4. Calculations were carried out using spectra derived for both 5 and 15% damping as indicated in columns (5) and (6) of the table. It can be seen that very similar results were obtained for the two damping values providing the scaling factor, S , that was used to scale the spectral displacements is reduced from 2.0 to 1.4 when the calculations are based on the 5% damped displacement spectrum instead of the 15% damped spectrum.

The two values of the scaling factor, S , may be compared with the modal participation factor of 1.5 that applies to a wall responding elastically in a mode like that shown in Figure 5.1(a). This means that if the cracked wall was responding elastically to an earthquake motion, the peak displacement at the centre of the wall would be 1.5 times that predicted using a SDOF displacement response spectrum providing the correct period and damping were used.

The scaling factor, S , of 2.0 for the 15% damped spectral displacements was selected to give results that would be conservative relative to the envelope of results predicted using the computer model. As the envelope of the computer model results corresponds mainly to the reduced level of damping considered, it can be seen from Figure 6.5(b) that the effective level of damping in the computer modeled walls was about 10% at the periods corresponding to a peak wall displacement of $.6Y_{\max}$ (see column (4) of table).

If future tests indicate that a higher level of damping is appropriate for face loaded walls the scaling factor values of 2.0 and 1.4 could be reduced.

Results of calculations for 2 other earthquake motions are also given at the bottom of Table 6.4. These motions were previously described in 6.5.1 and will be discussed further in section (7.2.1).

As demonstrated previously in Figure 6.4(a), the free vibration period of a face loaded wall increases with peak wall displacement. Also, spectral displacement usually increases with period. Therefore, using the period that corresponds to a maximum wall displacement of $0.6Y_{\max}$ to predict displacements using a displacement spectrum would normally result in a conservative prediction of the earthquake intensity required to generate a peak wall displacement of $0.6Y_{\max}$. However the displacement spectrum for the Weber earthquake motion shown in Figure 6.17(a) peaks at a period of 1.4 seconds and then declines. When the 2 x Scale wall has a peak displacement of $0.6Y_{\max}$ it responds with a period of 2.26 seconds (see column (4) of the table). The spectral displacement corresponding to this period is only 70%

TABLE 6.4 : CALCULATION OF EARTHQUAKE INTENSITY SCALING FACTOR REQUIRED TO GENERATE WALL DISPLACEMENT OF $0.6 Y_{MAX}$

EQ MOTION (1)	WALL SCALE (2)	60% Y_{max} (mm) (3)	CALCULATED PERIOD, T WHEN $Y = 0.6 Y_{MAX}$ (SECS) (4)	SPECTRAL DISPLACEMENT FOR PERIOD IN COLUMN (4) (λ = DAMPING, S = SCALING FACTOR)		PREDICTED EQ INTENSITY SCALING FACTOR	
				$\lambda = 15\%$ S = 2.0 (5)	$\lambda = 5\%$ S = 1.4 (6)	FROM (3)/(5) (7)	FROM (3)/(6) (8)
TABAS	1/2	93	1.13	250	243	0.37	0.38
	1	186	1.6	420	432	0.44	0.43
	2	372	2.2.6	651	700	0.57	0.53
WEBER	1/2	93	1.13	155	154	.6	.6
	1	186	1.6	176	173	1.05	1.07
	2	372	2.2.6	140 (200)*	126 (194)*	2.65 (1.86)*	2.95 (1.91)*
DZ4203	1/2	93	1.13	158	183	0.59	0.5
	1	186	1.6	275	295	0.67	0.63
	2	372	2.2.6	482	440	0.77	0.83
EL CENTRO NS X 1.3	1	186	1.6	220	173	0.81	1.07
DIAPHRAGM (SDOF MODEL)	1	186	1.6	282 (340)*	260 (375)*	0.65 (.54)*	.71 (.5)*

Notes: Col (3) Y_{max} calculated using equation 4

Col (4) Period of wall when peak displacement = $0.6 Y_{max}$ calculated using equation 10

Col (5) Spectral displacements corresponding to period T in col (4) scaled by factor S = 2.0, to allow for participation factor and a safety factor.

* Indicates peak spectral displacement corresponding to a period less than T used in calculations.

of the peak spectral displacement corresponding to the shorter period of 1.4 seconds. As the inelastic face loaded wall period varies with displacement it would appear more reasonable, in this case, to use the peak spectral displacement occurring at 1.4 seconds in the calculations instead of the value corresponding to a period of 2.26 seconds.

A similar "early" spectral displacement peak occurs for the "Diaphragm" earthquake motion. Alternative values of EQ Intensity Scaling Factor computed using the "early" peak spectral displacement are shown in the table enclosed within brackets. It can be seen that the predicted earthquake intensity required to generate a peak wall displacement of $0.6Y_{max}$ is less when the early peak of the spectral displacement is used in the calculations {see columns (7) and (9)}.

6.7.4 Comparison Between Proposed Formulae, Computer Model and ABK Methodology

The earthquake Intensity Scaling Factors required to cause wall collapse as predicted by the proposed formulae (see notes to Table 6.6), the computer model and the ABK methodology are compared in Table 6.5. The earthquake intensity scaling factors corresponding to a wall displacement of $0.6Y_{max}$ given in column (7) of Table 6.4 are reproduced in column (5) of the table. These values were increased by a factor of 1.2 to provide an estimate of the collapse earthquake intensity. {See column (6)}.

The earthquake Intensity Scaling Factors given in columns (9) and (10) of the table were read from the envelope of the wall responses given in Figures 6.11 to 6.13 and Figure 7.6(a). They correspond to the lower limit of the wall stability predicted by the computer model for the reduced level of damping considered.

The values given in columns (9) and (10) were computed using Figure 4.1 and the ABK Methodology outlined in section 4.3. Two values of peak velocity were used to compute the RMS of the velocities at the top and bottom of the wall element as required in the ABK methodology. These are shown in columns (2) and (3) of the table. V_1 is the Effective Peak Velocity (EPV) of the earthquake motion, which was calculated by dividing the pseudo spectral velocity at 1.0 second by an assumed amplification factor of 2.5. This method of evaluating effective peak ground velocity makes some allowance for the time interval that the peak velocity pulse acts as a short pulse will not produce as much response as a pulse of the same magnitude acting for a longer time. The pseudo spectral velocities were calculated from the 5% damped acceleration spectra using equation 13.

The method used by ABK (38(b)) to evaluate the EPV involved an additional refinement as the peak spectral pseudo velocity used by ABK was actually an average value in the period range 0.5 to 2.0 seconds. This refinement was not used in this study.

ABK do not state that the Effective Peak Velocity should be used as part of their methodology for evaluating the seismic resistance of face loaded walls. Nevertheless they do imply that using the EPV for an earthquake motion would be better than using the actual measured peak velocity.

TABLE 6.5 : COMPARISON BETWEEN PROPOSED FORMULAE, COMPUTER MODEL AND ABK METHODOLOGY

EQ MOTION (1)	PEAK VELOCITY (M/SEC)		WALL SCALE FACTOR (4)	EARTHQUAKE INTENSITY SCALING FACTORS PREDICTED BY:					
	V ₁ (2)	V ₂ (3)		PROPOSED FORMULAE		COMPUTER MODEL		ABK METHODOLOGY @ COLLAPSE USING:	
				@ Y = .6Y _{MAX} (5)	@ COLLAPSE = (5) X 1.2 (6)	@ Y = 0.6Y _{MAX} (7)	@ COLLAPSE (8)	V ₁ (9)	V ₂ (10)
TABAS	.41	1.12	1/2	0.37 (0.31)**	0.45 (0.37)**	0.45	0.475	1.47	0.54
			1	0.44	0.52	0.48	0.575	"	"
			2	0.57	0.68	0.67	1.0	"	"
WEBER	.24	.26	1/2	0.6 (1.02)**	.72 (1.23)**	1.25	1.34	2.5	2.3
			1	1.05	1.26	1.46	1.7	"	"
			2	2.67 (1.86)*	3.12 (2.2)*	2.0	2.4	"	"
DZ4203	.3	.4	1/2	0.59 (.72)**	0.7 (.86)**	0.95	1.0	2.04	1.53
			1	0.67	0.8	0.85	1.25	"	"
			2	0.77	0.92	1.13	1.4	"	"
EL CENTRO NS X 1.3	.41	.43	1	.84	1.0	1.08	1.12	1.47	1.4
DIAPHRAGM (SDOF MODEL)	0.6	1.03	1	.65 (.54)*	.78 (.65)*	0.5	0.65	1.0	.58

Notes: Col (2) effective peak velocity of EQ motion = psuedo spectral velocity at 1.0 sec + 2.5.
 Col (3) peak velocity of EQ motion calculated by integrating acceleration time history.
 Col (5) EQ intensity scaling factor predicted to give displacement of 0.6Y_{max} as calculated in Table 6.4. (** Scaling factor corresponds to 120% of EQ intensity required to open cracks. * peak spectral displacement corresponding to a wall period less than calculated by equation 10 used in calculation.)
 Col (7) & (8) read from envelope of wall responses in Figures 6.11 to 6.13 and 7.6(a)
 Col (9) & (10) calculated using ABK methodology (Fig 4.1) and velocities given in cols (2) and (3) respectively.

However the statistical analysis of their test results used the actual (target) velocity of the input motions imposed on their wall test specimens. This was calculated by differentiating the target displacements of the input motion used to test the wall specimens.

Column (3) of the table gives the actual peak velocities of the input motions used for the computer modelling of the face loaded walls in this study. The velocities were calculated by integrating the acceleration time histories. Where possible these were checked against published values for the earthquake records. It can be seen that the two methods of calculating peak velocity for use in the ABK methodology give similar results except for the Tabas and "Diaphragm" earthquake motions.

Two values of the Earthquake Intensity Scaling factors are given in columns (5) and (6) of the table for the half scale wall. The first value was obtained using the displacement spectrum for the DZ4203 earthquake motion and the Earthquake Intensity Scaling factor required to generate a displacement of $0.6Y_{\max}$ is given as 0.59.

It can be seen from Figure 6.11(c) that the computer model predicts that the wall is still responding elastically at this earthquake intensity. This could have been anticipated from the wall's elastic behaviour as the $1/2 \times$ scale wall model has a very short elastic period (.087 seconds) and its precracking elastic response lies on the rising branch of the acceleration response spectrum (see Fig 6.16(a)).

The second value given in column (5) of the table for the $1/2$ scale walls was calculated using the 15% damped acceleration spectra assuming that the earthquake intensity required to generate a wall displacement of $0.6Y_{\max}$ would be 20% greater than the earthquake intensity required to just open the cracks. In this case the wall's peak response was assumed to be equivalent to a uniformly distributed static load.

This provides an estimate of a lower limit to the $1/2 \times$ scale wall stability and can be seen to improve the correlation with values predicted by the computer modelling for the $1/2 \times$ scale modelled walls.

For $2 \times$ Scale walls and the Weber and Diaphragm earthquake motions, the correlation with the computer model predictions is also improved if the second value given in the table is used for the comparison. This value was computed using the "early" peak in the displacement response spectra that occurs for these two earthquake motions.

A comparison between the wall stability predicted by the ABK methodology and the computer modelling can be obtained by comparing the values of Earthquake Intensity Scaling factors required to cause wall collapse given in columns (9) and (10) with those in column (8) of the table.

The ABK methodology predicts that increasing the wall thickness should not affect the wall stability as all 3 scaled models of wall had the same H/t ratio. However, the computer model predicts that the earthquake intensity required to cause collapse will increase by 40 to 100% as the effective wall thickness is increased from 166 to 660mm. A better prediction of this trend is given by the proposed formulae.

It can also be seen that the use of EPV in the ABK methodology is generally unconservative (column (9)). This is particularly true for the Tabas earthquake motion which is a near fault earthquake record. Near fault records tend to have long acceleration pulses which give rise to high peak velocity/acceleration ratios. Use of the acceleration spectrum to compute pseudo velocity and hence an effective peak velocity appears to underestimate the earthquake intensity in this case.

The values given by the ABK methodology in column (10) correlate better with those predicted by the computer model. However, on average they tend to give a less conservative estimate of the wall's seismic resistance. This may be an indication that the level of damping on which the computer model results are based is too low and free vibration tests of URM walls are required to establish whether this is the case. In general it can be seen that the proposed formulae provide a better prediction of the results obtained from the computer model than would be predicted using the ABK methodology.

6.7.5 Example of Calculations Required to Compute the Seismic Stability of Face Loaded Walls

A summary of the calculations required to estimate the stability of a face loaded wall using the proposed formulae are given in Table 6.6. The calculations apply to a 330mm thick wall subjected to the DZ4203 earthquake motion. A range of wall slenderness ratios (H/t) and overburden to wall weight ratios (O/W) are considered. The weight of the wall is assumed to be 25 kN/m when the H/t ratio is 10 and the weight is assumed to increase linearly with height.

Results of the computations are plotted in Figure 6.19.

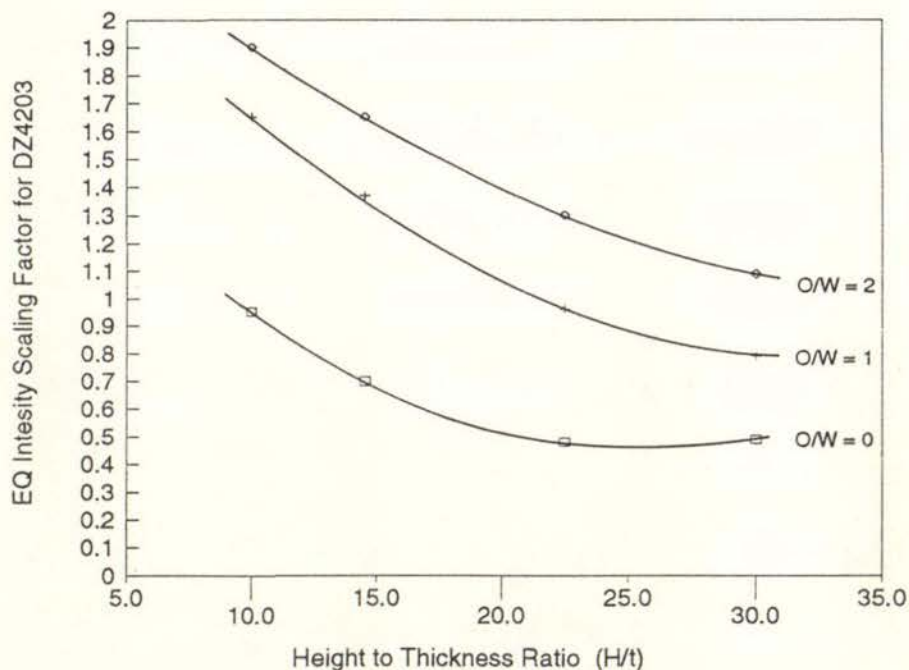


Figure 6.19 Predicted Seismic Resistance of a 330mm Thick URM Walls Using Proposed Formulae and DZ4203 EQ Intensity

TABLE 6.6 : EXAMPLE CALCULATION FOR COMPUTING THE SEISMIC STABILITY OF A FACE LOADED WALL USING PROPOSED FORMULAE (for 330m thick wall and DZ4203 EQ motion)

H/t	O/W	t (mm)	W (kN)	O (kN)	Y _{max} (mm)	V _{max} (kN)	T (Secs)	2 x Spectral Response for period T (mm)	0.60 Y _{max} = .6 x (6) (mm)	EQ Scaling Factor Required to produce:	
										0.6Y _{max} = (10)/(9) (11)	Collapse = (11) x 1.2 (12)
(1)	(2)	(3)	(4)	(5)	(6)	(7)	(8)	(9)	(10)	(11)	(12)
10	0	330	25	0	330	5.0	1.52	250	198	0.78	0.95
	1	330	25	25	275	12.4	.88	120	165	1.37	1.65
	2	330	25	50	264	20	.68	100	158	1.58	1.9
14.5	0	330	36	0	330	5.0	1.83	336	198	0.59	0.7
	1	330	36	36	275	12.4	1.06	144	165	1.14	1.37
	2	330	36	72	264	20	.82	114	158	1.38	1.66
22.5	0	330	56	0	330	5.0	2.28	492	198	0.4	0.48
	1	330	56	56	275	12.4	1.31	206	165	0.8	0.96
	2	330	56	112	264	2.0	1.02	140	158	1.12	1.35
30	0	330	74	0	330	5.0	2.64	486	198	0.4	0.49
	1	330	74	74	330	12.4	1.51	250	165	0.66	0.79
	2	330	74	148	264	2.0	1.17	174	158	0.9	1.09

Notes:

Col (1) wall height, H, to effective thickness, t, ratio

Col (2) overburden weight, O, to wall weight, W, ratio

Cols (4) & (5) wall weight and overburden scaled using the wall height, H

Col (6) displacement at which wall becomes statically unstable : $Y_{max} = \left(\frac{W+1.5O}{W+2O} \right) \dots\dots\dots 4$

Col (7) point load at wall mid-height required to open cracks :

$$V_{max} = \frac{2t}{H} (W + 1.5O) t \dots\dots\dots 3$$

Col (8) free vibration period of wall when peak displacement = 0.6Y_{max} : $T^2 = 0.0014 \frac{Y_{max}}{V_{max}} W \dots\dots\dots 10$

Col (9) spectral displacement read from Figure 6.16(b) for 15% damping and scaled by a factor S = 2.0 (a value of S = 1.4 should be used if 5% damped displacement spectra are used)

(1), (2) & (12) Results plotted in Figure 6.19

The general form of the plotted results may be compared with the design curves based on ABK's URM wall tests (compare Figures 4.1 and 6.19). It can be seen that the shapes of the two sets of curves are remarkably similar. However the proposed formulae would appear to indicate that the wall stability has a greater dependence on overburden load than was indicated by the ABK wall tests. Further computer modelling using higher O/W ratios than were used in this project is required to clarify this aspect of face loaded wall behaviour.

Also the proposed formulae are based on a low level of damping in the walls. With further testing of URM walls this may prove to be too conservative and the S factors (of 2.0 and 1.4) used to scale the spectral displacements may need to be reduced.

Before the proposed formulae could be used in practice, seismic resistance reduction factors that allow for the influence of diaphragm flexibility and amplification of seismic motions in the upper floors of a building are required.

7. BEHAVIOUR OF FACE LOADED WALLS WITH DIAPHRAGM INTERACTION

7.1 Behaviour of Walls Subjected to an Acceleration Pulse

7.1.1 Wall Modelling

The computer model used to evaluate the effect of diaphragm interaction on the behaviour of face loaded walls was practically the same as that described in section 6.2 for the full scale $4.8 \times 0.33\text{m}$ wall. However in this part of the project the diaphragms at the top and bottom of the wall element shown in Fig 6.1 were modelled using elastic truss members with stiffness damping. Also, in some cases, only 10% of the wall's vertical inertia was modelled to evaluate, or limit, the effects of impact on the wall behaviour.

7.1.2 Wall Modelled with 0.5 Second Period Diaphragms

Figure 7.1 shows the free damped vibration response predicted by the wall computer model when it was subjected to a $0.55g$ pulse for 0.2 seconds.

The total displacement at the mid-height crack level in the wall relative to the "ground" supports is shown (Figure 7.1(a)). The displacement at mid-height of the wall relative to a straight line joining the top and bottom of the wall is also shown in Figure 7.1(b). This is the component of the wall displacement generated by the opening and closing of the mid-height crack.

For this analysis the top and bottom diaphragms were modelled to have an elastic period of 0.5 seconds. To calculate the diaphragm stiffnesses required to give a diaphragm period of 0.5 seconds it was assumed that half the wall weight (inertia) acted with the top diaphragm and half acted with the bottom diaphragm as would normally be assumed in a design situation.

The amount of stiffness damping in the diaphragms ($\beta = .004$) was relatively low and corresponded to only 2.5% damping for a period of 0.5 seconds. The amount of damping in the wall was also very low. The wall damping factors used ($\alpha = 0$ and $\beta = .004$) corresponded to the "reduced damping" case detailed in section 6.5.8. Also, only 10% of the vertical inertia of the wall was included in the computer model to limit the effect of impact on damping.

In spite of these very low levels of damping it can be seen (Figure 7.1(b)) that the rocking wall motion associated with crack opening practically died out in only 3 cycles. This apparently anomalous behaviour can be explained by examining the diaphragm behaviour in greater detail.

The time histories of the forces in the top and bottom diaphragms are shown in Figure 7.2

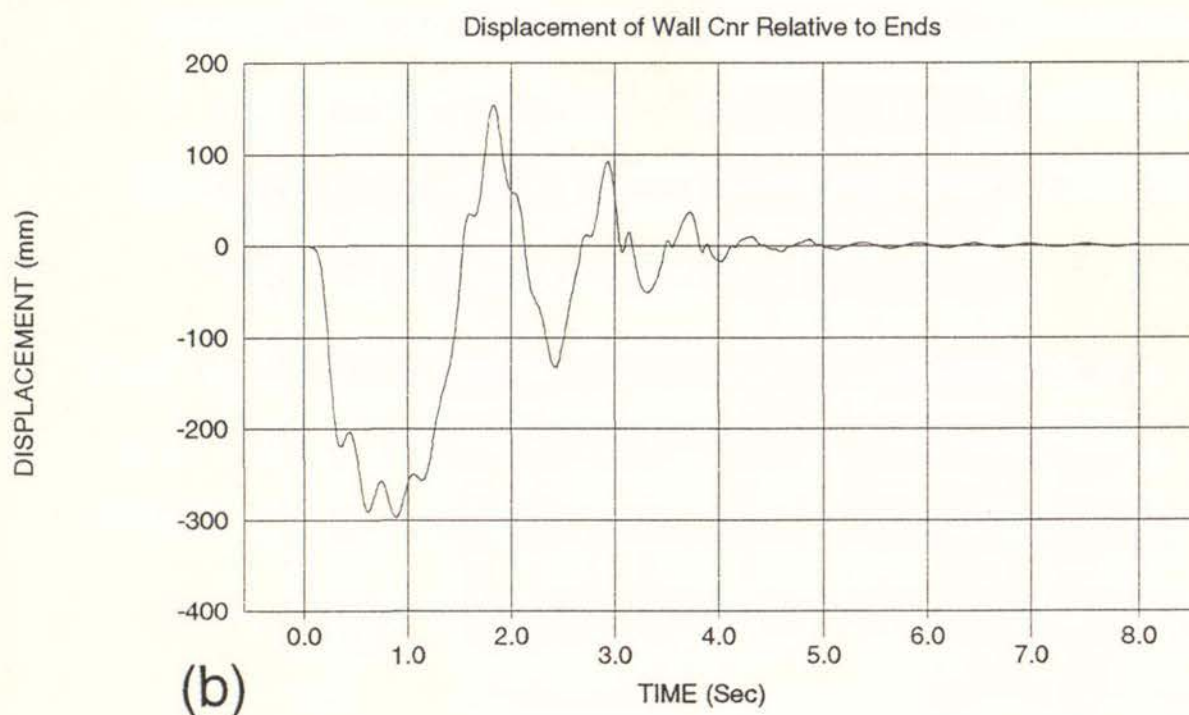
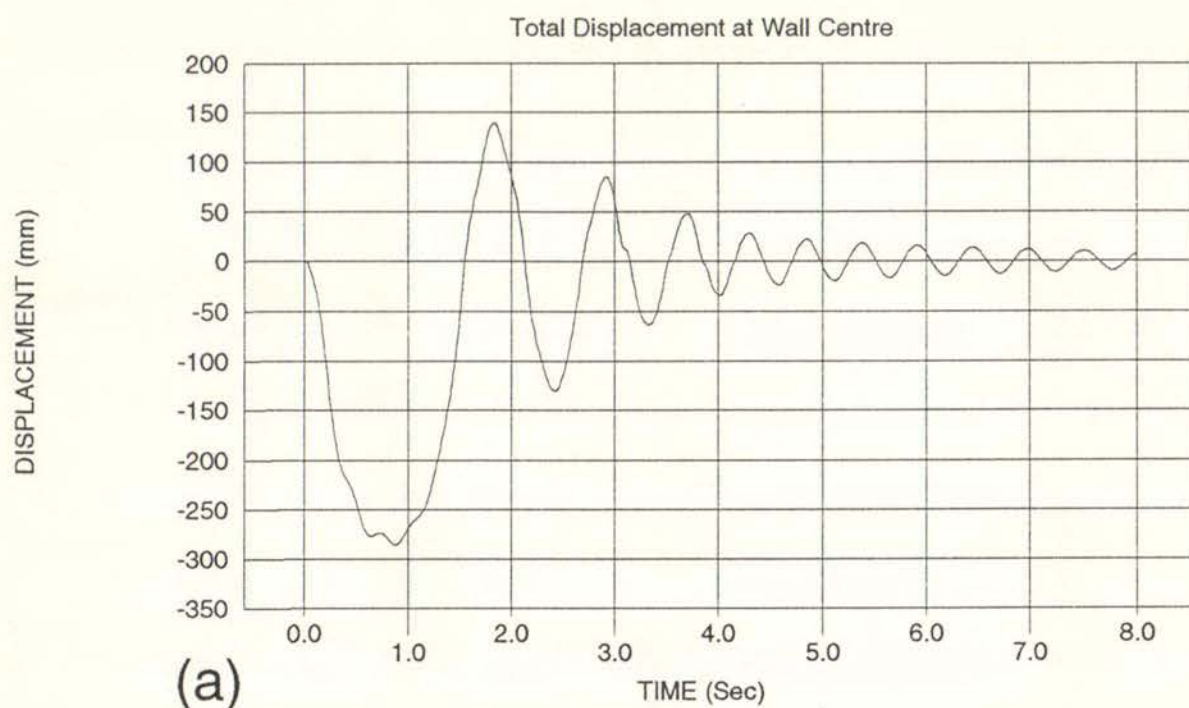


Figure 7.1 Displacement Time History at Mid-height of a Face Loaded Wall Modelled with 0.5 Second Period Diaphragms and subjected to an Acceleration Pulse for 0.2 seconds.

- a) Total Displacement at mid-height of wall including any components due to Deflection of Diaphragms and;
- b) Displacement at mid-height of wall excluding any components due to Deflection of Diaphragms.

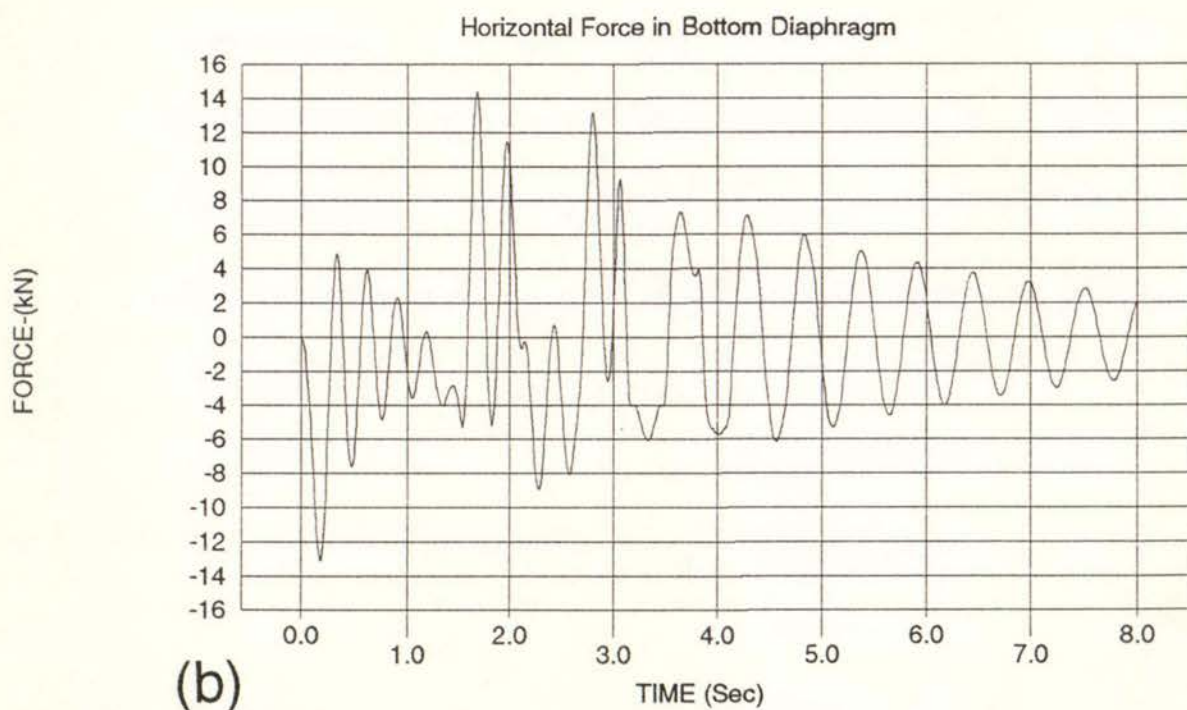
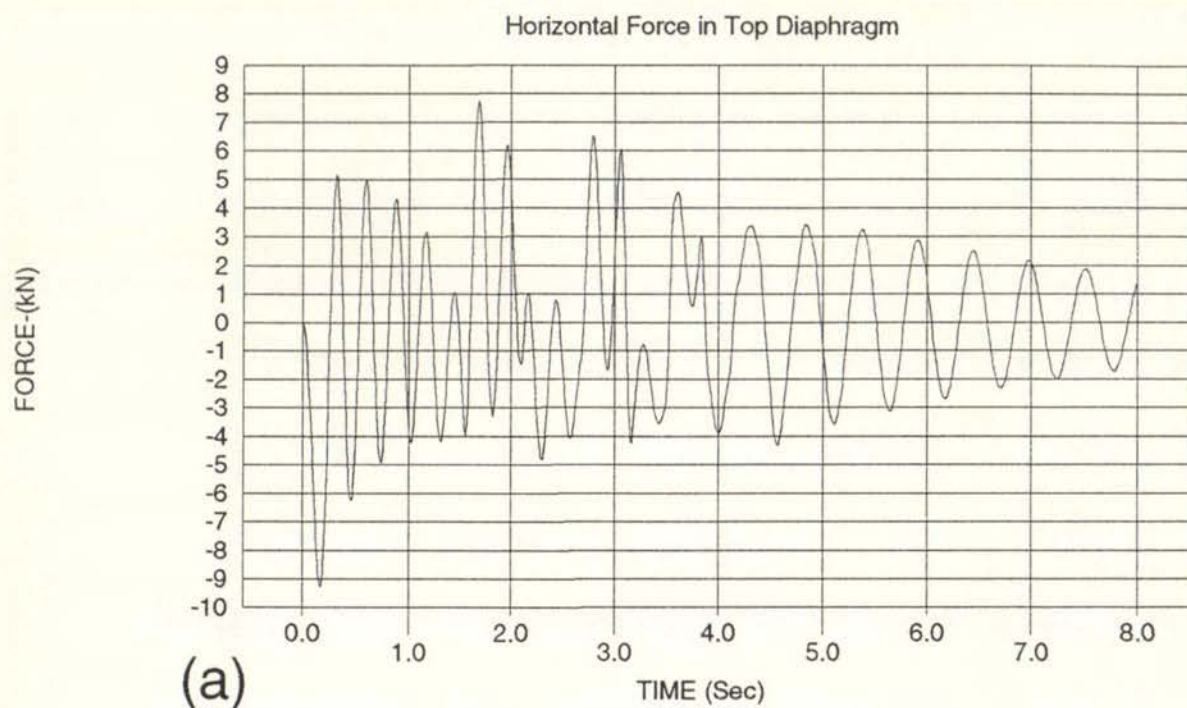


Figure 7.2

Time History of Diaphragm Forces for a Face Loaded Wall Modelled with 0.5 second Diaphragms and Subjected to an Acceleration Pulse for 0.2 seconds

- a) Force in Diaphragm at Top of Wall Element and;
 b) Force in Diaphragm at Bottom of Wall Element

By comparing Figures 7.2(a) and (b) with Figure 7.1(a) at the start of the time history, it can be seen that the forces in the diaphragms reach their first peak when the cracks in the wall just start to open. The peak forces in the diaphragms at this stage (9.2 and 13.0 kN) are significantly greater than the static forces (4.6 and 7.4 kN) that would correspond to the statically applied uniformly distributed load required to just open the cracks. Consequently, once the diaphragms reach their peak displacement they rapidly return to zero displacement and a high frequency diaphragm motion is generated.

This diaphragm motion is essentially a second mode response for the wall which may be visualised as the diaphragms oscillating while the centre of the wall remains stationary. In this mode the top and bottom halves of the walls are rotating rather than translating. Their effective mass in this mode is very much less than the 50% assumed to act with each diaphragm when the diaphragm periods were computed. Consequently the second mode diaphragm motion only has a period of approximately half that computed assuming 50% of the wall mass acts with the top and bottom diaphragms. The average period of the second mode response can be seen to be a little longer for the bottom diaphragm (0.3 seconds) than the top diaphragm (0.27 seconds) because the base fixity modelled at the bottom of the wall increases the effective wall mass acting with the bottom diaphragm.

The second mode diaphragm motion can be seen to die out at about 3.5 seconds into the time histories shown in Figure 7.2. This corresponds to the time at which the wall displacement associated with mid-height crack opening and closing also dies out (Figure 7.1(b)). Beyond this time the response is consistent with the wall and diaphragms responding in-phase with only the low damping (2.5% at 0.5 second period) that was provided in the diaphragms alone.

By comparing Figure 7.2 with Figure 7.1 it can be seen that the diaphragm motion doesn't start to decline until the wall motion associated with crack opening and closing has died out. This leads to the interesting observation that energy is being drawn from the wall motion and dissipated in the diaphragm preferentially. This helps explain why the wall motion associated with crack opening and closing dies out in only 3 cycles in spite of the low damping provided. The increased damping associated with the second mode of the wall motion is also a significant factor as the stiffness damping provided in the diaphragms is inversely proportioned to period. Hence the second mode damping in the diaphragm will be closer to 5% than the 2.5% associated with the first mode wall response period of 0.5 seconds.

7.1.3 Energy Loss In Diaphragms

It was demonstrated in Section 6.4.3 how the logarithmic decrement method can be used to evaluate the energy loss due to damping in each half cycle of an elastically responding element. The calculations required to evaluate the energy stored in an elastic member or in a face loaded wall at its peak displacement were also demonstrated.

These procedures were used to calculate the potential energy stored in the wall when it reached the two displacement peaks that occurred during the response at

approximately 1.9 and 2.9 seconds from the start of the time history (Figure 7.1(b)). The energy stored in the diaphragms at the same time steps was also calculated. This allowed the total energy loss that occurred in the system between 1.9 and 2.9 seconds to be evaluated.

The total energy loss in the diaphragms during this time interval due to damping was then calculated by summing the energy loss in each half cycle of the diaphragm responses. The calculations indicated that 73% of the total energy loss was due to damping in the diaphragms. This was in spite of the top and bottom diaphragms only having an average of 4.6 and 4.1% damping respectively during the time interval considered.

7.1.4 Walls Modelled with 1.0 and 2.0 Second Period Diaphragms

The stiffness of the diaphragms used in the 0.5 second diaphragm wall computer model were reduced by a factor of 1/4 and 1/16 to model 1.0 and 2.0 second period diaphragms. The stiffness damping coefficient for the diaphragms was also increased by a factor of 2 and 4 respectively to maintain the same diaphragm damping of 2.5% at the respective periods of 1.0 and 2.0 seconds and this resulted in approximately 5% damping for the second mode responses of the wall models.

Results for the wall model with 1.0 second diaphragms are similar to those already described for the 0.5 second diaphragm model and are not presented here.

The wall behaviour predicted by the computer model with 2.0 second diaphragms was significantly more complex, although it had some features that were similar to those obtained for the wall modelled with 0.5 second diaphragms.

Time histories for the wall displacements and diaphragm forces for the wall modelled with 2.0 second diaphragms are given in Figures 7.3 and 7.4 respectively. Once again it can be seen that the wall displacements associated with crack opening and closing die out more quickly than the diaphragm motion (compare Figure 7.3(b) with Figures 7.4(a) and (b)).

A detailed examination of the wall response indicates that it has been complicated by energy interchange between the wall and the diaphragms and large relative displacements occurring between the top and bottom of the wall element. The large relative displacements between the diaphragms are illustrated in Figure 7.5, which shows the deflected shape of the wall 1.8 seconds from the start of the time history. At this time the bottom diaphragm reaches its peak force and, as the diaphragms are elastic, this is also the time step that the diaphragm reaches its peak displacement.

It is interesting to note that this large relative displacement occurs even though the top and bottom diaphragms were modelled so that they had the same stiffness.

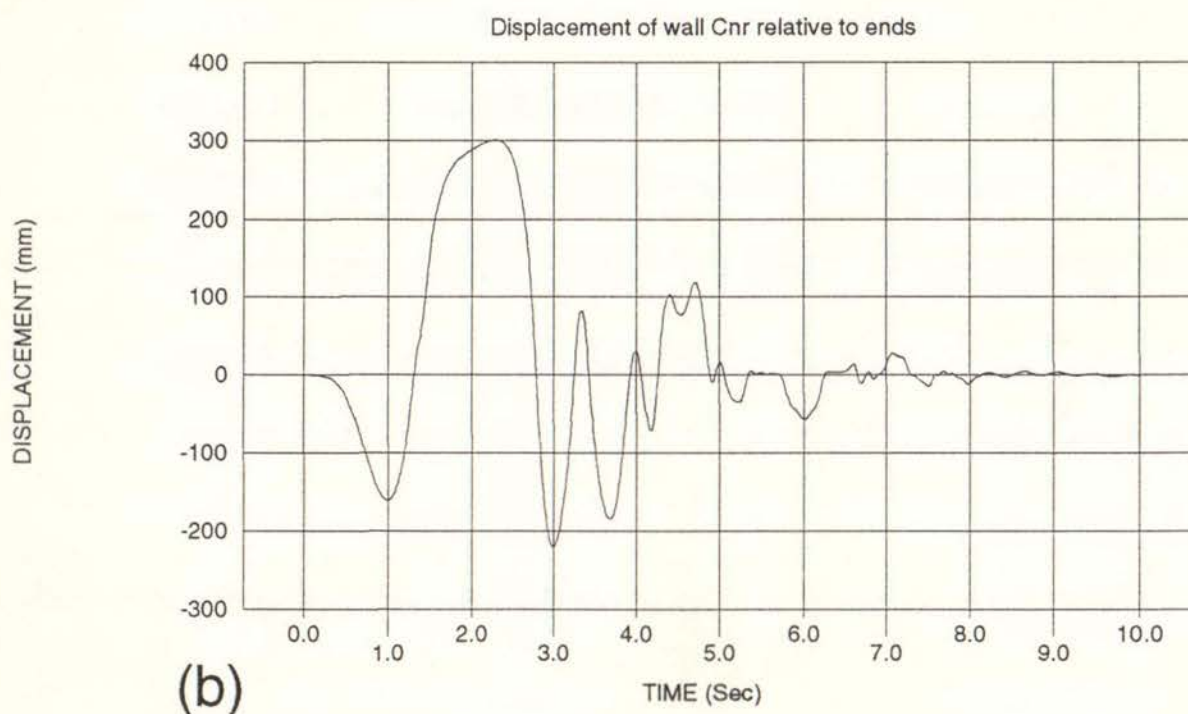
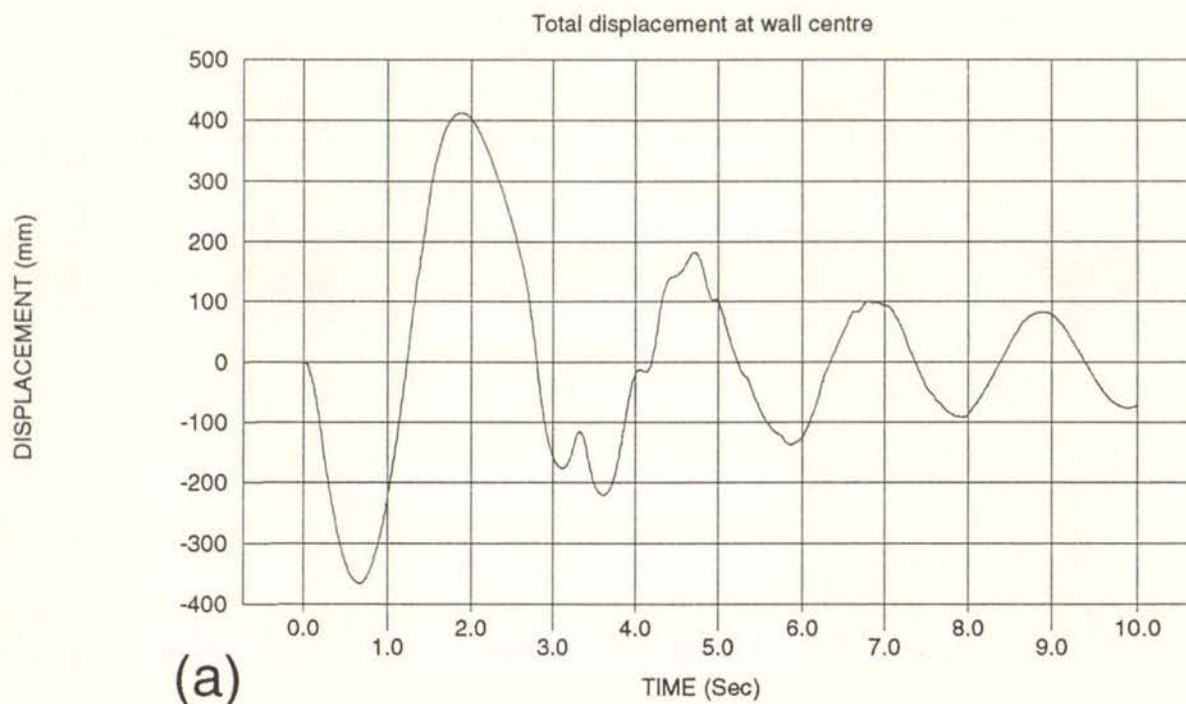


Figure 7.3

Displacement Time History at Mid-height of a Face Loaded URM Wall Modelled with 2.0 second Period Diaphragms and Subjected to an Acceleration Pulse for 0.2 seconds.

- a) Total Displacement at Mid-height of wall including any components due to Deflection of Diaphragms and;
- b) Displacement at Mid-height of wall excluding any components due to deflection of Diaphragms.

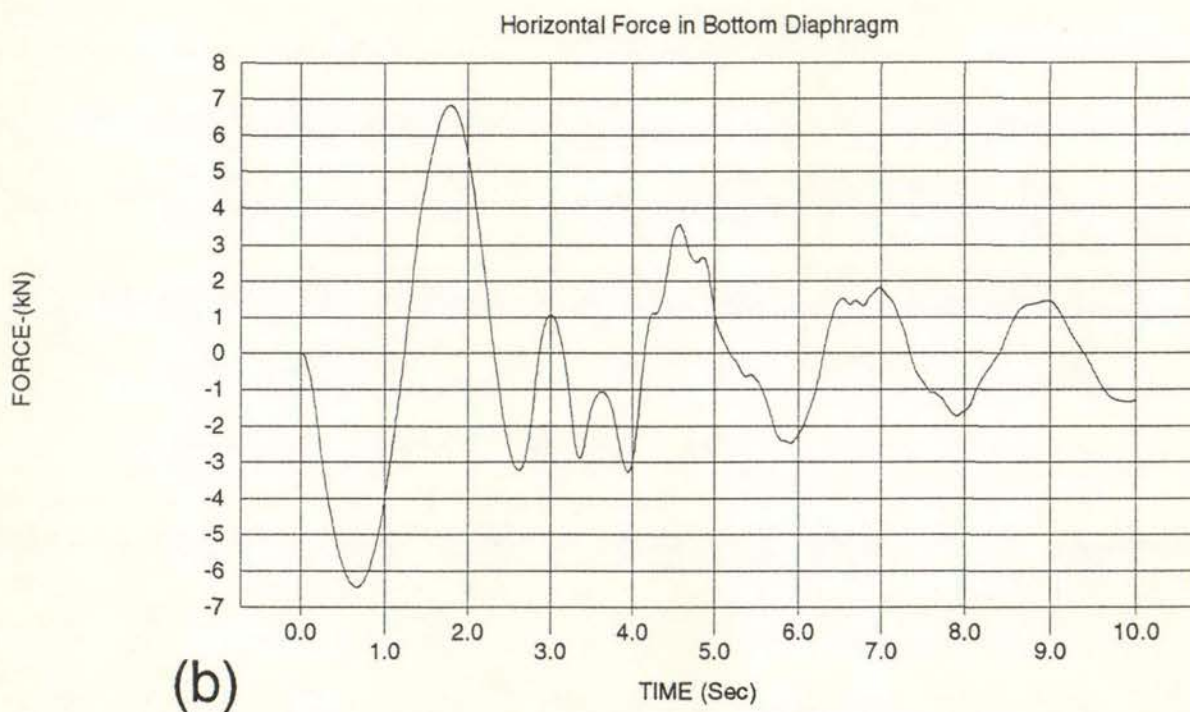
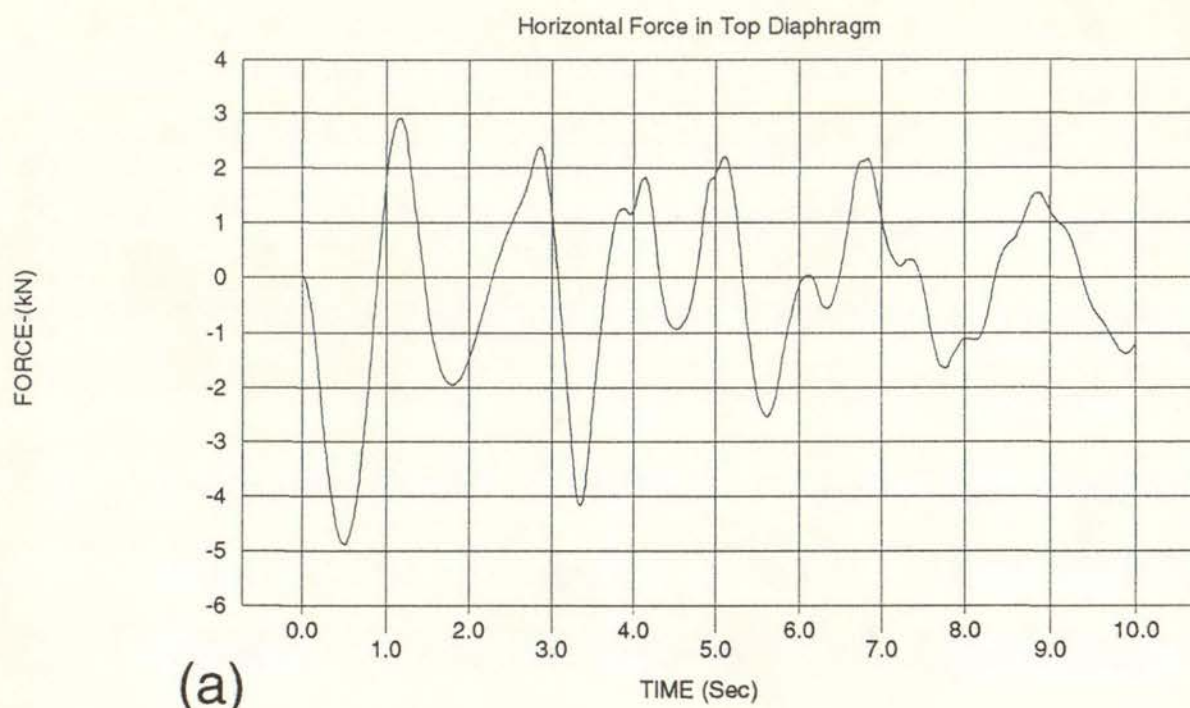


Figure 7.4

Time History of Diaphragm Forces for a Face loaded wall Modelled with a 2.0 second Diaphragm and Subjected to an Acceleration Pulse for 0.2 seconds

- a) Force in Diaphragm at Top of Wall Element and;
 b) Force in Diaphragm at Bottom of Wall Element

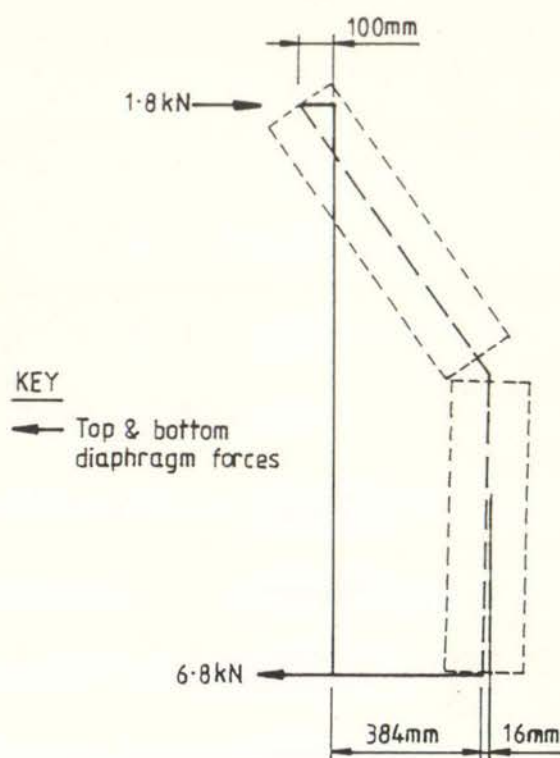


Figure 7.5 Deflected shape of Face Loaded Wall Model at 1.8 secs from start of Pulse Loading (Wall Modeled with 2.0 sec Diaphragms) (NTS)

7.2 Influence of Diaphragms on Seismic Response of Face Loaded Walls

7.2.1 Diaphragm Modelled Using ABK's Methodology

As detailed previously in sections 4.3 and 6.5.1, ABK used a diaphragm computer model to compute the response expected at the centre of a diaphragm. The diaphragm response was then used as the input motion at the top and bottom of their wall test specimens.

This method of modelling the influence of diaphragms on the response of a face loaded wall does not allow for any interaction between the responses of the diaphragm and the wall. Also, the test procedure used by ABK only controlled displacements. Therefore the procedure ignores the incompatibility between the forces that the diaphragm computer model would predict to be acting at the wall-diaphragm junction and the forces actually imposed on the wall specimen during the testing.

An investigation of this aspect of ABK's wall testing was carried out using the face loaded wall computer model. Details of the wall computer model were the same as those used for the acceleration pulse loading that were previously given in section 7.1.1.

In Section 6.5.1 it was described how a Single Degree of Freedom (SDOF) diaphragm computer model was used, as an approximation of ABK's more sophisticated diaphragm computer model, to obtain the stiff diaphragm input motion used by ABK to test their wall specimen. The SDOF diaphragm computer model, used for the approximation, had a period of 0.5 seconds and damping of 10% and the input motion used for the SDOF diaphragm model was 1.3 x the El Centro N-S earthquake record.

The approximation of ABK's stiff diaphragm motion obtain from the SDOF diaphragm model and 1.3 x the El Centro motion were used as input motions at the top and bottom of the face loaded wall computer model and the intensity of the input motion was varied by applying a scaling factor. The resulting displacements at the mid-height crack in the wall are shown in Figure 7.6(a). Details of the damping used in the analysis are as given in Table 7.1. (See "rigid diaphragm" case).

TABLE 7.1

Diaphragm Details (1)	Damping Case (2)	Diaphragm Damping (%)			Wall Damping Parameters		
		β (3)	Mode		Vertical Inertia (6)	α (7)	β (except links) (8)
			1 (4)	2 (5)			
Rigid Diaphragm	Full	N/A			100%	0.6	.004
	Reduced	N/A			100%	0.0	.004
0.5 Second Diaphragm	Low	.004	2.5	5	10%	0.0	.004
	High	.008	5	10	100%	0.6	.004
1.0 Second Diaphragm	1	.008	2.5	5	10%	0.0	.004
	2	.016	5	10	10%	0.0	.004
	3	.008	2.5	5	100%	0.6	.004
	4	.016	5	10	100%	0.6	.004
	5	.008	2.5	5	100%	0.0	.004
2.0 Second Diaphragm	1	.016	2.5	5	10%	0.0	.004
	2	.032	5	10	10%	0.0	.004
	3	.032	5	10	100%	0.2	.004
	4	.032	5	10	100%	0.0	.004

The envelopes of the results indicate that the EQ Intensity Scaling factor corresponding to wall collapse would be reduced from 1.12 to 0.65 when diaphragms are included in the model and the ABK method of modelling the influence of the diaphragms is used. This corresponds to a reduction factor of 0.58 in the seismic resistance of the wall.

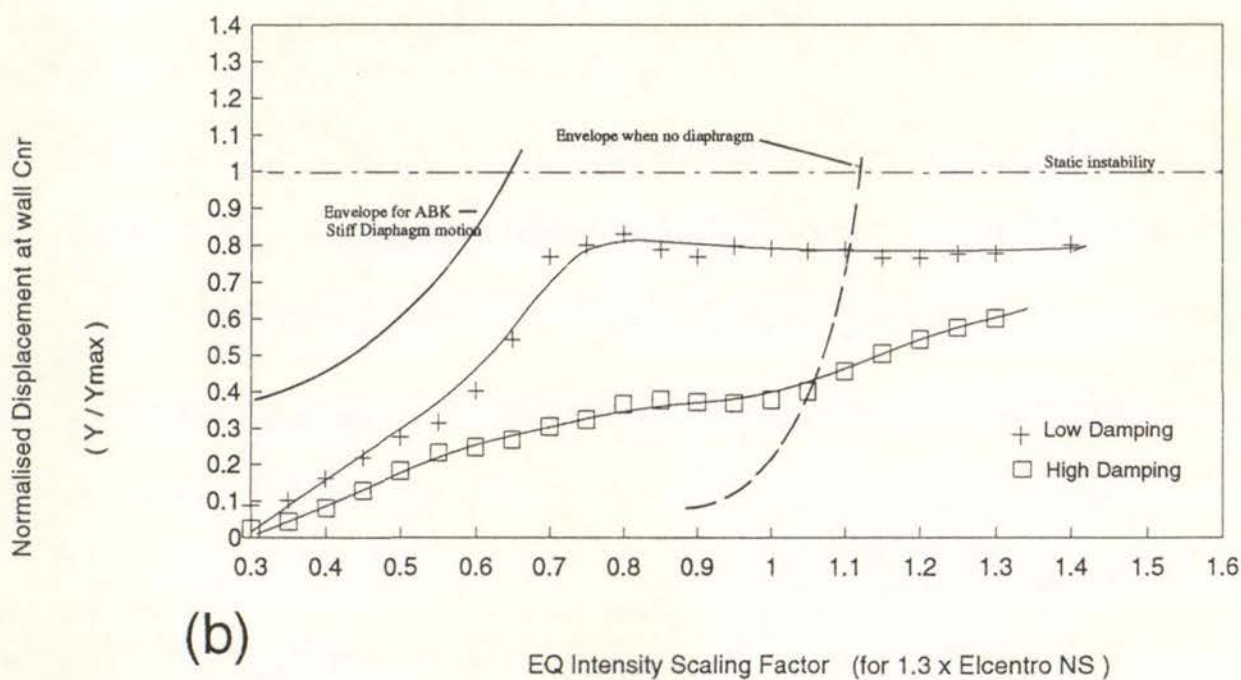
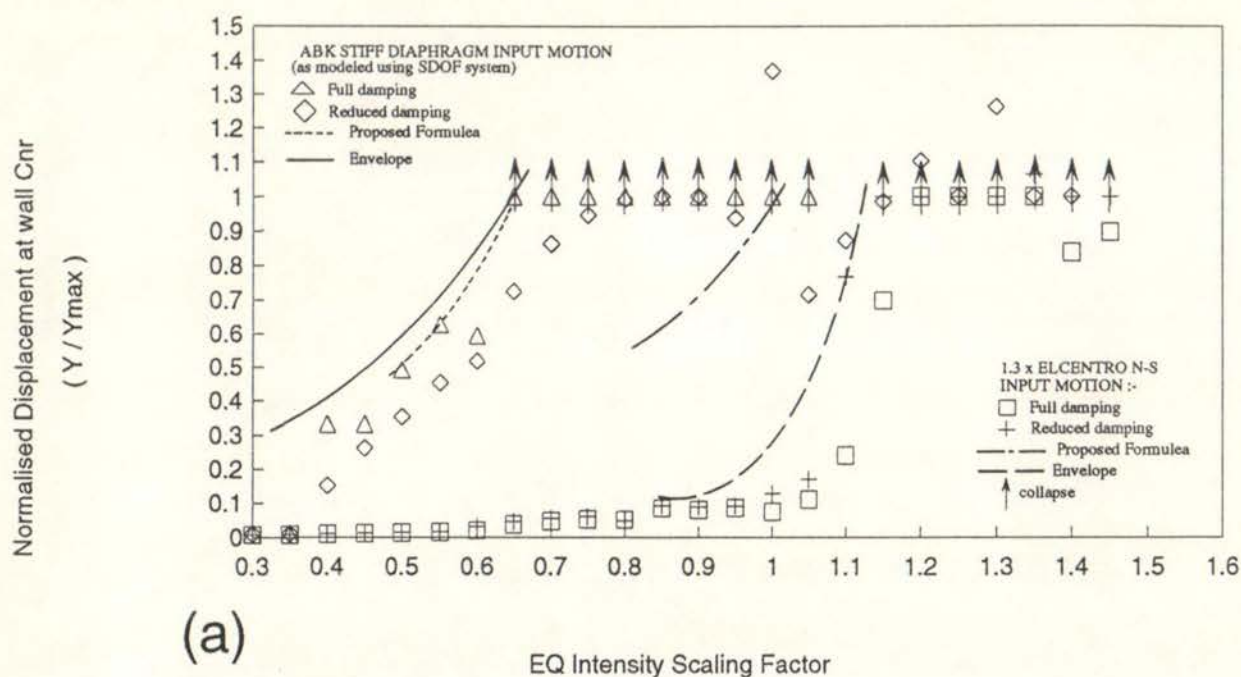


Figure 7.6 Peak Normalised Displacements at Mid-height of Face Loaded Wall Model Measured Relative to Line Joining Wall Element Ends.

- Wall Modelled with Rigid Diaphragms and subjected to 1.3 x El Centro NS EQ Motion and to ABK's Stiff Diaphragm Motion.
 - Wall Modelled with 0.5 second Diaphragms and subjected to 1.3 x El Centro NS EQ Motion.
- (See Table 7.1 for details of damping.)

In the ABK methodology the earthquake intensity (peak velocity) is scaled by a factor varying between 1.75 and 2.25 depending on the level of damping provided by the diaphragm and any timber crosswalls. The inverse of these amplification factors correspond to seismic resistance reduction factors of 0.57 and 0.44 respectively. These resistance reduction factors may be compared to the value of 0.58 predicted by the wall computer model when the diaphragms are modelled using the ABK test procedure and methodology.

Displacement and acceleration response spectra (for 15% damping) are given in Figure 7.7 for the 1.3 x the El Centro EQ motion and the ABK stiff diaphragm motion. These response spectra indicate that the diaphragm would be expected to have its greatest effect on the response of face loaded walls when they respond with a period close to the 0.5 second period that the diaphragm itself was modelled with.

However, as previously discussed in section 6.7.4, the wall period varies with displacement so that the "early" peak in the response spectrum that occurs at 0.5 seconds was used in the proposed formulae to predict the seismic resistance of the face loaded wall in this case.

Calculations using the proposed formulae to predict the seismic resistance of the walls for the ABK stiff Diaphragm motion and the 1.3 x El Centro motion were given previously in tables 6.4 and 6.5 and the predicted wall seismic resistances are reproduced in Figure 7.6(a). The agreement with the wall seismic resistance predicted by the computer model is good but the formulae tend to underestimate the effect of the diaphragms on the face loaded wall's stability.

7.2.2 Diaphragms Modelled with Flexibility

The method used to model the diaphragms so that they have nominal first mode vibration periods of 0.5, 1.0 and 2.0 seconds was described previously in sections 7.1.2 and 7.1.4.

When the computer modelled walls with these flexible diaphragms were subjected to an acceleration pulse it was shown in section 7.1 that they tended to respond with a 2nd mode period of about half the nominal periods given above. The SDOF diaphragm model used to obtain an approximation for ABK's stiff diaphragm motion had a period of 0.5 seconds. Therefore, the nominal period for the diaphragm to be used in the wall computer model for comparative purposes would be 0.5 or 1.0 for the 1st and 2nd modes respectively.

The displacements at mid-height of the wall modelled with a 0.5 second nominal diaphragm period are shown in Figure 7.6(b).

The input motion was 1.3 x the El Centro NS record and 2 levels of damping (see Table 7.1) were considered. Envelopes of the responses given in Figure 7.6(a) are reproduced in Figure 7.6(b) to facilitate a comparison between the two methods of

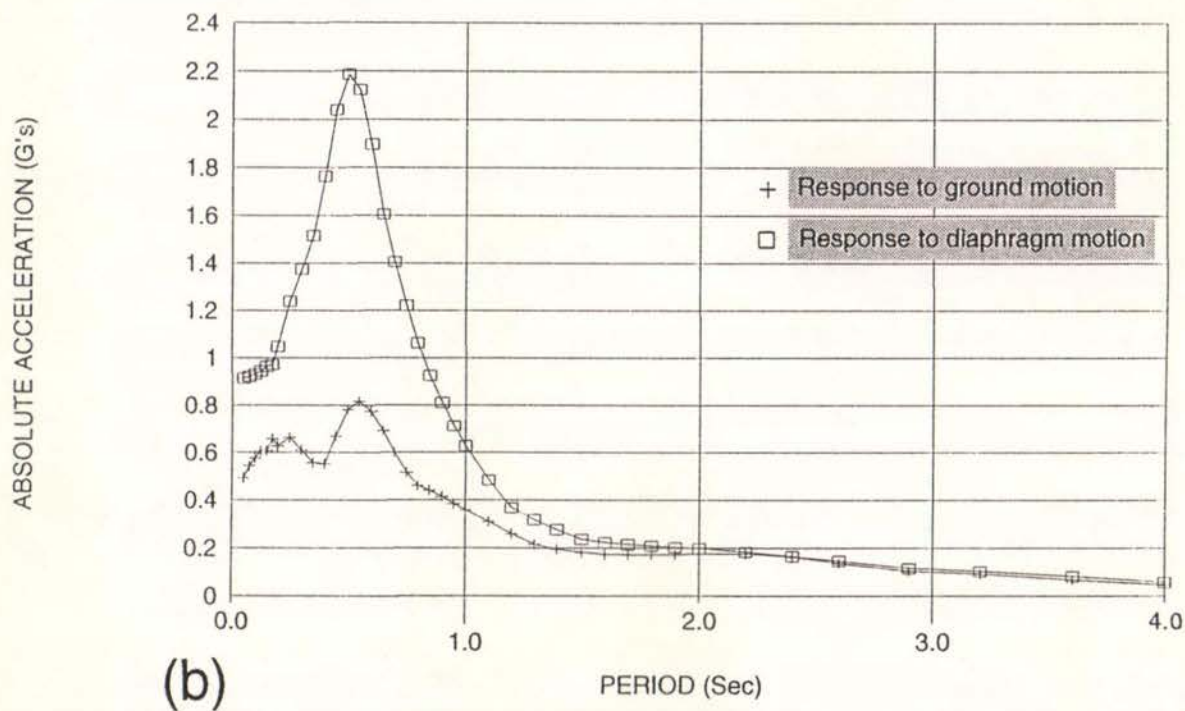
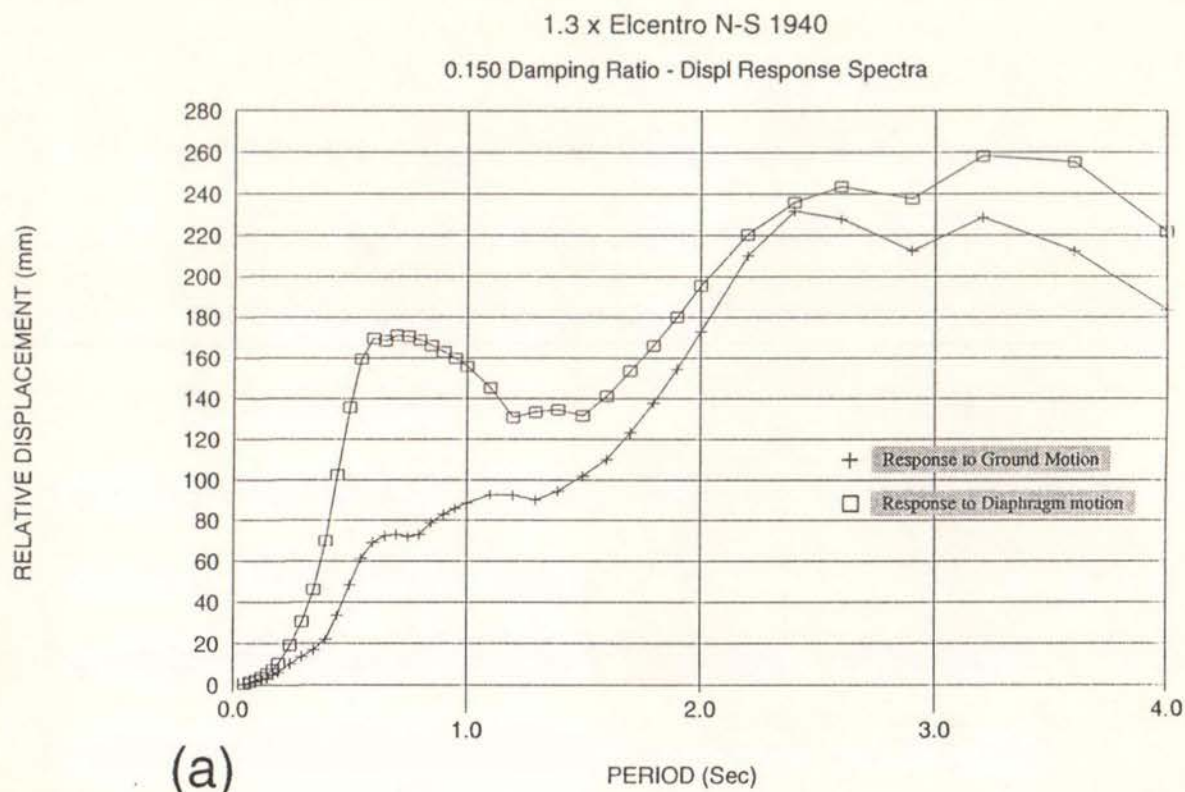


Figure 7.7 Elastic Response Spectra for 1st 15 seconds of the El Centro NS and ABK Stiff Diaphragm EQ Motions
 a) Displacement Response Spectra and;
 b) Acceleration Response Spectra

modelling the effects of diaphragms on the face loaded wall response.

It can be seen that the ABK methodology is conservative and that the degree of conservatism is dependent on the level of damping assumed for the computer model elements. For the low level of damping considered it can be seen from Table 7.1 (columns (3) and (4)) that the amount of damping provided in the diaphragm is only 2.5 and 5.0% for the first and second modes respectively. This is less than the 10% damping value used in the SDOF diaphragm computer model that was used to obtain the approximate ABK Stiff Diaphragm motion. The level of damping provided in the wall in the "low" damping case is also less than the "reduced" level of damping provided in the walls when the diaphragms were modelled using the ABK methodology. Therefore, results for the analyses with flexible diaphragms that should be compared with the envelope of the results obtained using the ABK methodology would lie between the "low" and "high" damping curves shown.

It can be seen in Figure 7.6(b) that the wall response in the low damping case did not increase when the EQ Intensity Scaling Factor was increased from about 0.7 to 1.4. Figure 7.8 indicates that there was a change in the response characteristics when the EQ Intensity Scaling factor reached 0.7. At this earthquake intensity the peak displacement at the mid-height of the wall, measured relative to a line joining the top and bottom of the wall, starts to exceed the displacement at mid-height of the wall measured relative to the diaphragms "ground" supports. This means that, at this earthquake intensity, the diaphragm displacements start to become at least partially out-of-phase with the mid-height wall displacements measured relative to a line joining the top and bottom of the wall element.

This change from in-phase to out-of-phase behaviour can also be seen for the high damping case in Figure 7.8. In this case the plateau in the response is much shorter. Some preliminary analyses using other earthquake records indicated that the long plateau in the response in the low damping case may only be a characteristic of the particular earthquake record used in the analyses.

Peak normalised displacements at mid-height of the face loaded wall when the diaphragms were modelled with a nominal period of 1.0 second are shown in Figure 7.9

Detailed inspection of the time histories of the diaphragm responses indicated that the approximately 0.5 second 2nd mode response of the diaphragms dominated the diaphragm response when the wall approached its collapse displacement. Therefore, the analysis results given in Figure 7.9 for the nominal 1.0 second diaphragm are also comparable with the results obtained using the ABK methodology and a 0.5 second diaphragm as given in Figure 7.6(a). The comparable level of damping used for the analysis of the walls with 1.0 second diaphragms would lie between damping cases 2 and 3 but closer to case 2. (See Table 7.1). The envelope of the results given in Figure 7.6(a) for the rigid (or no diaphragm case) has been reproduced in Figure 7.9. It can be seen that the method used by ABK to model the effects of the diaphragms on the wall response once again appears to be too conservative.

Peak normalised displacements at the mid-height of the face loaded wall when the diaphragms in the computer model were detailed to have a 2.0 second nominal

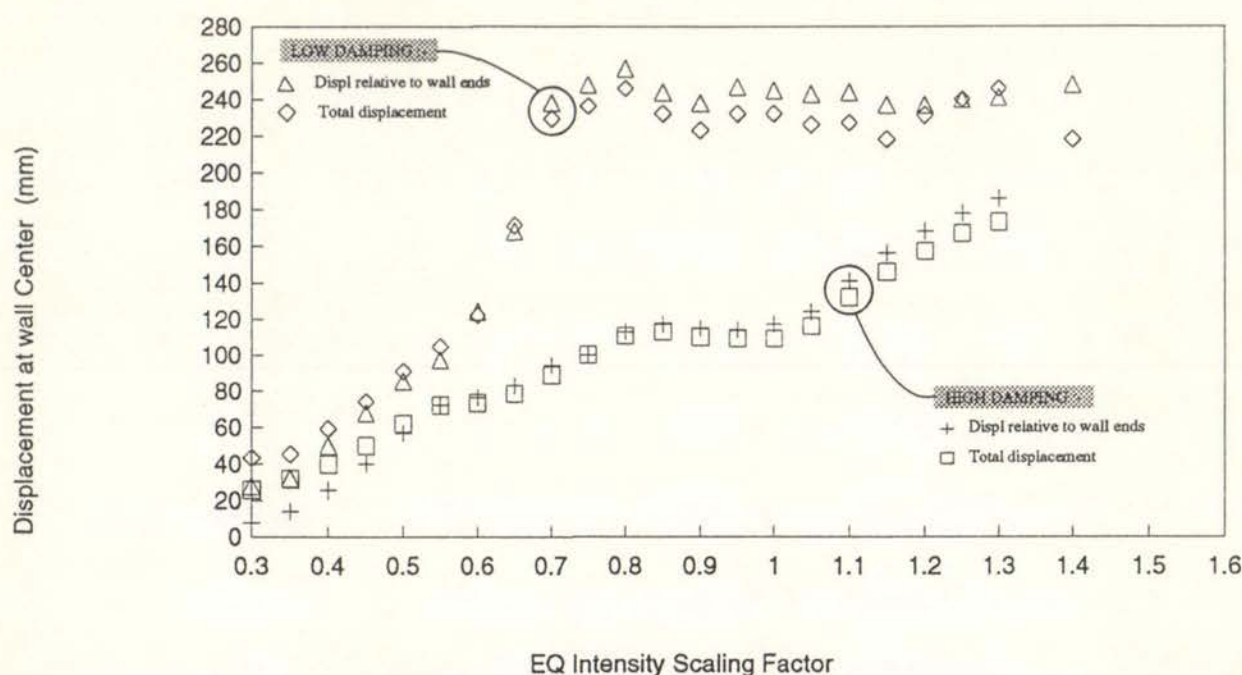


Figure 7.8 Peak Total and Relative Displacement at Mid-height of Face Loaded Wall when the wall is modelled with 0.5 second Diaphragms.

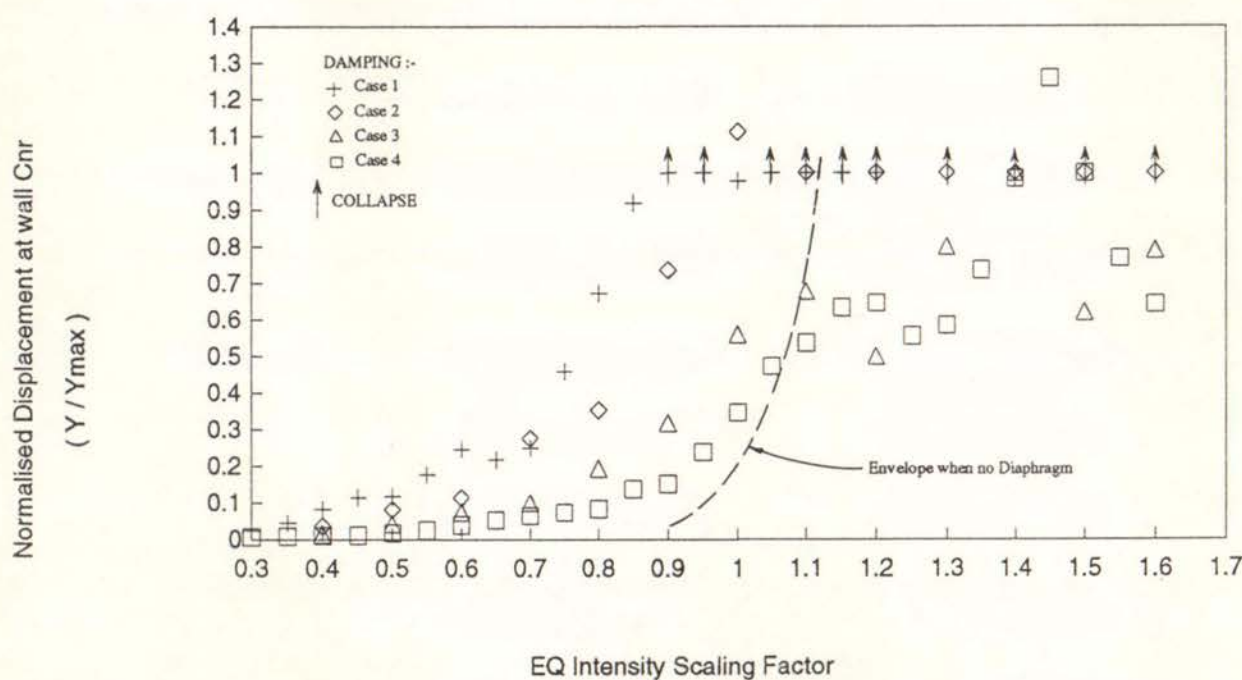


Figure 7.9 Peak Normalised Displacements at mid-height of Face Loaded Wall Model when the wall is modelled with 1.0 second Diaphragms. Displacements are measured Relative to Line Joining Ends of Wall Element and the input motion is 1.3 x El Centro NS (for details of Damping cases see Table 7.1).

period are shown in Figure 7.10. The envelope of the results expected when there is no diaphragm to affect the response, has been reproduced from Figure 7.9.

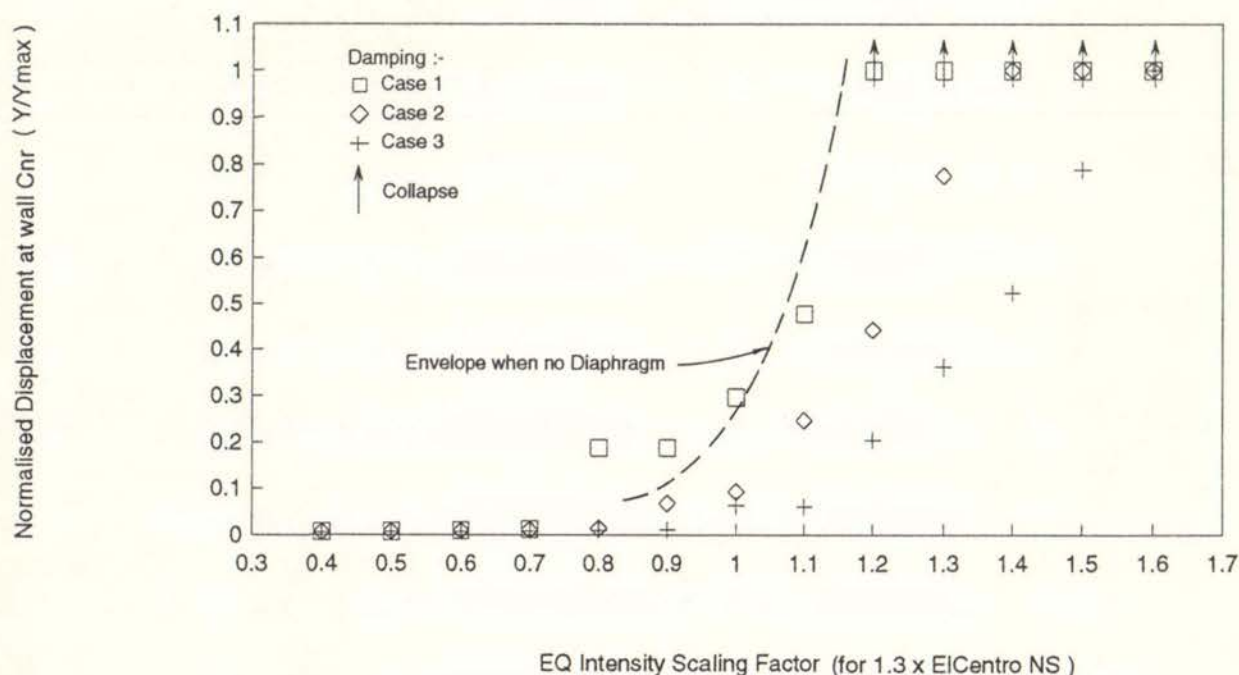


Figure 7.10

Peak Normalised Displacements at Mid-height of wall when wall modelled with 2.0 second Diaphragms. (For details of damping see Table 7.1)

The mass damping co-efficient, α used for the damping case 3 was 0.2. This is less than the 0.6 value used in comparable damping cases for the wall modelled with 0.5 and 1.0 nominal period diaphragms (see table 7.1). The mass damping co-efficient was reduced in this case because the mass damping also provides a significant component to the effective diaphragm damping when diaphragm displacements are large. If the wall was assumed to be rigid and the diaphragms responded in phase with a 2.0 second period, a mass damping co-efficient, $\alpha = 0.6$, would effectively produce an additional 15% damping for the diaphragms above that provided by the stiffness damping. A value of $\alpha = 0.2$ reduces this to 5% damping and places an upper limit of 5% on the additional effective damping provided by the diaphragms in the model.

The results presented in Figure 7.10 indicate that, for this earthquake record, it would be conservative to ignore the influence of the diaphragms on the stability of the face loaded walls when the diaphragms are very flexible.

7.2.3 Interaction Between Wall and Diaphragm Responses

As noted previously (Figure 7.9) the 0.5 second diaphragm displacements tend to move from in-phase to out-of-phase with the peak wall displacement measured relative to a line joining the top and bottom of the wall element.

The same type of behaviour was observed for the walls modelled with 1.0 second diaphragms as indicated in Figure 7.11. This suggests that the wall and diaphragms respond as an integrated system and helps explain why the method of modelling the diaphragms used for the ABK wall tests produces a different level of amplification of the face loaded wall response.

For the walls modelled with 2.0 second diaphragms the diaphragms tended to make an in-phase contribution to the peak wall displacement at all earthquake loading intensities as indicated in Figure 7.12. This was also evident when the time histories of the wall and diaphragm displacements were examined in detail.

It would appear that diaphragms and walls share the total displacement demand generated by the earthquake. This may help explain why the walls modelled with flexible 2.0 second diaphragms tended to be the most stable. However, the beneficial effect of the total displacement demand is counterbalanced to some degree by the influence of comparatively large relative displacements that developed between the top and bottom diaphragms.

These displacements would tend to destabilise the wall and reduce the wall displacement (measured relative to a line joining the top and bottom of the wall) at which the wall would become statically unstable.

The peak relative displacements between the top and bottom diaphragms are compared in Figure 7.13 with the peak displacements measured at the mid-height crack level of the walls. Figures 7.13(a) and (b) present the results for the walls modelled with 1.0 and 2.0 second diaphragms respectively.

For the wall modelled with 1.0 second diaphragms the peak relative diaphragm displacements are reasonably stable and reach a maximum of about 2/3 the peak (bottom) diaphragm displacement of 150 mm. An examination of the time history of the wall and diaphragm responses indicated that the relative diaphragm displacements were not having a significant effect on the face loaded wall stability in this case.

However, for the wall modelled with 2.0 second diaphragms, the relative diaphragm deflection can be seen to increase with earthquake intensity and reach a maximum of 280mm, which is about 80% of the peak (bottom) diaphragm displacement. A detailed examination of the wall and diaphragm response time histories indicated that these large relative diaphragm displacements were contributing significantly to the instability of the wall.

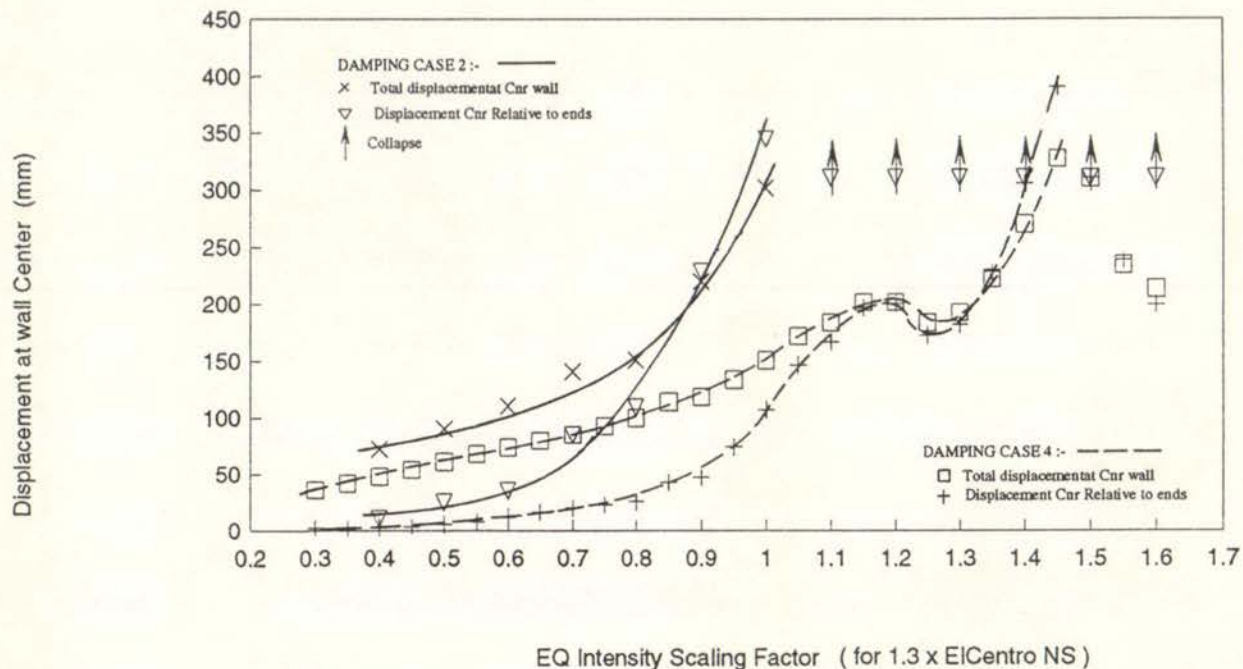


Figure 7.11 Total and Relative Displacements at the Mid-height crack level of Face Loaded Wall when wall modelled with 1.0 second period Diaphragms.

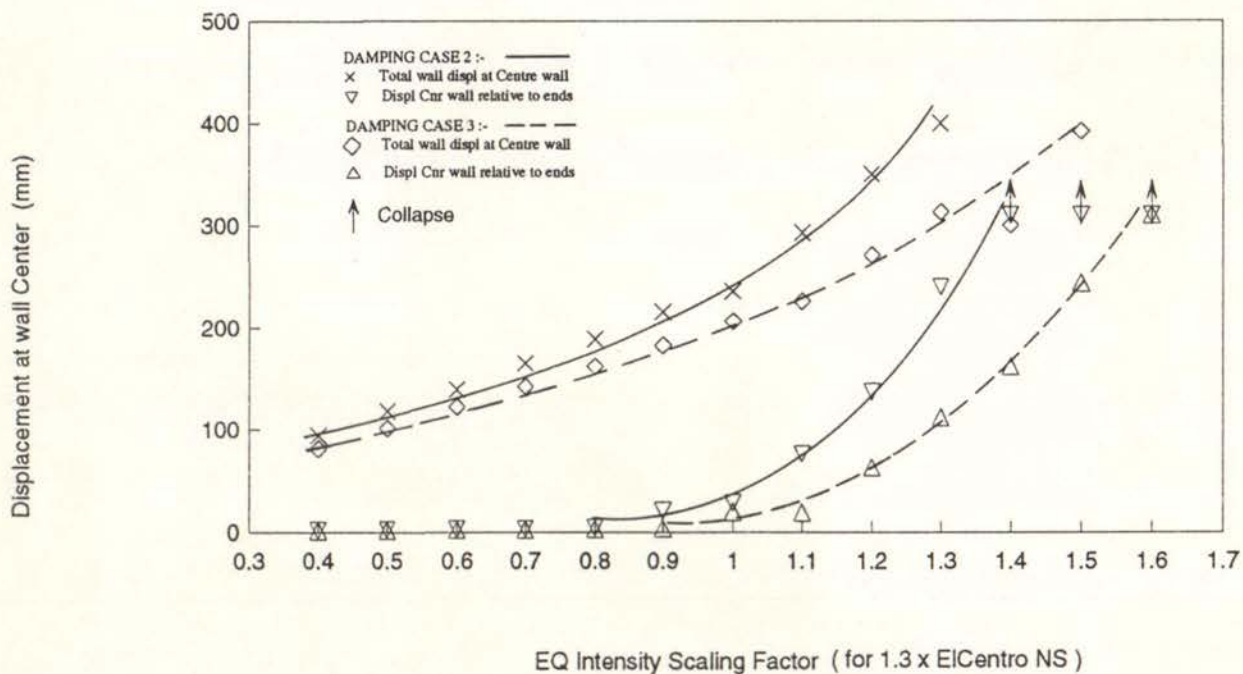


Figure 7.12 Total and Relative Displacements at Mid-height crack level of Face Loaded Wall when the Wall is modelled with 2.0 second Diaphragms

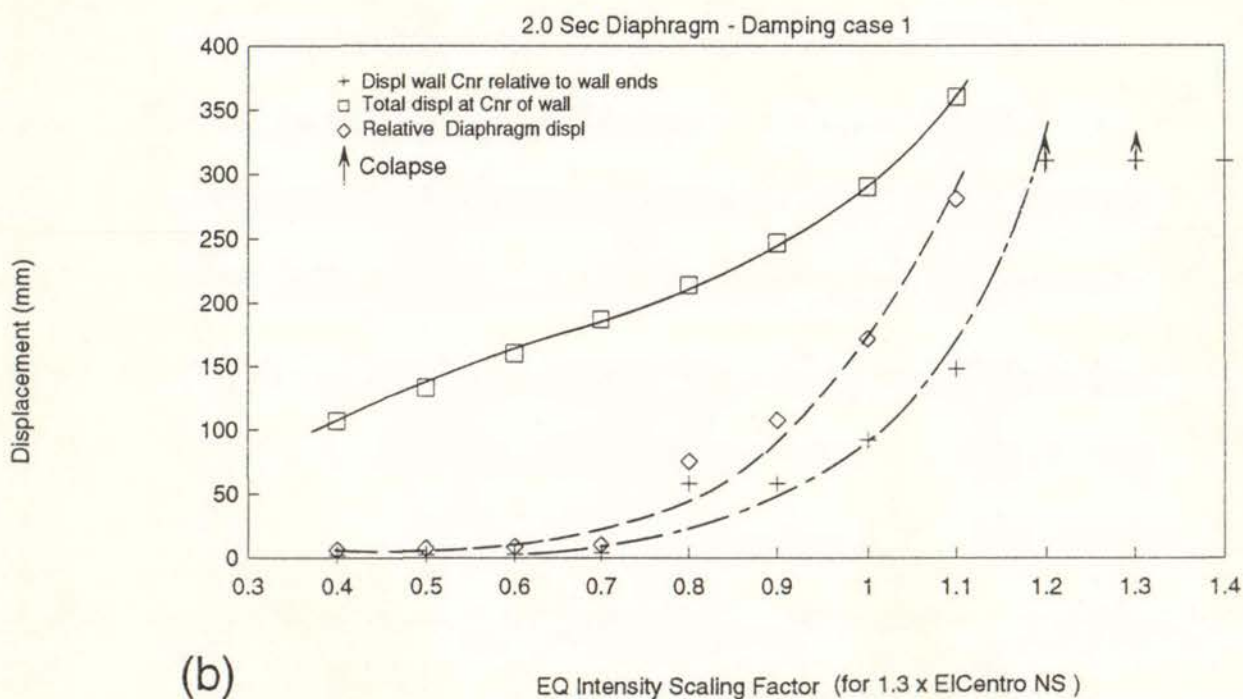
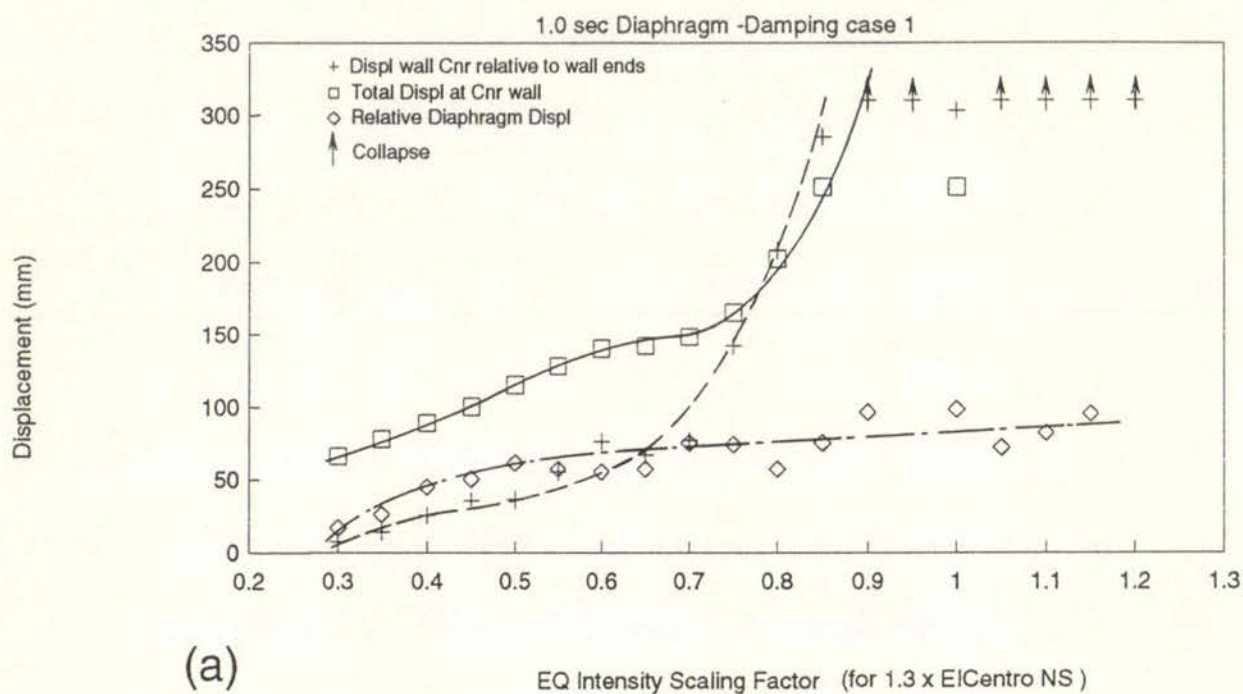


Figure 7.13

Comparison Between the Peak Relative Displacements of the Top and Bottom Diaphragms and the Peak Displacements at the Mid-height crack level of the wall;

- a) When the wall Modelled with 1.0 second Period Diaphragms and;
- b) When the wall Modelled with 2.0 second Period Diaphragms.

7.2.4 Effect of Impact on Damping

For the wall modelled with the 1.0 second diaphragms the parameters used for damping case 5 given in Table 7.1 were the same as those used for damping case 1 except that 100% of the wall's vertical inertia was modelled for damping case 5. Analysis results for damping case 5 were practically the same as those obtained for damping case 1 up to a wall displacement of 80% Y_{max} and have not been presented here.

Similar results were obtained for the wall modelled with 2.0 second diaphragms for damping cases 2 and 4.

These results indicate that impact may not be making a significant contribution to the total level of damping when the walls are modelled with flexible diaphragms.

This aspect of the wall modelling was not investigated further and no explanation is offered for this phenomenon.

7.2.5 Diaphragm Anchorage Forces Developed by Flexible Diaphragms

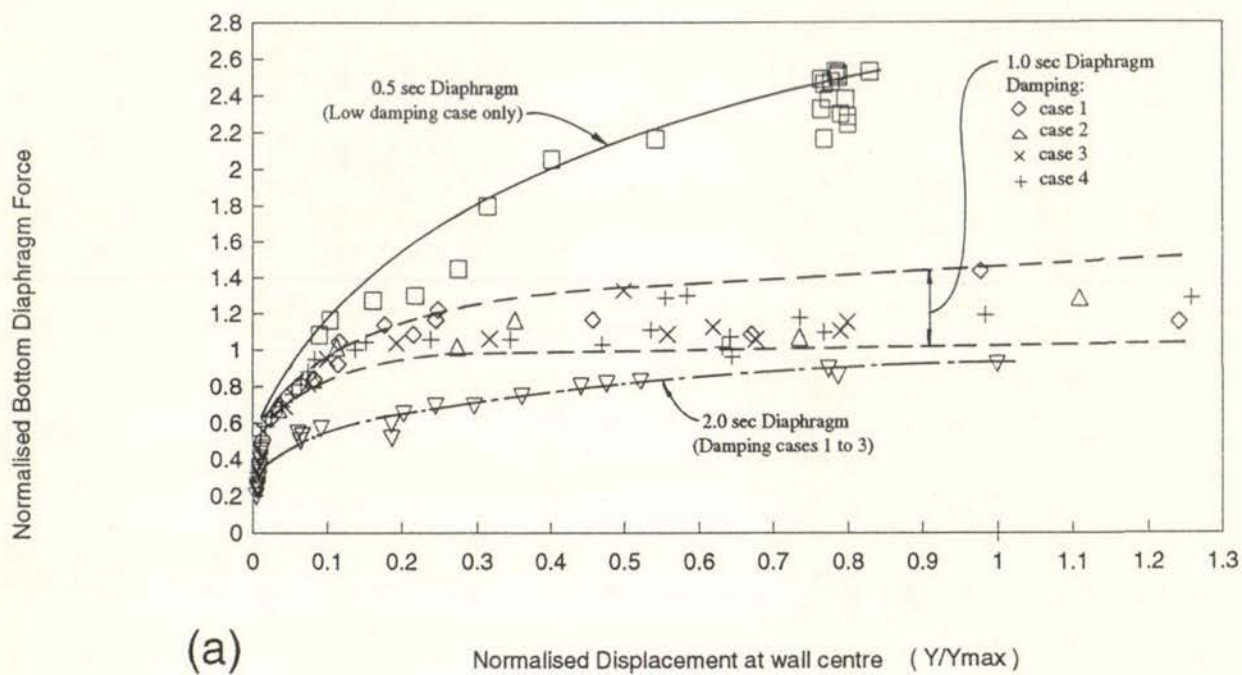
The peak anchorage forces that the wall computer model predicts will develop at the junctions between the wall and diaphragms at the bottom and top of the wall are shown in Figures 7.14(a) and (b) respectively. The anchorage forces have been normalised using the reaction that would develop at the top and bottom of the wall if a uniformly distributed load was applied to the wall that was just sufficient to open cracks assumed to be located at the base and mid-height of the wall (7.4 kN/m at bottom and 4.6 kN/m at top).

The normalised anchorage forces are shown plotted relative to the normalised displacement at the mid-height crack in the wall. The wall displacements in this case were measured relative to a line joining the top and bottom of the wall and the normalising displacement, Y_{max} , was computed using equation 4 and ignoring the effects of relative diaphragm displacements on the wall's stability. Details of the damping parameters used are given in table 7.1 and the same symbol is used to indicate results for the same damping case in both Figure 7.14(a) and Figure 7.14(b).

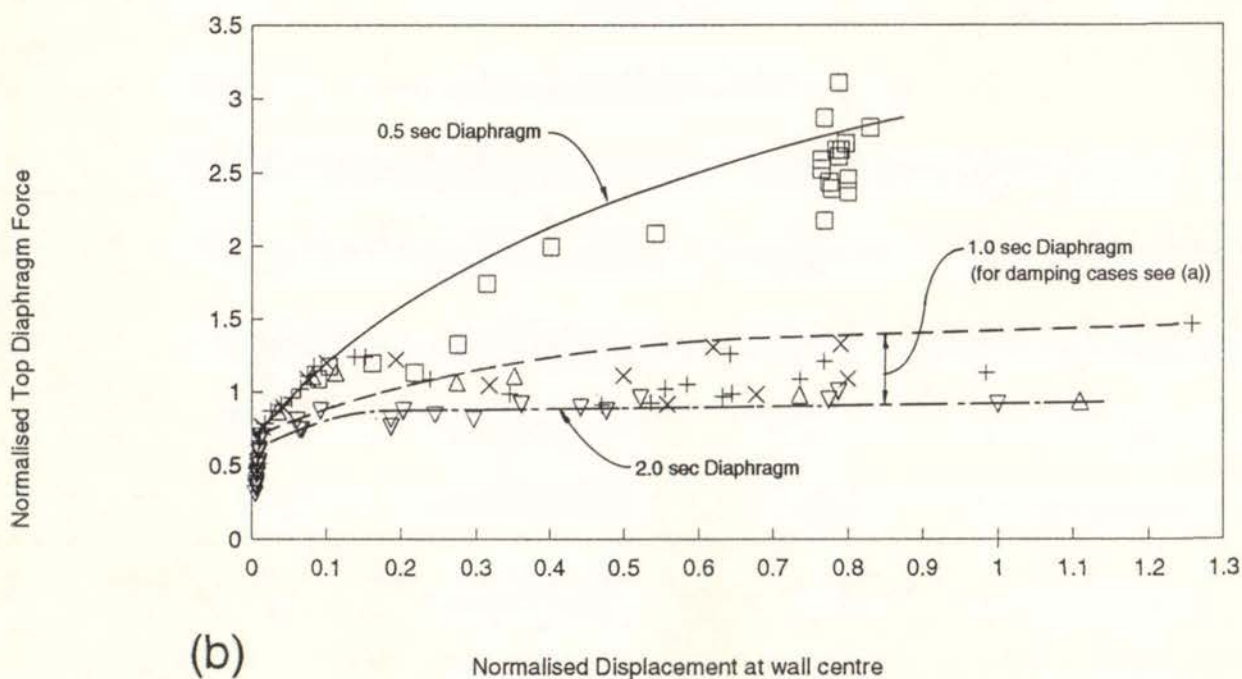
The anchorage forces can be seen to increase with increasing diaphragm stiffness and to be insensitive to the damping provided. The results for the walls modelled with 1.0 and 2.0 second diaphragms are similar to those obtained in section 6.6.4 for walls modelled with rigid diaphragms and ignoring the sharp peaks in the response generated by impact forces. For these two diaphragm periods it would appear that opening of the wall cracks is acting as a "fuse" so that an increasing wall response does not produce a significant increase in anchorage forces.

However, the results for the walls modelled with 0.5 second diaphragms indicate that the anchorage forces tend to increase significantly with wall response.

The possibility that the higher anchorage forces in this case were due to impact were investigated. One analysis with no vertical inertia provided in the wall model (so that impact forces were eliminated) indicated that the higher anchorage forces were



(a)

Normalised Displacement at wall centre (Y/Y_{max})

(b)

Normalised Displacement at wall centre

Figure 7.14 Relationship Between Peak Diaphragm Anchorage Forces and Peak Wall Displacements predicted by the Face Loaded Wall Computer Model for

- a) Bottom Diaphragm and;
- b) Top Diaphragm (for details of damping see table 7.1)

not the result of impact. However, further analyses for walls modelled with both rigid and stiff diaphragms and no vertical inertia are required to confirm this conclusion.

A normalised diaphragm anchorage force of 1.0 in Figure 7.14 corresponds to a lateral load design coefficient, C_d , of .33 (see equation 8) Therefore the analysis results given in Figure 7.14 indicate that relatively high levels of strength would need to be provided for anchorages and diaphragms if they are to remain elastic. For the walls with 0.5 second diaphragms the results indicate that anchorages and diaphragms would need to be designed for a strength corresponding to a lateral load coefficient of 1.0g to remain elastic.

If face loaded walls on either side of a diaphragm respond out-of-phase, a flexible diaphragm could act as a relatively rigid tie. In this case it would be unconservative to rely on diaphragm flexibility or yielding to limit the anchorage forces. In most cases the displacement capacity of wall anchors will be small relative to the wall and diaphragm displacements. Therefore it is unlikely that yielding could be used to significantly reduce the forces that may develop in the anchorages.

These considerations would lead to the conclusion that anchorages should be designed conservatively using a capacity design philosophy.

As pointed out above, the diaphragm modelled with a 0.5 second nominal period would need to have a strength corresponding to a lateral design coefficient of about 1.0g if it was to remain elastic for the range of earthquake intensities considered. If the diaphragm had been modelled with a lower strength it would have deformed inelastically (yielded) and performed more like the 1.0 and 2.0 second diaphragms with a higher level of effective damping. The analysis results indicate that the anchorage forces would then have been reduced and the stability of the face loaded walls would have been improved.

Conversely, the analysis results also indicate that if a flexible diaphragm is strengthened, anchorage forces will be increased and the stability of face loaded walls tied to the diaphragm may be reduced.

As noted above, a normalised diaphragm anchorage force of 1.0 in Figure 7.14, corresponds to a lateral design coefficient of .33g. This coefficient was computed for the full scale wall model that only had a small overburden load, O , representing a parapet. For lower storey walls with higher overburden pressures the lateral design coefficient corresponding to wall crack opening would be considerably higher.

Therefore, the results indicate that if diaphragms were designed with the minimum strength suggested by ABK of 0.2g (see section 4.3 and Figure 4.1(b)) large displacements and/or yielding demand would be imposed on the diaphragms.

However, the need for high strength or displacement capacity is not consistent with the lack of damage observed in diaphragms following earthquakes (see Section 2.10.4).

Further modelling of face loaded walls supported by low strength diaphragms, as

may be found in existing URM buildings in New Zealand, is required.

7.2.6 Analyses Using Other Earthquake Records

Similar analyses were performed using the wall computer model and the Coalinga earthquake motion.

Results of these analyses were given in Figure 2.3 and discussed in Section 2.8. Figure 2.3 indicates that flexible diaphragms had only a relatively moderate effect on the intensity of shaking required to cause collapse under face loading. This is in spite of using in the analyses, the lowest level of damping given in Table 7.1 for each of the diaphragm periods considered.

These results are consistent with those obtained for the El Centro record given above and support the conclusion that the method used by ABK to allow for diaphragm flexibility in their wall testing and methodology is too conservative.

When the predicted wall stability indicated by Figure 2.3 is compared with the actual level of damage in the Coalinga earthquake it may also be concluded that the computer model predictions are probably conservative, at least when low levels of damping are used in the computer model for the wall and diaphragm components.

Using the formulae and procedure given in Sections 6.7.3 and 6.7.4 the earthquake intensity required to cause wall collapse was estimated at 64% of the Coalinga earthquake intensity. This may be compared with the 78% earthquake intensity Scaling Factor predicted by the computer model for the rigid diaphragm condition as shown in Figure 2.3. This suggests that the proposed formulae are also conservative.

8. ANALYSIS OF REGENT THEATRE BUILDING - DANNEVIRKE

8.1 Details of Building

The Regent Theatre building is of interest because it is one of the largest buildings in Dannevirke and would appear, at first glance, to be vulnerable to earthquake damage. However, the building survived the Weber earthquake with relatively little damage that could be attributed with confidence to the earthquake. Further details of the Weber earthquake were given in Section 2.7.

The theatre was built in 1918 with a large upper circle but this was removed after the 1934 Pahiatua Earthquake. The remaining building is essentially a large 38 x 15m rectangular box as shown in Figure 8.1(a). A concrete band and diagonal steel bracing were added to the building at roof level, probably after the 1934 earthquake. These features are shown in Figure 8.1(a).

After the Weber earthquake two nuts from the ends of the rods in one of the bracing bays were found on the ground. The nuts had been filled with mortar to hide the fact that they only engaged a few threads on the bracing rods. The other end of the rods with the missing nuts were projecting 200-250 mm from the wall (see Figure 8.1(b)). This is the only evidence found that significant wall displacements had taken place at roof level. The building has recently been divided in half (circa 1988) by a transverse fire wall. This is a timber stud wall lined on both sides with gib board. Lighting within the building during the site inspection was poor but the lack of observed damage to the gib wall suggests that the roof level displacement at the centre of the longitudinal walls did not exceed more than 50 to 75mm. This would indicate that the 200- 250mm protrusion of the failed diagonal bracing rods from the wall face was generated progressively during the earthquake and not during a single cycle of the response.

The roof diaphragm consisted of straight board sarking clad with galvanised iron. A pinex ceiling diaphragm had been added at some stage but this was not continuous at the central gib clad fire wall.

The lime mortar exposed on the exterior faces of the building had weathered in places but could only be dug out with great difficulty using a car key. The mortar was tested using a builders hammer and a nail punch with a 3mm diameter point. In each test location the nail punch was driven into the vertical joints with 6 firm hammer blows. For 7 test locations on the exterior face of the building the nail punch penetration varied between 11 and 35mm with an average of 19.1mm. This mortar quality appeared to be typical of the lime mortar used in most of Dannevirke's commercial buildings.



Figure 8.1 Regent Theatre Building Dannevirke

- a) Building viewed from South.
- b) SW wall of Building and Location of anchor rods protruding 200-250 from wall.

8.2 Computer Modelling

The longitudinal walls of the theatre were analysed using DRAIN-2DX for the Weber EQ motion. The computer model used to analyse the face loaded walls of the theatre was essentially the same as that described in section 6.2. However adjustments were made for the height of the walls (7.5m) and the nominal (480mm) and effective (460mm) wall thicknesses. The lower diaphragm was also deleted from the model and replaced by a lateral ground support at the bottom of the wall.

Two conditions were assumed for support at the top of the wall; no support, or a weak support representing the combined effect of the central fire wall and the roof diaphragm.

ABK (38(h)) give the yield capacity of a single layer of T & G flooring or straight sheeting with roofing applied directly to the sheathing as 4.4 kN/m. However unpublished testing carried out at Works Central Laboratories on a section of existing T & G flooring showed that these types of diaphragm are very flexible. The section of floor tested by Works Central Laboratories had a span of 4.6m and depth of 2.7m and it was loaded at midspan statically and dynamically. The loads were applied cyclically with increasing peak displacements.

The secant modulus, G , representing the shear stiffness of the diaphragm was computed from the peak displacements and is given in Table 7.2. The secant modulus was calculated using the relationship:

$$y = V L/G \dots\dots\dots 15$$

where y was the peak displacement at midspan of the diaphragm, V was the shear flow at each of the diaphragms two supports and L is half the diaphragm span.

Table 7.2 Shear Stiffness of T & G Diaphragms

Displacement y (m)	Shear Flow V kN/m	Secant Modulus G kN/m
.013	1.1	195
.055	2.2	92
.125	2.5	46
.3	5.0	38

For the Regent Theatre it was assumed that the central fire wall and roof diaphragm would only provide support for the face loaded longitudinal walls in the central half of the building. The remaining sections of the longitudinal walls were assumed to be supported by a combination of the concrete band at roof level, horizontal spanning of the face loaded walls and the diagonal steel bracing that was still effective, at least in the end bays.

Using these simplifying assumptions and data published in reference (48) it was estimated that the peak strength developed by the central fire wall and roof diaphragm would be 5.5 kN per metre of face loaded wall and that the displacement at the top of the wall at midspan of the diaphragm would be 75mm when this load developed. At this displacement the diaphragm only developed a shear flow of 1.1 kN/m and contributed only 16% of the restraining force. The total restraining force of 5.5 kN/m corresponded to a lateral load design co-efficient, C_d , of only 0.14g based on the weight of the top half of the face loaded walls and the parapet. The central fire wall and roof diaphragm were modelled in the face loaded computer model as an elastic truss member that yielded elasto-plastically at a force of 5.5 kN/m and displacement of 75mm.

The earthquake record used to represent the Weber earthquake was the N67E component of the ground accelerations recorded at the Dannevirke PO site located in the adjacent city block to the Regent Theatre. This component of the record had an orientation that was normal to the longitudinal walls of the Regent Theatre.

8.3 Predicted Response of Regent Theatre Face Loaded Walls

Displacement time histories for the Regent Theatre longitudinal walls predicted by the wall computer model are shown in Figure 8.2. In this case the walls were modelled without a roof diaphragm (i.e. as a free standing cantilever) and input motion for the computer model was 1.0 x the Weber earthquake intensity. Displacements predicted at the top of the wall are shown in Figure 8.2(a) and those predicted to occur at the mid-height crack level, measured relative to a line joining the top and bottom of the wall, are shown in Figure 8.2(b)

If the wall responded as a rigid body rocking on its foundation, it would not become statically unstable until the displacement at the top of the wall exceeded the effective wall thickness of 460mm. It can be seen (Figure 8.2(a)) that the peak displacement at the top of the wall was only 165mm so that the computer model predicts that the wall would have remained stable even without any support from the roof diaphragm or fire wall.

The relative displacements given in Figure 8.2(b) correspond to the wall displacements generated by the mid-height crack opening and closing. They may also be viewed as a measure of the contribution made to the wall displacements by a second mode wall response. In this second mode response, wall displacements are generated by the top half of the wall rocking back and forth on the lower half of the wall.

For the second mode, a negative displacement in Figure 8.2(a) corresponds to a positive contribution to the displacement at the top of the wall that is shown in Figure 8.2(a). Therefore it is evident that the second mode is generally in phase with the first mode and makes a positive contribution to displacements at the top of the wall. This type of in phase behaviour was not observed when diaphragms were modelled at the top of the wall.

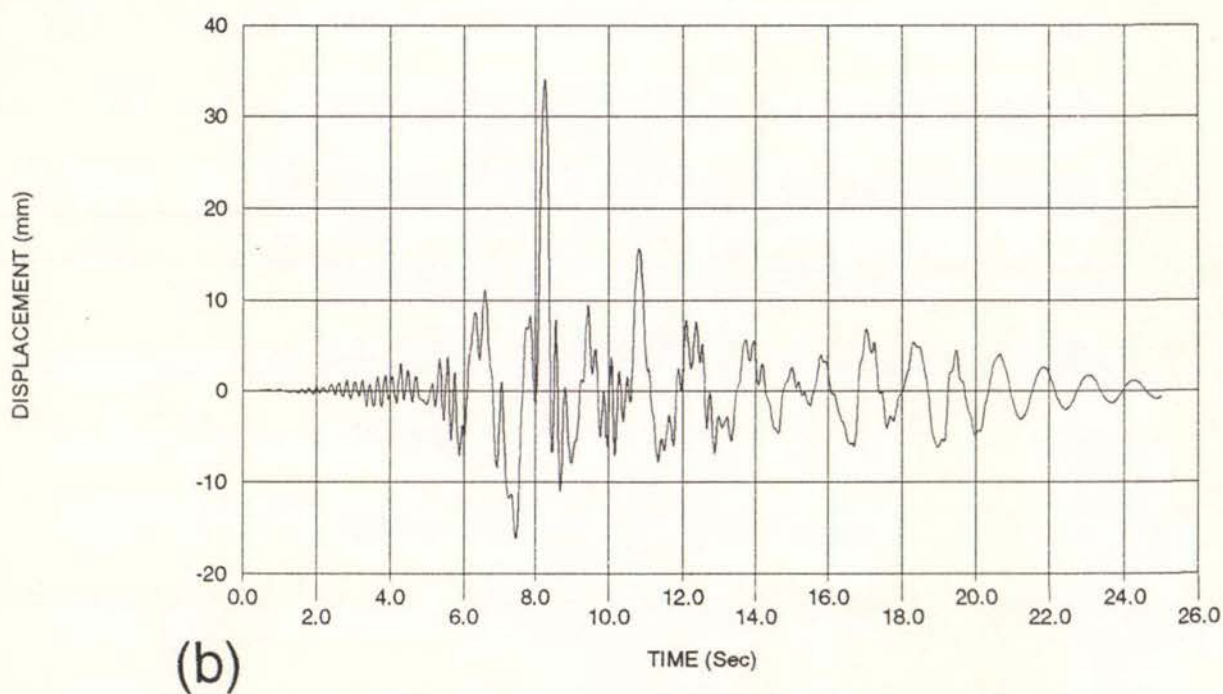
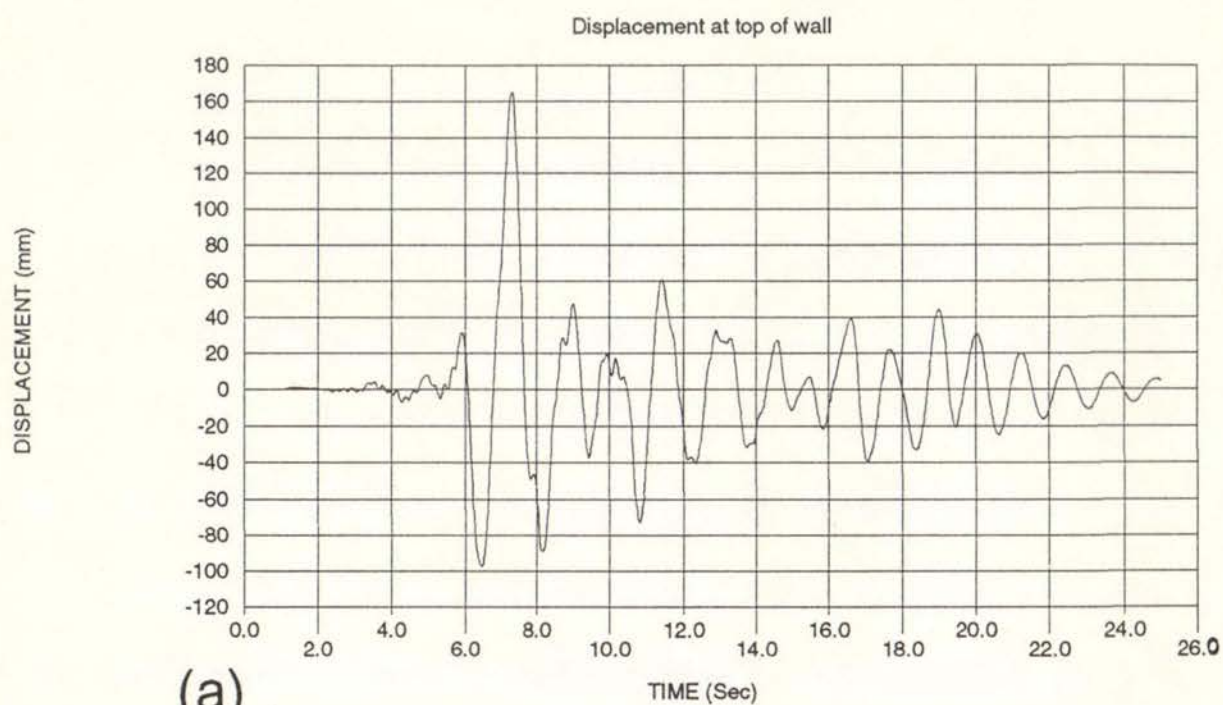


Figure 8.2 Displacement of Regent Theatre Longitudinal Walls when walls modelled without a Roof Diaphragm and subjected to 1.0 x WEBER EQ Motion.

- a) Displacements at Top Wall and;
- b) Displacements at Mid-height crack level measured Relative to Line Joining Top and Bottom of Wall.

The analysis that produced the time histories given in Figure 8.2 used the first 25 seconds of the earthquake record. For the remaining analyses of the Regent Theatre walls, only the earthquake motion in the record between 5 and 18 seconds was used as the input motion for the computer model. Peak displacements recorded for these analyses are shown in Figure 8.3.

Two levels of wall damping were considered, "full" and "reduced". These damping levels were previously described fully in section 6.5.8. Two levels of damping were also considered for the roof "diaphragm" element in the model. For the "full" level of diaphragm damping, a stiffness damping coefficient, $\beta = .024$ was used for the diaphragm element. The level of damping that this coefficient would have produced in the diaphragm when it was close to its peak displacement was calculated using the period estimated from the time histories of the diaphragm responses. This procedure indicated that the diaphragm damping was generally in the range 5 to 10% with the level of damping decreasing with increasing diaphragm displacement.

For the "low" diaphragm damping a stiffness damping coefficient, $\beta = .002$ was used. This would have produced about 10% of the above damping levels.

When the results given in Figure 8.3 for the range of damping parameters considered are compared, it is evident that the addition of a diaphragm, even if it has low damping, is the most effective method of reducing wall displacements. This can be confirmed by comparing results for (a) the case with no roof diaphragm and reduced wall damping and; (b) the case with low roof diaphragm damping and reduced wall damping. The reduction of wall displacements due to additional wall and/or diaphragm damping is then seen to be relatively marginal.

As the "diaphragm" in the computer model primarily models the effect of the transverse timber fire wall located at midspan of the longitudinal face loaded walls, the analysis indicates that the addition of timber shear walls is an effective means of reducing face loaded walls displacements in moderate earthquakes. However, if this building was subjected to a major earthquake that induced displacement at the top of the wall closer to the limit that would produce instability of the face loaded walls (i.e. 460mm), the timber fire wall would probably be effectively destroyed as a load resisting element early in the response. Under these conditions its contribution to the stability of the face loaded walls may not be significant.

The lack of damage observed in the timber fire wall after the Weber earthquake suggests that the displacement at the top of the wall was not more than about 50 to 75mm. The displacements at the top of the wall given in Figure 8.3(a) for an EQ Intensity Scaling Factor of 1.0 are generally greater than this limit and indicate that either; damping in the system was higher than the upper limits assumed, the horizontal spanning of the face loaded walls was more effective than assumed or that the remaining diagonal steel bracing in the ceiling plane was more effective than assumed in the computer model. Damping associated with soil-structure interaction may also have been significant.

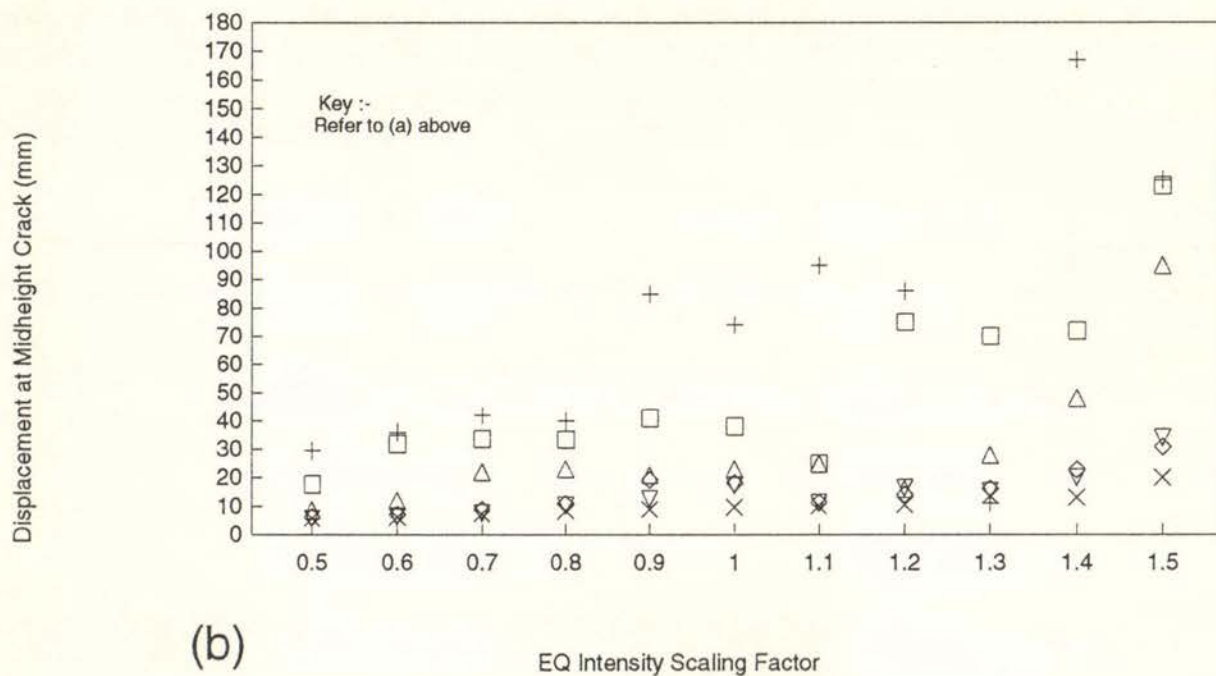
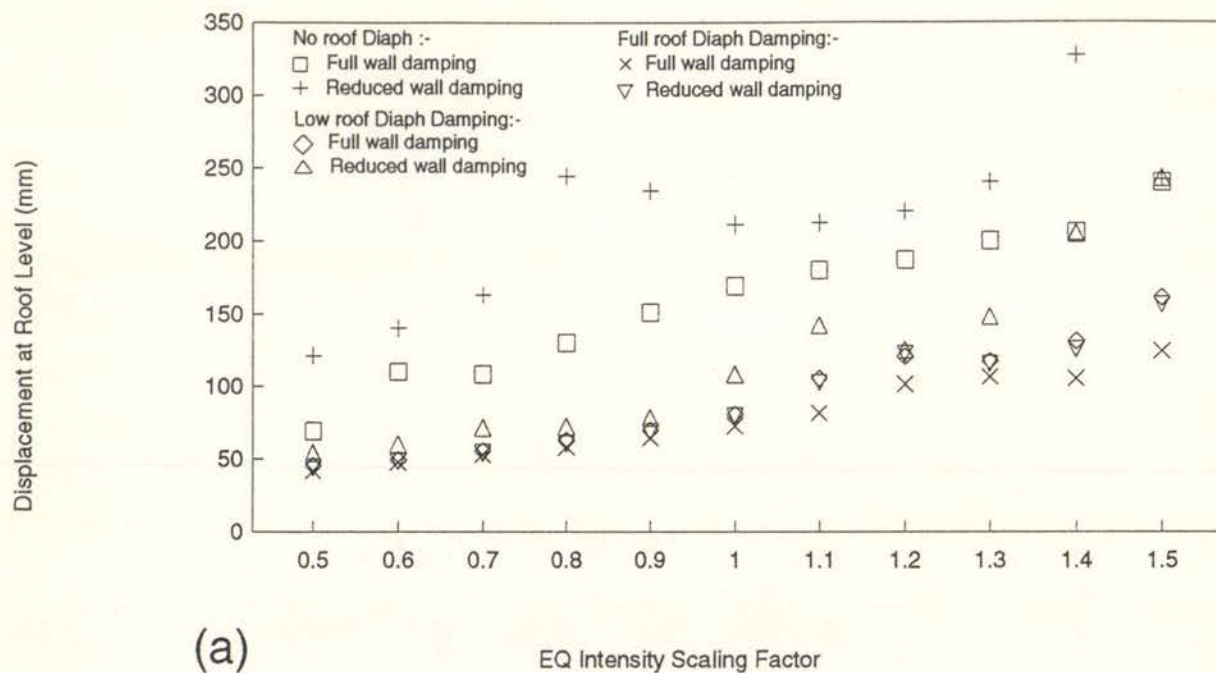


Figure 8.3 Displacement of Regent Theatre Longitudinal Walls Predicted by Computer Model for a Range of WEBER Earthquake Intensities and Damping Parameters.

- Displacements at Top of Wall and;
- Displacements at Mid-height Crack level Measured Relative to Line Joining the Top and Bottom of the Wall

9 METHODOLOGY FOR EVALUATING THE SEISMIC RESISTANCE OF FACE LOADED URM WALLS.

9.1 Introduction

In this section of the report a methodology is proposed for evaluating the seismic resistance of face loaded URM walls. Initially the steps required to evaluate a wall using the proposed methodology are summarised. A more detailed explanation of the procedures required for each step is then given. Finally, aspects of the proposed methodology that require further research are outlined.

9.2 Summary of Proposed Methodology

Step 1

Evaluate the earthquake intensity required to cause the wall to collapse if the building had rigid diaphragms and shear walls.

Step 2

Apply a resistance reduction factor to allow for the effects of diaphragm flexibility.

Step 3

Apply a further seismic resistance reduction factor to the earthquake intensity evaluated in Step 2 to allow for any amplification of the seismic motions in the upper floors of multi-storey buildings.

Step 4

Evaluate the anchorage forces that are required at the wall diaphragm junctions to maintain wall stability and the minimum diaphragm strength required to control diaphragm displacements.

9.3 Details of Proposed Methodology

9.3.1 Step 1 : Seismic Resistance of Face Loaded Walls with Rigid Diaphragms

The procedure to be used to evaluate the seismic resistance of face loaded walls with rigid diaphragms is detailed in Section 6.7.

In this procedure the free vibration period of a face loaded wall is estimated using a semi empirical formula. (Equation 10).

The period calculated from the formula corresponds to the free vibration wall period expected when the face loaded wall reaches a peak displacement that is 60% of the displacement at which the wall becomes unstable, Y_{max} .

This period is used in conjunction with a displacement response spectrum to estimate the earthquake magnitude required to cause the wall to reach a peak displacement

of $0.6 Y_{\max}$. It is then assumed that the wall would collapse if the earthquake intensity was increased by a further 20%.

The earthquake motion used for the analysis may be a specific earthquake record or a design spectrum. In either case a displacement response spectrum is required for the analysis. This may be derived from an acceleration response spectrum as described in Section 6.7.2.

To obtain the peak face loaded wall displacement expected in an earthquake a scaling factor has to be applied to the displacement value read from the displacement response spectrum. This scaling factor is required to allow for the difference between the response expected for a multi-degree of freedom face loaded wall and that expected for a single degree of freedom system. It also provides for a "factor of safety". The magnitude of the scaling factor to be used in the proposed methodology also depends on the damping value that was used to derive the displacement response spectrum. Scaling factors of 2.0 and 1.4 are recommended when displacement spectra are derived using 15 and 5% damping respectively.

These scaling factors are based on wall analyses using what are believed to be conservative levels of damping. If tests show that higher levels of wall damping can be expected it may be possible to reduce these scaling factors significantly.

Sample calculations for this step of the proposed methodology are set out in Section 6.7.5.

9.3.2 Step 2 : Effect of Flexible Diaphragms

In the ABK methodology the implied reduction factor that needs to be applied to the seismic resistance of face loaded walls to allow for the influence of flexible diaphragms is between 0.44 and 0.58.

The computer model analyses used in this project indicate that the ABK method of modelling the effect of diaphragm flexibility on the stability of face loaded walls is too conservative as it ignores the interaction that can take place between the wall and the diaphragm response. The computer analyses used in this project indicate that a seismic resistance reduction factor between 0.7 and 1.0 could be used (see Section 7.2).

The actual reduction factor to be used would depend on the flexibility of the diaphragm (ie its natural period) and its expected level of damping. However, future analyses with a range of wall thicknesses and different earthquake records may require the magnitude of the scaling factors given above to be adjusted.

9.3.3 Step 3 : Effect of Shear Wall Amplification

In multi-storey URM buildings the in-plane response of the shear walls will result in an amplification of seismic motions in the upper floors of the building. In the ABK methodology no amplification is assumed. This is likely to be unconservative, especially where the building's in-plane shear walls respond with significant rocking motion of the wall elements between window openings.

The procedure for estimating the amplification of peak accelerations at various levels of multi-storey buildings as suggested by Priestley (42) could be used to evaluate appropriate seismic resistance reduction factors for this stage of the methodology.

However, the Priestley procedure is expected to be too conservative as amplification factors recently recorded in a URM building indicate that a higher level of damping than that assumed by Priestley is required to account for the effects of soil structure interaction. (See Section 4.5)

Also, in most cases, the shear walls will be relatively stiff when loaded in-plane and can be expected to amplify the high frequency components of earthquake motion more than low frequency components. The computer analyses carried out as part of this project indicated that the face loaded walls of a URM building have a relatively low frequency response when nearing collapse. Therefore, shear wall flexibility may not effect the stability of face loaded walls as much as the magnitude of the peak acceleration amplification factors measured in multi-storey buildings would suggest.

9.3.4 Step 4 : Anchorage Forces and Diaphragm Strengths

Factors affecting anchorage forces are discussed in Section 7.2.4.

In the ABK methodology anchorages are designed to have sufficient capacity to resist the seismic loads that correspond to a lateral load coefficient of $C_d = 1.0g$. This anchorage capacity is required by the ABK methodology for earthquakes with an effective peak ground acceleration of $0.4g$.

Analyses carried out for this project indicate that the response of a face loaded wall may limit the anchorage forces developed.

Formulae are presented that allow peak anchorage forces to be calculated under static loading conditions. The peak static anchorage forces are assumed to develop when cracks in the face loaded wall just start to open and the wall is subjected to a uniformly distributed face load.

Under dynamic conditions the peak static anchorage force may be exceeded by a margin that depends on the diaphragm stiffness and strength. Out-of-phase responses of the face loaded walls on opposite edges of a diaphragm may also result in increased anchorage forces.

It is recommended that anchorages be designed for $2 \times$ the peak static anchorage forces. However, where diaphragms are stiff and strong the dynamic amplification factor should be increased from 2 to 3.

In the lower floors of a multi-storey URM building, where the overburden load is large or where the wall has a low H/t ratio, the above procedure will result in anchorage forces close to or greater than that expected for an elastic response. Under these conditions the wall may not even crack under face loads and anchorage forces corresponding to an elastic response should be used.

When mortar quality is poor or the overburden pressure is low the anchorage

capacity may be limited by the shear strength of the brickwork (see Section 2.10.3).

In the ABK methodology, a minimum diaphragm strength is required to limit diaphragm displacements (See Section 4.3) because large diaphragm displacements are likely to result in large relative diaphragm displacements between storeys which, theoretically, should affect the stability of face loaded walls. When the effects of relative diaphragm displacement on the static stability of a face loaded wall are considered it is evident that the detrimental effect of relative diaphragm displacement should be dependent on the ratio of the relative diaphragm displacement to the wall thickness. Therefore the minimum diaphragm strength should also be dependent on the thickness of the face loaded walls anchored to it. However, wall thickness is not considered as a parameter in ABK's methodology for evaluating diaphragms.

Minimum diaphragm strengths required by the ABK methodology for short span diaphragms are relatively low when compared with the anchorage forces predicted by the analyses carried out for this project. Further analyses are required to evaluate the affect of low strength and yielding diaphragms on the response of face loaded walls before recommendations can be made for the minimum diaphragm strength required.

9.4 Further Research Required

This research project has indicated that further research is required in the following areas:

- Further inelastic dynamic analyses are required to confirm that the formulae proposed for estimating the stability of face loaded walls are applicable for a range of wall slenderness ratios and overburden to wall weight ratios.
- Free vibration tests on face load wall specimens are required to establish appropriate levels of damping to use in computer modelling. Test parameters need to include the mortar type (soft or strong) and the wall thickness. Tests could be carried out on short sections of wall. The test specimens could either be isolated in the wall of a building that is about to be demolished or they could be constructed in the laboratory.
- Inelastic dynamic analyses are required to evaluate the interaction between the seismic responses of walls in adjacent storeys and to determine the appropriate boundary conditions that should be used to model single storey wall elements.
- The face loaded computer model used in this project needs to be extended to include a parapet wall section that is able to rock back and forth on a crack located at the level of the top diaphragm. The effect of treating the parapet as a central point load when modelling the supporting wall in the storey below the parapet could then be evaluated. It should also be possible to develop a methodology for evaluating the seismic stability of parapets that is similar to the methodology proposed in this project for face loaded walls. The effect of parapet bracing could also be evaluated.
- Analyses in this project and by Zoutenbier (43) (on more slender and flexible

walls) has indicated that the seismic stability of face loaded walls is not effected by the presence of flexible diaphragms as much as the ABK methodology would suggest. Further analyses with a range of earthquake motions and wall thicknesses are required to confirm this conclusion. In the methodology proposed in this project for evaluating the seismic resistance of face loaded walls a reduction factor is applied to take into account the effects of diaphragm flexibility. Further analyses would allow the magnitude of this reduction factor to be stated with more confidence and clarify parameters that effect it.

- Further inelastic dynamic analyses are required to evaluate the effects of diaphragm yielding on the stability of face loaded walls and on anchorage forces.
- Testing is required to establish the minimum quality of mortar and/or overburden pressure that is required to prevent anchorage pull through or shear failures in the brickwork.
- The face loaded computer model used in this project needs to be extended to incorporate flexible masonry shear walls that transmit the earthquake motion to the floor diaphragms and can be expected to amplify the earthquake motion in the upper levels of a multi-storey URM building.

The analysis of a 5 storey URM face loaded wall by Zoutenbier (43) showed that the seismic resistance of the face loaded wall elements in each storey generally decreased with increasing height. However, it was not possible to separate the influence of reduced over burden load from the effects of amplification of the earthquake motion in the upper storeys. Analyses that isolate the influences of these two parameters are required.

- Face loaded URM walls are usually able to span horizontally as well as vertically. The additional restraint provided by end walls and partitions has not been considered in this project.

Horizontal spanning can be expected to increase the stiffness of face loaded walls and reduce their seismic displacements.

In some cases face loaded walls with weak mortar have been left bowed in the horizontal plane after earthquakes, indicating that the bricks have rotated relative to one another at the horizontal mortar joints. This could be a significant source of additional damping for the seismic response of some face loaded walls.

10 SUMMARY AND CONCLUSIONS

The principal objectives of this project were to obtain a better understanding of the behaviour of URM buildings in earthquakes, to identify the main factors influencing their vulnerability and to develop procedures for evaluating URM buildings in New Zealand. The investigation encompassed a review of the performance of URM buildings in past earthquakes and a review of previous research into the dynamic stability of face loaded walls. The behaviour of URM walls under severe earthquake loading in the out-of-plane direction was also modelled analytically using inelastic dynamic analysis.

The review of earthquake damage concentrated on New Zealand and Californian experience in areas of MM VII or higher intensity shaking. California was selected because of its similar style and history of URM construction. All URM buildings in the two regions are pre 1933/35 vintage and most have two or three wythe thick structural walls and timber roof framing and floors. Except in the CBD areas of the larger cities, very few of the buildings are over three stories high and most are either one or two stores high. In both regions, many URM buildings in the highest seismicity areas have lightly reinforced bands and/or existing wall anchors.

The analytic investigations undertaken were directed at assessing the collapse behaviour of URM walls under dynamic face loading. The wall element modelled was based on one of the clay brick wall specimens tested by the ABK joint venture in the early 1980's. The wall behaviour predicted was compared with the test results reported by ABK. Analyses were also performed using historic acceleration records to assess the predicted response in terms of the observed extent of damage to URM buildings in the earthquakes.

Conclusions and recommendations from the investigation are given below. Further specific conclusions and recommendations are presented in the respective sections covering the review of past damage and the analytic investigations.

1. Collapse and partial collapses of individual walls occurred in some earthquakes at MM VII intensity and total collapses of buildings were reported in all areas of MM VIII and higher intensity shaking for the earthquakes reviewed. Numerous instances of catastrophic collapse occurred in MM X areas. Parapet failures occurred in all of the areas reviewed.
2. In areas of up to MM VII intensity shaking, collapse or partial collapse of walls was primarily due to face load failure. In most cases, collapse was restricted to either single storey walls or the top storey in multistorey buildings and occurred as a result of either a lack of anchors or failure of the anchors tying the tops of the walls to the roof framing. Prior failure of parapets or collapse of walls may have caused some of the apparent anchorage failures but low overburden and poor mortar quality were factors in most of the collapses. Examples were found where even through-wall anchorages with external plates had partially pulled through walls, and in other cases there were out-of-plane shear displacements on a horizontal plane under a line of anchors. There were also several instances in the Loma Prieta earthquake where wall anchorages failed by tearing out sections of a horizontal timber diaphragm.

The failure of diaphragm anchors in these earthquakes points to the need for a tightening of requirements for design and for brickwork testing, particularly for anchors at the tops of walls where there is little overburden.

3. Wythe delamination and spalling were observed in several Californian earthquakes. These failures were also restricted to the upper sections of walls and were associated with poor quality or deteriorated mortars and poor filling of the vertical joints between wythes.
4. The predicted face load response of URM wall elements was found to be consistent with observed damage when recorded ground motions were used in the analytical model. In particular, for wall elements with a height to thickness ratio of 14 that are adequately anchored top and bottom, the ground motions recorded in four areas of MM VII shaking were not strong enough to induce face load collapse. These results are consistent with the behaviour observed in the 1990 Weber (NZ) and 1979 Imperial Valley (Calif) earthquakes. In both cases, most URM walls had been tied to floor and/or roof diaphragms and there was minimal face load damage to URM walls. Analyses using the same wall element and analysis parameters indicate that under unfavourable conditions, face load collapse could occur at as low as 50% - 80% of the 1983 Coalinga record (MM VIII), which is again consistent with the high level of damage to URM buildings in this earthquake. Further comparative analyses are required to confirm these results.
5. Corner damage observed in several Californian earthquakes points to the need to ensure satisfactory transfer of diaphragm shear forces into the end walls and in particular, to restrain the diaphragms from sliding in shear relative to the walls. At higher shaking intensities, wall junction failures also resulted in face walls separating from cross and end walls, significantly increasing the risk of wall collapse.
6. Examples of damage due to pounding between buildings were evident in most of the earthquakes, particularly in areas subjected to MM VIII or higher intensity shaking. While there are limited options for preventing pounding, some form of mitigation is required in situations where there is a risk of wall pounding causing building collapse.
7. Cracking failures due to in-place loading were common in most earthquakes. This damage does not appear to have caused collapse of URM buildings subjected to MM VIII or lower intensity shaking. However, at higher intensities, in-plan failures were identified as a significant cause of the collapse.
8. A survey of some of New Zealand's unreinforced masonry (URM) building stock that have been identified as earthquake risks, indicated that very few have more than three storeys and that the majority have only one or two storeys. It was concluded that New Zealand's research effort into the behaviour of URM buildings should be concentrated on buildings with three or less storeys.
9. The computer model indicated that diaphragms in buildings subjected to MM

VII or higher shaking would be highly stressed or deformed. However, this has generally not been reflected in the damage observed in areas subjected to earthquake intensities up to MM VIII, even though very few of the diaphragms had been strengthened. Further research into the interaction between wall and diaphragm behaviour is required.

10. It was found that the time history analyses could not accurately model the short time interval during the wall response when the cracks in the brickwork closed and large impact forces were generated in the walls, though this did not significantly affect the overall behaviour predicted by the model. Difficulties were also experienced in representing damping in the walls and diaphragms. Further investigation of this aspect is required. Nevertheless, agreement between the predicted and observed displacements of the wall specimens was very good given uncertainties relating to the actual earthquake input motions used in the ABK tests.
11. The analyses showed that for any given earthquake record, a wall subjected to face loading is not unstable at all load intensities above the minimum level required to cause collapse. When the intensity of face loading is increased above the minimum collapse load by scaling the earthquake record, the wall collapses at some load intensities but may be stable at other higher intensities. This occurs because the wall response is highly nonlinear at large displacements and as a result, varying the load intensity changes the phase relationship between the wall response and the imposed earthquake excitation. Because of this behaviour, results based on only a small number of tests or analyses can produce a misleading estimate of collapse load. This behaviour also indicates that the differences between collapse and non-collapse of nearby apparently similar buildings (as often observed) may in some cases, be simply due to phase differences between the wall response and earthquake loading, rather than reflecting a difference between the seismic load resistances of the buildings or differences in the level of seismic loading imposed.
12. Results of the analyses indicate that the testing method used by ABK overestimates the detrimental effect that diaphragm flexibility is likely to have on the seismic resistance of face loaded URM walls. While the intensity of loading imposed prior to the wall fracturing can be significantly amplified as expected from elastic theory, the EQ intensity required to collapse a wall is generally not affected as significantly by the presence of a flexible diaphragm and may be increased, depending on the spectral characteristics of the earthquake loading imposed and the diaphragm period.
13. The results of the analyses also showed that the seismic resistance of a face loaded wall is a function of both wall thickness and height to thickness ratio, rather than only the latter as assumed in the ABK methodology. For walls with a constant height to thickness ratio, the computer model predicts increased seismic resistance as the wall thickness is increased from 166 to 660mm. The size of the increase varied between 40 and 100% depending on the earthquake record used in the analyses.

In general the computer analyses and review of earthquake damage reports carried out as part of this project indicate that many URM buildings in New Zealand should be able to resist moderate earthquakes without collapse providing the walls are adequately anchored to the building's floor and roof diaphragms.

However, the performance of URM buildings in a major earthquake is expected to be poor.

The Tabas earthquake record represents the type of earthquake motion that can be expected close to the epicentre of a major earthquake. An earthquake motion of this intensity could be generated, for example, in Wellington's CBD which is located within only 1-2km of the Wellington Fault. Computer analyses using the Tabas earthquake motion indicate that many New Zealand URM buildings would not be able to withstand an earthquake of this intensity without, at least, partial collapse. Face loaded walls in the top storey of a multi-storey URM buildings are expected to be the most vulnerable elements and the vulnerability of these walls will increase with increasing slenderness. Earthquake damage reports indicate that URM buildings would also become susceptible to collapse at this earthquake intensity due to in-plane damage to walls.

An alternative methodology for assessing the seismic resistance of face loaded URM walls has been presented. In this methodology the effective period of the face loaded wall motion is computed using semi-empirical formulae. The effective period is then used in conjunction with an elastic displacement response spectrum to predict the earthquake magnitude required to cause the face loaded wall to collapse. Further research required to develop and refine the proposed methodology is outlined. However, even at this stage of its development, the proposed methodology is expected to provide a more realistic assessment of face loaded wall stability than other currently used procedures.

REFERENCES

1. NZNSEE "Earthquake Risk Buildings, Recommendations and Guidelines for Classifying, Interim Securing and Strengthening", *NZ National Society for Earthquake Engineering Study Group Recommendations*, 1985.
2. Noland JL, Kingsly GR and Atkinson RH (1988), "Utilization of Nondestructive Techniques into the Evaluation of Masonry", *Proceedings of the Eighth International Brick and Block Masonry Conference*, Dublin, Ireland, September 1988.
3. Callaghan FR (1933), "The Hawke's Bay Earthquake - General Description" in *Report of the Hawke's Bay Earthquake, 3rd February 1931*, NZ Dept. of Scientific and Industrial Research, Bulletin No. 43, Wellington, 1933, pp. 3-38.
4. Brodie A and Harris AG (1933), "Damage to Buildings" in *Report of the Hawke's Bay Earthquake, 3rd February 1931*, NZ Dept. of Scientific and Industrial Research, Bulletin No. 43, Wellington, 1933, pp. 108-115.
5. Hull AG (1990), "Tectonics of the 1931 Hawke's Bay Earthquake", *NZ Journal of Geology and Geophysics*, 1990, Vol. 33, pp. 309-320.
6. Dowrick DJ and Smith EGC (1990), "Surface Wave Magnitudes of Some New Zealand Earthquakes 1901-1988", *Bulletin NZNSEE*, Vol. 23, No. 3, September 1990.
7. Sritharan S and McVerry GH (1990), "Analysis of Strong Motion Records for Microzoning Central Wellington", *Regional Natural Disaster Reduction Plan - Seismic Hazard*, Wellington Regional Council, May 1990
8. Johnston JAR (1960), "A Brief History of Damaging Earthquakes in Wellington City and Developments in Multi-storey Building Construction in New Zealand", *Proc. of the Second World Conference on Earthquake Engineering*, Tokyo 1960, Vol. 1.
9. Aked WE (1945), "Damage to Buildings in the City of Wellington by Earthquake, 1942", *Proc. the New Zealand Institution of Engineers*, Vol. XXXI, 1945.
10. Kariotis J, Barkley B, Ewing B and Johnson A (1980), "Unreinforced Masonry Performance - 1979 Imperial Valley Earthquake", *Reconnaissance Report - Imperial County, California, Earthquake* October 15, 1979, EERI, February 1980.
11. Reitherman R, Cuzner GJ, Zsutty TC & Smith GW (1984), "Performance of Unreinforced Masonry Buildings", in *Coalinga, California, Earthquake of May 2, 1983*, Reconnaissance Report, EERI Report No. 84-03, Calif., Jan. 1984.

12. Kariotis J (1984), "Survey of Unreinforced Masonry Buildings", in *Coalinga, California, Earthquake of May 2, 1983*, Reconnaissance Report, EERI Report No. 84-03, Calif., Jan. 1984.
13. Stover CW (1983), "Intensity Distribution and Isoleismal Map", in *The 1983 Coalinga, California Earthquakes*, Special Publication 66, California Department of Conservation, Division of Mines and Geology, Sacramento CA, 1983.
14. Leeds DJ (1983), Commissioned report for Scientific Service, Inc, Redwood City, CA, prepared by David J Leeds and Associates, Los Angeles, CA, July 1983.
15. Borchardt R, personal communication, 1992.
16. Jones BG and Nicolaidis CN (1988), "The Whittier Narrows, California Earthquake of October 1, 1987 - Buildings at Risk", *Earthquake Spectra*, Vol. 4, No. 1, EERI, 1988.
17. Deppe K (1988), "The Whittier Narrows, California Earthquake of October 1, 1987 - Evaluation of Strengthened and Unstrengthened Unreinforced Masonry in Los Angeles City", *Earthquake Spectra*, Vol. 4, No. 1, EERI, 1988.
18. Hart GC, Kariotis J, and Noland JL (1988), "The Whittier Narrows, California Earthquake of October 1, 1987 - Masonry Building Performance Survey", *Earthquake Spectra*, Vol. 4, No. 1, EERI, 1988.
19. Moore TA, Kobzeff JH, Diri J, and Arnold C (1988), "The Whittier Narrows, California Earthquake of October 1, 1987 - Preliminary Evaluation of the Performance of Strengthened Unreinforced Masonry Buildings", *Earthquake Spectra*, Vol. 4, No. 1, EERI, 1988.
20. Doc Xuan Nghiem (1988?), "October 1, 1987, Whittier Narrows Earthquake Damage Survey", Earthquake Div., City of Los Angeles, LA, California (unpublished?).
21. Benuska L (1990) -Tech. Editor, "Loma Prieta Earthquake Reconnaissance Report", *Earthquake Spectra*, Supplement to Vol. 6, EERI, May 1990.
22. Holmes WT, Lizundia B, Brinkman S, Conrad J, Reitherman R, Dong W, Burton J, and Bailey A (1990), "Damage to Unreinforced Masonry Buildings in the Loma Prieta Earthquake of October 17, 1989", Report prepared by Rutherford & Chekene for the California Seismic Safety Commission, Sacramento, CA, July 1990.
23. Smith EGC (1990), "1990 Southern Hawke's Bay Earthquakes", Earthquake Seminar, Hawke's Bay Branch IPENZ, Century Theatre, Napier, Nov. 1990.
24. Eiby GA (1980), "The Marlborough Earthquakes of 1848", *New Zealand DSIR Bulletin* 225, New Zealand Department of Scientific and Industrial Research, Wellington, 1980.

25. Steinbrugge KV and Schader EE (1973), "Earthquake Damage and Related Statistics", in *San Fernando, California Earthquake of February 9, 1971*, National Oceanic and Atmospheric Administration, U.S. Department of Commerce, Washington, D.C., 1973.
26. Scott NH (1973), "Felt Area and Intensity of San Fernando Earthquake", in *San Fernando, California Earthquake of February 9, 1971*, National Oceanic and Atmospheric Administration, U.S. Department of Commerce, Washington, D.C., 1973.
27. Jin Guoliang (1979), "Damage in Tianjin During Tangshan Earthquake", in *The 1976 Tangshan, China Earthquake*, 2nd U.S. National Conference on Earthquake Engineering, Stanford University, August 1979, EERI March 1980.
28. Hu Yuxian (1979), "Some Engineering Features of the Tangshan Earthquake", in *The 1976 Tangshan, China Earthquake*, 2nd U.S. National Conference on Earthquake Engineering, Stanford University, August 1979, EERI March 1980.
29. Steinbrugge KV and Cloud KW (1965), "Preliminary Engineering Report", in *The Puget Sound, Washington Earthquake of April 29, 1965*, Coast and Geodetic Survey, U.S. Department of Commerce, Washington, 1965.
30. Algermissen ST and Harding ST (1965), "Preliminary Seismological Report", in *The Puget Sound, Washington Earthquake of April 29, 1965*, Coast and Geodetic Survey, U.S. Department of Commerce, Washington, 1965.
31. Wailes CD, Jnr and Horner AC (1933) "Survey of Earthquake Damage at Long Beach, California", City of Long Beach files, published in *Engineering News-Record*, May 25, 1933, as "Earthquake Damage Analyzed by Long Beach Officials".
32. Martel RR (1936), "A Report on the Earthquake Damage to Type III Buildings in Long Beach", *Earthquake Investigations in California, 1934-1935*, U.S. Coast and Geodetic Survey, Special Publication No. 201, 1936.
33. NZS 4203:1992, "New Zealand Standard Code of Practice for General Structural Design And Design Loadings For Buildings", Standards Association of New Zealand, Wellington, 1992.
34. Prakash V and Powell GH (1992), "Drain 2DX Version 1.02 User Guide", Dept. of Civil Engineering, University of California / NISEE Computer Applications, Jan. 1992.
35. Dr R Razani, S H Razani "Pictorial Report about the causes of failure, Modes of Failure, and Weak Points of Unreinforced Structures (URM), Semi-Reinforced, and Confined Masonry buildings During June 1989 Earthquake in Gilan-2 anjan Provinces and other Recent Earthquakes in Iran". Draft report constituting part of UNDP-UNCHS (Habitat) Project IRA/90/004 - Assistance in the implementation of a Post Earthquake Reconstruction Programme, United Nations Industrial Development Organisation, Vienne.

36. "Newcastle Earthquake Study", The Institute of Engineers, Australia, 1990.
37. RGA # 1-87, "Establishing an Alternative Design Methodology for Unreinforced Masonry Buildings", City of Los Angeles, Department of Building & Safety, **Rule of General Application # 1-87.**
38. ABK Joint Venture "Methodology for Mitigation of Seismic Hazards in Existing Unreinforced Masonry Buildings". El Segundo, C A Agbajian Associates.

ABK-TR-01 (1981) - Catagorisation of Buildings
ABK-TR-02 (1981) - Seismic Input
ABK-TR-03 (1981) - Diaphragm Testing
ABK-TR-04 (1981) - Wall Testing : out-of-plane
ABK-TR-05 (1982) - Interpretation of Diaphragm Tests (not available)
ABK-TR-06 (1982) - Interpetation of Wall Tests : out-of-plane
ABK-TR-07 (1983) - Anchorage - not available
ABK-TR-08 (1984) - Methodology
39. Kariotis J C, Ewing R D, Johnson A W " Predictions of Stability of Unreinforced Masonry Shaken by Earthquakes", *proceedings of 3rd N American Masonry Conference*, June 1985.
40. DZ 4203/2 "Draft NZ Standard for General Strucutural Design and Design Loading for Buildings", *Standards Association of New Zealand*, Private Bag, Wellington, 1991.
41. Division 88 Los Angeles Municipal Code "Earthquake, Hazard Reduction in Existing Buildings" also RGA - Unreinforced Masonry Bearing Wall Buildings - Alternative Design to Division 88 April 21, 1987.
42. Priestly, M J N: "Seismic Behaviour of Unreinforced Masonry Buildings", *Bulletin of NZNEE*, Vol 18, No. 2, June 1985. (Also Discussion Vol 19, No. 1 March 1986).
43. Zoutenbier, J: "The Seismic Response of Unreinforced Masonry Buildings", *ME Project Report*, Department of Civil Engineering, University of Canterbury, February 1986.
44. Moore T A, Kobzeff J H, Diri J and Arnold C, "The Whittier Narrows, California Earthquake of October 1, 1987 - Preliminary Evaluation of the Performance of Strengthened Unreinforced Masonry Buildings", *Earthquake Spectra*, Vol. 4, No. 1, Feb 1988.
45. Tena-Colunga A, "Seismic Evaluation of Unreinforced Masonry Structures with Flexible Diaphragms", *Earthquake Spectra*, Vol 8, No. 2, 1992.
46. Allahabadi R, "DRAIN-2DX, Seismic Response and Damage. Assessment for 2D Structures", *PhD dissertation*, University of California, Berkely, 1987.

47. Psycharis I M, "Effort of Base Uplift on Dynamic Response of SDOF Structures" *ASCE Journal of Structural Engineering*, Vol 117, No. 3, March 1991.
48. Dean J A, Lapiash E B, "Gibraltar Board Sheathed Bracing Walls" *Report prepared for Winstones Wallboards Limited, Auckland, NZ by CLC Consulting Group.*